CRUISE SCIENCE REPORT: RR#2004; R/V ROGER REVELLE

Post-cruise summary of the second cruise of the National Science Foundation project, "Collaborative Research: Biogeochemical and Physical Conditioning of Sub-Antarctic Mode Water in the Southern Ocean" (by Balch, McGillicuddy, Morton, Bates, Long and Brownlee). Presenting cruise narrative and reports of each group within the science party. Version 3; 5/6/2021

Cruise to the Pacific Sector of the Southern Ocean- Honolulu, HI (26 December, 2020) to Honolulu, HI (23 February, 2021).

Cruise Science Report: RR#2004 R/V Roger Revelle

Table of Contents

21 Feb 2021

Cruise Science Report Narrative: RR2004 R/V Roger Revelle 26 December, 2020 – 23 February, 2021

William Balch, Bigelow Laboratory for Ocean Sciences, E. Boothbay, ME

Dennis McGillicuddy, Woods Hole Oceanographic Inst., Woods Hole, MA

Peter Morton, Florida State University, Tallahassee, FL

1. Overview and Cruise Narrative

Cruise #2004 of the R/V Revelle was the second research cruise funded as part of the National Science Foundation project, "Collaborative Research: Biogeochemical and Physical Conditioning of Sub-Antarctic Mode Water in the Southern Ocean" (by Balch, McGillicuddy, Morton, Bates, Long and Brownlee). Subantarctic Mode Water (SAMW) is a major Southern Ocean (SO) water mass, subducted equatorward in all three SO sectors. Two classes of biomineralizing phytoplankton, diatoms and coccolithophores, grow in SAMW formation regions. Diatoms dominate at the Polar Front, while the coccolithophores are concentrated to the north at the Subantarctic Front and Subtropical Front in a zonal band of high-reflectance water known as the Great Calcite Belt (GCB). Both algal groups produce dense mineral shells that ballast organic debris, driving the biological pump; they condition the water before and during subduction. SAMW chemistry and biology dominate marine ecosystems and the biological pump in subtropical and tropical waters; it is estimated that SAMW controls 75% of the biological production of waters north of 30ºS, as well as the functional groups of algae that grow there on contemporary to glacial/interglacial time scales (Sarmiento et al., 2004). Our goal on this cruise was to quantify how coccolithophore and diatom production in SAMW conditions water mass chemistry. Furthermore, experiments aboard ship were designed to evaluate whether the production balance between these two groups impacts their growth at low latitudes. One unique feature of the region of study for this cruise is the presence of mesoscale eddies that form at the various frontal boundaries; these are rich in either coccolithophore or diatom assemblages and associated microbial communities. Such eddies provide an ideal, semi-enclosed, water parcel to observe the rates of conditioning of SAMW over time scales of months, enabling estimates of the physiological and ecological controls on nutrient, trace metal, and carbonate system composition of SAMW. **The three goals of this cruise:** The ***first*** goal was to determine the rates that SAMW coccolithophores and diatoms condition the CO_2-carbonate chemistry (alkalinity, dissolved inorganic carbon, pH, pCO_2, $CaCO_3$ saturation state (Ω) plus nutrient and trace metal concentrations). The taxonomic and physiological diversity was also assessed across the study area using microscopy plus traditional and next-generation sequence profiling for DNA and RNA. The ***second*** goal was to experimentally determine whether the conditioning of SAMW water was limited by iron, silicate and/or nitrate, and understand the controls on algal species assemblages and genetic diversity. An important question was whether these SO waters act as a net CO_2 source or sink. The ***third*** goal of this work (post-cruise) is ultimately to combine these

findings with the best estimates of Ekman- and eddy-driven subduction of SAMW to estimate the biogeochemical impact to the basin scale, using both observations and global numerical models. We occupied PIC-rich and PIC-poor mesoscale features and measured changes in their ecology, production (both inorganic and organic), alkalinity, pH, pCO_2, Ω, plus nutrient concentrations of the SAMW at its point of formation. We performed a meridional survey from 30°S-60°S to characterize the larger-scale variability of the carbonate chemistry, nutrients, productivity, genetics and biomass of various plankton groups as the SAMW was subducted northwards. This cruise integrated ocean physics, chemistry and biology.

As explained above, SAMW sustains primary production and controls the ecology and chemistry of the lower latitudes. Global data show that SAMW waters, initially conducive to coccolithophore growth in the GCB, show the lowest surface coccolithophore concentrations by the time SAMW is upwelled at the equator some 40 years later (lower than in subtropical gyres). Iron and nutrient conditioning appear to play integral roles in determining which algal classes dominate (with obvious ramifications to the biological pump) and whether the waters act as a net CO_2 source or sink.

This cruise work extended the research findings of the project into educational opportunities beyond the oceanographic community. Three undergraduates participated in the cruise (Lauren Hearn, FSU), Hannah Primiano (Drew University) and Ben Gustafson (Colby College). Both Primiano and Gustafson also participated in Bigelow's Research Experiences for Undergraduates program this past year. Three graduate students participated: Julia Middleton (WHOI), Logan Tegler (WHOI), and Andrew Hirzel (WHOI). One postdoc, Hilde Oliver (WHOI), also participated. An educator, Dr. Guiliana Viglione (Bigelow), was brought on the cruise to broaden public and classroom outreach. She made initial contact with multiple schools around the country to introduce the scientific problem of this work, and organized interactions with the students, answering questions, blogging, using social media, all to broaden outreach in a quantifiable fashion.

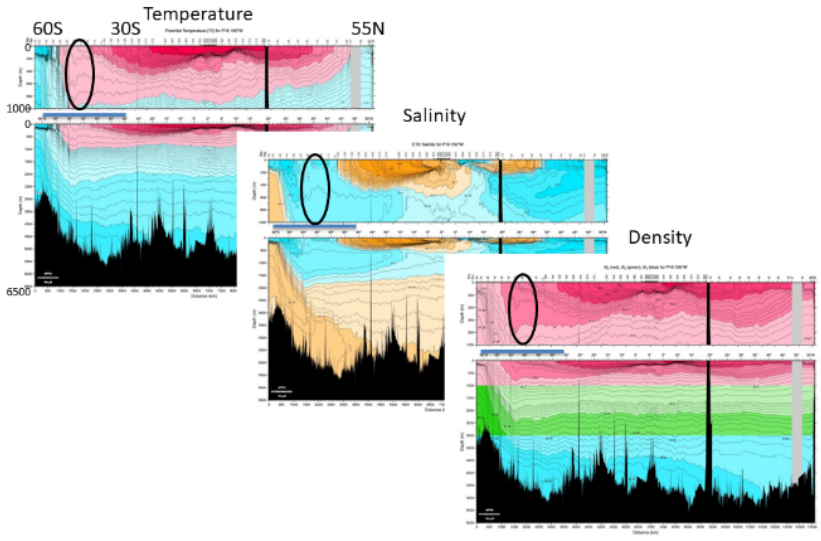

Figure 1. Temperature, salinity, and density sections from P16. Oval shape indicates SAMW. Source: WOCE Atlas Volume 2: Pacific Ocean, http://whp atlas.ucsd.edu/pacific/p16/sections/sct_menu.htm

Unfortunately, two of the science party, Daniela Sturm and Joost de Vries (from the Brownlee laboratory in the UK) were not allowed to fly to Hawaii to join the ship at the last minute. This was due to a

recently imposed federal prohibition on travelers coming to the US from Europe and the United Kingdom, which had recently put in place during the covid pandemic.

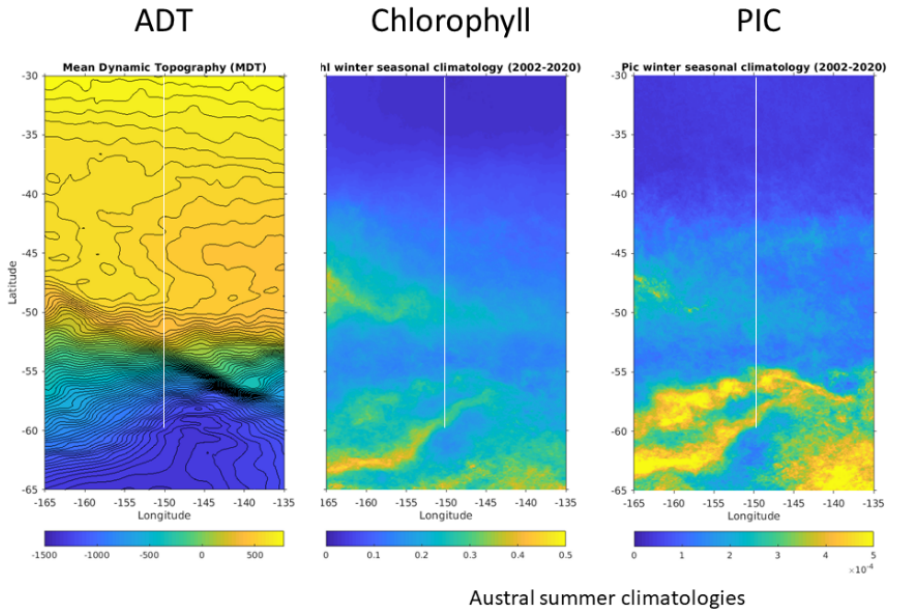

Figure 2. Climatologies of absolute dynamic topography (ADT), chlorophyll, and PIC.

2. Ship track

This cruise departed Honolulu, Hawaii on 26 December 2020 (following two weeks of strict quarantine/isolation for covid plus 4d of loading of the ship within the Revelle's covid "bubble." The ship transited south along the great circle route from Honolulu to 30ºS x 150ºW. We targeted this meridian for several reasons. First, SAMW is formed in the Southern Ocean at high rates in the vicinity of this meridian (Cerovečki et al., 2013)(Fig. 1). This water is subsequently subducted and gets carried northward at depths of 500-700m, where it is brought closer to the surface in about 40 years time in the equatorial regions, influencing the productivity of these waters as well as those further into the northern hemisphere (Sarmiento et al., 2004). Second, ocean color satellite data over the last 23 years has shown elevated reflectance from the Great Calcite Belt between the latitudes of 40ºS to 50ºS but this region is extremely remote and few actual observations exist to confirm this (Balch et al., 2016) (Fig. 2). Third, ocean color imagery has also revealed regions of elevated coccolithophore-like reflectance further south than 50ºS latitude along this meridian, but these waters have temperatures well below the preferred temperature range of the common coccolithophore species of the Southern Ocean, *Emiliana huxleyi*, hence we suspected another particle type likely is responsible (Fig. 2). There is strong topographic steering of the currents along the subantarctic front, the polar front and the southern Antarctic Circumpolar current by the Pacific Antarctic Ridge and its associated Udintsev and Eltanin Fracture Zones (Fig. 3, 4). Fourth, this region has elevated frequencies of eddy formation, with trapped high-reflectance waters, which provide opportunities to follow these semi-enclosed parcels and their trapped populations in space and time. A meridional transect along 150ºW provided an opportunity to track the formation of SAMW and its age using Freon measurements (to be performed ashore by the laboratory of Dr. Rana Fine (Rosenstiel School of Marine and Atmospheric Sciences, Miami, FL) (Fine, 1993, 2011; Fine et al., 2002; Fine et al., 2008). Knowing the age of SAMW will allow determination of the rates that SAMW is being

conditioned by diatoms, coccolithophores and other classes of phytoplankton on its trek to the north.

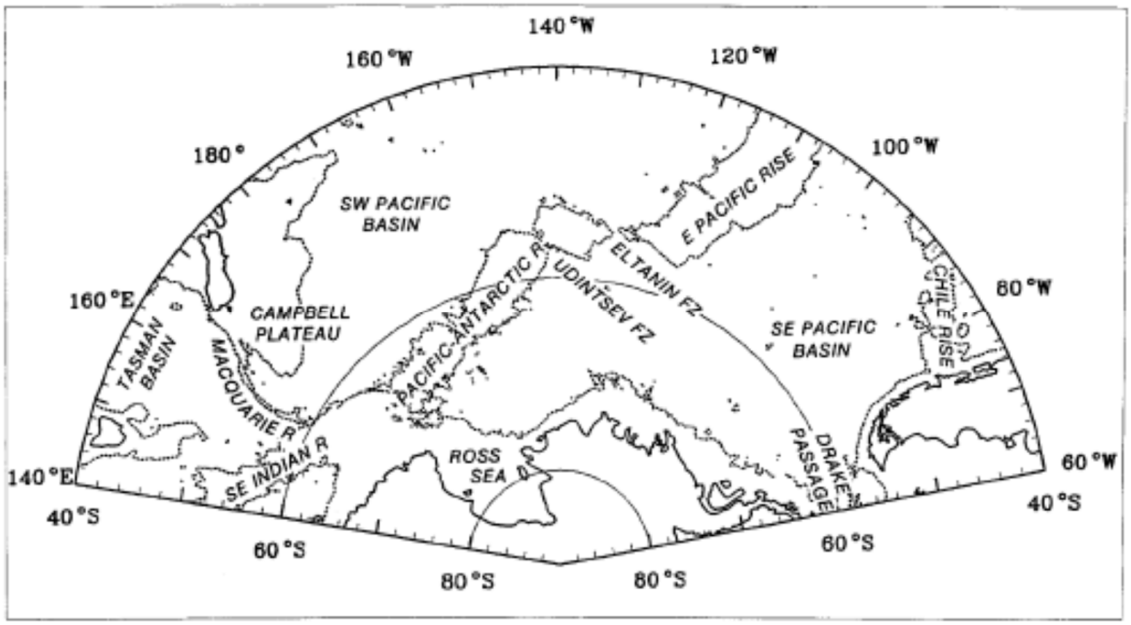

Figure 3- Major bathymetric features of the Pacific Sector of the Southern Ocean. Dashed line is the 3,500m isobaths. Note locations of the Udintsev and Eltanin Fracture Zones. Taken from Patterson and Whitworth (1989).

We began the meridional transect (with CTD casts at 0.5° latitude resolution at 30°S-47°S), and we switched to a higher resolution of sampling from 47°S to 60°S (so-called "enhanced meridional transect at 0.33° latitude resolution), plus the addition of VPR tows, in order to better define mesoscale features that we encountered (with both satellite and ship data) along the 150°W meridian. The enhanced meridional transect was done in 180-240 nautical mile segments along 150°W, which allowed for more flexible scheduling of the VPR transects during good weather days, allowing safer VPR deployment and recovery, whereas the CTD stations could be performed safely on the many more inclement days with higher sea states when the VPR could not be deployed safely. Five carboy experiments were performed during the trip to investigate factors limiting to the phytoplankton production (see more below).

After completion of the meridional transect (both reduced-resolution and enhanced resolution), we headed east for the first crossing of the polar front which was shown through altimetry to be topographically-steered through the Udintsev Fracture Zone. Moreover, satellite remote sensing of this feature showed it to be of high reflectance. After crossing the Polar Front the first time, we surveyed a mesoscale eddy which contained waters with elevated reflectance around the edge (hereafter referred to as "Eddy A") performing two radial surveys with complete VPR and hydrographic sections. Two productivity and trace-metal casts were performed in Eddy A along with a carboy experiment, as well. The ship then transited south and east to perform a cross frontal VPR and hydrographic survey (which crossed the same polar frontal boundary

crossed earlier during the meridional transect, as well as during the transit to Eddy A; this transect was called the "Cross Frontal Transect").

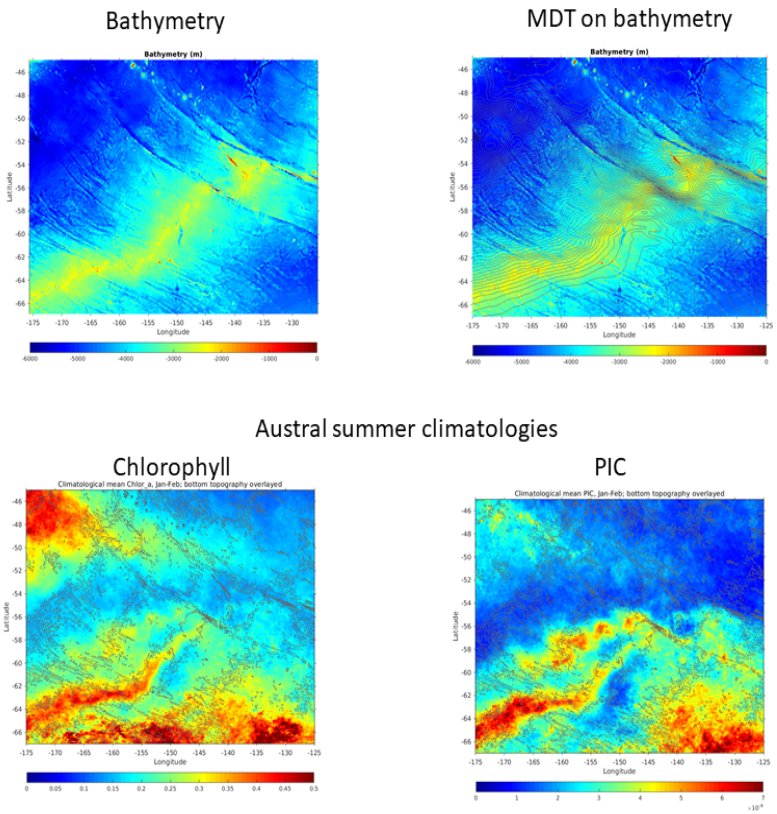

Figure 4. Upper left: bathymetry; upper right: contours of mean dynamic topography (MDT) overlaid on bathymetry; lower left: austral summer chlorophyll climatology with bathymetric contours overlaid; lower right: austral summer PIC climatology with bathymetric contours overlaid.

At this point of the cruise, French Polynesia announced that the ports in Tahiti would be closed for the ship to disembark scientists at the end of February. This meant that the ship would have to return to Honolulu at cruise end, which, in turn, meant that we would lose about one week of science time for the long transit back to Honolulu. Therefore, we devised a streamlined cruise plan for the remainder of the cruise in order to achieve all of our objectives. The ship then visited a small mesoscale eddy (Eddy C) which contained a highly focused, high-reflectance core which we had observed in satellite imagery for several weeks. We performed one VPR tow and one hydrographic survey along one diameter across the small eddy and left Eddy C with VPR in tow, to do a repeat crossing of Eddy A, then onward to a high-reflectance meander of the SubAntarctic Front for collection of water for the fourth experiment and documentation of the conditions of the SAF. We then headed for the portion of the meridional survey where we had seen low levels of coccolithophores three weeks prior. This region had remained cloud covered for weeks, thus we had little idea of what awaited us. Shortly after leaving the Meander station, the estimates of acid-labile backscattering (an optical proxy for PIC) began rising and for the next 400 nautical miles saw PIC concentrations three times higher than anything we had seen previously along the 150°W meridian (or elsewhere for that matter).

3. Sampling overview

There were five types of measurements that were made during most segments of this cruise.

1) **Video Plankton Recorder:** The video plankton recorder is a 360kg towed device that undulates through the water column between the surface and 100m. It measures hydrographic variables (temperature, salinity and depth), as well as oxygen concentration, chlorophyll

fluorescence plus total optical backscattering at 532nm wavelength. A stroboscopic camera documents the types and concentrations of particles larger than 30-50 microns. These are subsequently identified and sorted post-cruise using advanced machine learning techniques.

2) **Surface Underway Measurements:** Surface underway measurements were made to map surface features in real time. The data sets collected by this underway system were: temperature, salinity, fluorescence, total backscattering at 532nm and acidified backscattering at 532nm (after reducing the pH below the dissociation point for calcite). The difference between total and acidified backscattering represents "acid-labile backscattering", which is an optical proxy for the concentration of PIC (Balch and Drapeau, 2004). Also part of the underway sampling system was a bow-mounted Surface Acquisition System with hyperspectral radiometers (HyperSAS; SeaBird) which gathered downwelling irradiance, upwelled water radiance and sky radiance at 136 bands across the UV, Visible and near IR spectrum. The radiometers viewed 90º-110º from the solar azimuth using an automated underway aiming system. This optimized the surface reflectance signature for calculating normalized water-leaving radiance (Mueller et al., 2003). The ship's underway sampling system also was running (with salinity, temperature, chlorophyll fluorescence, oxygen and an underway pCO_2 SAMI sensor).

3) **Hydrographic Sections:** Following a transect of the VPR, hydrographic profiles were performed along the same transect with the CTD (the "full-water cast"), sampling for Freons, dissolved oxygen, DIC, alkalinity (and all other parameters of the carbonate cycle using the CO2-SYS program), extracted chlorophyll, nutrients, POC, PIC, biogenic silica, coccolithophore counts and FlowCAM analyses (for enumerating and classification of nanoplankton and microplankton species). We alternated each CTD full-water cast with a "trip-on-fly" water cast. These later casts were used only to sample full water properties at the surface only, as well as DIC and nutrients at eight depths. These trip-on-fly casts served to provide greater resolution in hydrographic sections across the features. A separate Digital Autonomous VPR (DAVPR) was also attached to the CTD for recording distributions of organisms over 1000m casts. Once per day, typically pre-dawn, CTD casts included samples drawn for primary productivity and calcification. These measurements involved the use of ^{14}C-bicarbonate and all manipulations were done in a portable UNOLS radioisotope van.

4) **Trace Metals:** Sampling for trace metals was performed daily using nine Niskin-X bottles clamped to nonmetallic Aracom line, hung at depths to ~1000m and tripped with non-metallic messengers. All trace-metal-clean manipulations were performed in a trace-metal-clean laboratory or a plastic bubble built within the ship's wet lab. 5) Five carboy experiments were performed over the cruise, which involved incubating surface, trace-metal-clean water collected by a "Big Jon" surface sampler (towed from the side of the ship at 1-3kts, which maintained a distance of 5-10m from the side of the ship as it pumped surface water into two 200-L plastic tanks within the wet lab bubble). For three of the carboy experiments we performed triplicate incubations of untreated control water plus five treatments (three replicates each) in plastic, acid-cleaned cubitainers with a) 5% dilution with subsurface water, b) 20 μM trace metal-clean nitrate, (c) 20 μM trace metal-silicate, (d) 1 nM of iron and (e) 1 nM of iron+20 μm of silicate

(exact details in Morton-Trace Metal section below). The cubitainers were then sampled approximately every other day for 4-5 days while being incubated under surface light conditions in an on-deck incubator, with temperature maintained at T0 *in-situ* surface conditions. The carboys were sampled about every two days by the Balch group for chlorophyll, nutrients, PIC, POC, biogenic silica, quantitative coccolithophore counts and quantitative FlowCAM samples (for enumeration of algal classes, cell volumes, and slope of the particle-size distribution). Later in the cruise, for two of the carboy experiments, due to time constraints with two simultaneous incubations, we were only able to perform incubations with a control and two treatments of (a) 5% subsurface water and (b) 2 nM iron). Ph.D. student, Julia Middleton (Ph.D. student of Dr. Tristan Horner, WHOI) performed experiments on barite formation in parallel with the carboy experiments of this trip. Ph.D. student, Logan Tegler (Ph.D. student of Dr. Tristan Horner, WHOI) performed experiments on cadmium isotopic composition in parallel with the carboy experiments.

5) **Other Ancillary Measurements:** There were several important other ancillary measurements critical to the scientific goals of the cruise. Daily updated altimetry, SST and ocean color imagery provided essential basin scale views of the study area for understanding physics and phytoplankton variability. Ocean color data from NASA's MODIS Aqua, VIIRS and JPSS were used to define PIC concentration and chlorophyll concentration regionally and to plan cruise tracks. Parallel space-based SST measurements were made along with the ocean color measurements. These SST data helped to link specific water mass information to the various phytoplankton features. However, extensive cloudiness made for significant gaps in coverage of surface PIC and chlorophyll concentrations for weeks at a time. Fortunately, the altimetry data are not compromised by cloudiness and they provided reliable day-to-day positions of sea surface dynamic height features associated with prior ocean color images.

On days with acceptable weather and sky conditions when the ship was stopped near Local Apparent Noon we deployed an Ocean Color Profiler (Satlantic) over the fantail to characterize the upwelling and downwelling light field in the surface 100m of the water column. We were able to perform 11 of these profiles over the course of the cruise.

There were other observations that were made real-time aboard ship for validation. For each productivity cast, two filtrations were performed with water from the surface and fluorescence maximum to provide semi-quantitative microscope analysis using the filter-freeze-transfer (FFT) method (Hewes and Holm-Hansen, 1983) to concentrate phytoplankton and provide real time semi-quantitative estimates of species abundance. Moreover, a plankton net was mounted on the CTD periodically to provide vertical net hauls of material to compare with DAVPR images. Surface underway samples were performed every three hours during extended transit periods and were processed for DIC/Total Alkalinity, nutrient concentrations (nitrate, nitrite, phosphate, ammonium and silicate), POC, PIC, biogenic silica (BSi), extracted chlorophyll, coccolithophore counts, and FlowCAM counts.

Along the meridional transect, 10 profiling floats were deployed for the SOCCOM program (Lynne Talley, SIO) and another 10 profiling floats were deployed for NOAA (Elizabeth Steffen, PMEL). Those floats along with their deployment locations are identified in Table 1.

Table 1- Profiling floats deployed, event numbers (GMT year, month, day.time: YYYYMMDD.TTTT) and locations.

Event #	Instrument	Station	Cast/action	Lat (dec.deg) [+N;-S]	Lon(dec.deg)[+E;-W]	Deployed for
20201231.0833	PMEL NAVIS Argo Drifter #F0999	N/A	N/A	3.997	-155.236	NOAA PMEL/Steffen
20201231.1956	PMEL NAVIS Argo Drifter #F0990	N/A	N/A	2.011	-154.940	NOAA PMEL/Steffen
20210101.0702	PMEL NAVIS Argo Drifter #F0984	N/A	N/A	0.002	-154.642	NOAA PMEL/Steffen
20210101.1742	PMEL NAVIS Argo Drifter #F0997	N/A	N/A	-1.998	-154.344	NOAA PMEL/Steffen
20210102.0402	PMEL NAVIS Argo Drifter #F0986	N/A	N/A	-4.002	-154.037	NOAA PMEL/Steffen
20210108.0152	SOCOMM 19018	1		-29.997	-149.998	SOCCOM/Talley-SIO
20210110.0209	Navis 0887	11	3	-35.000	149.900	SOCCOM/Talley-SIO
20210111.0317	Navis 1115	17	2	-38.000	-150.000	SOCCOM/Talley-SIO
20210112.1417	Navis Float #1204	25	3	-42.003	-150.000	SOCCOM/Talley-SIO
20210112.2320	Deep Solo Float #12041	27	3	-43.001	-150.004	NOAA PMEL/Steffen
20210114.0740	Apex float 19072	33	3	-45.998	-149.999	SOCCOM/Talley-SIO
20210116.2026	Navis float F1205	37	3	-47.672	-150.003	SOCCOM/Talley-SIO
20210117.1815	Apex float 8690/17328	43	3	-49.679	-149.987	SOCCOM/Talley-SIO
20210118.2041	Deploy Apex Float 19085	45	3	-53.002	-149.986	SOCCOM/Talley-SIO
20210119.1846	Deep Solo Float #12040	51	3	-51.000	-149.999	NOAA PMEL/Steffen
20210124.1740	Apex float #19327/8917	63	3	-59.993	-150.000	SOCCOM/Talley-SIO
20210126.0546	APEX float #19067	73	3	-56.670	-149.998	SOCCOM/Talley-SIO
20210209.0026	Navis F0998	101	2	-43.864	-150.001	NOAA PMEL/Steffen
20210209.1755	Navis F0991	N/A	N/A	-40.996	-150.326	NOAA PMEL/Steffen
20210210.0920	Navis F0985	N/A	N/A	-38.001	-150.755	NOAA PMEL/Steffen

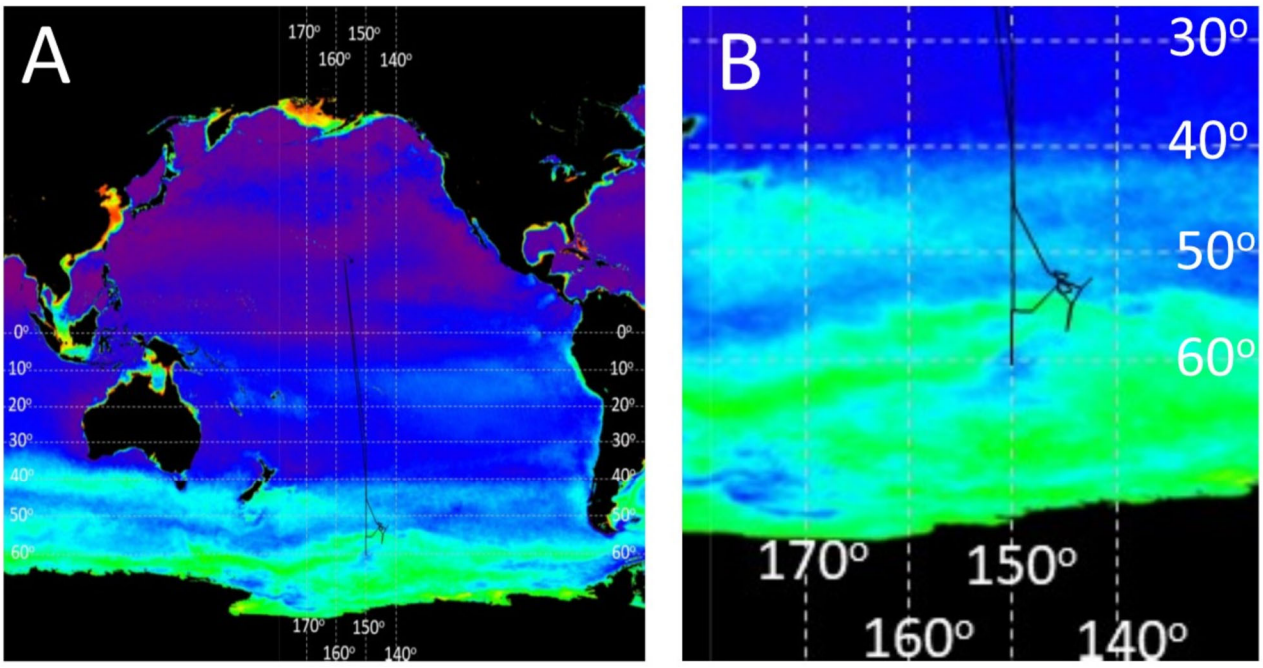

Figure 5-Nineteen-year PIC climatology from MODIS Aqua ocean color database (NASA Goddard Space-Flight Center). Revelle#2004 cruise track overlaid onto climatology (black line). A) Large-scale view showing the entire Pacific Basin and the cruise track (black line). B) Enlarged view showing sample area between 30°S-60°S centered along 150°W.

4. Cruise Track Relative to Remote Sensing Climatology

The ship's 12,500 nautical mile cruise track is shown superimposed over the 19-year austral-summer climatology of NASA's Aqua PIC determination using the merged two-band/three-band algorithm (Balch et al., 2005; Gordon et al., 2001) (Fig. 5). The results show that the ship traversed through the expected high-reflectance features over the course of the trip: a) the Great Calcite Belt (before and after the bloom formation), b) regions of high-reflectance Southern Ocean features associated with the Pacific Antarctic Ridge and Udintsev Fracture Zone (both Polar Front and South Antarctic Circumpolar Current boundaries), meanders and eddies. The cause of this high reflectance has never been known due to lack of shipboard validation data but has long been suspected to not be caused by coccolithophores since the water temperatures are so cold (<=2°C). Results from this cruise suggest that indeed the PIC concentrations were low, but we must await processing of our analytical filters for PIC to know for sure. Certainly, the FFT polarized microscopy performed on this trip suggest that the high reflectance was NOT due to coccolithophores.

5. Detailed Leg Summary

Leg 1: Departure from Honolulu, HI to 30ºS x 150ºW; Dec 26, 2020-7 January, 2021 (Days 1-13)

During this leg of the voyage, various test deployments were performed for the VPR, trace-metal/Niskin-X sampling bottles and Ocean Color Profiler (OCP), along with deployment of five NOAA Navis Argo profiling floats, one each at 4ºN, 2ºN, equator, 2ºS and 4ºS along the great circle route between Honolulu and 30ºS x 150ºW. The surface underway system was started at 27º 23'S x 150º 34'W, in international waters at 1022h GMT, on 7 January 2021.

Leg 2: Meridional Transect along 150ºW (half-degree spacing) 7-14 January 2021; (Days 13-20)

During this leg of the cruise, we performed a total of 38 CTD casts located at each half degree of latitude along the 150ºW meridian. These consisted of (1) 18 CTD casts with full water sampling, double tripping 10L Niskin bottles between the 1000m and the surface, (2) 18 trip-on-fly CTD casts [with 24 depths tripped "on the fly" as they pass the following 24 depth targets: 1000m, 900m, 800m, 700m,600m 500m, 450m, 400m, 350m, 300m, 250m, 200m, 150m, 120m, 110m, 100m, 90m, 80m, 70m, 60m, 50m, 40m, 25m, 5m] and (3) two deep casts to within several hundred meters of the seafloor. Of the 18 full water CTD casts, seven qualified as morning productivity casts, sampling from six specific light depths between the surface and the base of the euphotic zone. Following each productivity cast, a trace-metal clean cast was performed using nine Niskin-X bottles over the upper 1000m depth. Eleven light casts were performed daily with the OCP during local apparent noon during this leg.

Leg 3: Enhanced Meridional Transect (1/3 degree spacing/VPR towing); 14-25 January 2021; (Days 20-31)

During this leg, we began the enhanced meridional transect in order to sample the Subantarctic, Polar and Southern Antarctic Circumpolar frontal regions. This involved three "zig-zag" operations over each 180 or 240 nautical mile stretch (333-445km): a) towing the VPR the entire length in one direction, b) performing a hydrographic survey at 20 nautical mile resolution (37km) and 1000m CTDs in the opposite direction and c) steaming to the beginning of the next segment. This sample design allowed us flexibility to run the VPR tow during the best weather periods. During this leg of the expedition, we performed four 18-27h VPR tows, 18 full CTD water stations (including eight productivity casts), 18 alternating Trip-on-fly CTD stations. We also performed eight Niskin-X trace-metal casts, seven OCP casts and two carboy experiments.

Leg 4: Eddy A survey 25-31 January 2021; (Days 31- 36)

This leg included the eastward departure from the 150ºW meridian towing the VPR 65h, crossing the Polar Front for a second time on our way to the cyclonic Eddy A. The survey of Eddy A involved two radial surveys with the VPR along with a 4h search near the eddy center

for the precise location of the eddy center. The VPR was then towed for the remainder of the two-radial survey after which the VPR was recovered. Two hydrographic sections of five stations each, separated by 25 miles (46km) were back-tracked along the previous VPR survey. This involved six full water stations (including two productivity CTDs) and 4 trip-on-fly stations. Two Niskin-X casts were performed and one Big Jon deployment to collect water for the next carboy experiment at station 82, at eddy center. On day 36 (30 January) we encountered severe weather, so the ship had to heave-to for ~12h as we waited for the bad conditions to subside.

Leg 5: Frontal survey over Udintsev Fracture Zone 31 January- 2 February 2021; (Days 36-39)

We departed eddy A for the third crossing of the Polar Front ("cross-frontal survey). This began with a 12h VPR tow over the 120 nautical mile (222km) length of the feature, followed by a 7 CTD hydrographic section (1000m depth), alternating full CTD stations (including a dawn productivity cast) and trip-on-fly stations, separated by 20nmiles (37km) each. There was one Niskin-X cast at the same station as the productivity cast (station 87). There was a mid-day OCP cast at station 89.

Leg 6: Eddy C survey; 2-3 February 2021; (Days 39-40)

Following the cross-frontal survey we steamed directly to Eddy C, a cyclonic eddy centered at 54º 4.8'S x 138º 1.5'W, with an highly-reflective inner core, which we observed in multiple ocean color images, as recently as 20 January. Time only permitted us to do one 25.5h VPR radial survey across Eddy C followed by one hydrographic section in the reciprocal direction: three full CTD stations (including one productivity station) and two trip-on-fly stations separated by 25 nautical miles (46km).

Leg 7: Revisit Eddy A and SubAntarctic Front Meander; 3-5 February 2021; (Days 40-42)

Following our visit to Eddy C, the ship, with VPR in tow, headed for a repeat section through Eddy A on its way to a meander of the Subantarctic Front, which had previously been observed as a bright, PIC-rich feature in satellite imagery. We steamed across the entire meander, then returned to a station in the middle of the feature located at 44º52' x 150ºW, for a series of casts (Niskin-X cast, full CTD/Productivity cast, and Big Jon sampling for the fourth carboy experiment).

Leg 8: Coccolithophore Bloom Survey; 5-8 February 2021; (Days 42-45)

We left the Subantarctic Front and headed for 47ºS x 150ºW: a location that we had sampled along the meridional transect some 23d earlier. For this 390 nautical mile (723km) transit which lasted 35h, we had the surface underway sampling system running as well as we were taking underway samples every three hours. On 6 February, at 0640GMT, at a position of 50º 22'S x 147º 12'W we entered the southern end of a dense coccolithophore bloom of mostly *Emiliania huxleyi* (as based on our FFT polarized compound microscopy aboard ship), with significantly elevated b_b' values exceeding $2E^{-3}$ m^{-1}. Up to this point, these were the highest b_b' values

observed for the entire trip. We remained in this feature for the next 232 miles (430km) until we arrived at 47ºS x 150ºW, then an additional 250 nautical miles (463km) to the north (for 482 miles total transit (or 890km)). We then steamed 10 miles (18.5km) further north out of the feature until we reached 43º11'S x 150ºW. At this position, we deployed the VPR and steamed a reciprocal course to the south along 150ºW, back into the bloom for a 100 mile VPR tow, recovering the VPR at 44º52' x 150ºW at 1130hGMT on 8 February. We then proceeded with a six-station hydrographic survey to the north (four full-water CTD stations and two trip-on-fly CTD stations, spaced every 20miles (37km) and ending at 43º 11.0'S x 150ºW). This hydrographic section was completed by 2330h local on 8 February (0900h, 9 February GMT), after which we stopped all VPR and CTD sampling for the remainder of the cruise.

Leg 9: Northbound underway survey 8-12 February 2021; (Days 45-49)

The last science leg for the trip was the collection of underway surface data as the ship headed along the great circle route towards Honolulu (see section 3 above). We also deployed an additional three profiling floats for NOAA/PMEL along the route at 44ºS, 41ºS and 38ºS. (See Table 1 for precise locations). All science sampling was stopped at 26ºS x 152º 19.5'W, once *R/V Revelle* left international waters.

Leg 10: Transit to Honolulu; 11-23 February 2021; (Days 48-60)

All science sampling was stopped during this segment of the cruise

6. Ship's data

The R/V Revelle's underway surface sampling system collects a huge amount of data, beyond the scope of this report. However, some of the data sets gathered routinely during the cruise were: ADCP current velocity profiles, bathymetric measurements using the ship's multibeam system, meteorological data and underway surface water properties (e.g. temperature, salinity, fluorescence, O_2 and pCO_2).

Acknowledgements

We would like to thank Captain Wes Hill, officers and crew of the *R/V Roger Revelle*. The Covid pandemic presented *major* challenges for this cruise (both at the beginning [dealing with pre-cruise quarantine,] and at the end, when French Polynesia shut down Tahiti for the disembarkation of scientists). The fact that we were still able to accomplish the original objectives of this trip is a real testimonial to the seamanship and "can-do" attitude of the ship's crew. The Scripps marine technicians that accompanied us (Matt Durham and Charlie Brooks) provided excellent oversight of all deck operations and utmost safety at all times, Scripps ODF chemists Melissa Miller and Megan Roadman were indispensable for the accurate measurements of oxygen, nutrients and salts. Norman Kuring (NASA Goddard Space Flight Center, Greenbelt, MD) provided us with daily basin-scale MODIS imagery before, during and after RR#2004. This imagery was instrumental to help us plan our cruise track. We are also grateful to Olga Kosnyrev (WHOI) who provided mapped images of PIC, chlorophyll, and absolute dynamic topography in real time. All the members of the ship operations office at the Scripps Inst. of

Oceanography, UCSD are to be thanked for the immense organizational and logistical tasks associated with the planning a cruise of this size during a global pandemic (Bruce Applegate, Steven Kelty, Andrew Brighton, Hannah DeLapp, Lee Ellett, Katelin Pedersen, and others too numerous to mention here). Without their help, we could have never completed this expedition. Support of the National Science Foundation for this project is gratefully appreciated. We particularly acknowledge Hedy Edmunds and Rose Dufour, who were instrumental in getting our previously-scheduled cruise moved from the Indian Ocean to the Southwest Pacific after the onset of the pandemic, as well as helping with the myriad of logistical hurdles for a cruise of this magnitude, imposed by covid.

Science party participants

Table 2- Science party participants of R/V Thompson RR#2004 and their affiliations/roles.

Number	Title	First Name	Last Name	Institution	Position
1	Mr.	Phil	Alatalo	Woods Hole Oceanographic Inst. Woods Hole, MA, USA	Research Associate
2	Dr.	William	Balch	Bigelow Laboratory for Ocean Sciences, East Boothbay, ME, USA	Chief Scientist/ Principal Investigator
3	Mr.	Bruce	Bowler	Bigelow Laboratory for Ocean Sciences, East Boothbay, ME, USA	Senior Res. Assoc.
4	Mr.	Charles	Brookes	Scripps Inst. Oceanography	Marine Technician
5	Mr.	David	Drapeau	Bigelow Laboratory for Ocean Sciences, East Boothbay, ME, USA	Senior Res. Assoc.
6	Mr.	Matthew	Durham	Scripps Inst. Oceanography	Marine Res. Tech
7	Mr.	Matthew	Enright	Bermuda Inst. Of Ocean Sciences, Prince George, Bermuda	Research Specialist
8	Ms	Rebecca	Garley	Bermuda Inst. Of Ocean Sciences, Prince George, Bermuda	Senior Res. Assoc.
9	Mr.	Benjamin	Gustafson	Colby College	Undergrad Student
10	Ms	Lauren	Hearn	Florida State University, Tallahassee	Undergrad Student
11	Mr.	Andrew	Hirzel	Woods Hole Oceanographic Inst. Woods Hole, MA, USA	Graduate Student
12	Dr.	Dennis	McGillicuddy	Woods Hole Oceanographic Inst. Woods Hole, MA, USA	Principal Investigator
13	Ms.	Julia	Middleton	Woods Hole Oceanographic Inst. Woods Hole, MA, USA	Graduate Student
14	Ms.	Melissa	Miller	Scripps Inst. Oceanography	Marine Res. Tech
15	Dr.	Peter	Morton	Florida State University, Tallahassee	Principal Investigator
16	Dr.	Hilde	Oliver	Woods Hole Oceanographic Inst. Woods Hole, MA, USA	Post-doc
17	Ms	Sunny	Pinkham	Bigelow Laboratory for Ocean Sciences, East Boothbay, ME, USA	Technician
18	Ms.	Hannah	Primiano	Drew University	Undergrad Student
19	Ms	Megan	Roadman	Scripps Inst. Oceanography	Marine Technician
20	Ms	Logan	Tegler	Woods Hole Oceanographic Inst. Woods Hole, MA, USA	graduate student
21	Mr.	Clayton	Tompkins	Scripps Inst. Oceanography	Computer tech
22	Dr.	Giuliana	Viglione	Freelance Science Writer	Scientific Writer

Science party photo

Fig 6- Science party for RR#2004 (left to right): Phil Alitalo (WHOI), Hilde Oliver (WHOI), Megan Roadman (SIO), Andrew Hirzel (WHOI), Sunny Pinkham (BLOS), Matt Enright (BIOS), William Balch (BLOS), Dennis McGillicuddy (WHOI), Mellisa Miller (SIO), Peter Morton (FSU), Giliana Viglione (Freelance Writer), Rebecca Garley (BIOS), Hannah Primiano (BLOS REU), Logan Tegler (WHOI), Matt Durham (SIO), David Drapeau (BLOS), Ben Gustafson (Bigelow REU/Colby), Bruce Bowler (BLOS), Julia Middleton (WHOI, Lauren Hearn (FSU), Charlie Brooks (SIO).

Summary of Deck Operations

Table 3-Summary of cruise events during RR#2004

Deck operation/analysis	Number or duration of operations (days)
CTD full-water casts	55
CTD "Trip-on-fly" casts	48
CTD Deep casts	3
Trace Metal Niskin-X casts	21
VPR tows	13
D-VPR casts (to within 100m of ocean bottom)	94
D-VPR net hauls	54
Surface Trace Metal-Clean collections for experiments	5
Number 24h Productivity/calcification incubations	21
Underway surface samples for Chl, POC, PIC, BSi, FlowCAM, coccolith microscopy	45
Surface underway nutrient analyses	43
Surface underway DIC measurements	44
Filter-Freeze-Transfer microscopy samples viewed at sea	49
Carboy experiments (4day)	5
Days continuous underway inherent optical property measurements (b_{bp531}, $b_b'_{531}$, $a(\lambda)$, $c(\lambda)$)	37
Days continuous underway apparent optical property measurements (bow hyperspectral radiometry)	36
Days continuous underway total alkalinity and pCO2 measurements	45
Number CTD nutrient samples processed (not including one mis-sampled)	1140
Number Trace Metals nutrient samples processed	173
Number incubation nutrient samples processed	224
Number CTD oxygen samples processed (not including 3 lost due to operator error)	1138
Number CTD salt samples processed (not including one mis-sampled)	1140
Number Trace Metals salinity samples processed	173
Number incubation salinity samples processed	23
Number DIC/TA CTD samples processed	1102
Number DIC/TA incubation exp. samples processed	189
Number chlorophyll samples filtered/processed	1021
Number biogenic silica samples filtered for analysis ashore	725
Number PIC samples filtered for analysis ashore	725
Number POC samples filtered for analysis ashore	725
Number of coccolithophore count samples for analysis ashore	725
Number of CFC (Freon) samples for analysis ashore	277
Number of DNA samples filtered (to be processed ashore)	130
Number of FlowCAM samples processed (begun at sea with more analysis ashore)	725
Days of remote sensing imagery processed for PIC, chlorophyll and SST	79
Number of trace metal samples for analysis ashore	674
XBT casts	56
Number of HPLC samples (from SOCCOM stations)	30
Number of pH samples (from SOCCOM stations)	186
Ocean Color Profiler (OCP) profiles	11
SOCCOM profiling floats deployed	10
NOAA profiling floats deployed (Argo and Deep Solo)	10
Number Cd incubation/biomass decay studies	4
Number of Ba incubation/barite formation studies	4
Number of dissolved barium samples taken	172
Number productivity casts	21
Posts on Bigelow blog (by Giuliana Viglione)	18
Tweets using #SAMW21 hashtag as of 20 February (Giuliana's professional account)	36
Impressions on #SAMW21 tweets as of 20 February	45,000
Comments on SAMW21 Ask Me Anything	75
SOCCOM blog posts as of Feb 12, 2021 (by Melissa Miller)	7
hits on SOCCOM blog posts as of Feb 14, 2021	740
posts to Twitter @RVRogerRevelle as of Feb 12, 2021 (by Melissa Miller)	34

References

Balch, W. M., Bates, N. R., Lam, P. J., Twining, B. S., Rosengard, S. Z., Bowler, B. C., Drapeau, D. T., Garley, R., Lubelczyk, L., Mitchell, C. E., and Rauschenberg, S., 2016, Factors regulating the Great Calcite Belt in the Southern Ocean and its biogeochemical significance: Global Biogeochemical Cycles p. doi: 10.1002/2016GB005414.

Balch, W. M., and Drapeau, D. T., 2004, Backscattering by Coccolithophorids and Coccoliths: Sample Preparation, Measurement and Analysis Protocols, *in* Mueller, J. L., Fargion, G. S., and McClain, C. R., eds., Ocean Optics Protocols For Satellite Ocean Color Sensor Validation, Revision 5: Biogeochemical and Bio-Optical Measurements and Data Analysis Protocols, Volume 5, Chapter 4: Greenbelt, Maryland, National Aeronautical and Space administration, Goddard Space Flight Space Center, p. 27-36.

Balch, W. M., Gordon, H. R., Bowler, B. C., Drapeau, D. T., and Booth, E. S., 2005, Calcium carbonate budgets in the surface global ocean based on MODIS data: Journal of Geophysical Research Oceans, v. 110, no. C7, p. C07001, doi:07010.01029/02004JC002560.

Cerovečki, I., Talley, L. D., Mazloff, M. R., and Maze, G., 2013, Subantarctic mode water formation, destruction, and export in the eddy-permitting southern ocean state estimate: Journal of Physical Oceanography, v. 43, no. 7, p. 1485-1511.

Fine, R. A., 1993, Circulation of Antarctic intermediate water in the South Indian Ocean: Deep-Sea Research Part I, v. 40, no. 10, p. 2021-2042.

-, 2011, Observations of CFCs and SF 6 as ocean tracers: Annual Review of Marine Science, v. 3, p. 173-195.

Fine, R. A., Rhein, M., and Andrié, C., 2002, Using a CFC effective age to estimate propagation and storage of climate anomalies in the deep western North Atlantic Ocean: Geophysical Research Letters, v. 29, no. 24, p. 80-81.

Fine, R. A., Smethie, W. M., Jr., Bullister, J. L., Rhein, M., Min, D. H., Warner, M. J., Poisson, A., and Weiss, R. F., 2008, Decadal ventilation and mixing of Indian Ocean waters: Deep-Sea Research Part I: Oceanographic Research Papers, v. 55, no. 1, p. 20-37.

Gordon, H. R., Boynton, G. C., Balch, W. M., Groom, S. B., Harbour, D. S., and Smyth, T. J., 2001, Retrieval of coccolithophore calcite concentration from SeaWiFS imagery: Geochemical Research Letters, v. 28, no. 8, p. 1587-1590.

Hewes, C. D., and Holm-Hansen, O., 1983, A method for recovering nanoplankton from filters for identification with the microscope: The filter-transfer-freeze (FTF) technique.: Limnology and Oceanography, v. 28, p. 389-394.

Mueller, J. L., Morel, A., Frouin, R., Davis, C., Arnone, R., Carder, K., Lee, Z. P., Steward, R. G., Hooker, S. B., Mobley, C. D., McLean, S., Holben, B., Miller, M., Pietras, C., Knobelspiesse, K. D., Fargion, G. S., Porter, J., and Voss, K., 2003, Ocean optics protocols for satellite ocean color sensor validation, Revision 4, Volume III: Radiometric measurements and data analysis protocols Greenbelt, MD, Goddard Space Flight Center, p. 78.

Patterson, S. L., and Whitworth, T., 1989, Chapter 3 Physical Oceanography, *in* Glasby, G. P., ed., Antarctic Sector of the Pacific: New York, Elsevier, p. 55-93.

Sarmiento, J. L., Gruber, N., Brzezinski, M. A., and Dunne, J. P., 2004, High-latitude controls of thermocline nutrients and low latitude biological productivity: Nature, v. 427, p. 56-60.

RR2004 VPR Team Cruise Report
Draft February 22, 2020

Dennis McGillicuddy
Phil Alatalo
Andrew Hirzel
Hilde Oliver

Shoreside team: Olga Kosnyrev, Valery Kosnyrev, Josh Eaton, Fred Thwaites

Contents

Figures

1. Introduction

The SAMW 2021 cruise was redirected from the South Indian Ocean to the Pacific Sector of the Southern Ocean. The pre-cruise planning process included extensive deliberations on the precise location for the operational area, and we settled on the 150W meridian where prior measurements along the P16 line indicate ample volume of SAMW in this region (Figure 1). Patterson and Whitworth (1989) provide an excellent review of the descriptive physical oceanography of the region; locations of the primary fronts are described in Orsi et al. (1995). Extensive biogeochemical measurements were carried out along 170W as part of the JGOFS AESOPS Program (Anderson and Smith 2001; Smith and Anderson 2003; Smith et al. 2000)

Summertime climatologies of chlorophyll and particulate inorganic carbon (PIC) show similar patterns, with relatively modest expressions of the Great Calcite Belt (GCB; Balch et al. 2016) in the 43-55S latitude band (Figure 2). Farther south, filaments of enhanced chlorophyll and PIC correspond to fronts in Mean Dynamic Topography (MDT). Topographic steering by the Pacific-Antarctic Ridge (Figure 3) causes a confluence of the Subantarctic, Polar, and Southern Antarctic Circumpolar Current fronts (SAF, PF, SACCF; Orsi et al. 1995; Patterson and Whitworth 1989). Seasonal climatologies of PIC show distinctive variations in the 45-67S latitude band (Figure 4).

The overall cruise plan consisted of (1) a meridional transect from 30-60S along 150W, supplemented by VPR tows from 47-60S (**Section 2**), (2) Mesoscale surveys of fronts and eddies of interest (**Section 3**), and revisitation of a portion of the 150W transect, during which a coccolithophore bloom was observed (**Section 4**). Distribution of an unexpected planktonic "spindle" is described in **Section 5**. **Appendix 1** provides information on evaluation and calibration of CTD conductivity and oxygen sensors.

Plankton were sampled using three distinct methods: high-speed video sampling using the towed VPRII platform, self-recording video using the DAVPR on the CTD rosette for discreet casts, and a small 150um plankton net mounted on the rosette that was used opportunistically. Overall impressions for this cruise were similar to the South Indian Ocean mission last year, with regards to the lack of zooplankton in the sub-tropical regions. Initially we were getting very low image counts in both optical instruments and plankton hauls were very meager. As we approached the 60S on the meridional transect, the number of images captured increased dramatically, particularly as we passed through the various frontal regions further south.

Diagnostic plankton species are quite useful to validate water masses. Given the remote area, lack of sampling, and confluence of distinct water masses, we were especially cognizant of distinct particles that either dominated or were present in various regions. For this cruise, we were surprised to see great numbers of very small pteropods, polychaete worms, and unusual diatom formations several times. While limacinid pteropods are not unusual, they occurred sometimes in great numbers often together with worms and an unidentified organism, which we have tentatively identified as *Thalassiothrix antarctica* colony (**Section 5**). While forams and phaeodarians were fairly common, acantharian radiolarians formed dense patches in the lower salinity water of the meander in the northern section of the meridional transect. The colonial alga *Phaeocystis antarctica* occurred briefly several times, presumably indicating water from the

SubAntarctic Front. Large diatom mats were present in high abundance at the Polar Front and swamped the VPRII camera with images. These mats were often found at depth with the DAVPR, indicating that they were sinking out of the system. Regarding larger taxa such as krill, gelatinous predators, and fish larvae, these organisms were present, but never in huge abundances. Much more often, we were surprised by the lack of organisms; our last VPRII tow netted a record low of images for a 13-hour tow, while we towed through the coccolithophore bloom from 43-50S (**Section 4**).

Use of the Convolutional Neural Network (CNN) approach to image classification provided for some real-time mapping of selected taxa, using CNN classifiers trained on images from prior cruises. Initial vetting of the CNN results, along with preliminary analysis of new taxa to be added to the classifier, is presented in **Appendix 2**. **Appendix 3** contains an atlas of the hydrographic, bio-optical, and taxonomic plots for all VPR tows combined.

Note: higher resolution figures are available in the accompanying powerpoint file.

2. Meridional transect

Seventy-four CTD casts spanning from 30-60 S were conducted from 8 to 26 January 2021 along the 150 W meridian. The transect was divided into two sections: a northern "classic meridional transect" extending from 30-47 S and a southern "enhanced meridional transect" extending from 47-60 S. "Classic" meridional transect casts (Casts S1 to S35) were spaced 0.5 degrees apart, while "enhanced" transect casts (Casts S35 to S74) were spaced 1/3 degrees apart, and were complemented by four VPR II tows for high-resolution hydrographic and bio-optical surveys of the surface ocean.

Over the span of the meridional transect, the surface ocean became substantially cooler, fresher, and denser (Figure 5, Figure 6, Figure 7). Four major oceanographic fronts were crossed: 1) the STF at ~36 – 39 S (salinity at 100 m drops from 35.0 to 34.6), 2) the SAF at ~53.0 – 53.5 S (where temperature at 400 m dips below 5ºC and salinity at 300 m becomes fresher than 34.2), 3) the PF at ~ 55.5 S (where the temperature minimum rises above 200 m), and 4) the SACCF at ~57.5 (where the temperature minimum above 150 m goes below 0ºC and the salinity maximum below 800 m rises above 34.73) (Orsi et al. 1995). SAMW (defined where 26.5 kg m^{-3} < σ_θ < 27.1 kg m^{-3}) was present at all stations north of the SACCF; casts south of 37.5 S were extended from 900 m to 1000 m to better encapsulate the 27.1 kg m^{-3} isopycnal. SAMW was present at the surface between the SAF and SACCF.

Chlorophyll concentrations estimated from florescence varied widely over the span of the meridional transect (Figure 8). The Subtropical Zone (STZ, north of the STF) was characterized by deep (> 100 m), low magnitude (< 1 µg/L) chlorophyll maxima. South of 42 S, higher chlorophyll concentrations were present in the upper 100 m, with maximum chlorophyll concentrations generally increasing southward. The highest chlorophyll concentrations measured along the meridional transect (> 8 µg/L) were observed just north of the PF. High (> 3 µg/L) concentrations were also measured in the vicinity of the SACCF, before dropping off at the southern terminus of the transect.

While the oxygen saturation of the upper water column was consistently high through the meridional transect, oxygen saturation below 150 m varied substantially (Figure 9). In the subtropical zone, the several-hundred-meter thick SAMW layer was characterized by slightly elevated oxygen saturation relative to the overlying and underlying waters. South of the STF and north of the PF, oxygen was highly saturated (> 90%) from the surface down to deeper than 300 m, with the σ_θ = 27.1 kg m^{-3} isopycnal (the densest SAMW) bounding the deepest high-oxygen waters. This deeper, highly oxygenated water disappears with the outcropping of the σ_θ = 27.1 kg m^{-3} isopycnal at ~ 57.5 S. The denser waters that then extend to ~150 m south of the σ_θ = 27.1 kg m^{-3} isopycnal outcropping have a much lower oxygen saturation of ~50-60%, with an oxygen saturation minimum between the σ_θ = 27.6 kg m^{-3} and the σ_θ = 27.7 kg m^{-3} isopycnal. With the sub-zero temperatures characterizing the southern transect terminus, these casts were the site of both the highest and lowest oxygen concentrations observed during the entire meridional transect.

Along the "enhanced" transect south of 47 S, VPR Tows 2, 3, 4, and 5 ran from 47 S to 60 S along the 150 W meridian to provide higher resolution of the surface ocean in that interval (Figure 10, Figure 11, Figure 12, Figure 13). Pairing the VPR tows across the dynamic frontal regions with the CTD cast data demonstrates how submesoscale variability in temperature, salinity, density, and fluorescence measured in the top 100-120 m relates to deeper mesoscale ocean variability. As in the CTD data, the largest chlorophyll concentrations measured by the VPR were captured between the SAF and the PF, with the highest chlorophyll concentrations closely following density surfaces (Figure 13).

Nutrient (nitrate, phosphate, nitrite, ammonium, silicate) data across the meridional transect were collected, compiled, and made available by the Scripps ODF team (Figure 14). Nitrate and phosphate were depleted north of 42 S, with nitrate drawn down to the approximate detection limit. At 42 S (Station 25), surface nitrate concentrations rise to ~ 1 μM, and the chlorophyll maximum was 35 m below the sea surface, shallower than the deeper (90 m or deeper) chlorophyll maxima for stations further north (Figure 8). Moving southward, all measured nutrients typically increased. An exception was surface silicate, which was somewhat patchier than other macronutrients. While surface silicate was depleted to < 1 μM over much of the STZ, it was also drawn down north of the SAF and north of the PF. We calculated Silicate* (Si*, silicate – nitrate) over the entirety of the meridional transect to assess the relative drawdown of silicate relative to nitrate. As demonstrated in Sarmiento et al. (2004), the SAMW layer was distinguished from overlying and underlying waters by its comparatively low Si* values (~14 μM). The lowest Si* values observed over the meridional transect (< -20 μM) were observed near the PF, the location where the highest chlorophyll concentrations were observed (Figure 8). South of the PF, Si and Si* values rapidly rise.

Carbonate system data for the meridional transect were collected and provided by the BIOS team aboard (Figure 15). Throughout the transect, the SAMW layer had higher DIC than less dense waters and lower DIC than denser waters. Total alkalinity (TALK) was low in the surface waters north of the STF and high for waters denser than σ_θ = 27.1 kg m^{-3}, with low TALK found in the subsurface SAMW in the Subantarctic Zone corresponding to high oxygen saturation. Upper water column pCO_2 was lowest where the largest chlorophyll concentrations were observed: in the region north of the SAF extending to the SACCF, with the lowest pCO2 observed north of

the PF. Below the surface in the SAMW layer north of 42 S, low pCO_2 was associated with enhanced oxygen saturation (like TALK). This deeper depletion of pCO_2 and TALK was not observed in waters denser than $\sigma_\theta = 27.1$ kg m^{-3}.

Nutrient and other water mass properties vary systematically in temperature-salinity space (Figure 16, Figure 17). Several water masses were captured over the transect: SAMW (26.5 kg $m^{-3} < \sigma_\theta$ 27.1 kg m^{-3}), warm and salty Subtropical Surface Water (STSW) north of ~39 S, slightly fresher and less warm Subantarctic Surface Water (SASW) between the SAF and the STF, cold and fresh Antarctic Intermediate Water (AAIW) and Antarctic Surface Water (AASW), and slightly wamer-and-saltier-than-AAIW upper circumpolar deep water (UCDW). North of 42 S, temperature is the primary control on density, and the highest oxygen saturations are associated with the warmest waters. Here, chlorophyll concentrations are low, and nitrate, silicate, and Si* are all near zero. South of 42S, the SAMW layer moves closer to the surface, chlorophyll concentrations increase, and surface nitrate concentrations increase while surface silicate concentrations remain low, and surface Si* becomes negative. Both AAIW and UCDW had high nitrate and silicate concentrations, and positive Si*.

Despite overall consistently cloudy conditions, the enhanced portion of the meridional transect crossed several distinct PIC (Figure 18) and chlorophyll (Figure 19) features detected by satellite ocean color. The northern portion of VPR 2 (47 to 50 S) traversed a low-chlorophyll, high PIC eddy (Figure 20, Figure 21); satellite measurements of absolute dynamic topography (ADT) show cyclonic “Eddy 1” at ~47.5 S (Figure 22). VPR bio-optical measurements confirmed Eddy 1 as a region of low chlorophyll and high backscatter (b_b) down to ~60 m (Figure 20). Farther south, satellite ADT also revealed a meander of the ACC at ~50.25 S, and anticyclonic “Eddy 2” at ~51.6 S depressing the main pycnocline (Figure 23, Figure 24). VPR 4 (53 to 56 S) also crossed two bands of high PIC and high chlorophyll measured by satellites at ~53.5 S and ~55.5 S, which were both captured by the VPR fluorescence and b_b measurements (Figure 25). The dropping sea surface height shown by satellite ADT and rapid currents measured by the ship ADCP suggest that VPR 4 was towed through the ACC (Figure 26).

The VPR was towed across three major oceanographic fronts as determined by the CTD meridional transect profiles: 1) the SAF at ~53.0 – 53.5 S, 2) the PF at ~ 55.5 S, and 3) the SACCF at ~57.5 S (Figure 20). Between the SAF and the SACCF, isopycnals are sloped; north and south of the frontal region isopycnals are relatively flat. Upon encountering the SAF, the entire water column freshened, and both chlorophyll and b_b increased. Chlorophyll and b_b were also enhanced on both sides of the PF, and on the southern side of the SACCF. The highest b_b of the VPR enhanced transect was recorded at the PF, and the highest chlorophyll was measured just north of the PF.

Results from the individual VPR tows comprising the enhanced meridional transect (VPR 2-5) will now be presented in detail.

VPR 2 crossed through Eddy 1 and clipped the northeast flank of a meander in the SAF (Figure 21, Figure 22). Selected taxonomic distributions (Figure 23) reveal a patch of acantharians associated with a warm surface layer in the meander spanning 49.5 – 49.8S. Diatoms were distributed throughout the tow, with peak abundances in between Eddy 1 and the meander.

Calanoid copepods were present within Eddy 1, and observed only occasionally in waters south of 48.4S.

VPR 3 extended the sampling of a meander in the SAF initiated in VPR 2, passed through Eddy 2, and then crossed the SAF itself (Figure 24, Figure 25). Another patch of acantharians was observed at the edge of the SAF; diatoms, marine snow, and copepods were abundant in a band centered on 51 S between the meander and Eddy 2 (Figure 26).

VPR 4 continued sampling of the SAF initiated in VPR 3, extending into the northern flank of the PF (Figure 27, Figure 28). The high fluorescence regions in the southern SAF and northern PF were manifested in the "Phaeo bloom" taxon by the classifier (Figure 29). Upon examination of the sorted ROIs, it was clear the classifier put the following plankton types into this taxon: colonial algae, diatom mats, *P. antarctica*, and ghost colonies (Figure 30). Pteropods, polychaetes, and copepods were also abundant in these high fluorescence regions (not shown).

VPR 5 continued through the PF, crossed the SACCF and into the Ross Gyre (Figure 31, Figure 32). The southern flank of the PF contained a high abundance of diatoms, as well as same the collection of plankton types allocated to "Phaeo bloom" by the classifier in VPR (Figure 33). *Chaetoceros*, "spindles" (*Thalassiothrix antarctica*?), and segmented diatom chains were also present in the polar front, as well as pteropods and worms. The southern edge of the polar front (57.5S-58.5S) contained a dense diatom bloom composed of *Chaetoceros*, "spindles", and segmented diatom chains. Pteropods and worms were absent in this area. Waters of the Ross Gyre (58.5S south) contained mostly large zooplankton (e.g., krill, amphipods, and salps) and fecal strings.

To summarize the dominant trends in microplankton biogeography in VPR 2-5, based on the above taxonomic distributions plus additional qualitative analysis:

- Subantarctic Front
  - Acantharians (northern flank)
  - Large colonial phytoplankton (*Phaeocystis*?)
  - Polychaetes
  - Pteropods
- Interstitial region
  - *P. Antarctica*
- Polar Front – northern branch
  - Warm, fresh, high F, b_b
  - Aggregates of small rod-shaped diatoms
- Polar Front – southern branch
  - Cold, salty, low F, b_b
- Polar Front zooplankton
  - Pteropods
  - Copepods
- Ross Gyre
  - Large zooplankton (e.g., krill, amphipods, and salps)
  - Fecal Strings

Satellite imagery received after the completion of the enhanced meridional transect revealed high PIC and chlorophyll associated with the SACCF, consistent with the VPR results (Figure 34, Figure 35).

Note that the starting points of VPR 4 and VPR 5 were moved farther north in order to provide two time points bracketing CTD observations. Overlap regions for VPR 3-4 and 4-5 are shown in Appendices 4 and 5, respectively.

3. Feature surveys

3.1 Survey of Eddy A

After completion of the 30-60 S meridional transect, the VPR was towed northeastward from to survey Eddy A, a persistent mesoscale cyclonic feature with relatively high satellite-detected PIC (Figure 36) and chlorophyll concentrations (Figure 37). The VPR was towed across the PF during transit to the center of Eddy A (VPR 6, 7), then towed in a bow-tie pattern to complete the eddy survey (VPR 7-9). Note that the strobe failed during the latter part of VPR 6 and ROIs were not available for that portion of VPR 6 or VPR 7.

The transit towards Eddy A allowed for additional high-resolution surveying of the high-fluorescence, high-backscatter PF (Figure 38, Figure 39). East of 150 W, the PF (at ~55.5 S on 150 W) splits into northern and southern branches, which were both measured by the VPR (Figure 39). The more southern of the two branches was colder and saltier with lower fluorescence and backscatter. Taxonomic observations (Figure 40) show a similar distribution to that of the southern branch of the PF on the meridional survey. Predominant taxa are Chaetoceros, “spindles”, segmented diatoms, copepods, pteropods, and worms. From 147W to 146W, there was a cold and salty anomaly with lifted isopycnals separating the two branches of the polar front. This anomaly was characterized by lower chlorophyll, backscatter, and overall plankton abundance than either of the two branches. The more northern of the two is warmer and fresher (33.85) with higher fluorescence and backscatter, with conditions more similar to those of the crossing of the PF on the 150 W meridional transect. The taxonomic distribution reflected that seen in the northern branch of the PF in the meridional survey, with overall lower abundance than the peak concentrations seen in VPR4.

Hydrographic properties measured by the VPR and XBTs, satellite ADT, and ADCP data were used to pinpoint the center of Eddy A (Figure 41, Figure 42,Figure 44). Like the northern branch of the PF and the 150 W meridional transect, the core of Eddy A was characterized by low salinity (33.85) (Figure 41). Unlike the high-chlorophyll and high b_b PF, however, fluorescence and b_b in the core of Eddy A were moderate. Zooplankton were abundant in the eddy though; the VPR captured images of copepods, pteropods, marine snow, and chaetognaths. The northern edge of the eddy was comprised of the SAF and had both high chlorophyll and high b_b. Image data recommenced just prior to making the turn southeast at the northwest corner of the eddy (Figure 43); this high-biomass area was characterized by colonial alga, *P. antarctica*, pteropods, and worms, similar to that which was seen within waters of the SAF during the meridional survey.

Following the VPR survey, ten CTD profiles comprising two transects crossing Eddy A were conducted (Figure 45, Figure 46, Figure 47). Like the VPR data, the CTD profiles indicate a colder eddy core than the outer eddy regime. In the top ~200 m, the eddy core is fresher; at depth it is saltier than the surrounding water. Nutrient data collected by the Scripps ODF team reveal the upward doming of nutriclines. This high-nutrient water doming at eddy center is also associated with low oxygen saturation, a signature of UCDW.

High-resolution satellite imagery of Eddy A suggests that the presence of a spiral streamer of high PIC / chlorophyll around the eddy (Figure 48, Figure 49). Cross-eddy variability in temperature and salinity captured by VPR hydrographic measurements also indicates a cold spiral streamer (Figure 41). This potentially indicates lateral entrainment and advection of colder, fresher, high chlorophyll, and high b_b waters from high-biomass frontal regions to form the ring of high chlorophyll and high backscatter in the periphery of the eddy.

The origin of Eddy A was estimated by comparing the eddy core water to the 150 W meridional transect in temperature-salinity space (Figure 50). The eddy core appears to have originated from the northern flank of the PF based on its water mass characteristics. Comparing CTD cross sections of Eddy A and the meridional transect also suggest consistency between water observed at the core of Eddy A and the PF region (Figure 51). The deeper waters of the core of Eddy A appear to be a mixture of AAIW and UCDW; the upper water column is likely to be composed of warmed AASW.

3.2 Survey of Polar Front at 141W

Satellite ocean color images from mid-December revealed high PIC (Figure 52) and high chlorophyll (Figure 53) across the PF at 141 W. The frontal configuration at 141 W differed from than at 150 W, however, due to topographic steering by the Pacific Antarctic Ridge. The SACCF and PF converge in the vicinity of the Udintsev Fracture Zone, as illustrated by ADT overlaid on bathymetry (Figure 54). These differences between the PF at 141 W relative to the 150 W meridian motivated an extensive VPR cross-sectional survey (VPR 10). February satellite imagery suggests that PIC and chlorophyll may have declined in the PF since December (Figure 55, Figure 56), though high PIC and chlorophyll appeared to continue in the Southern ACC front.

Consistent with satellite measurements, high fluorescence and backscatter were detected in the SACCF during VPR 10 (Figure 57). Backscatter and chlorophyll were enhanced to a lesser degree at the PF, which had converged with the SACCF (Figure 58), with the strongest signals detected ~50 m below the surface. In the PF (56.8 – 57.2 S), diatom mats predominated from ~ 60-80m below the surface. In the SACCF (57.6-58.0 S; Orsi et al. 1995), diatom mats were abundant in the surface layer. The tow was characterized by sharp horizontal gradients in bio-optical measurements, with “vertical walls” in chlorophyll and b_b detected at 56.8 S, 57.55 S, and 57.95 S.

Colonial alga and diatom mats were common throughout the tow. *P. antarctica*, pteropods, and worms were present within the PF. South of 57.5 S, those three taxa were replaced with

Chaetoceros, “spindles”, and segmented diatom chains typical of the southern branch of the PF and the SACCF.

3.3 Survey of Eddy C

Satellite images from 20 January 2021 indicate a hotspot of PIC and chlorophyll in the interior of cyclonic “Eddy C” (Figure 59, Figure 60), motivating a VPR eddy survey from its southwest to northeast corners on 2 February (Figure 61). An XBT survey was used to help pinpoint eddy center (Figure 62). Whereas original expectations were for Eddy C to be a younger version of Eddy A, their hydrographic and bio-optical properties were quite different. In contrast to Eddy A, the interior of Eddy C contained a warm and salty interior, low fluorescence, low microplankton abundance, but high b_b (Figure 63). Also unlike Eddy A, nutrient measurements made during CTD profiles through the eddy document high ammonium at eddy center (Figure 64, Figure 65, Figure 66). Patches of higher chlorophyll consisting of diatom mats were detected on the eddy flank (Figure 67); *P. antarctica*, pteropods, and worms were also present.

In the center of the eddy, the higher backscatter reaches the surface, creating a “Bull’s eye” backscattering pattern consistent with the satellite imagery. As PIC concentrations are estimated by the relation PIC ~ b_b / (a + b_b) (Gordon et al. 1988), low values of *a* can allow the PIC to shine forth, which we suspect may have been the case for Eddy C.

Zooplankton (e.g., copepods, pteropods) were present in eddy center, but the overall abundance of ROIs was extremely low. Eddy center had roughly 300 ROIs/hour for 5 straight hours, as compared to a typical hour of 1-2k ROIs and blooms which have upwards of 6-20k ROIs.

3.4 Revisitation of Eddy A

After completion of the Eddy C survey, Eddy A was revisited while transiting to the meander of the SAF for VPR 12. The VPR 12 track was designed to bisect Eddy A, then travel into the eddy south of the SAF meander (“Eddy D”) before entering the SAF itself (Figure 68, Figure 69). As the configuration of the meander had shifted in the period since its first occupation on 19 January, a short northeastward segment following our passage through Eddy D ensured we had indeed traveled across the SAF. High fluorescence and backscatter signals were still present in low-salinity Eddy A during its revisitation (Figure 70), and zooplankton remained abundant.

3.5 Survey of Eddy D / Subantarctic Front

While satellite images suggested the presence of high PIC and chlorophyll waters wrapping around the southern flank of Eddy D, this was not detected by VPR sensors; fluorescence and b_b remained low throughout the Eddy D cross section (Figure 70).

Fluorescence increased somewhat when entering the SAF, however backscatter remained near background levels. At no point in VPR12 did colonial algae or diatom mats appear in similar abundance to prior visitations of the SAF (Figure 71). *P. antarctica* was still present.

4. A coccolithophore bloom along 150W

During the transit north to re-occupy a portion of the meridional transect along 150W, a bloom of coccolithophores was detected from 50.5S to 43.3S, with b_b' values of up to 3E-3 (Figure 72). These values were almost an order of magnitude larger than what we have observed up to this point. VPR 13 surveyed the northern edge of this bloom (Figure 73), spanning the background conditions to the north (warm SST, > 16C; low fluorescence, low backscatter) into the bloom interior with b_b' values of ~2E-3. The total backscatter mimics the pattern of b_b', with an increasing trend from north to south, interrupted by a dip in the vicinity of 44.1S. Note that the surface expressions of peaks in b_b' centered at 43.8S and 44.6S both have subsurface extensions to the north. Salinity anomalies centered at 43.5S and 44.5S appear to be associated with a frontal meander (Figure 74). Based on satellite imagery, the dip in b_b' at 44S (Figure 72) coincides with an eddy with low PIC in the interior (Figure 75, left panel).

A satellite image subsequent to the survey reveals PIC-rich water to the east of where high b_b' was observed along 150W (Figure 75, right panel).

Comparison of the CTD data from the two occupations of this portion of the meridional transect reveals surface warming (Figure 76), as to be expected this time of year. However, near-surface waters also freshened by ~0.2 psu, indicating the presence of a different water mass (Figure 77). The associated nutrient data (Figure 78) reveal some deepening of the nitracline and an increase in ammonium.

Ten Southern Ocean Carbon and Climate Observations and Modeling (SOCCOM) BGC Argo floats were deployed over the 30-60 S, 150 W meridional transect (float IDs 19018, 0887, 1115, 1204, 19072, 1205, 17328, 19085, 19327, 19067 (Figure 79); for details see SOCCOM section of the SAMW21 cruise report). Every ten days, each float reports a profile of hydrographic and bio-optical measurements; these data can inform how the waters originating at the 150 W meridional transect evolved over the cruise period, in a quasi-Lagrangian framework. An eleventh, older SOCCOM float (12701) was also near 60 S, 150 W during the January-February 2021 cruise period, providing data for the southern terminus of the meridional transect, where RR2004 SOCCOM floats were not deployed until later in January. The optical nitrate sensor on float 0887 deployed at 35 S was not operational, and the backscatter measurements from float 17328 between ~600 and 850 m are problematic.

The SOCCOM float data corroborate the increased temperature and decreased surface salinity found between 50.5 S to 43.3 S during the reoccupation of the 150 W transect (Figure 80 Figure 81). 10 m salinities for float 19072 deployed at 46 S declined from 34.48 to 34.26 between 15 January and 14 February. Float 19072 also saw increasing chlorophyll (Figure 82) and backscatter (Figure 84), which was also found during the second occupation of the meridional transect. The trajectory of float 19072 suggests net northwestward transport, and ADCP data from VPR 13 also show generally northward transport from 0-700 m south of 43.5 S (Figure 85), where enhanced backscatter was observed (Figure 73).

Analysis of the DAVPR data provides an initial assessment of changes in the plankton community between the first and second occupations of this portion of the 150W transect. We

found that the first transect in early January showed a mix of zooplankton species and a modest number of ROIs (average = 66) or images captured per cast to 1000m. The second survey in early February showed slightly higher numbers of RIOs (average = 86). While a diverse assemblage of zooplankton was present in both surveys, forams, copepods, and gelatinous organisms were more common in January. By February, fecal strings and marine snow dominated most of the stations. More noticeable, however, were diatom chains which were present in all casts in January, had all but vanished in February. Oddly, chlorophyll was greater in February, light transmission less, and slightly higher phosphate, silicate, nitrite, and ammonium ion. Temperatures had increased at the surface along with a fresher lens of seawater.

Low microplankton abundance was also evident in VPR13, which contained only 653 total ROIs over a 10 hour towing period (excluding the first and last hours of the tow). Zooplankton (e.g., copepods, krill) were more abundant in higher chlorophyll waters to the south (Figure 86).

5. Distribution of planktonic "spindles" perhaps *Thalassiothrix antarctica*

An unusual plankton specimen appeared in the video images of both the DAVPR and the VPRII about halfway through the cruise, which had a distinctive, lined, elongated ovoid shape, about 1 mm long (Figure 87, Figure 88). Although it had the shape of a dinoflagellate, it was like nothing seen in routine identification manuals. Occurrences of what we called 'spindles' were common enough to be larval invertebrates or large phytoplankton; eventually collection in the 150um plankton net secured a more positive identification as a colonial diatom.

Spindles appear abruptly at Sta. 69, at 58S, where they were very abundant, present with many other types of zooplankton, except copepods. Coincidentally, the tow before it, Sta. 68 (58.3S), had virtually all marine snow particles. The next two stations (up to 57.3S) Stations 70 and 71 had abundant spindles and other diatoms such as rods and *Chaetoceros sp*. as well as a diverse zooplankton fauna. Then just as abruptly, they vanished from the next station, #72 at 57.0S. Small pteropods were very abundant at both stations 71 and 72, but the associated spindles were gone in the more northern station. This one-degree of latitude (57 to 58) is south of the PF and at the convergence of SAMW water and the cold fresh SACCF.

The next occurrence of spindles in the DAVPR videos are at Stations 85, 86, and 87 as part of the survey across the PF at 141W, just south of Eddy B. Moving north, spindles showed up at 58S (Station 85) together with a diverse zooplankton assemblage including abundant acantharians and diatom mats. Stations 86 and 87 were also rich with many zooplankton and phytoplankton along with spindles. Spindles abruptly disappeared at Station 88, 57.1S, but small pteropods, worms, and diatom mats were particularly abundant in this diverse assemblage. This water appeared to be the transition from PF to SACCF waters: salinity was about 34.1 ppt, 3C, with chlorophyll values ranging from 2.5 to 4 and backscatter of 3 to 5 * 10^{-4}.

Corroboration with the plankton samples was problematic in that the net was not always deployed on every DAVPR cast and consisted of a small mouth opening. Still, spindles were found in abundance at Station 85 for the PF section. Only 2 specimens were found at Station 71 and a single specimen at Station 72, where none were seen on video. While our current

identification is the diatom colony *Thalassiothrix antarctica*, we hope to confirm this in the laboratory and to better define the association with the water mass at this location.

6. Summary of VPR tows

VPR #	Date	Description	Operational notes
1	28-Dec	Test tow	
2	Jan 15-16	Section 47-50	Tail skid broke
3	Jan 17-18	Section 50-53	
4	Jan 20-21	Section 53-56	
5	Jan 23-24	Section 56-60S	
6	26-Jan	Eastward, northeastward section	Strobe failed, replaced bulb and board
7	27-Jan	Northeastward section Eddy A center determination	Strobe failed; then CTD / bio-optical data failed
8	27-Jan	Continuation of VPR7, restarted deck	
9	Jan 27-28	Completion of eddy A survey	New board failed (burnt diodes); put new bulb back into old board; tail skid broke during haul back
10	31-Jan	Polar front transect	
11	2-Feb	Eddy C transect	
12	Feb 3-4	Eddy A revisitation; meander survey	
13	Feb 7-8	Revisitation of meridional transect	

7. Acknowledgements

We gratefully acknowledge support of this research by the National Science Foundation. The Video Plankton Recorder II was kindly made available as shared use equipment by the Dalio Family Foundation; the Digital Autonomous Video Plankton Recorder was kindly made available as shared use equipment from WHOI's Biology Department. The VPR team very much appreciates the superb efforts of ResTechs Matt Durham and Charlie Brooks, as well as assistance from our RR2004 shipmates in launch and recovery operations.

8. References

Anderson, R. F., and W. O. Smith. 2001. The US Southern Ocean Joint Global Ocean Flux Study: Volume Two. Deep Sea Research Part II: Topical Studies in Oceanography **48:** 3883-3889.

Balch, W. M., N. R. Bates, P. J. Lam, B. S. Twining, S. Z. Rosengard, B. C. Bowler, D. T. Drapeau, R. Garley, L. C. Lubelczyk, C. Mitchell, and S. Rauschenberg. 2016. Factors regulating the Great Calcite Belt in the Southern Ocean and its biogeochemical significance. Global Biogeochemical Cycles **30:** 1124-1144.

Gordon, H. R., O. B. Brown, R. H. Evans, J. W. Brown, R. C. Smith, K. S. Baker, and D. K. Clark. 1988. A semianalytic radiance model of ocean color. Journal of Geophysical Research: Atmospheres **93:** 10909-10924.

Orsi, A. H., T. Whitworth, and W. D. Nowlin. 1995. On the meridional extent and fronts of the Antarctic Circumpolar Current. Deep Sea Research Part I: Oceanographic Research Papers **42:** 641-673.

Patterson, S. L., and T. Whitworth. 1989. Chapter 3 Physical Oceanography, p. 55-93. *In* G. P. Glasby [ed.], Elsevier Oceanography Series. Elsevier.

Sarmiento, J. L., N. Gruber, M. A. Brzezinski, and J. P. Dunne. 2004. High-latitude controls of thermocline nutrients and low latitude biological productivity. Nature **427:** 56-60.

Smith, W. O., and R. F. Anderson. 2003. US Southern Ocean JGOFS Program (AESOPS): Part III. Deep Sea Research Part II: Topical Studies in Oceanography **50:** 529-531.

Smith, W. O., R. F. Anderson, J. K. Moore, L. A. Codispoti, and J. M. Morrison. 2000. The US Southern Ocean Joint Global Ocean Flux Study: and introduction to AESOPS. Deep-Sea Research II **47:** 3073-3093.

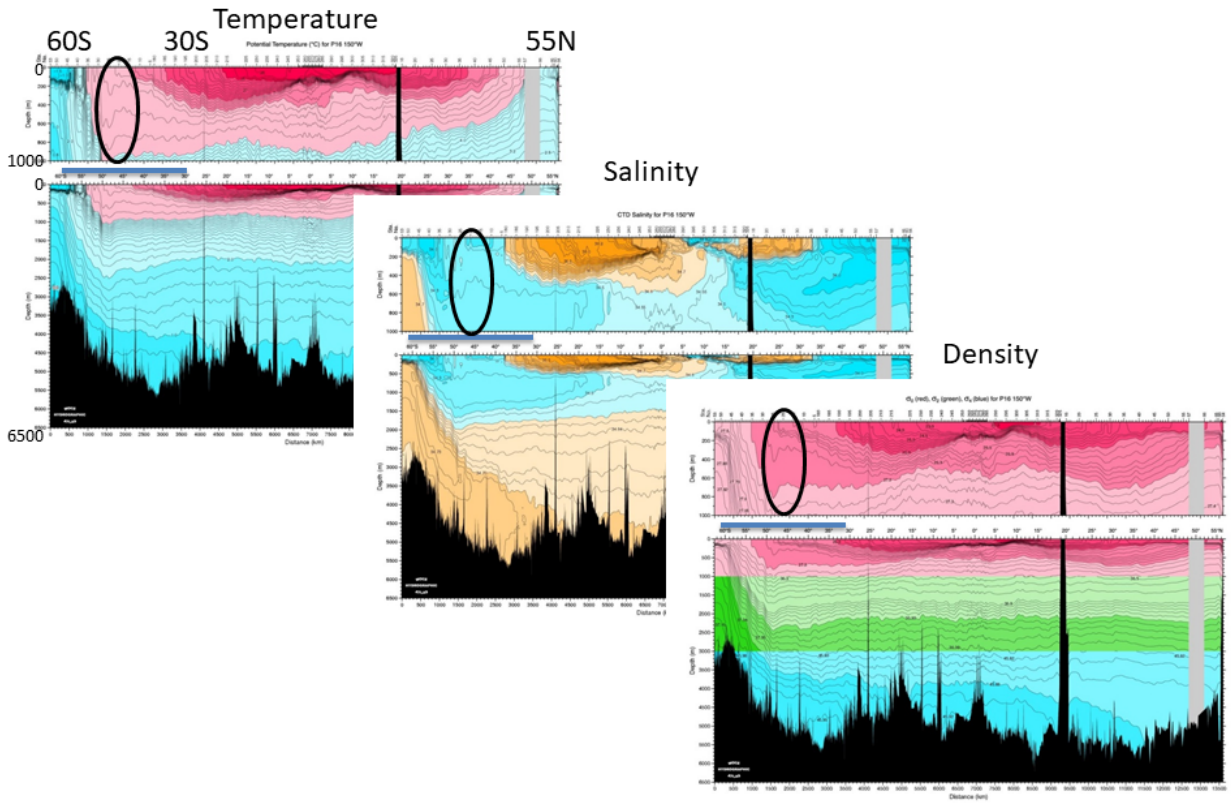

Figure 1. Temperature, salinity, and density sections from P16. Oval shape indicates SAMW. Source: WOCE Atlas Volume 2: Pacific Ocean, http://whp-atlas.ucsd.edu/pacific/p16/sections/sct_menu.htm

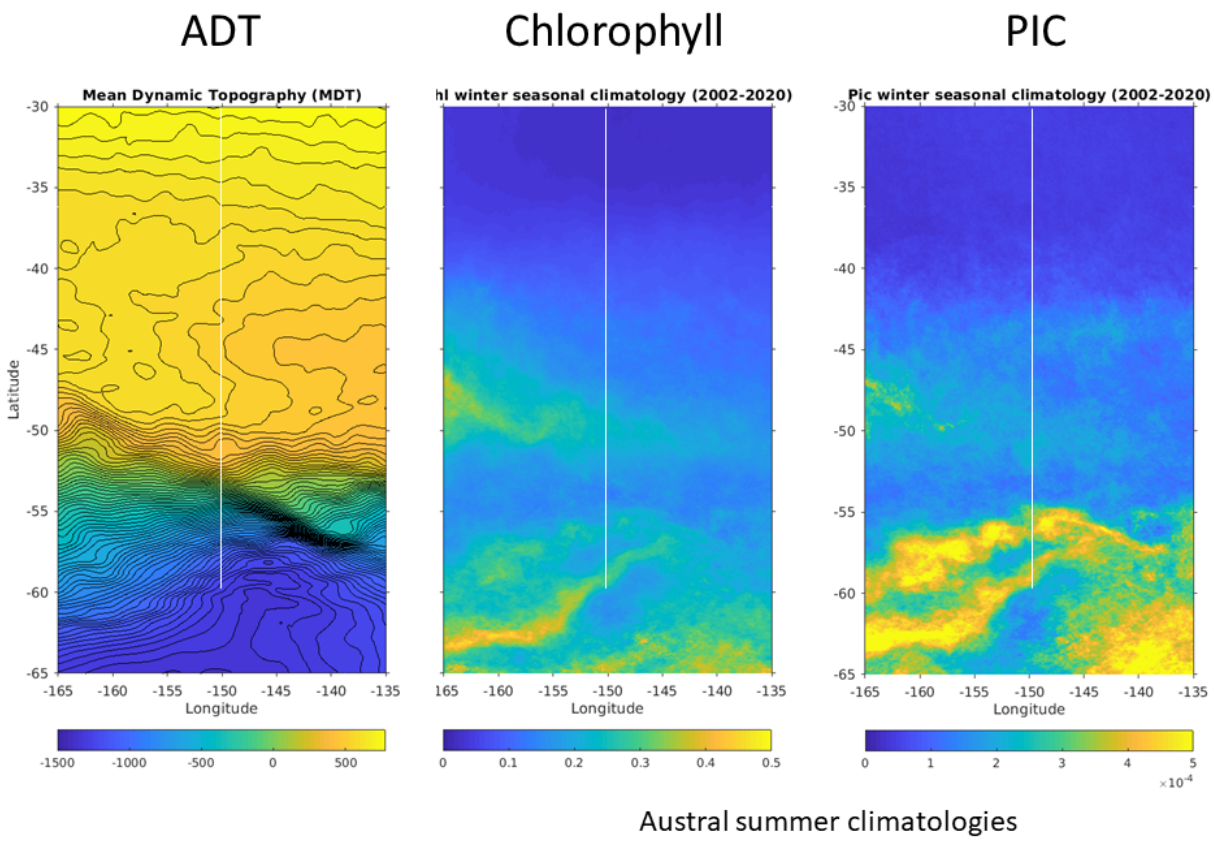

Figure 2. Climatologies of absolute dynamic topography (ADT), chlorophyll, and PIC.

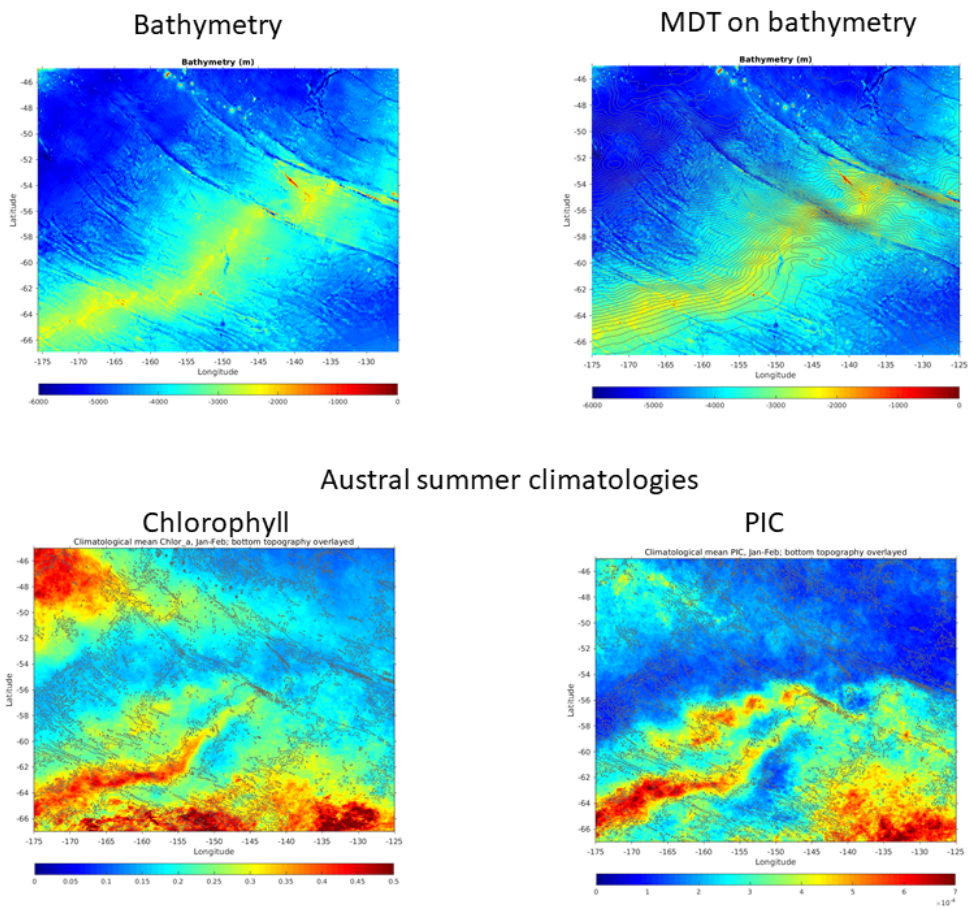

Figure 3. Upper left: bathymetry; upper right: contours of mean dynamic topography (MDT) overlaid on bathymetry; lower left: austral summer chlorophyll climatology with bathymetric contours overlaid; lower right: austral summer PIC climatology with bathymetric contours overlaid.

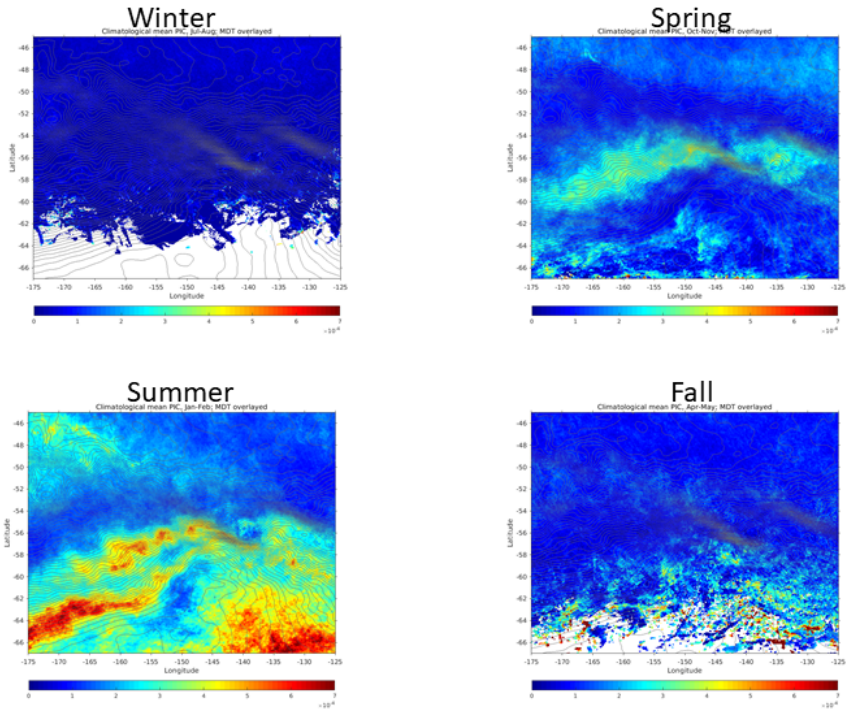

Figure 4. Seasonal PIC climatology, 45-67S.

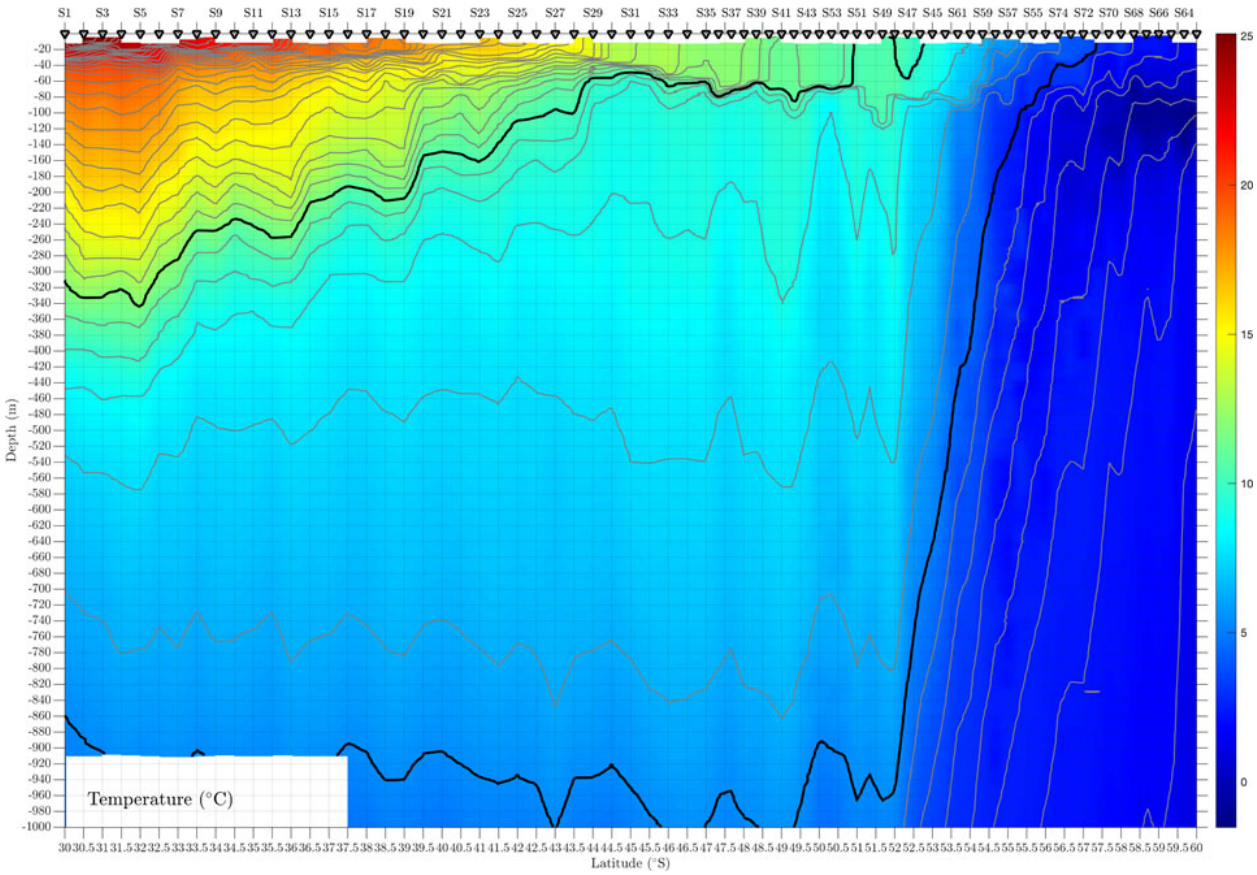

Figure 5. Temperature from 30-60S along 150W.

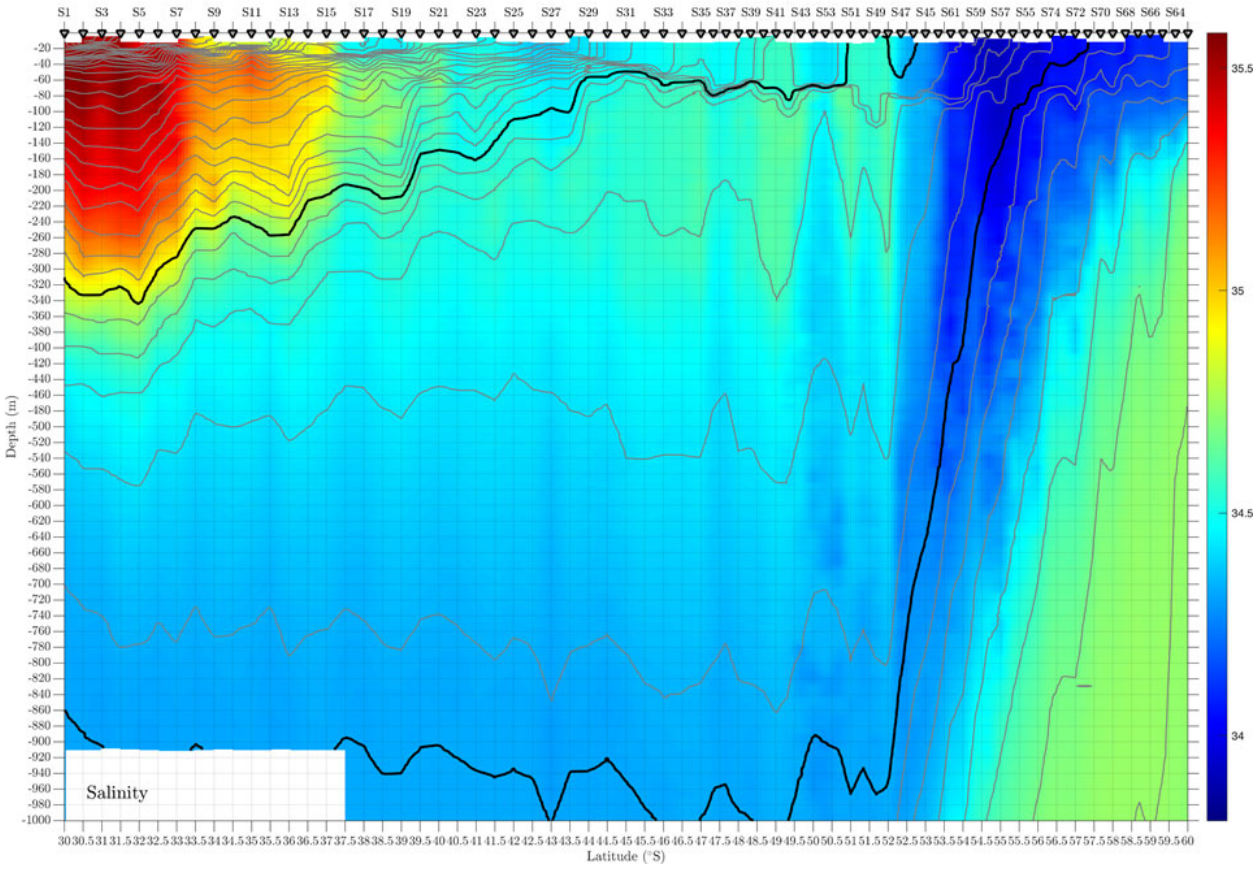

Figure 6. Salinity from 30-60S along 150W.

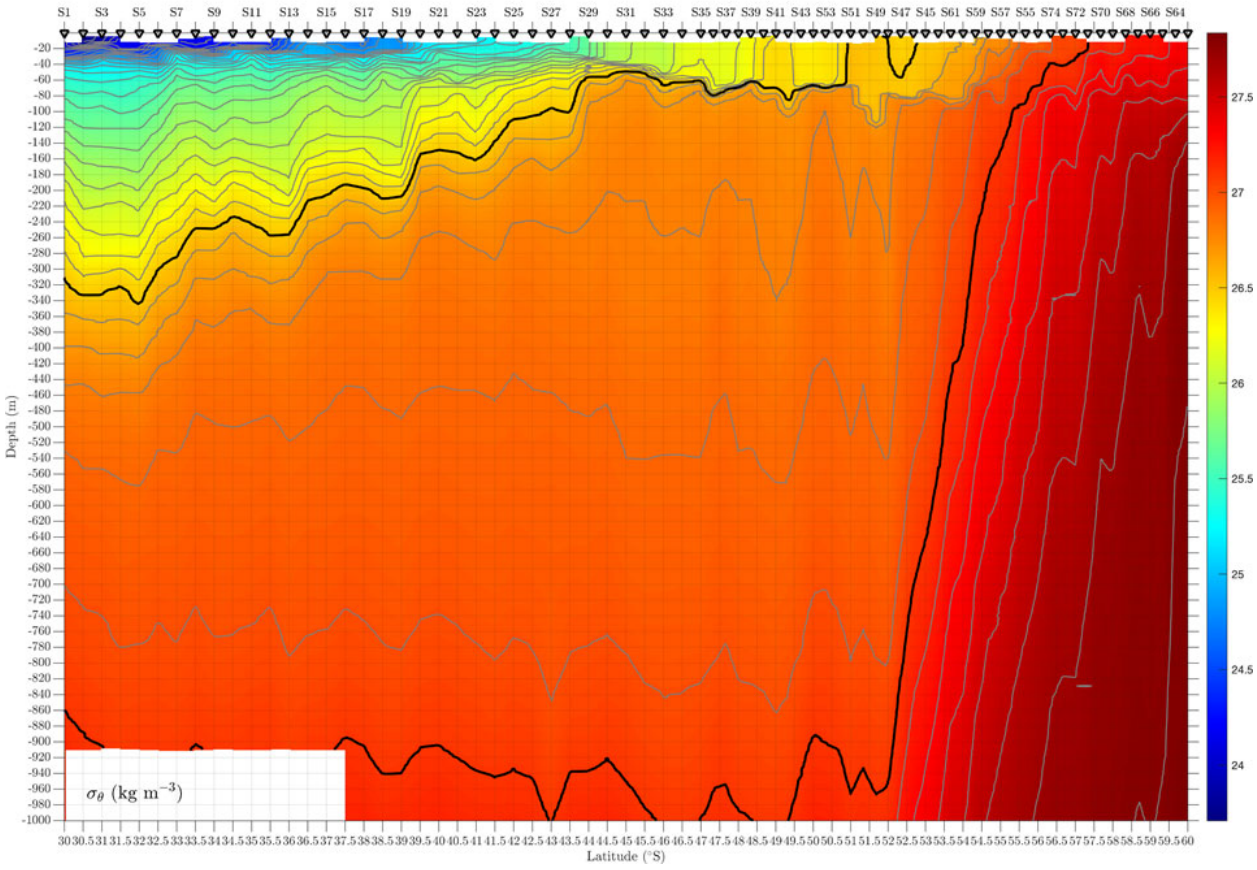

Figure 7. Density from 30-60S along 150W.

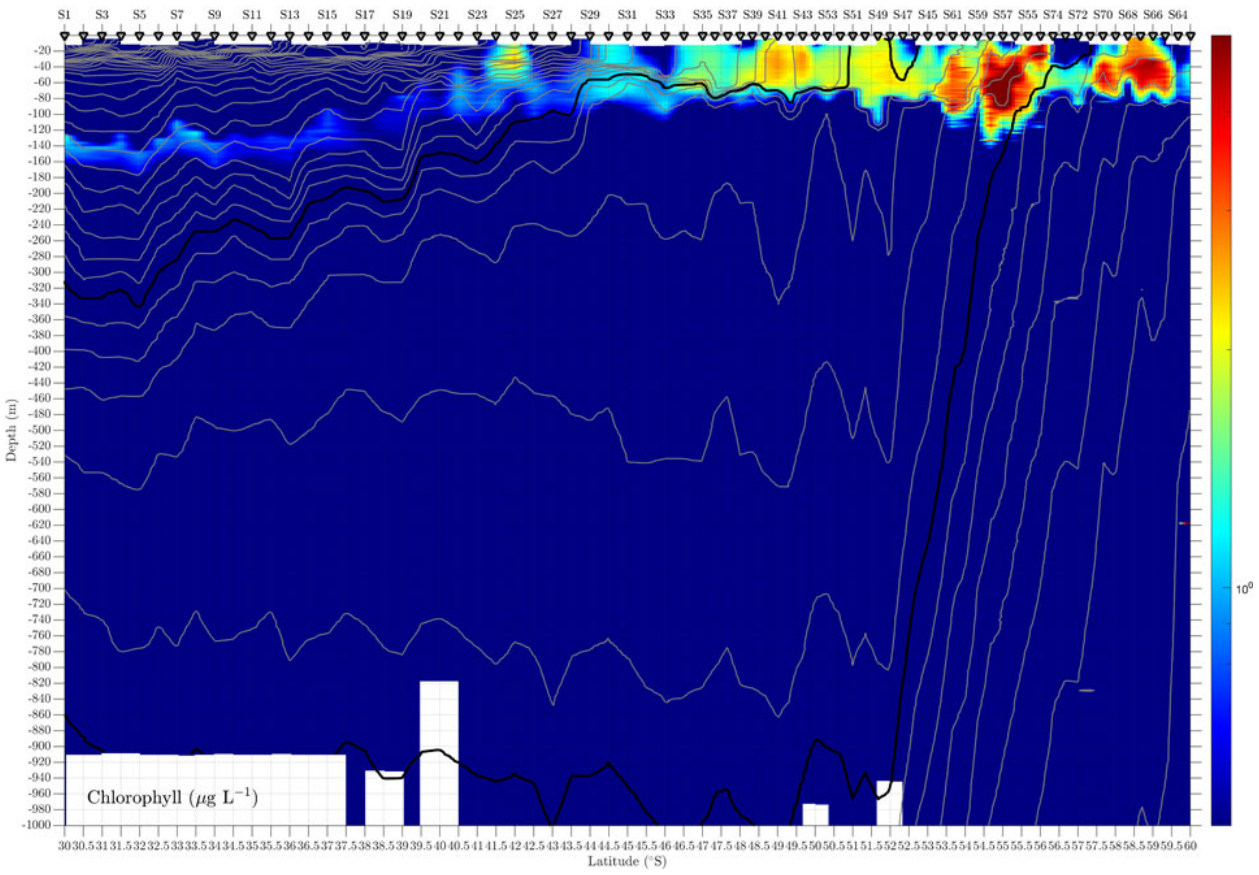

Figure 8. Fluorescence from 30-60S along 150W.

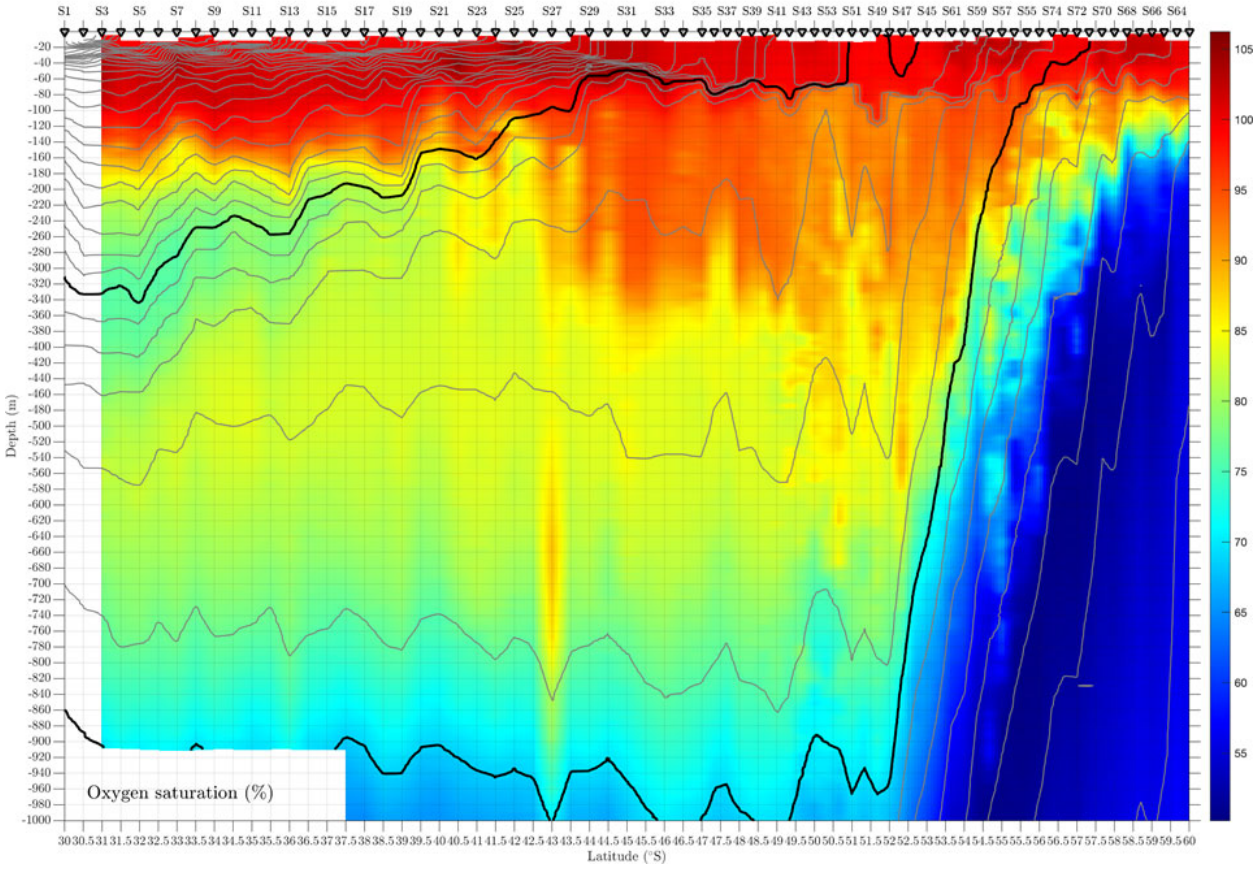

Figure 9. Oxygen saturation from 30-60S along 150W.

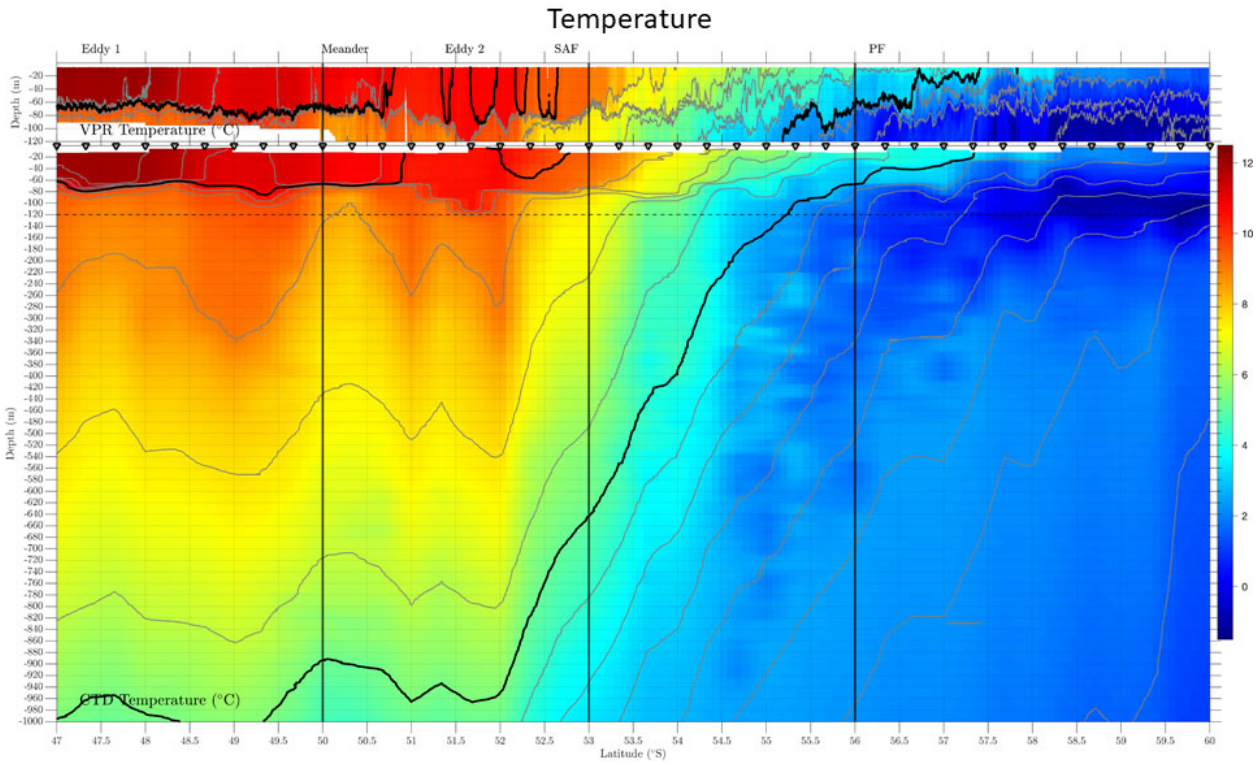

Figure 10. Temperature along 150W from VPR (top) and CTD (bottom) between 47 and 60S.

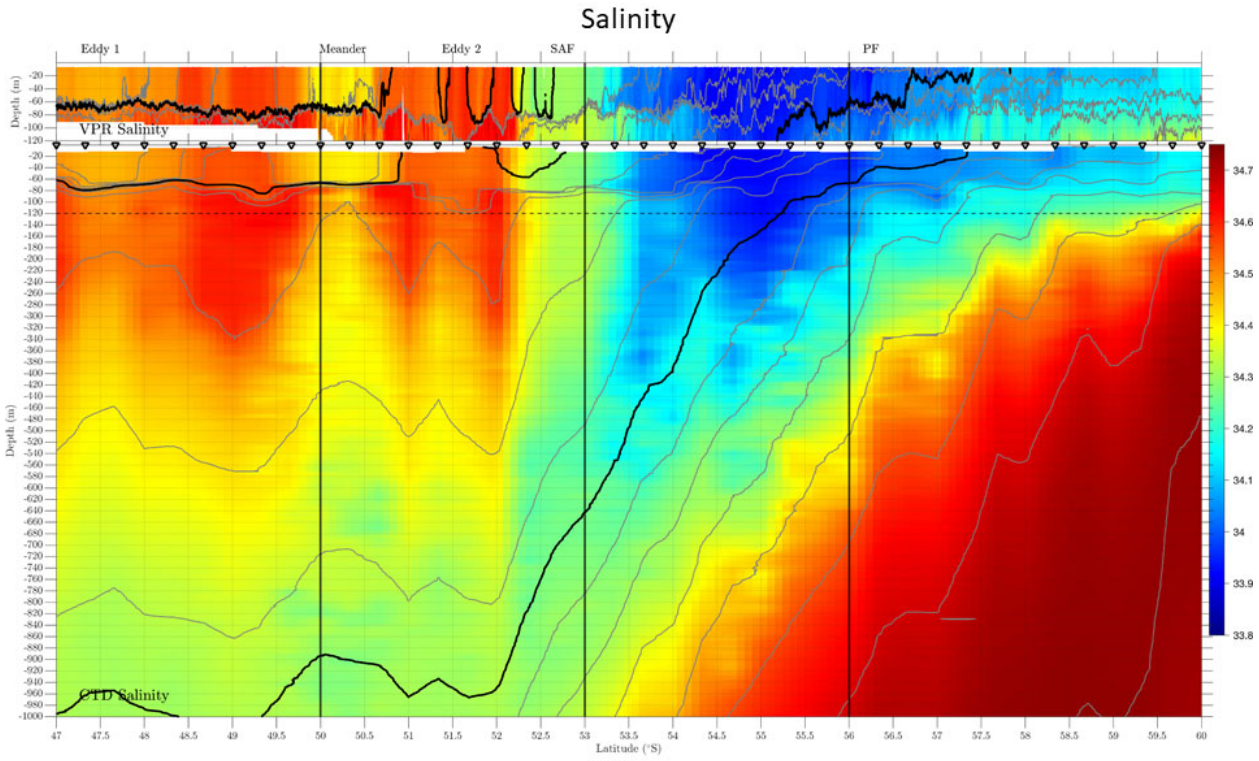

Figure 11. Salinity along 150W from VPR (top) and CTD (bottom) between 47 and 60S.

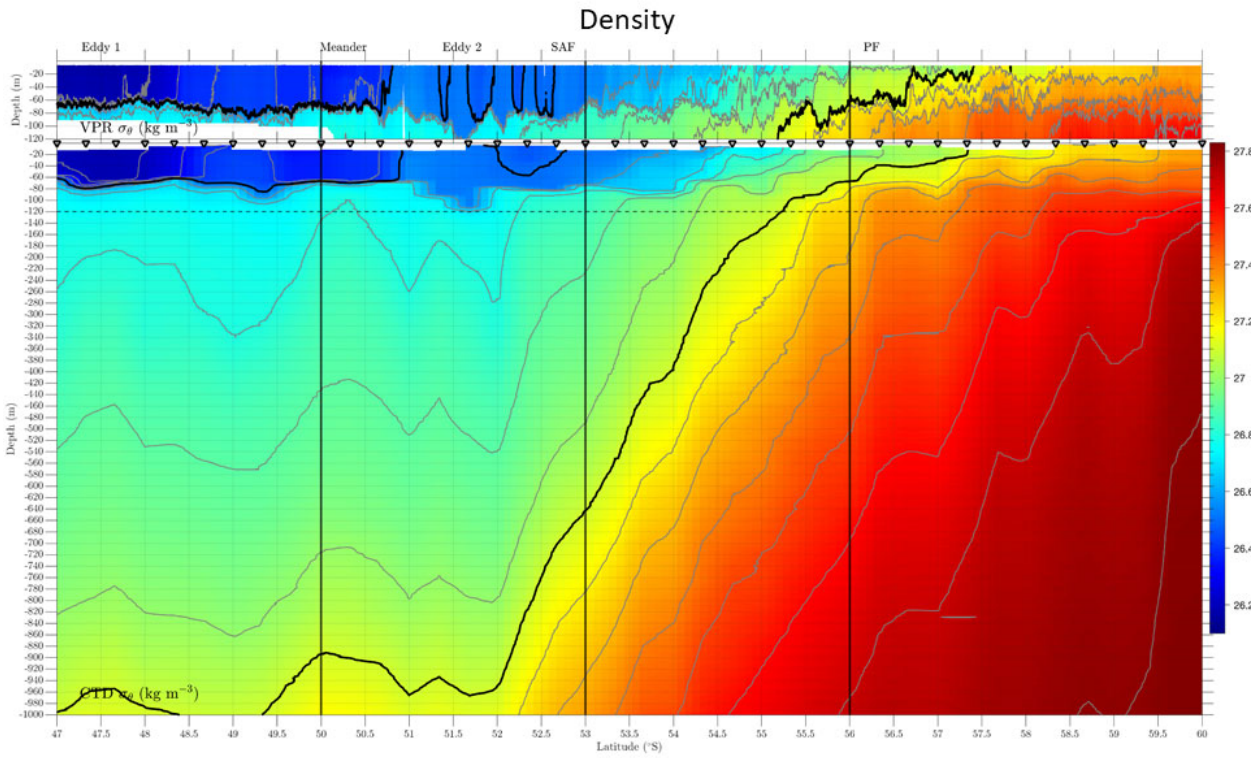

Figure 12. Density along 150W from VPR (top) and CTD (bottom) between 47 and 60S.

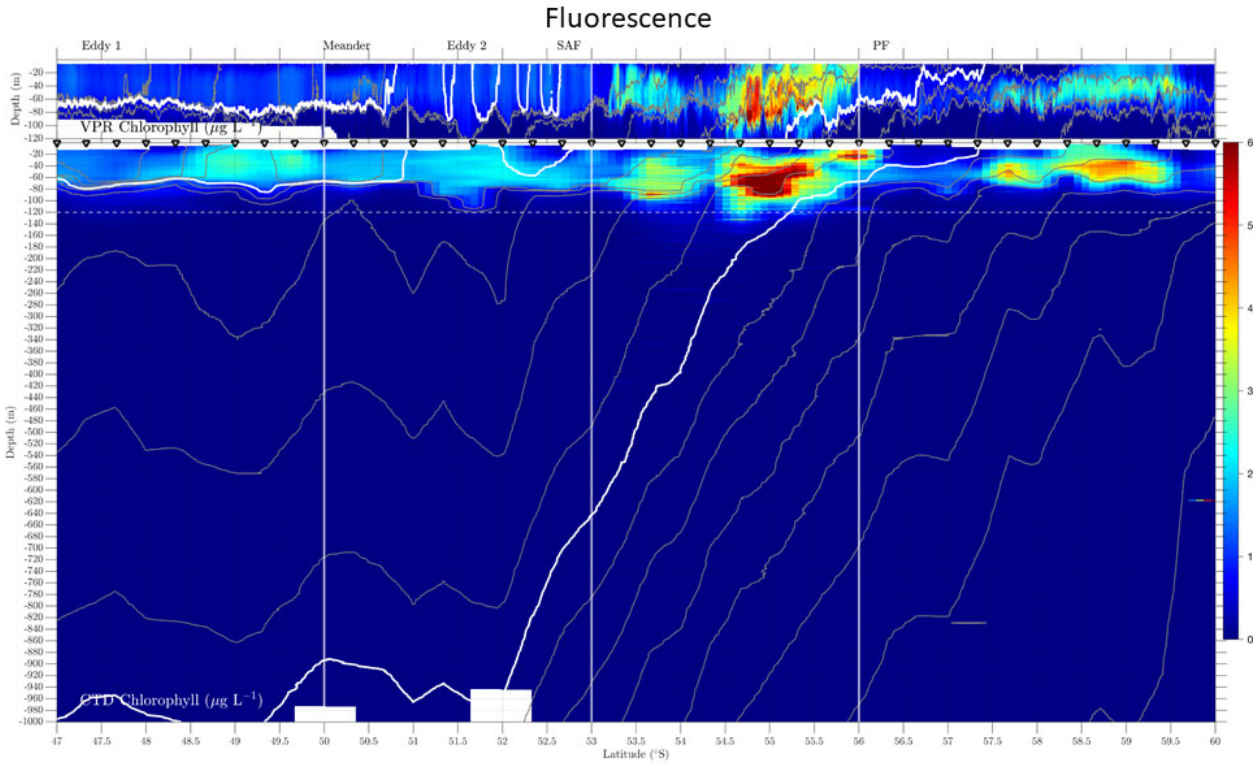

Figure 13. Fluorescence along 150W from VPR (top) and CTD (bottom) between 47 and 60S.

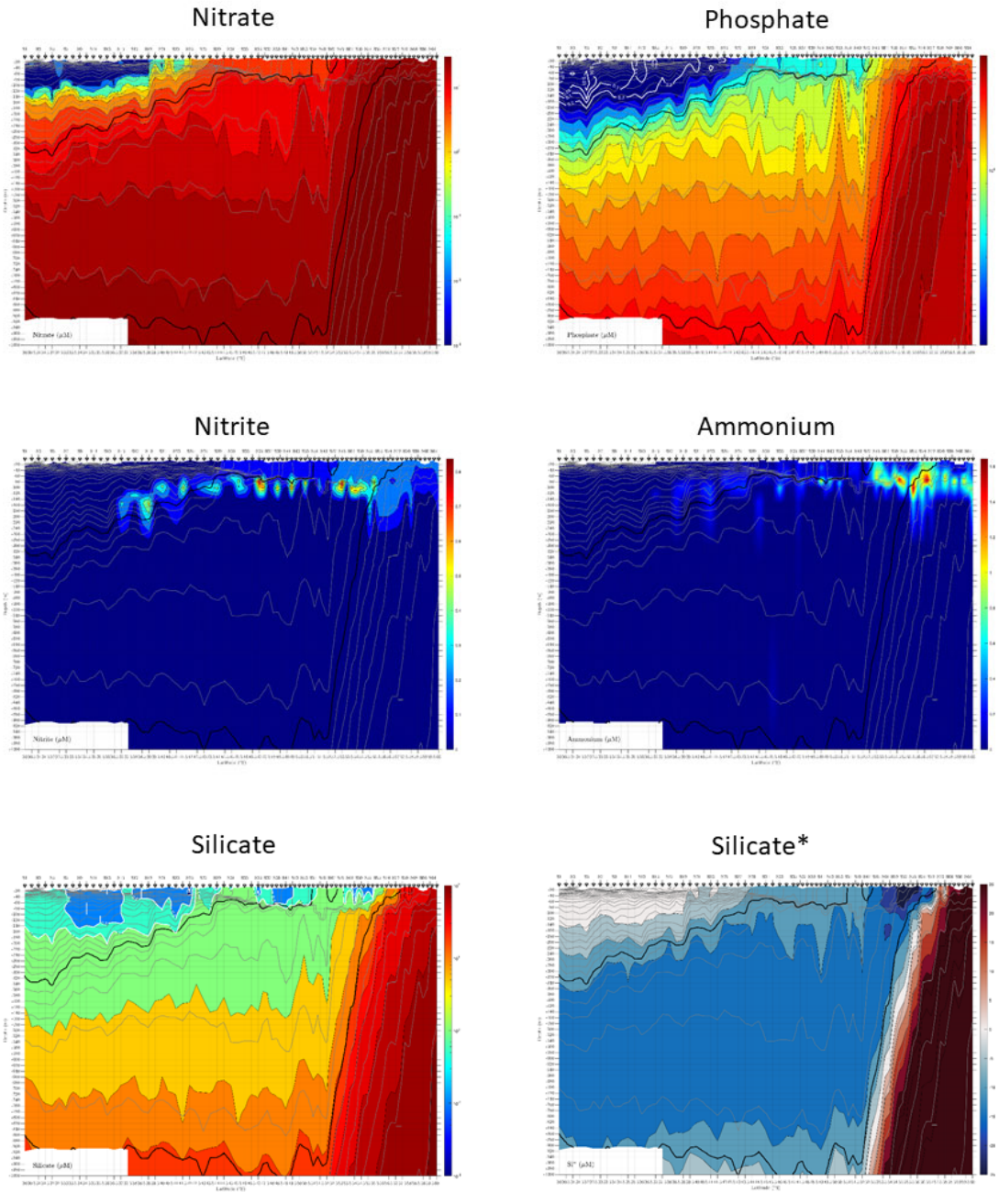

Figure 14. Nitrate, phosphate, nitrite, ammonium, silicate, and silicate from 30-60S along 150W.*

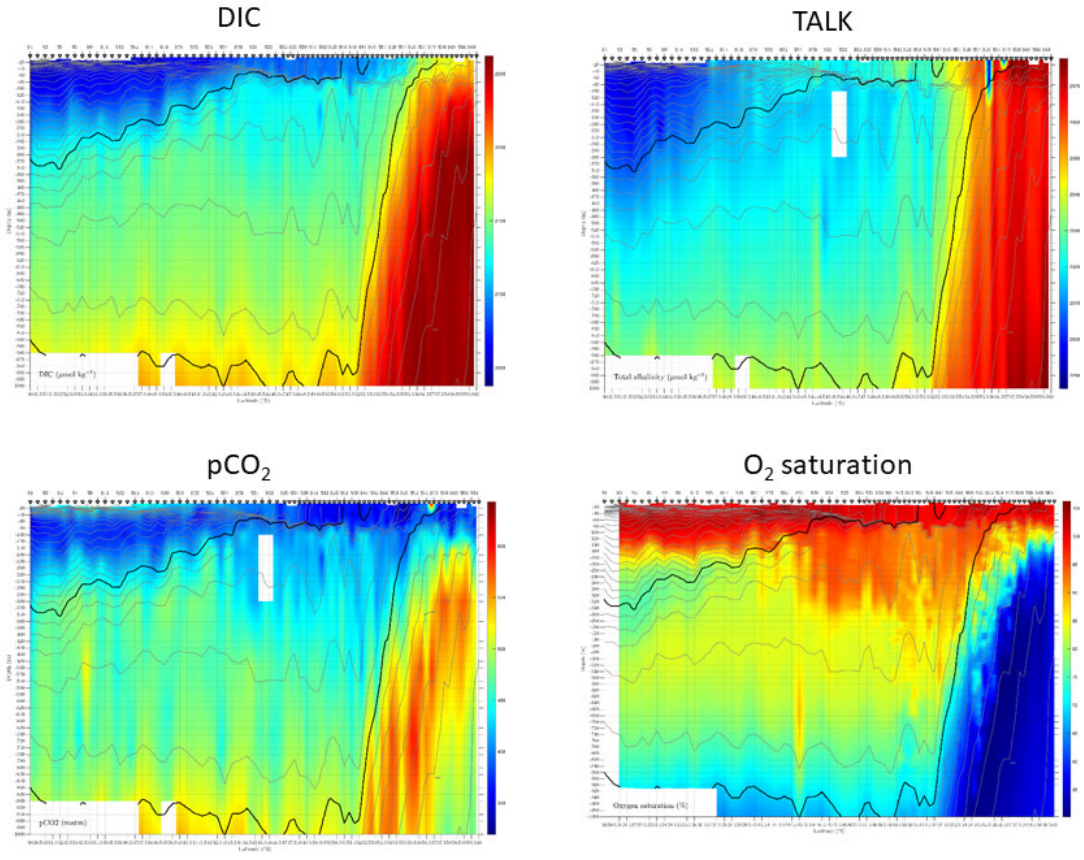

Figure 15. DIC, Total Alkalinity, pCO_2, and O_2 saturation from 30-60S along 150W.

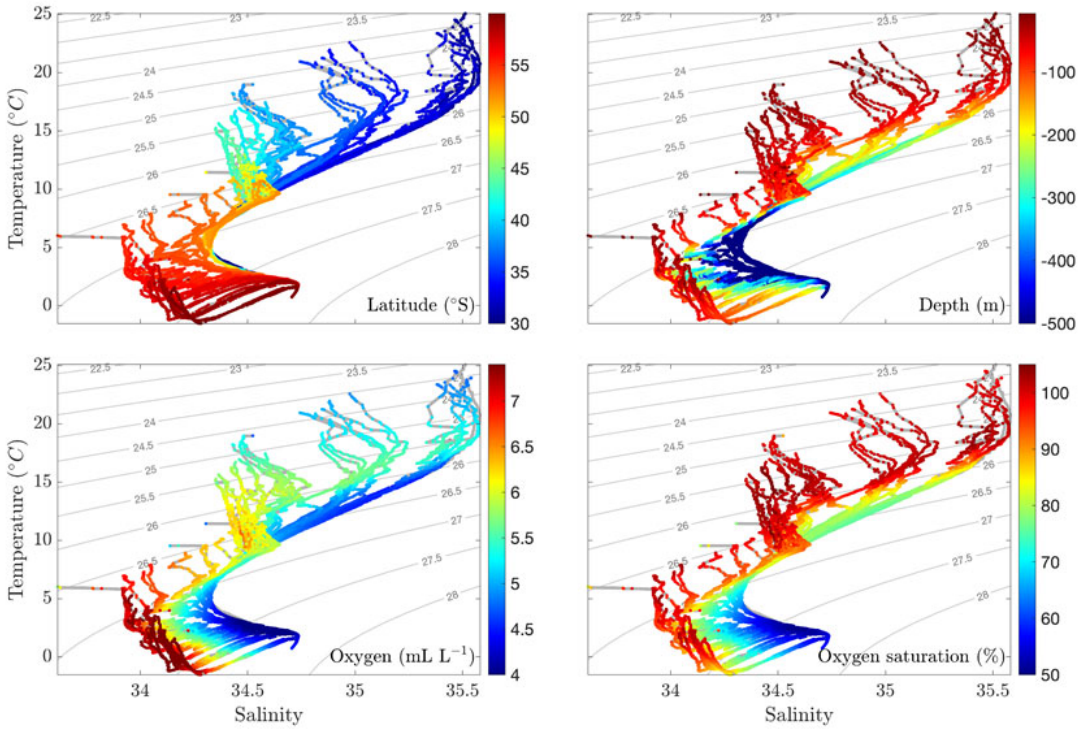

Figure 16. Temperature - salinity characteristics from 30-60S along 150W.

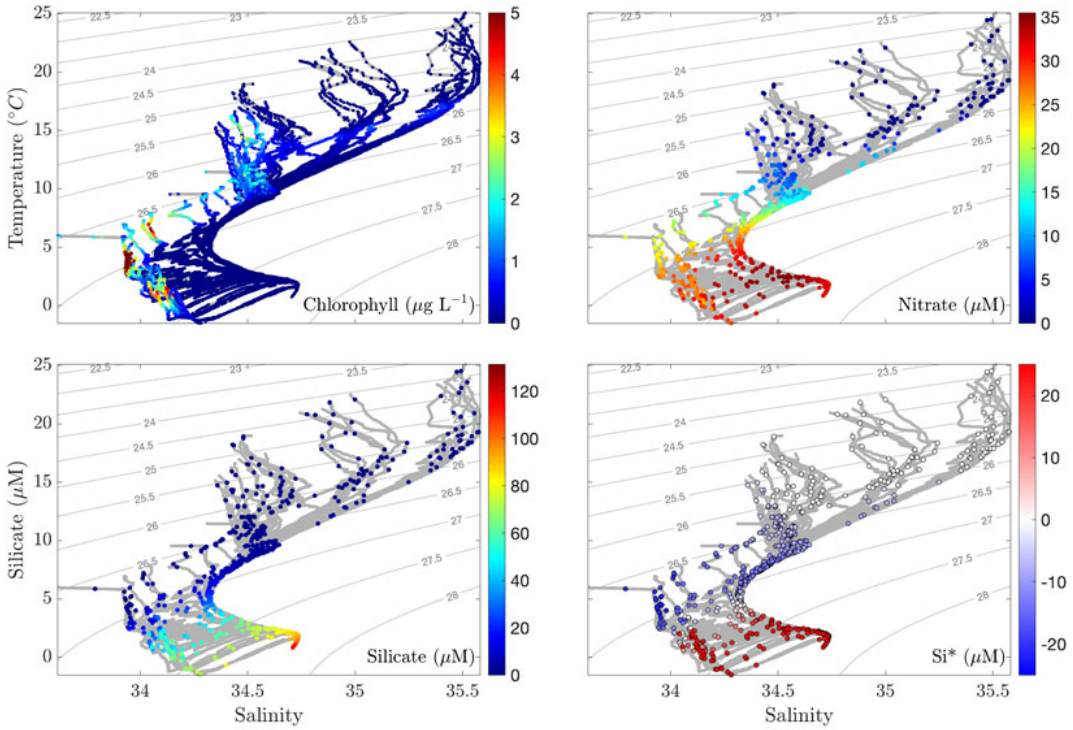

Figure 17. Temperature - salinity characteristics from 30-60S along 150W.

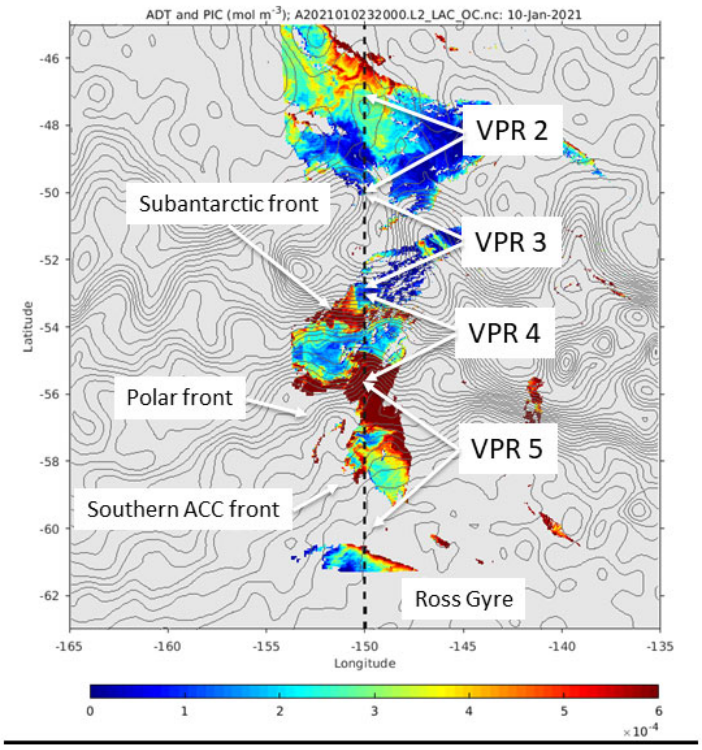

Figure 18. VPR 2-5 locations with contours of ADT and PIC indicated in color.

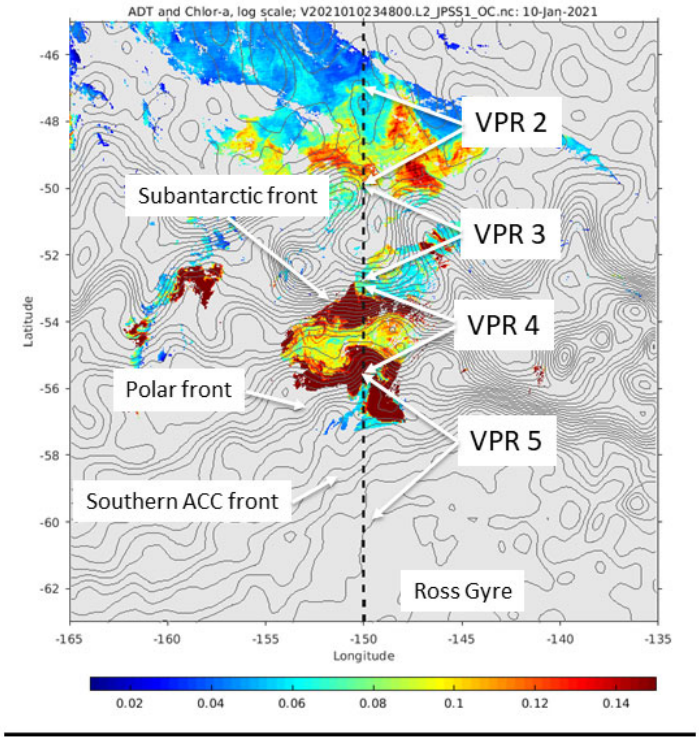

Figure 19. VPR 2-5 locations with contours of ADT and chlorophyll indicated in color.

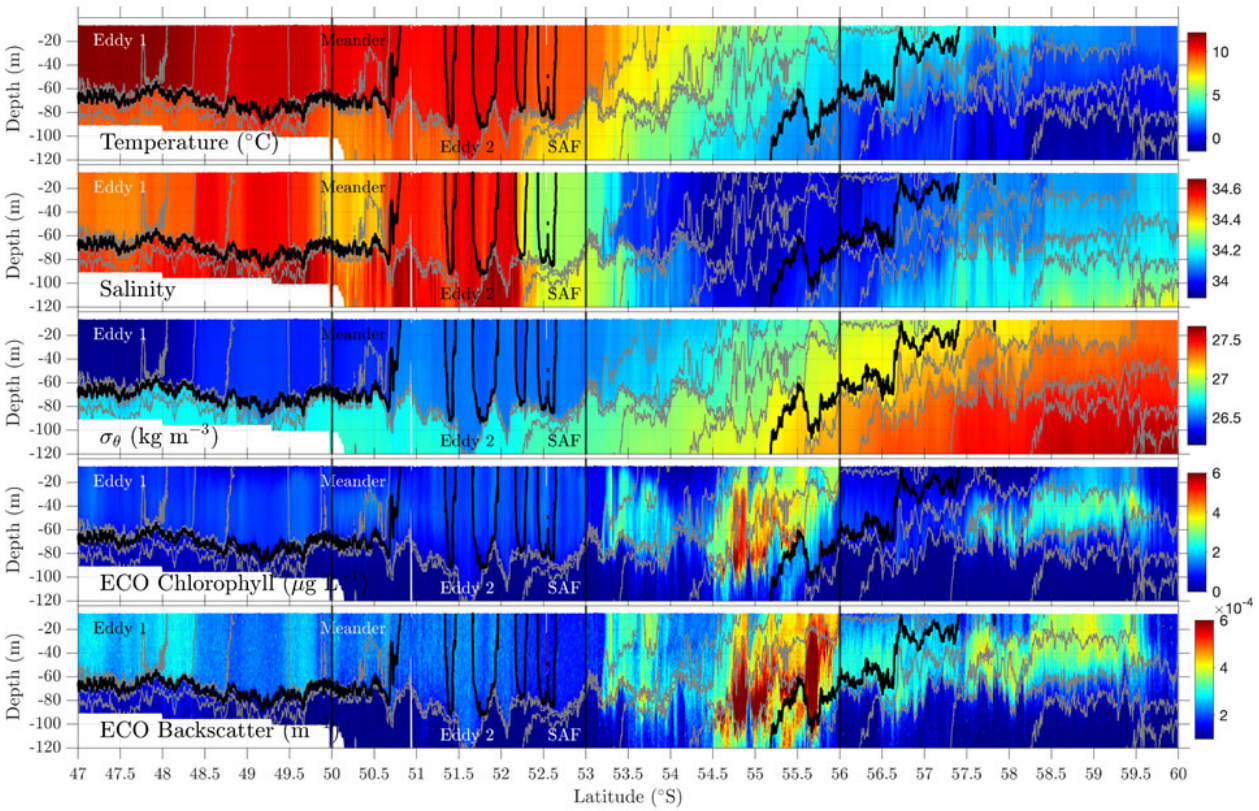

Figure 20. VPR 2-5 Temperature, salinity, density, fluorescence, and backscatter along 150W from 47-60S.

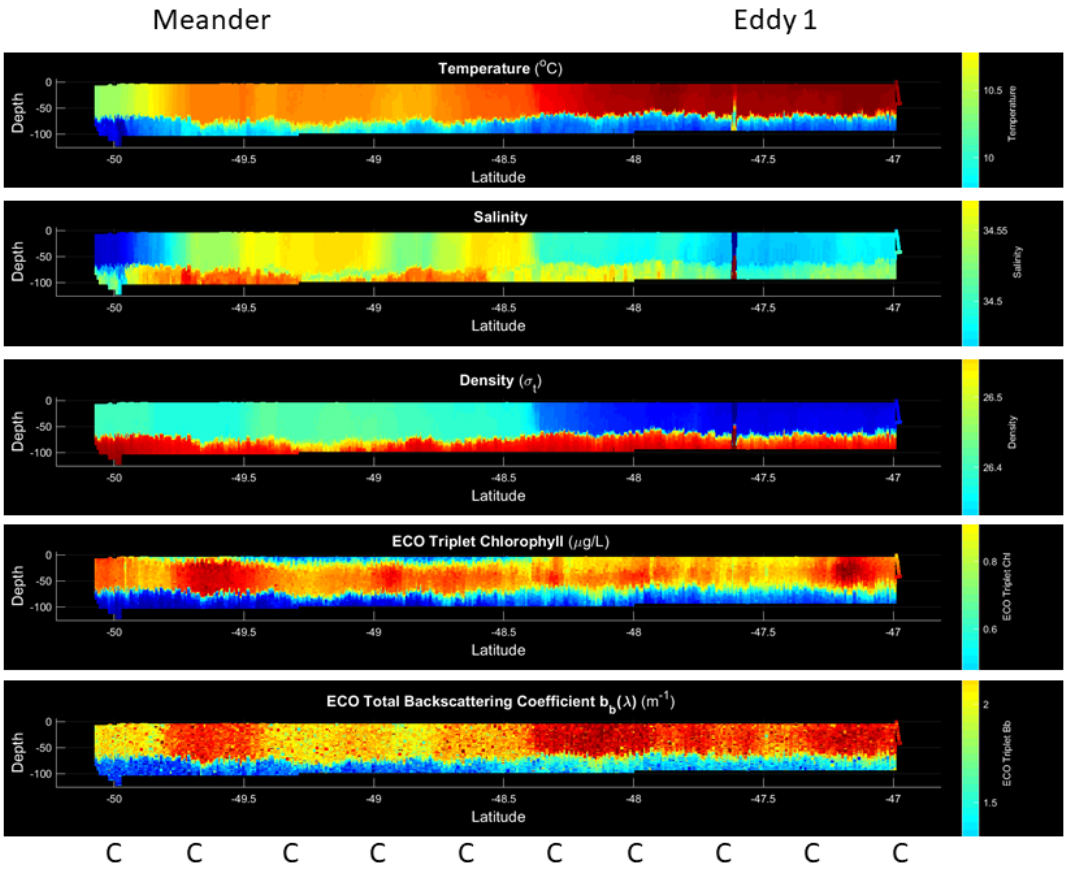

Figure 21. VPR 2 temperature, salinity, density, fluorescence, and backscatter.

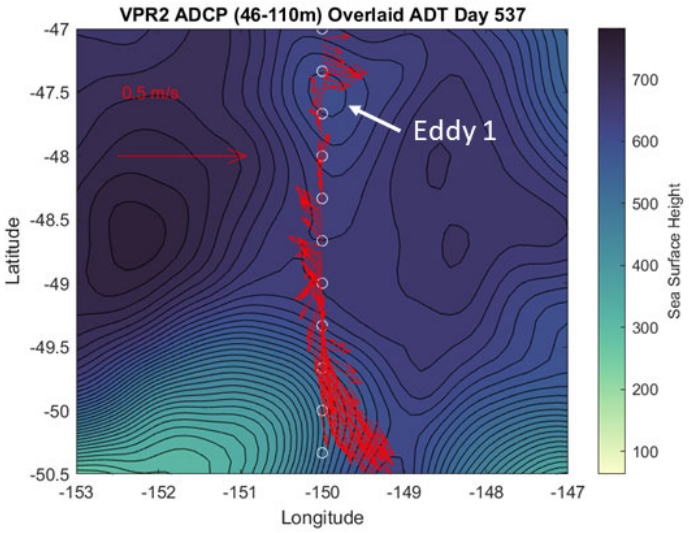

Figure 22. ADCP currents along VPR 2 track.

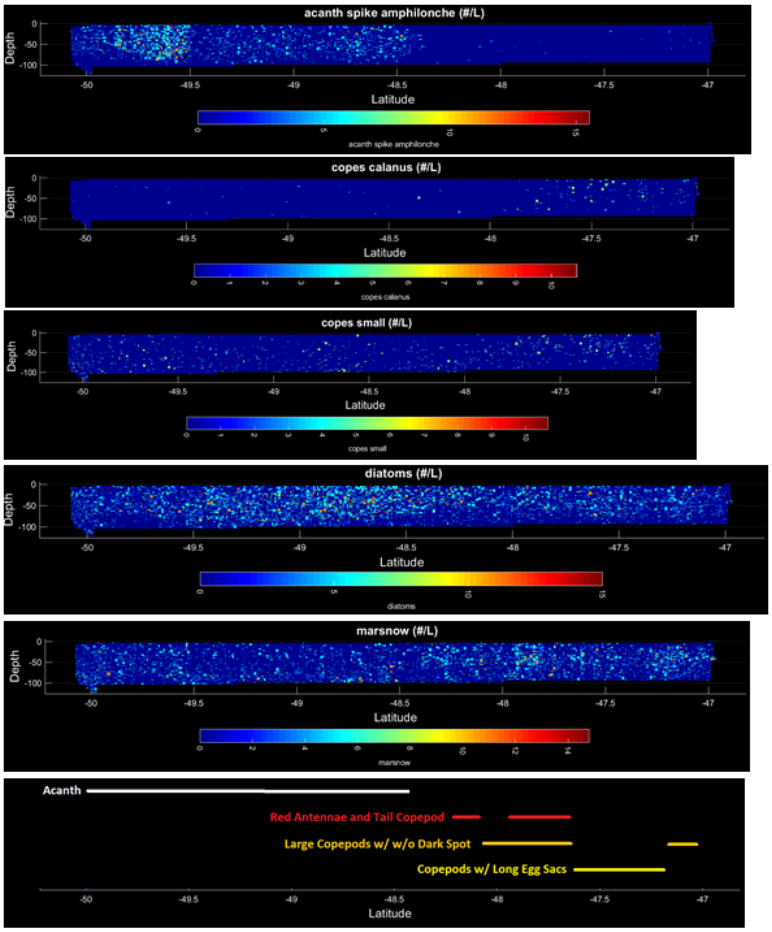

Figure 23. VPR 2 taxa plots (see text).

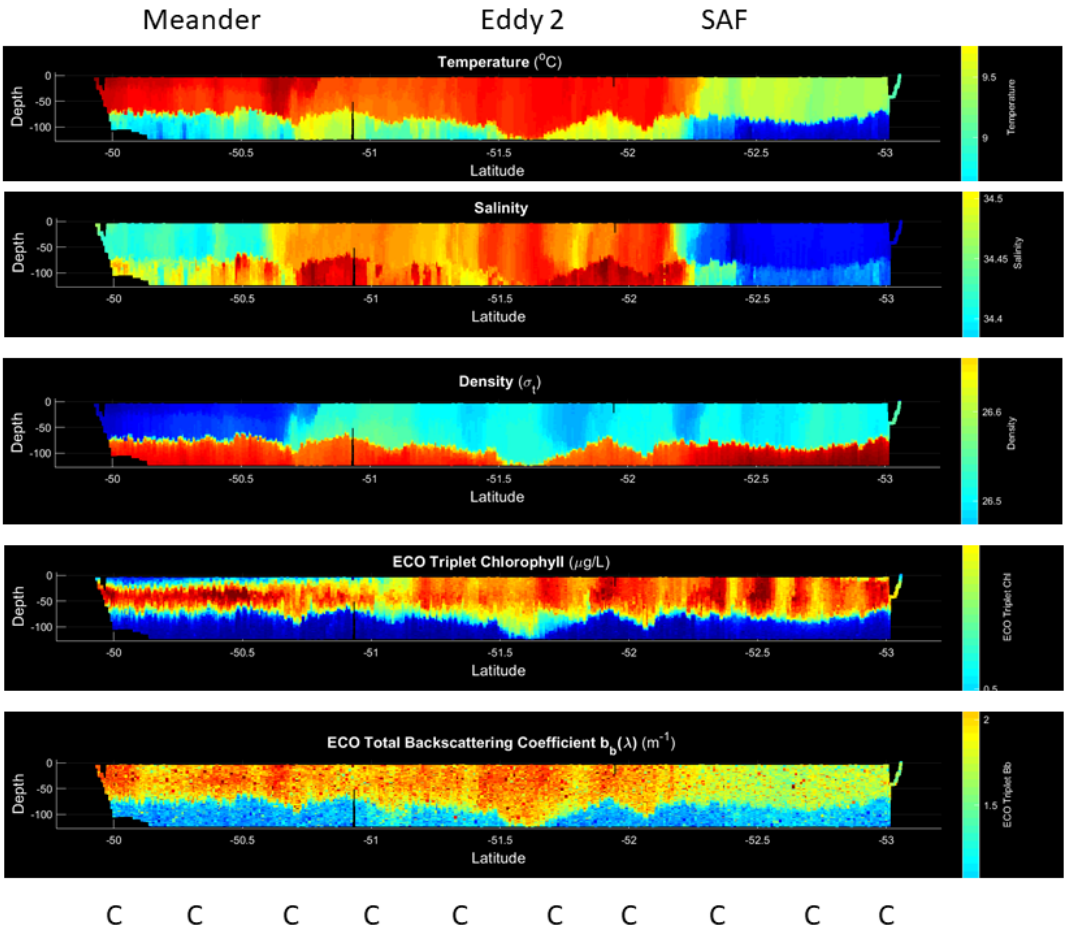

Figure 24. VPR 3 temperature, salinity, density, fluorescence, and backscatter.

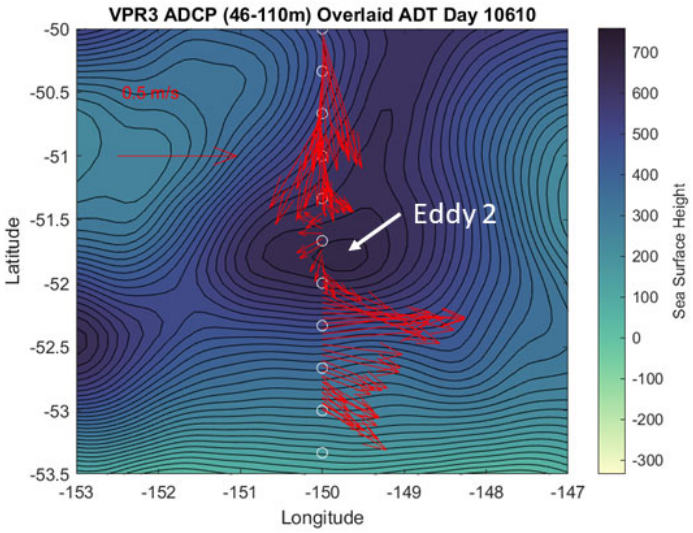

Figure 25. ADCP currents along VPR 3 track.

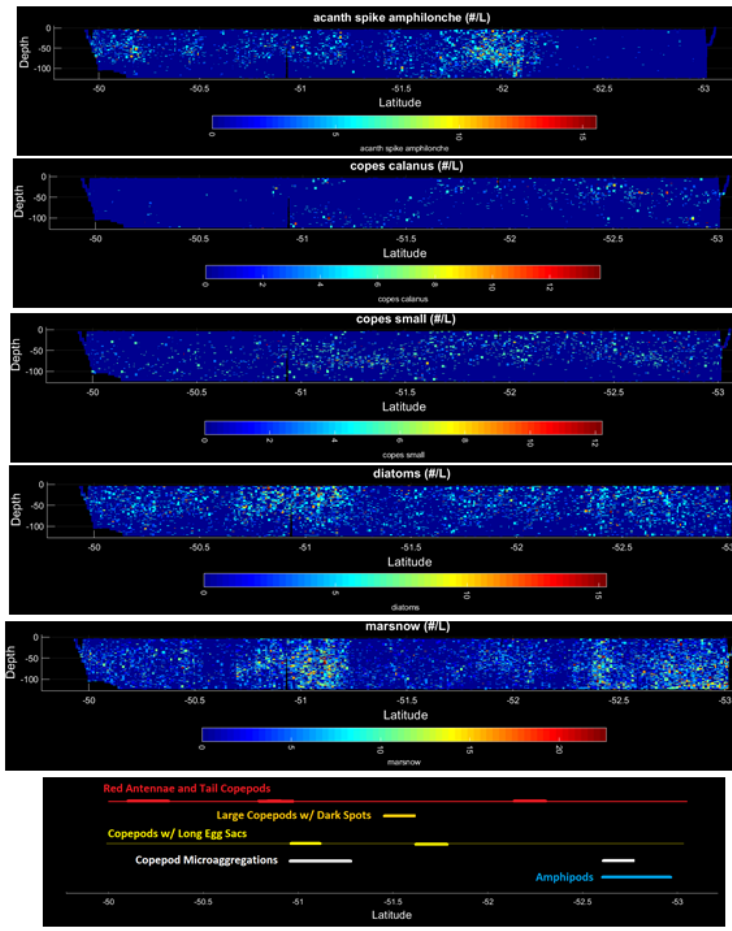

Figure 26. VPR3 taxa plots (see text).

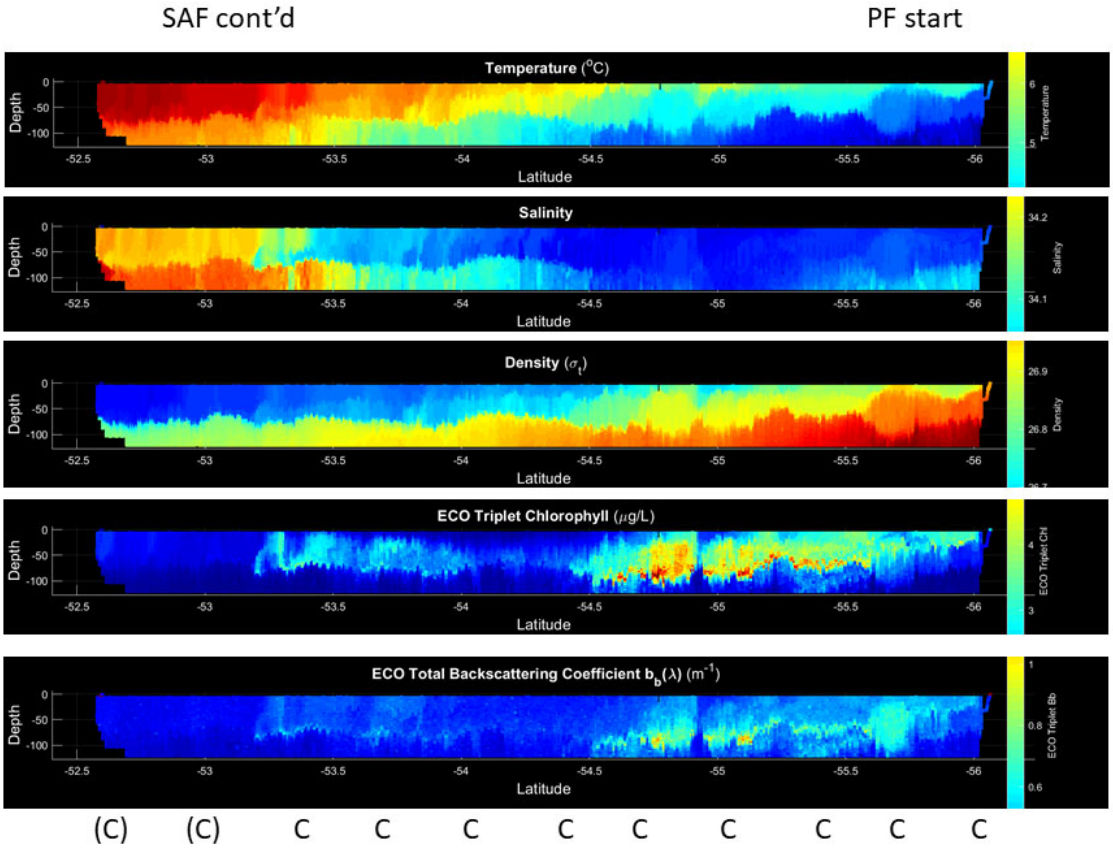

Figure 27. VPR 4 temperature, salinity, density, fluorescence, and backscatter.

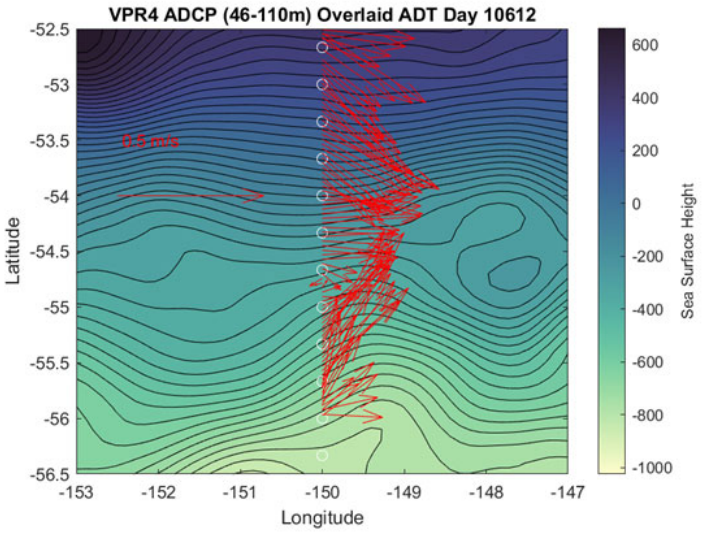

Figure 28. ADCP currents along VPR 4 track.

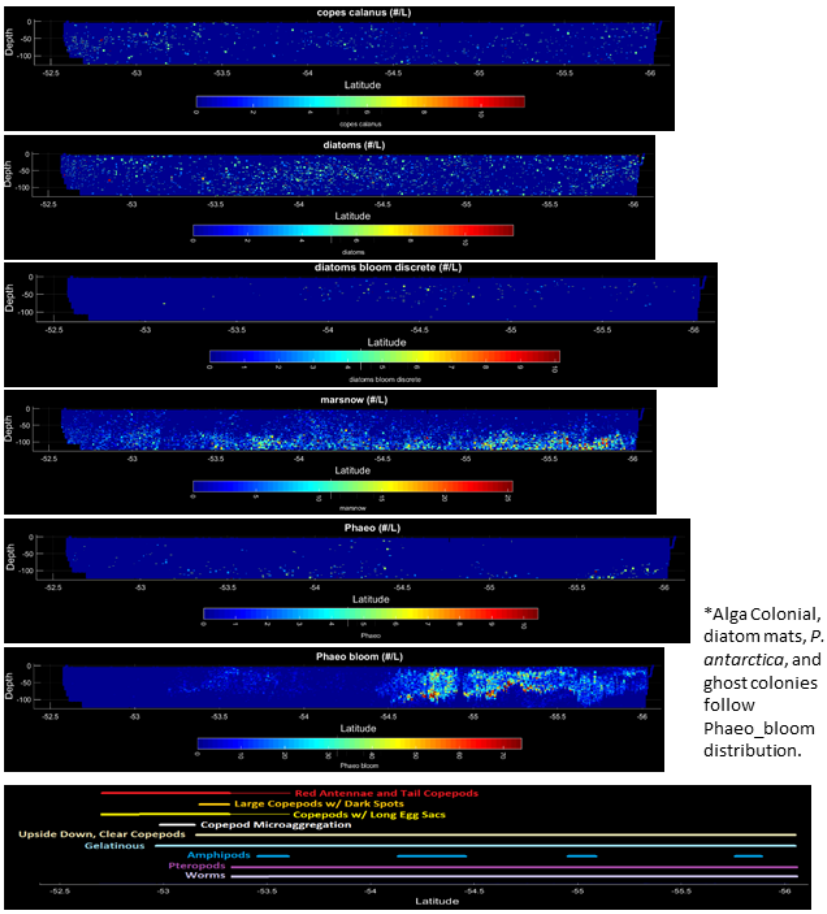

Figure 29. VPR4 taxa plots (see text).

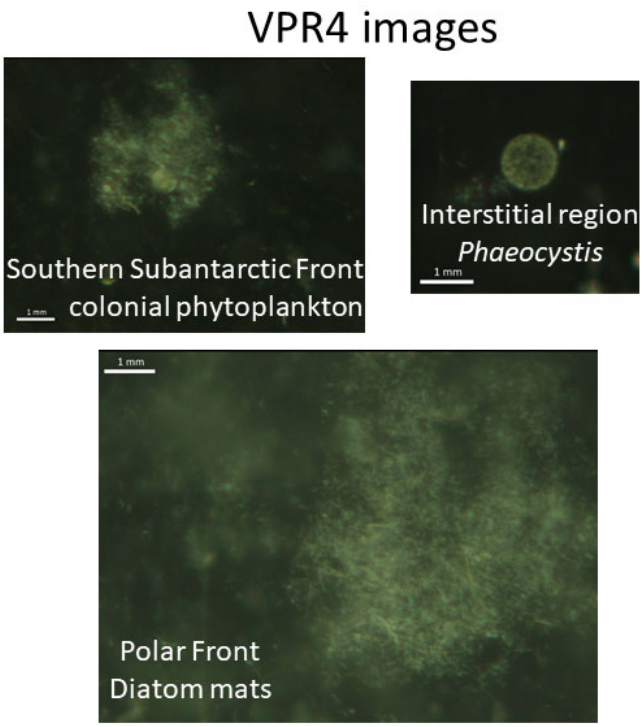

Figure 30. Sample images from VPR 4.

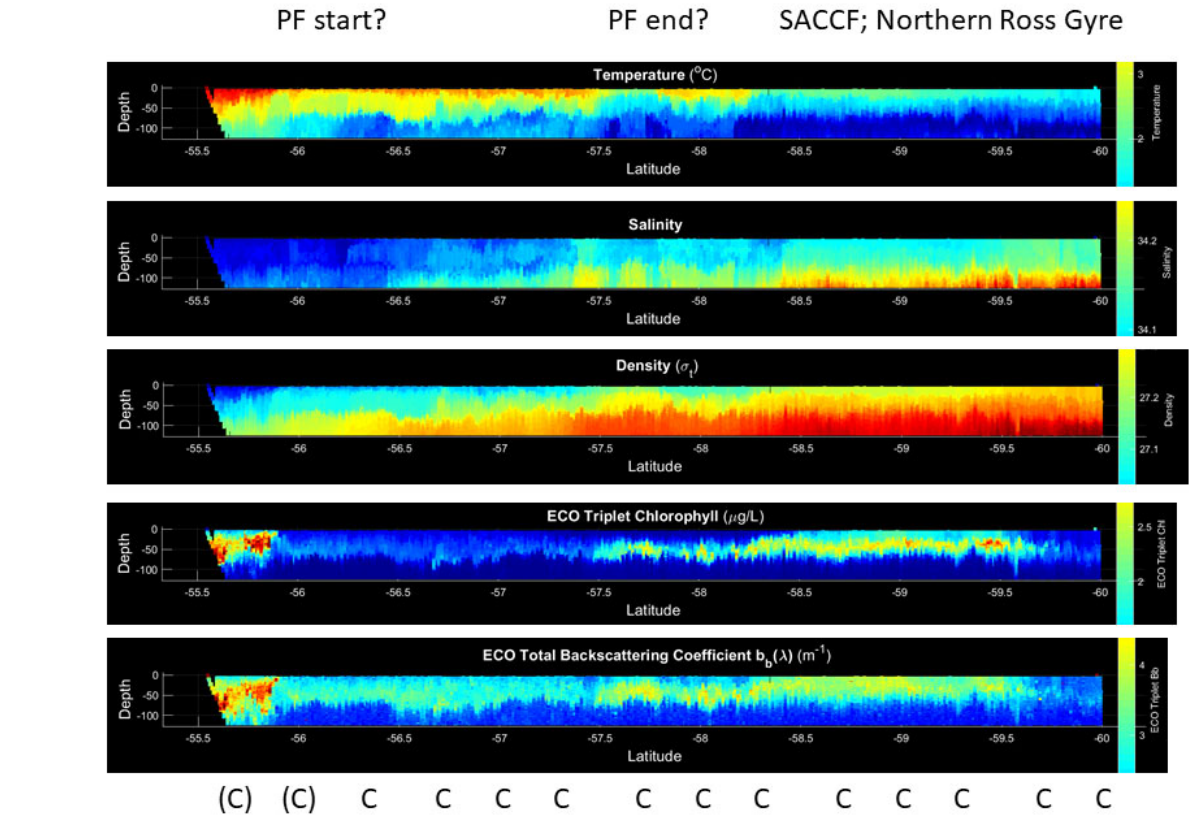

() = second pass through previously occupied stations

Figure 31. VPR 5 temperature, salinity, density, fluorescence, and backscatter.

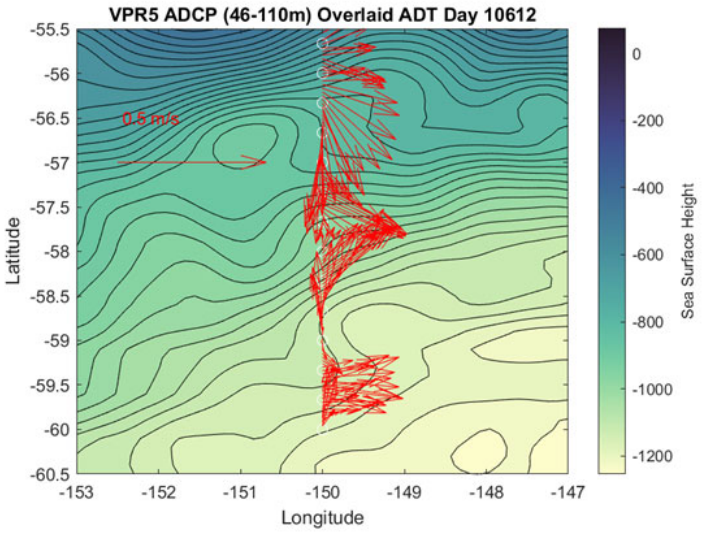

Figure 32. ADCP currents along VPR 5 track.

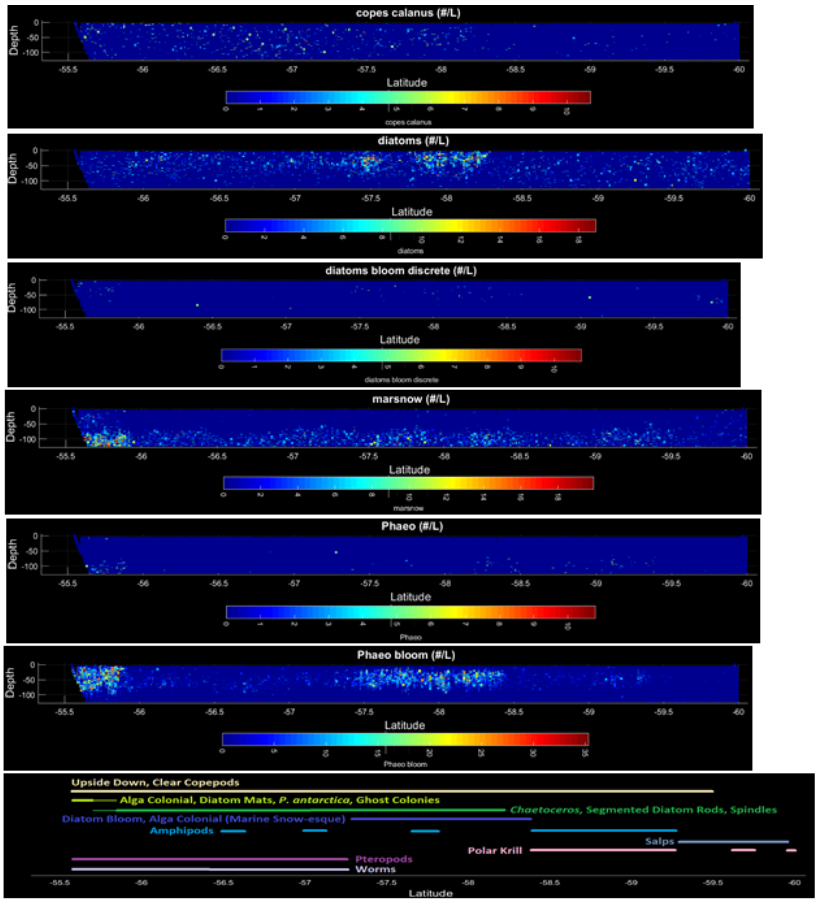

Figure 33. VPR5 taxa plots (see text).

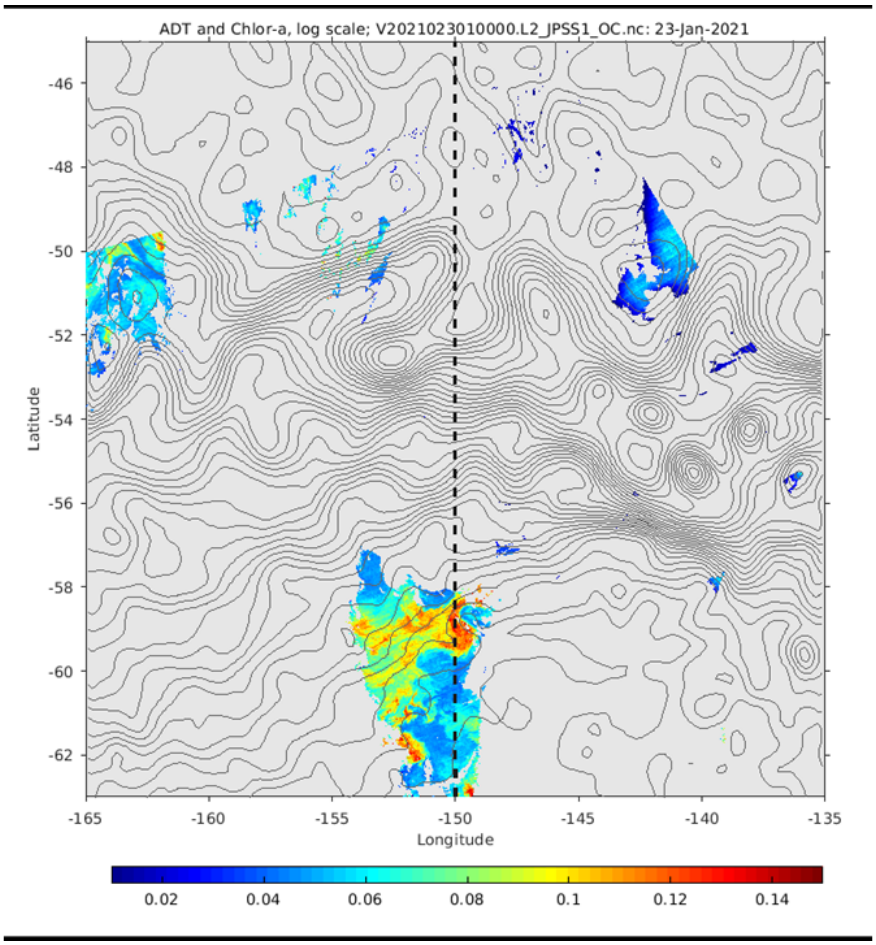

Note high chl / PIC filament 58.5-59.5S consistent with VPR survey

Figure 34. PIC image revealing structure at the Southern ACC Front.

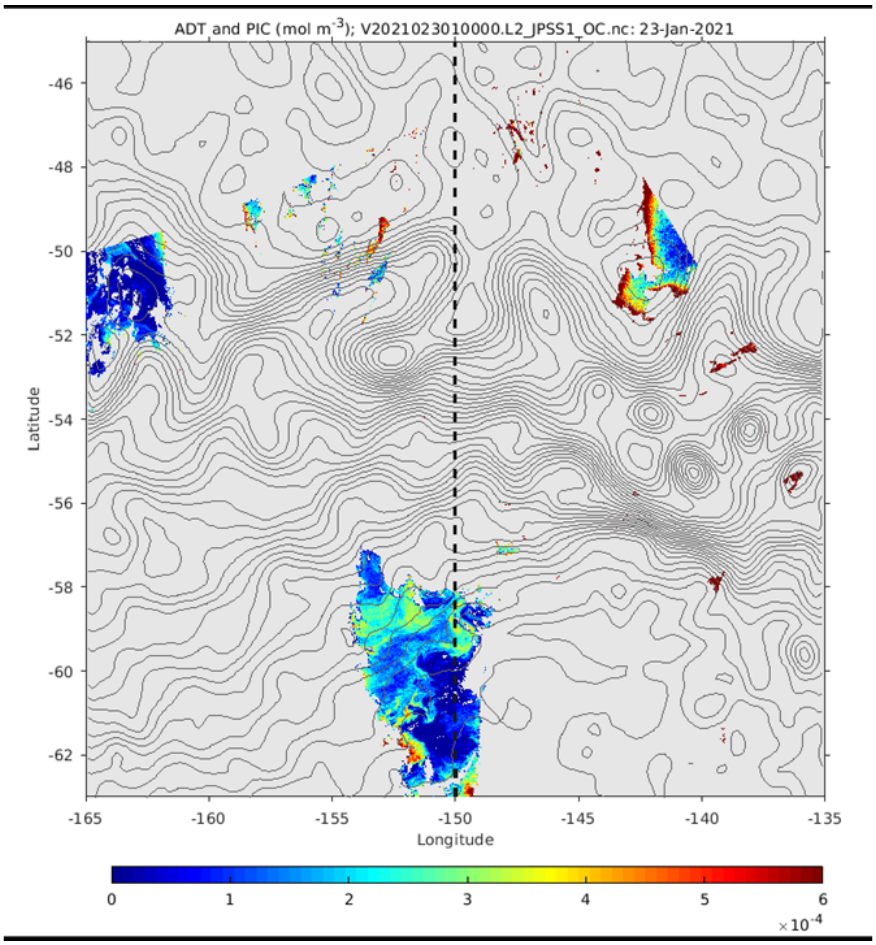

Figure 35. Chlorophyll image revealing structure at the Southern ACC Front.

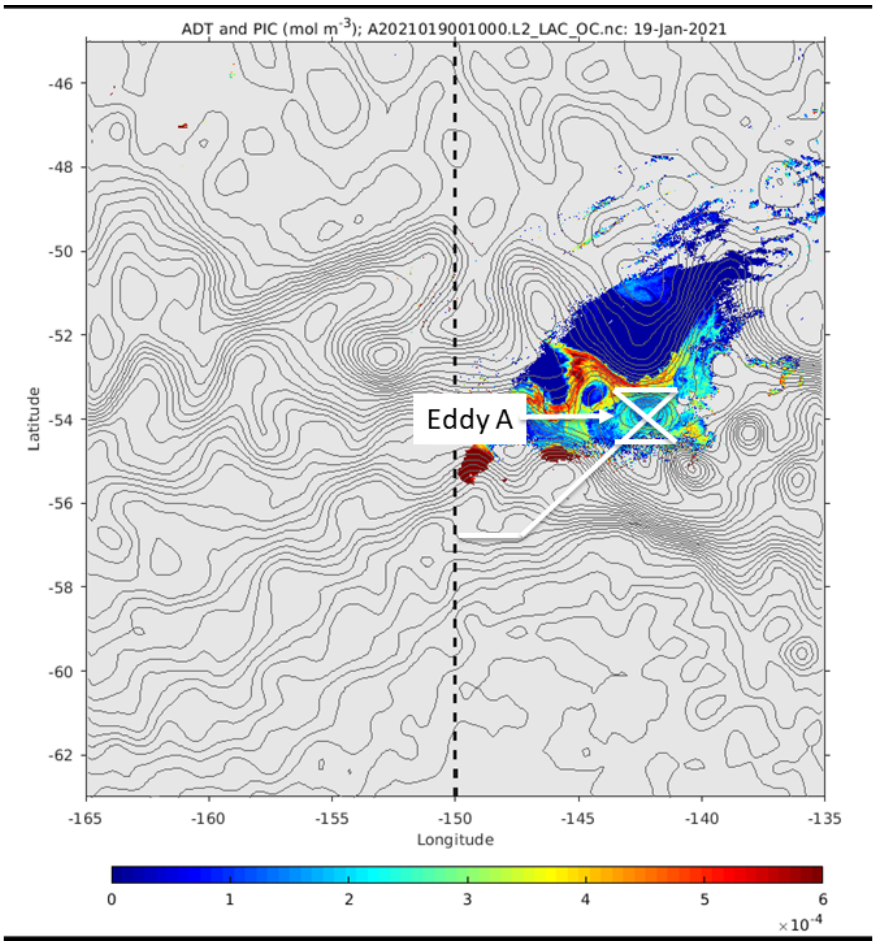

Figure 36. VPR 6, 7, [8], 9 tracks with contours of ADT and PIC indicated in color.

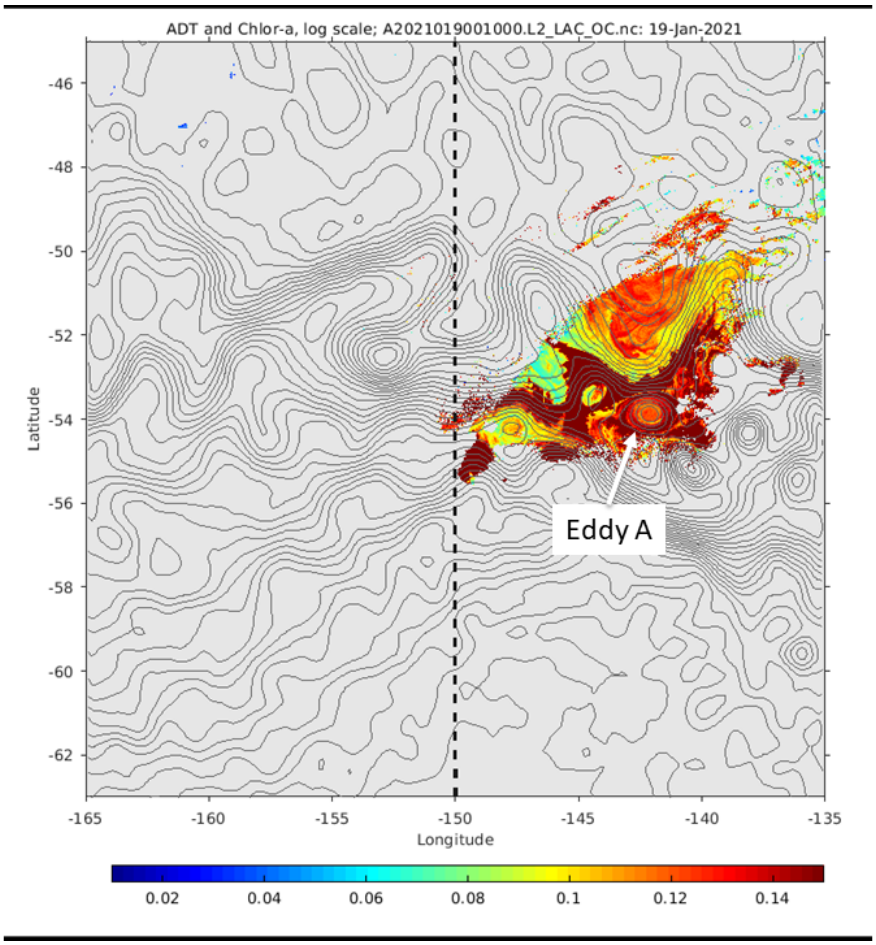

Figure 37. VPR 6, 7, [8], 9 tracks with contours of ADT and chlorophyll indicated in color.

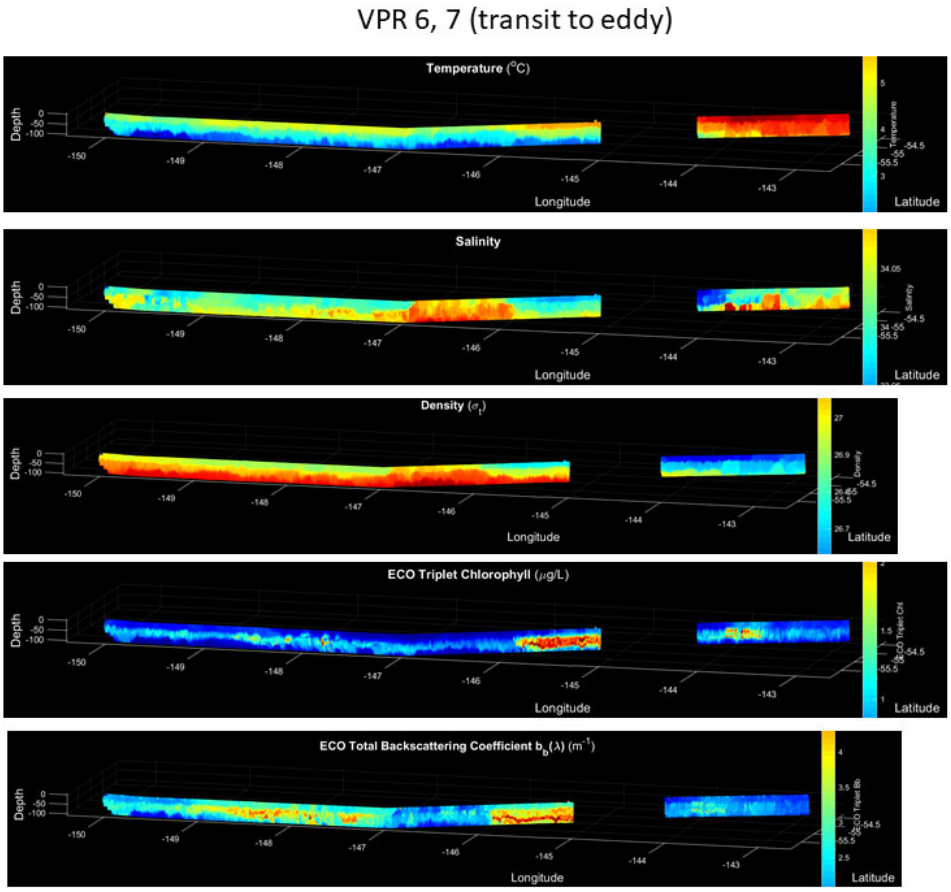

Figure 38. VPR 6, 7 (partial) temperature, salinity, density, fluorescence, and backscatter.

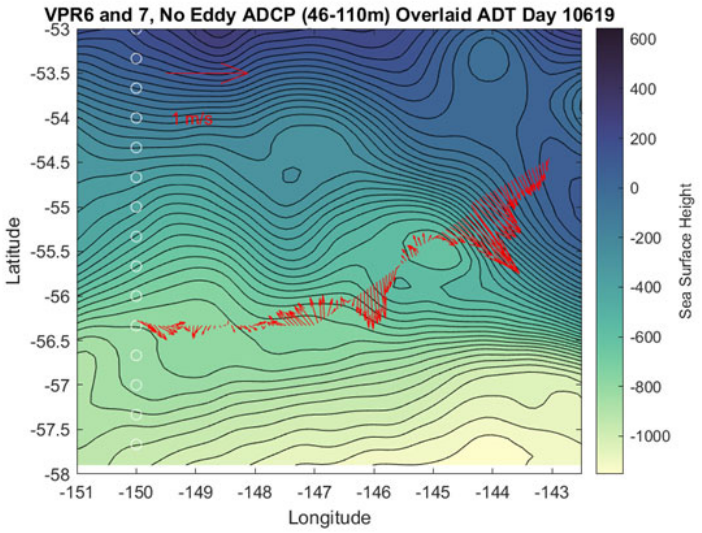

Figure 39. ADCP currents along VPR 6,7 (partial) tracks.

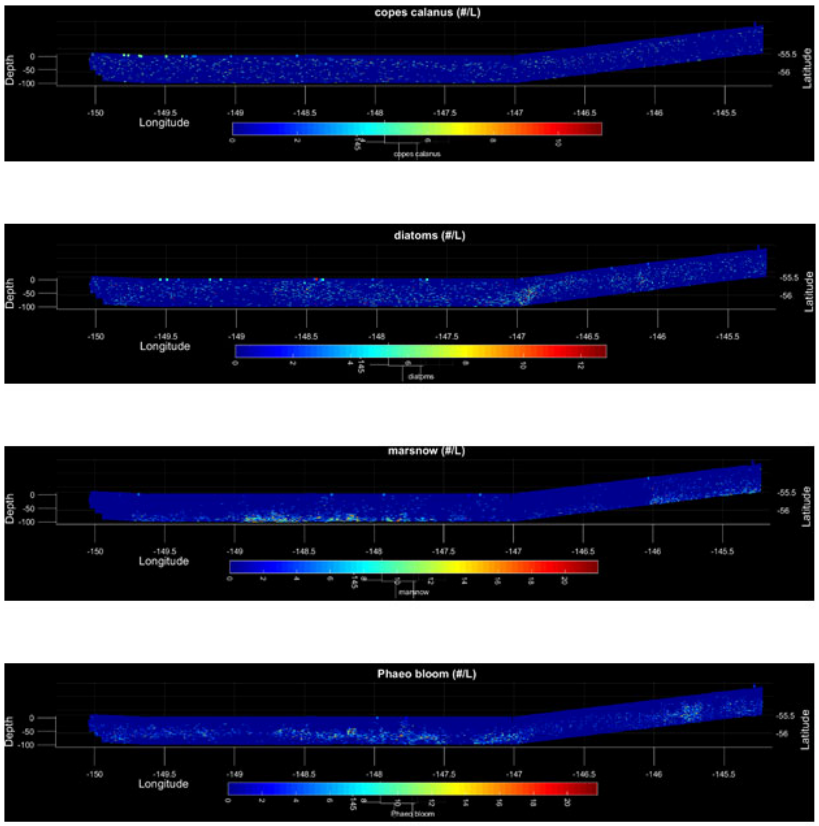

Figure 40. Taxon plots for VPR 6. Note that the strobe failed and so ROIs were not available for VPR 7; only the hydrographic and bio-optical data for VPR 7 are shown in Figure 38.

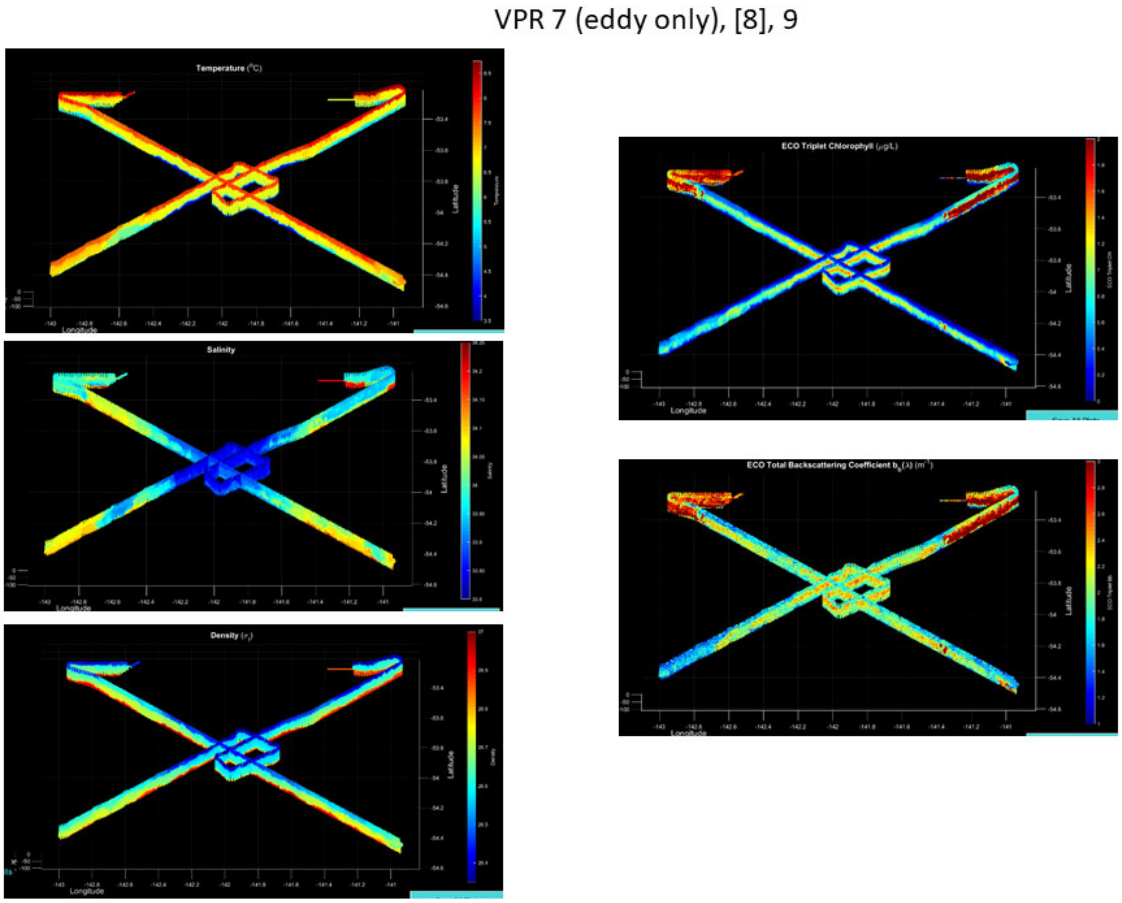

Figure 41. VPR 7 (partial), [8], and 9 temperature, salinity, density, fluorescence, and backscatter.

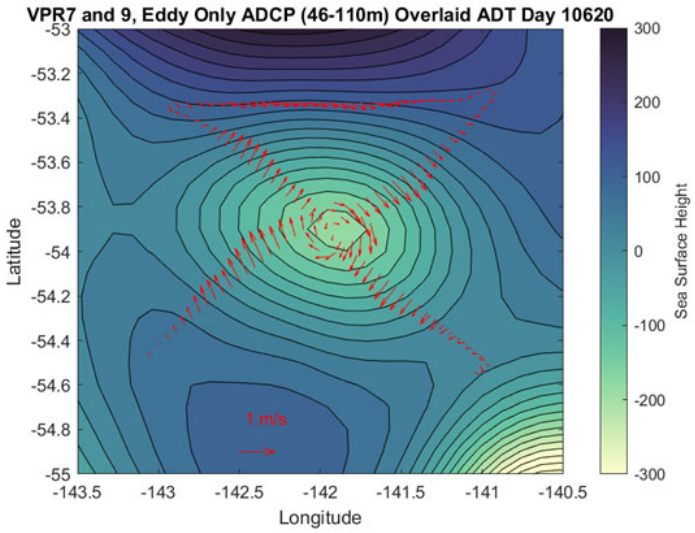

Figure 42. ADCP currents along VPR 7 (partial), [8], and 9 tracks.

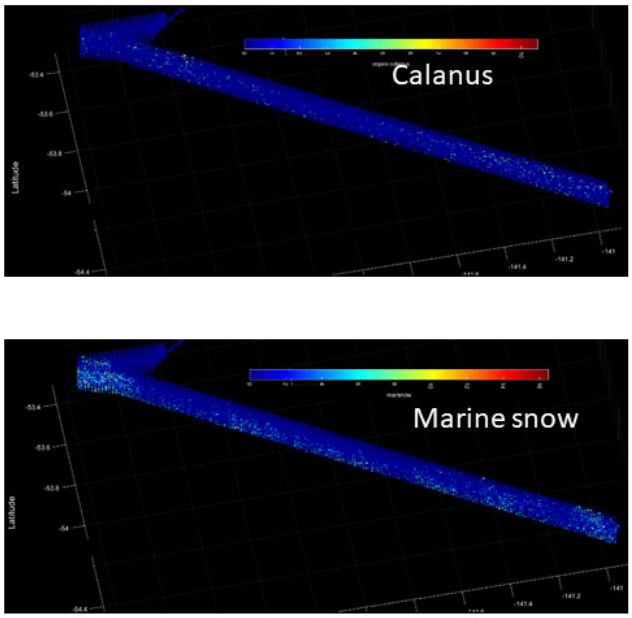

Figure 43. Taxon plots for VPR 9, turning southeast at the northwest corner of Eddy A.

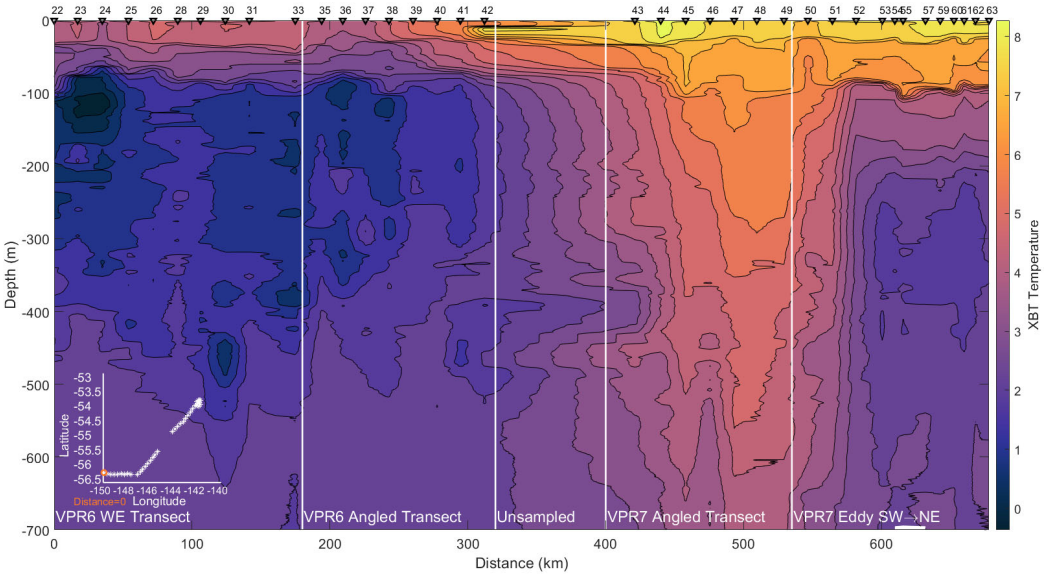

Figure 44. XBT survey used to help locate the center of Eddy A.

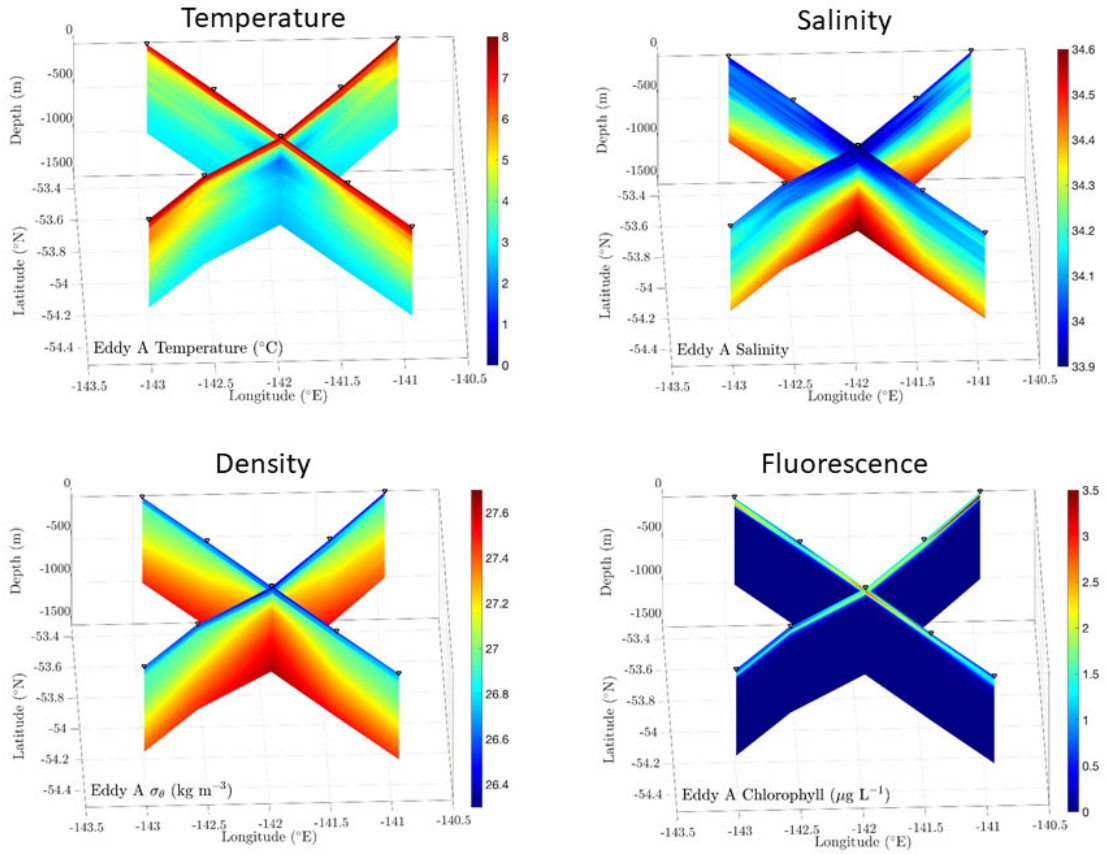

Figure 45. CTD cross sections of Eddy A: temperature, salinity, density, and fluorescence.

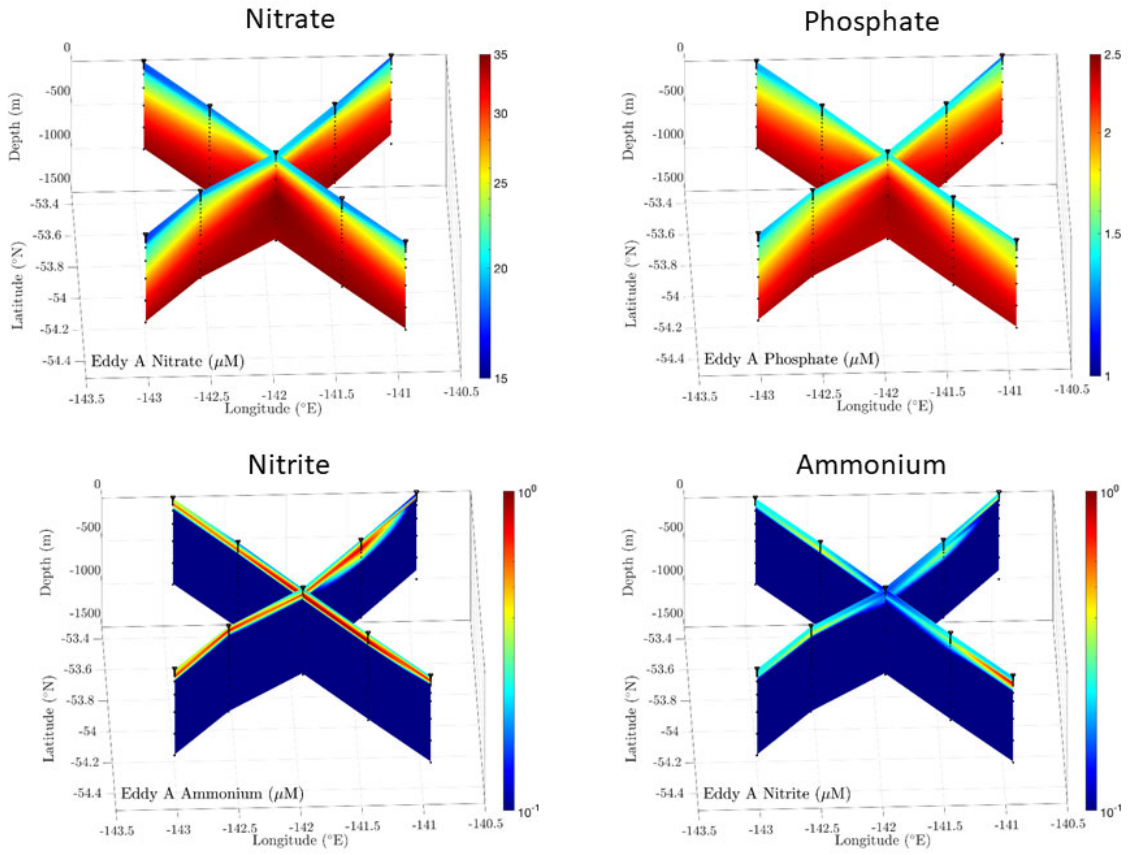

Figure 46. CTD cross sections of Eddy A: nitrate, phosphate, nitrite, and ammonium.

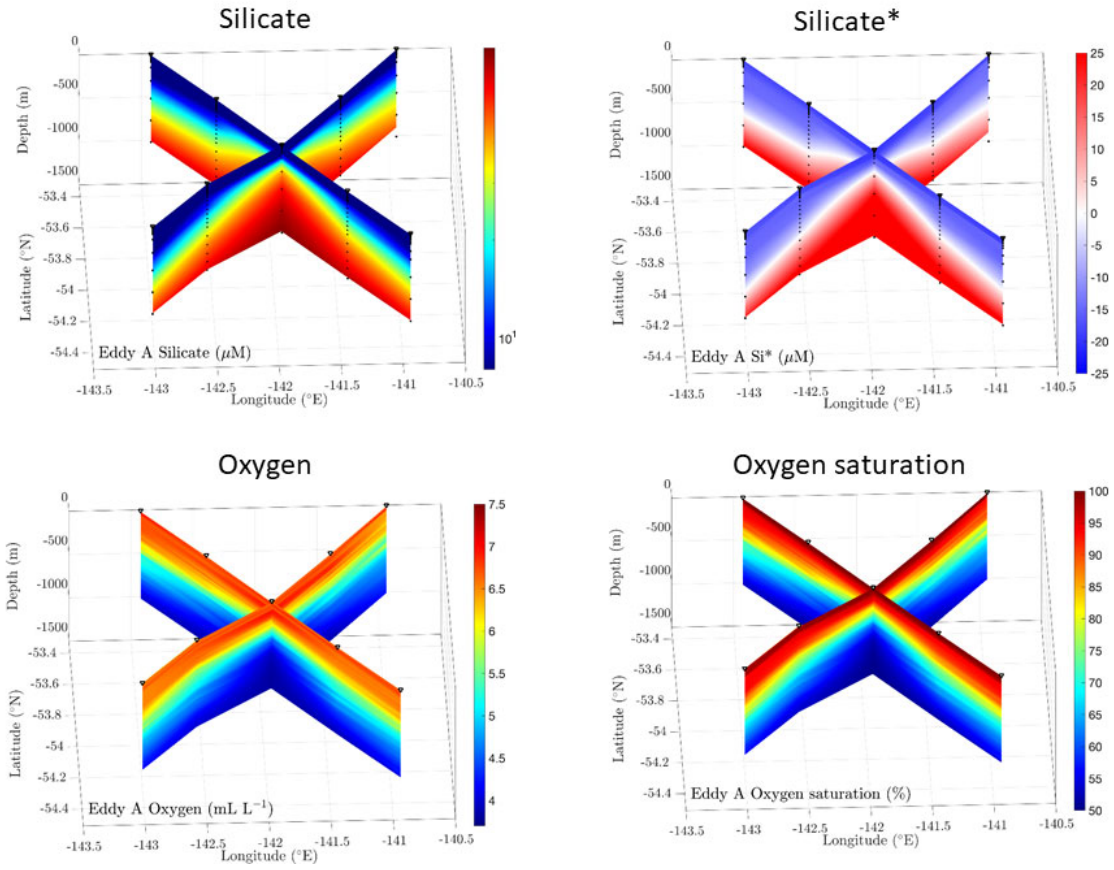

Figure 47. CTD cross sections of Eddy A: silicate, silicate, oxygen, and oxygen saturation.*

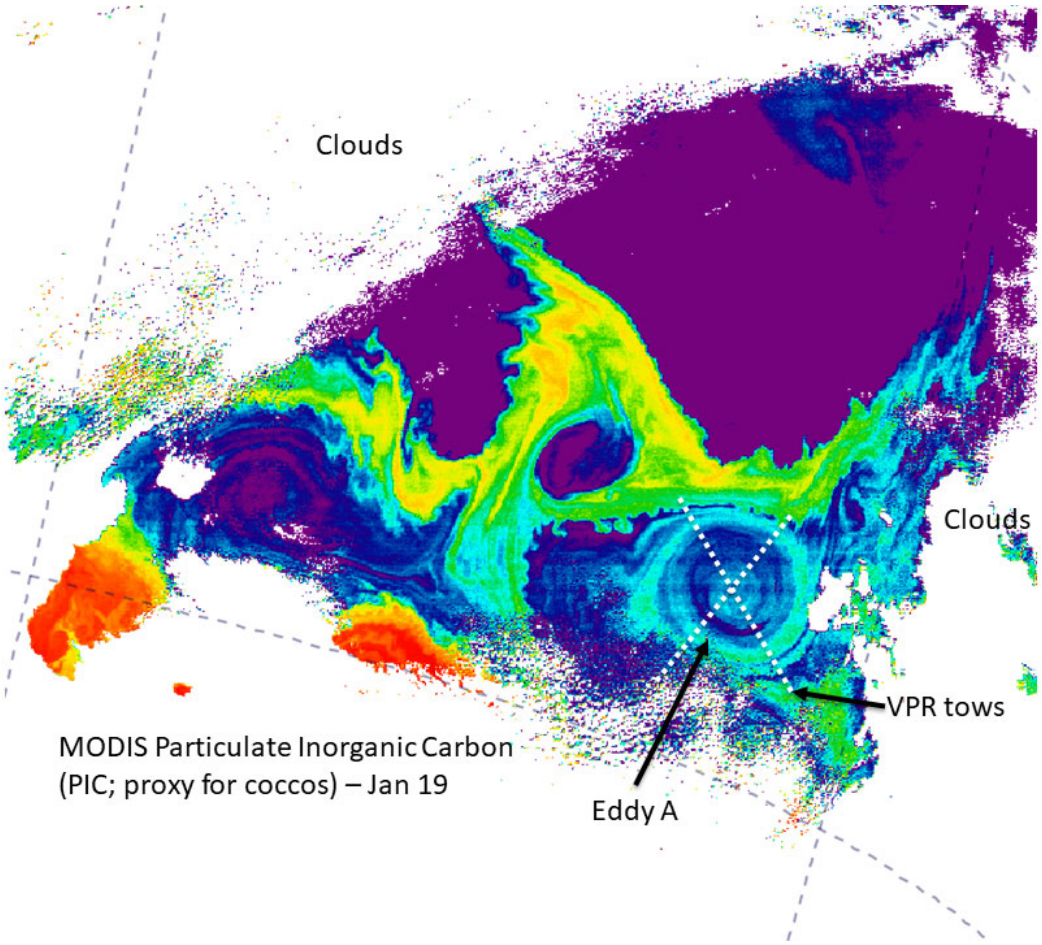

Figure 48. High resolution PIC image of Eddy A.

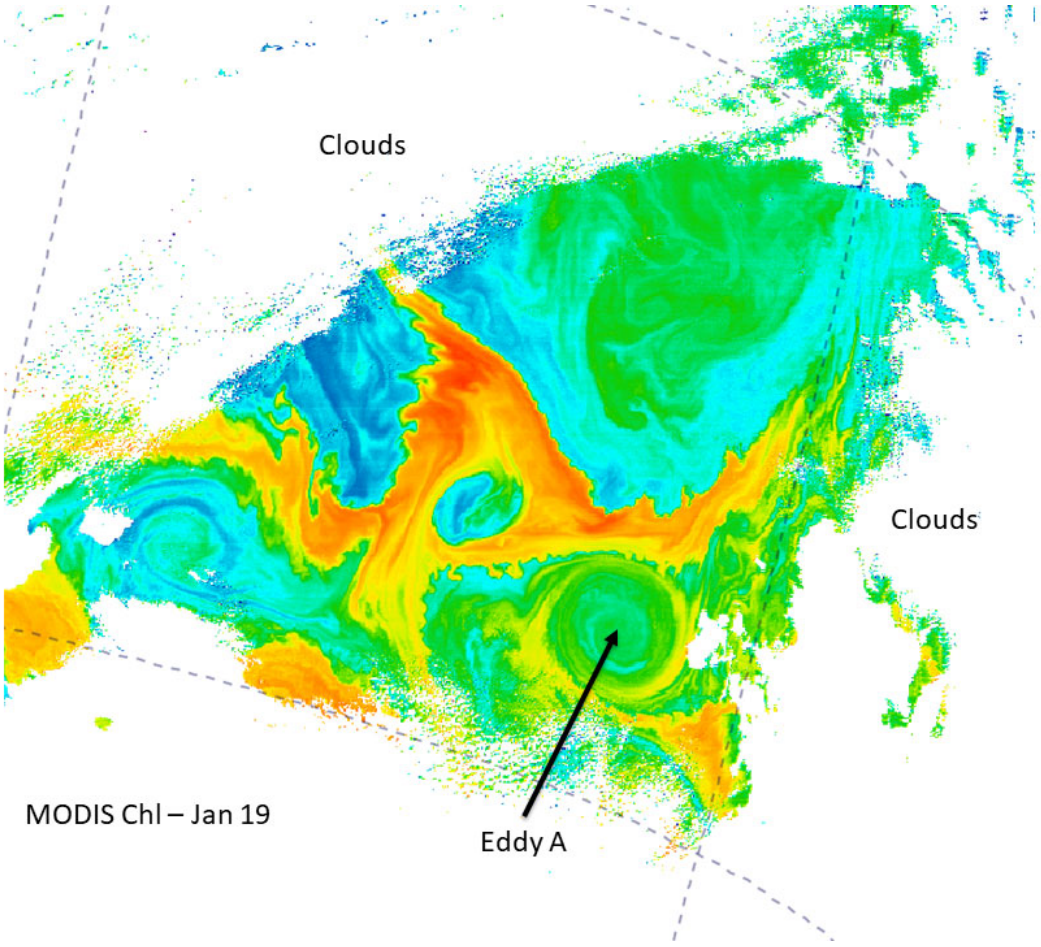

Figure 49. High resolution chlorophyll image of Eddy A.

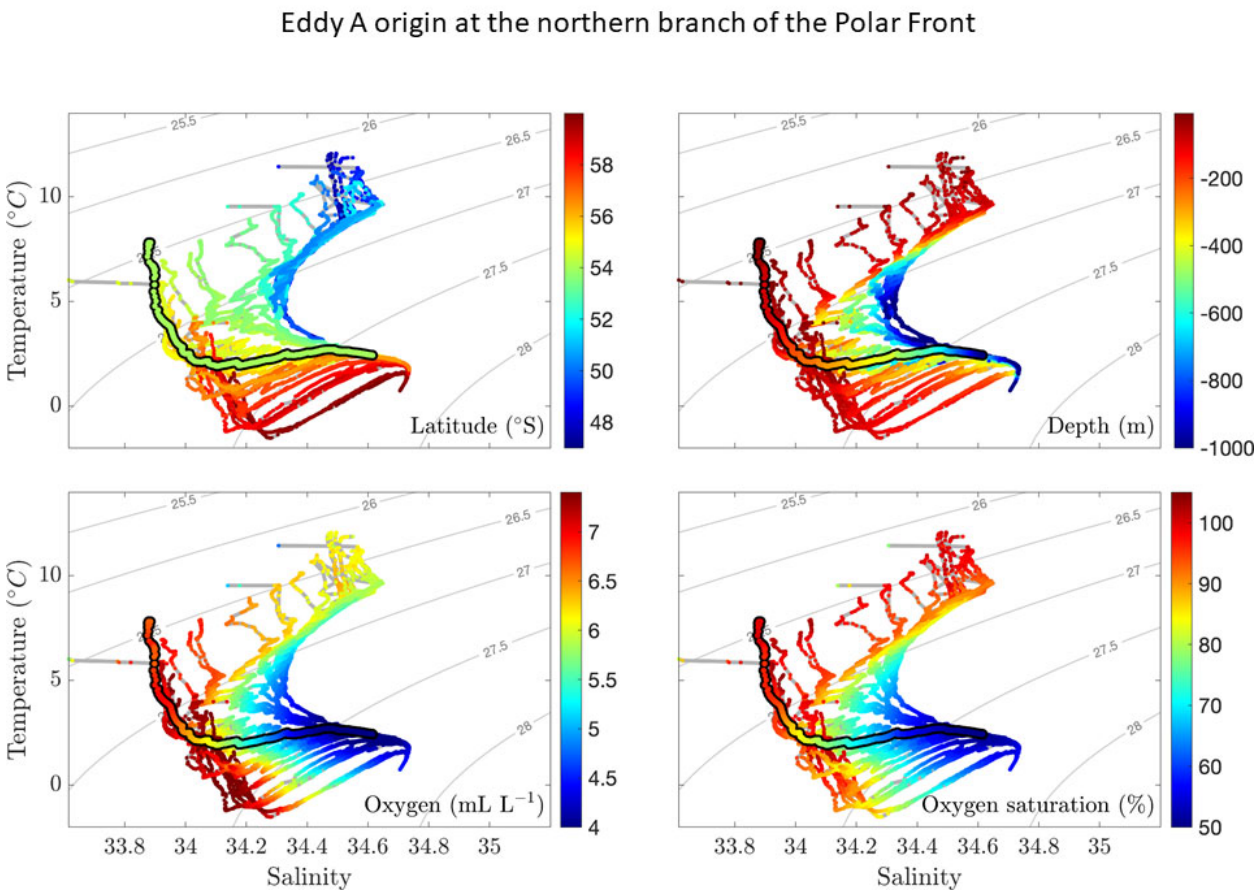

Figure 50. Temperature - salinity characteristics from Eddy A center (green) superimposed on those from the meridional transect.

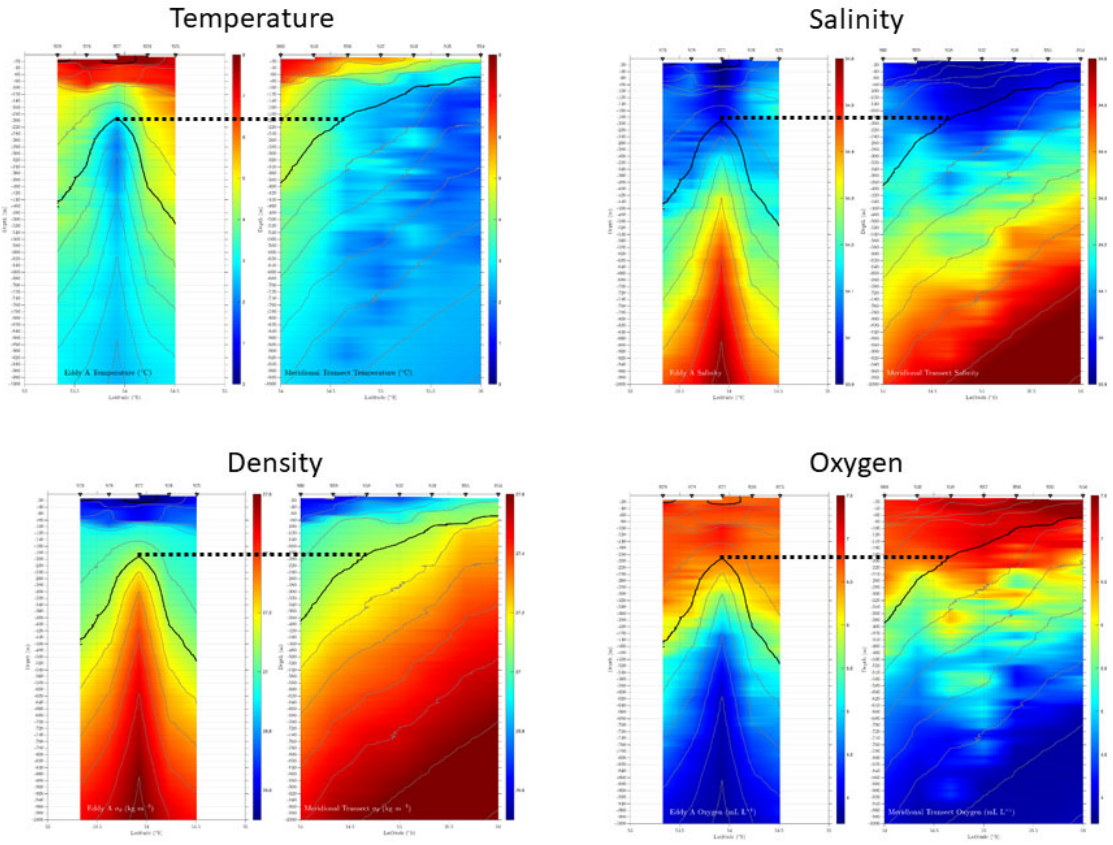

Figure 51. Cross-sections of temperature, salinity, density, and oxygen in Eddy A (left) versus the meridional transect (right). Horizontal line connects the peak in the 27.1 isopycnal (lighter bound of SAMW) within Eddy A to its level in the meridional transect.

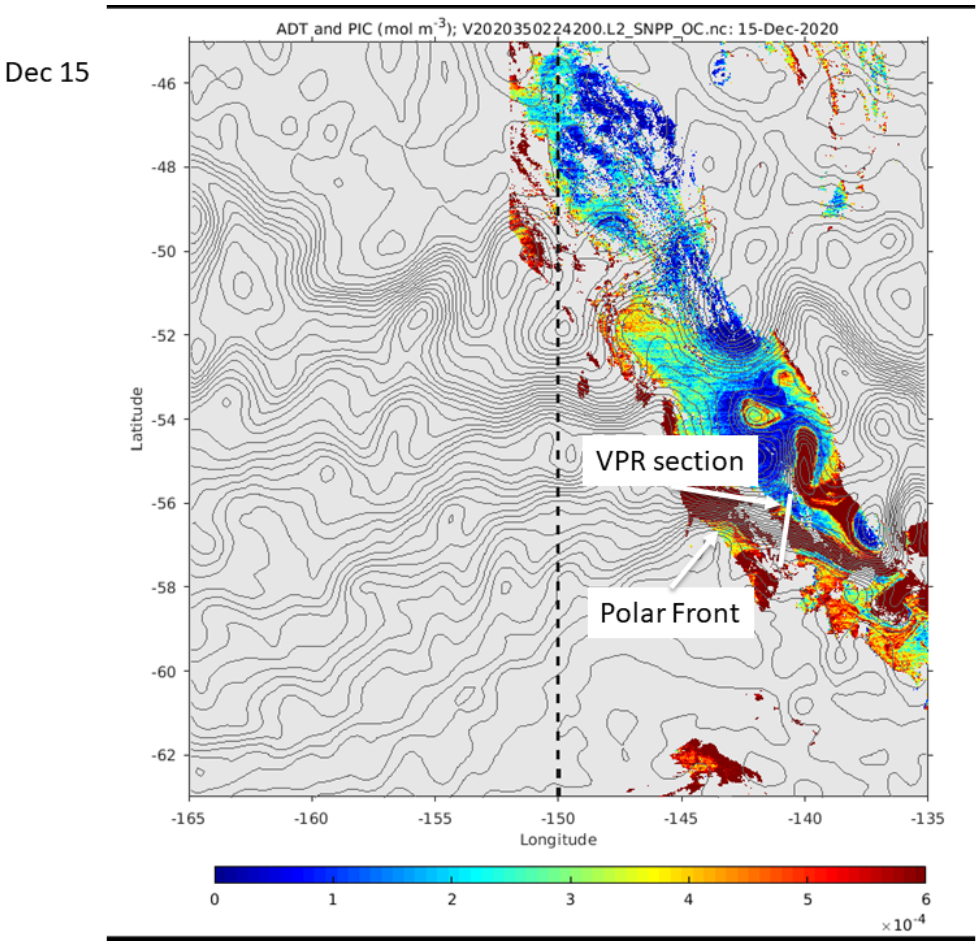

Figure 52. VPR 10 section across the Polar Front at 141W with contours of ADT and PIC indicated in color (image from 15 December 2020).

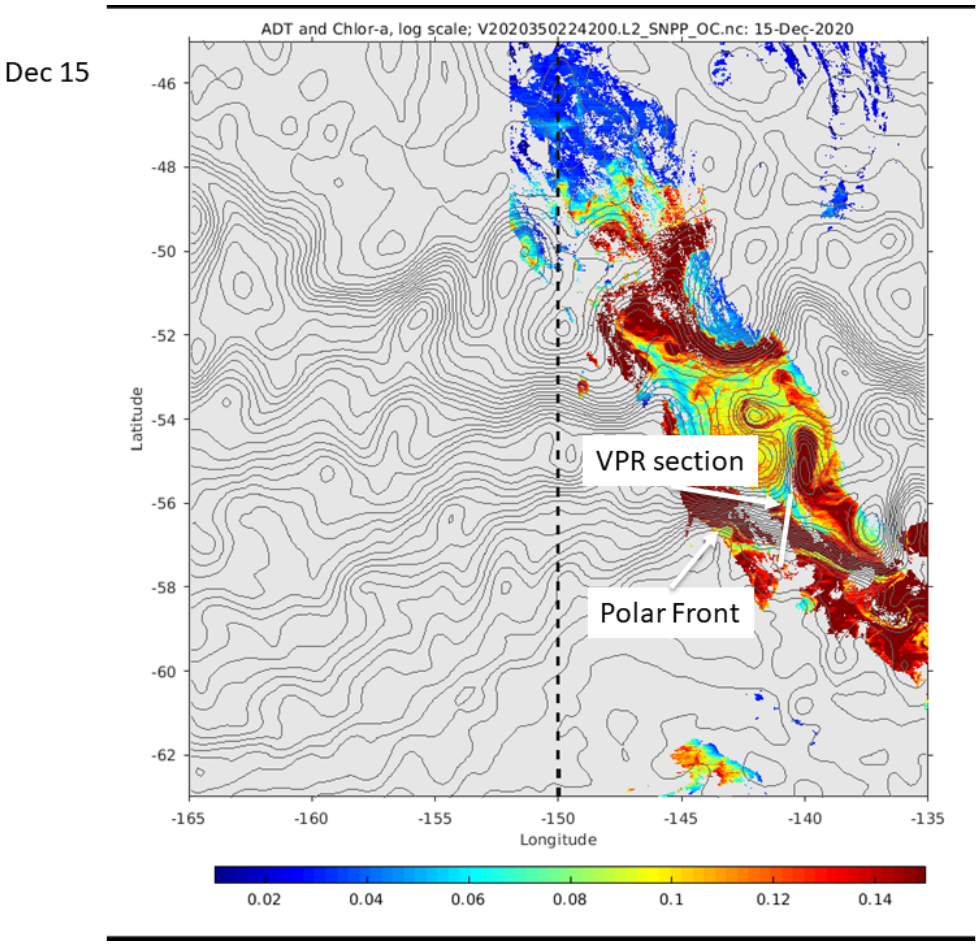

Figure 53. VPR 10 section across the Polar Front at 141W with contours of ADT and chlorophyll indicated in color (image from 15 December 2020).

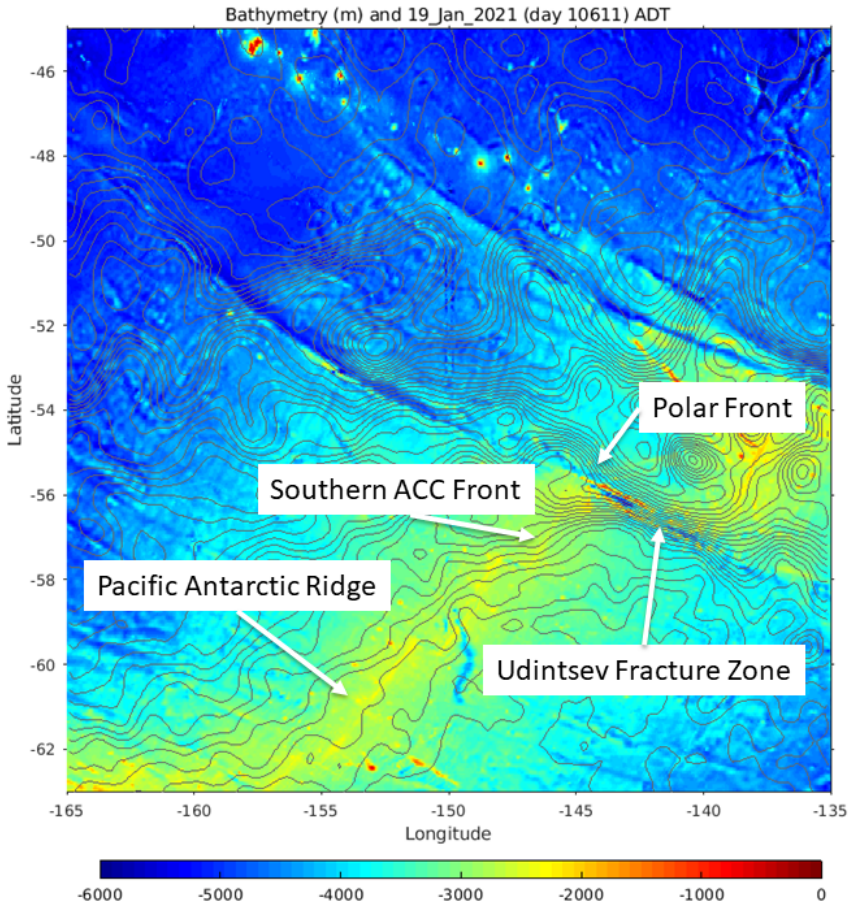

Figure 54. Contours of ADT overlaid on bathymetry.

Feb 2

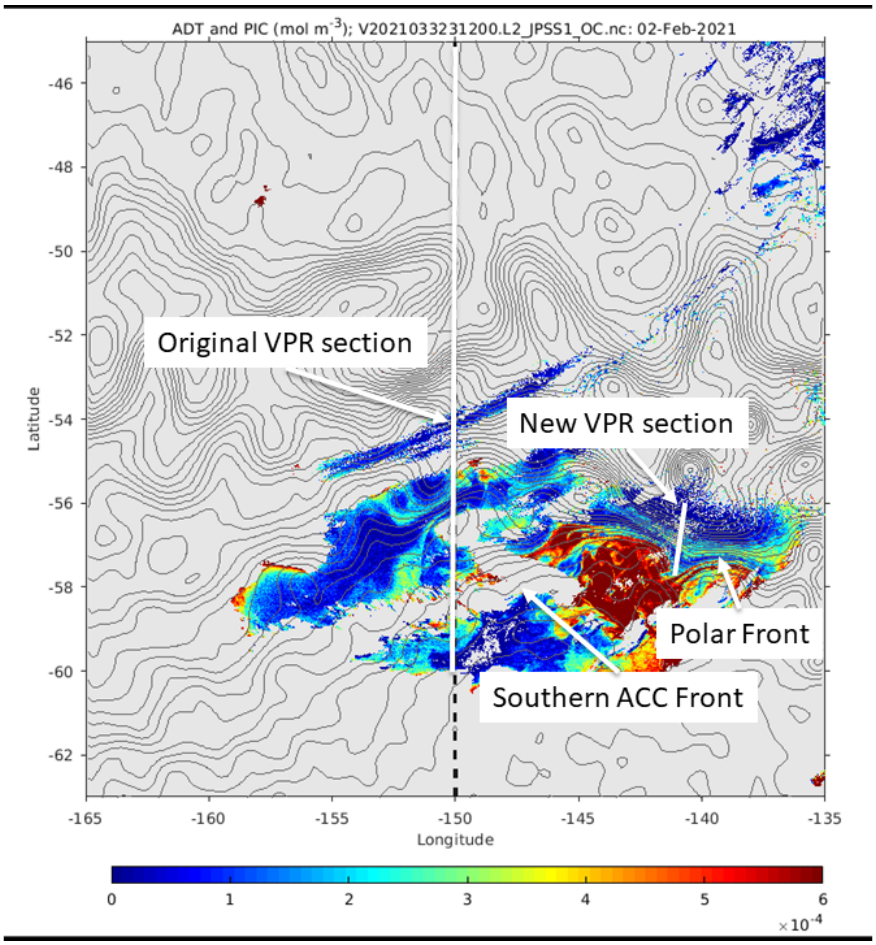

Figure 55. VPR 10 section across the Polar Front at 141W with contours of ADT and PIC indicated in color (image from 2 February 2021).

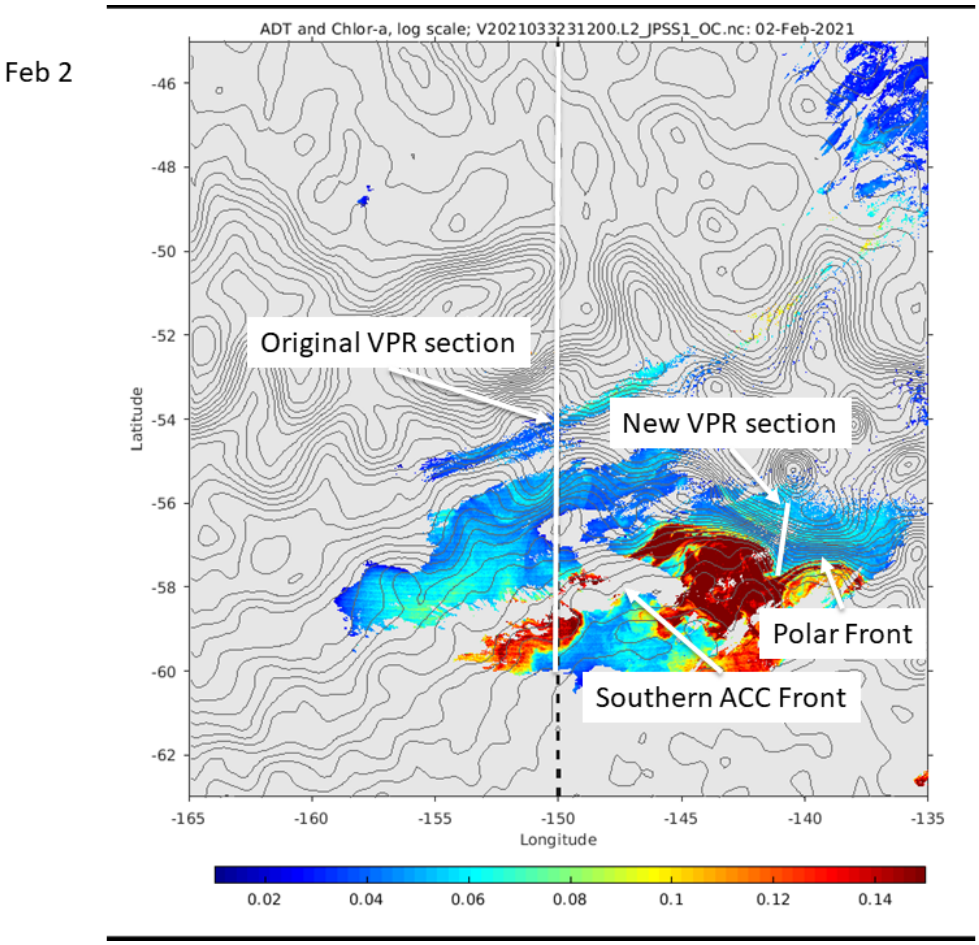

Figure 56. VPR 10 section across the Polar Front at 141W with contours of ADT and chlorophyll indicated in color (image from 2 February 2021).

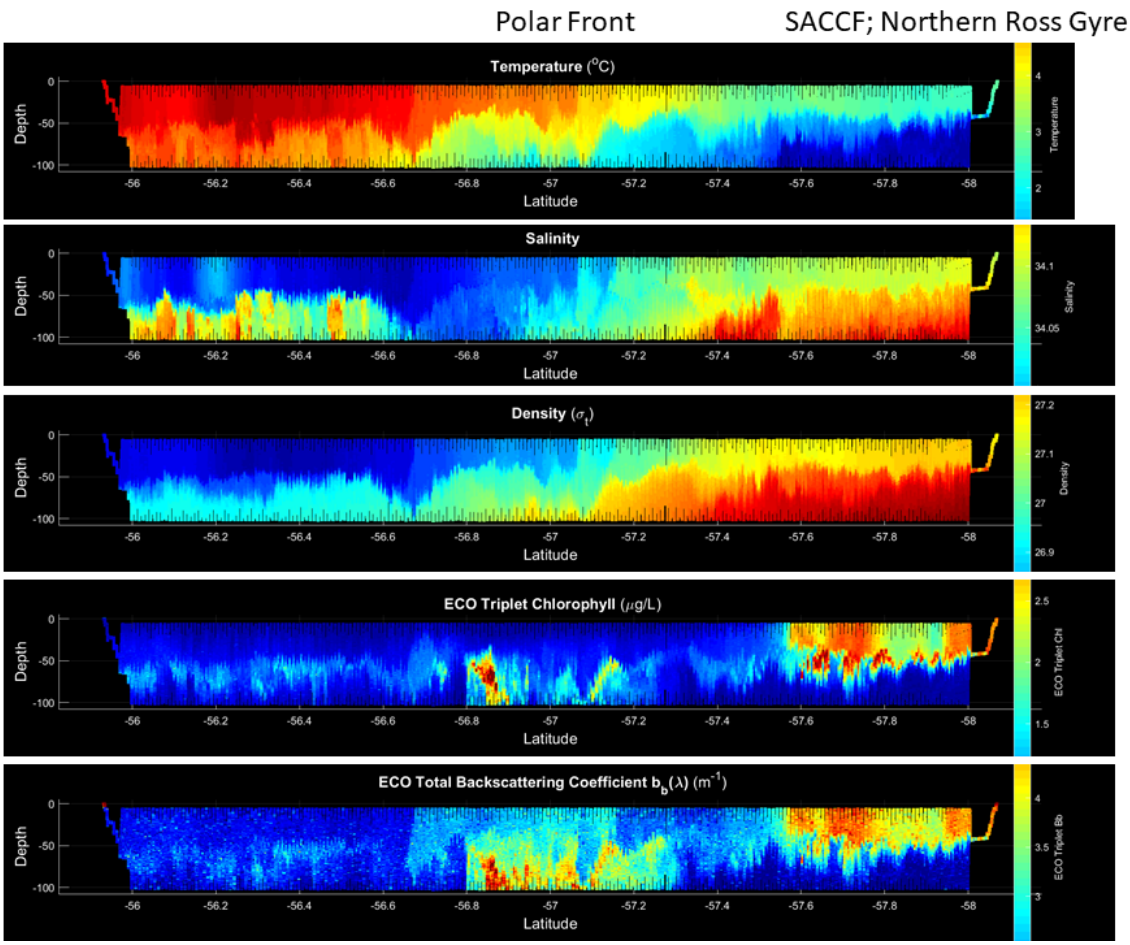

Figure 57. VPR 10 temperature, salinity, density, fluorescence, and backscatter.

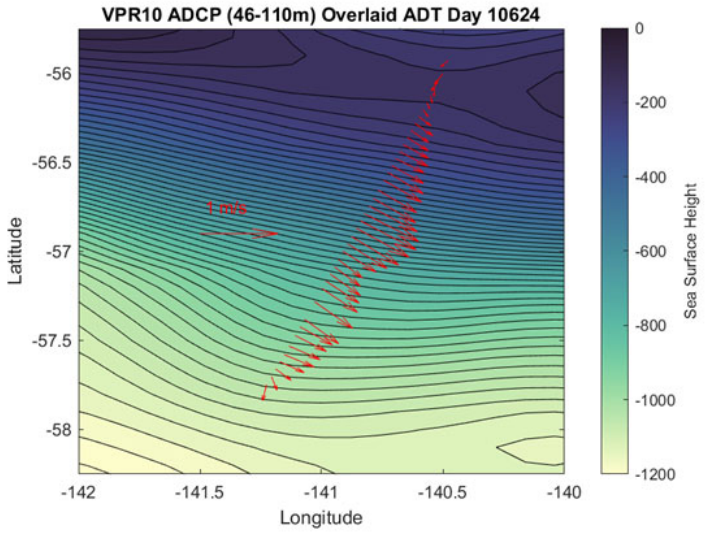

Figure 58. ADCP currents along VPR 10 track.

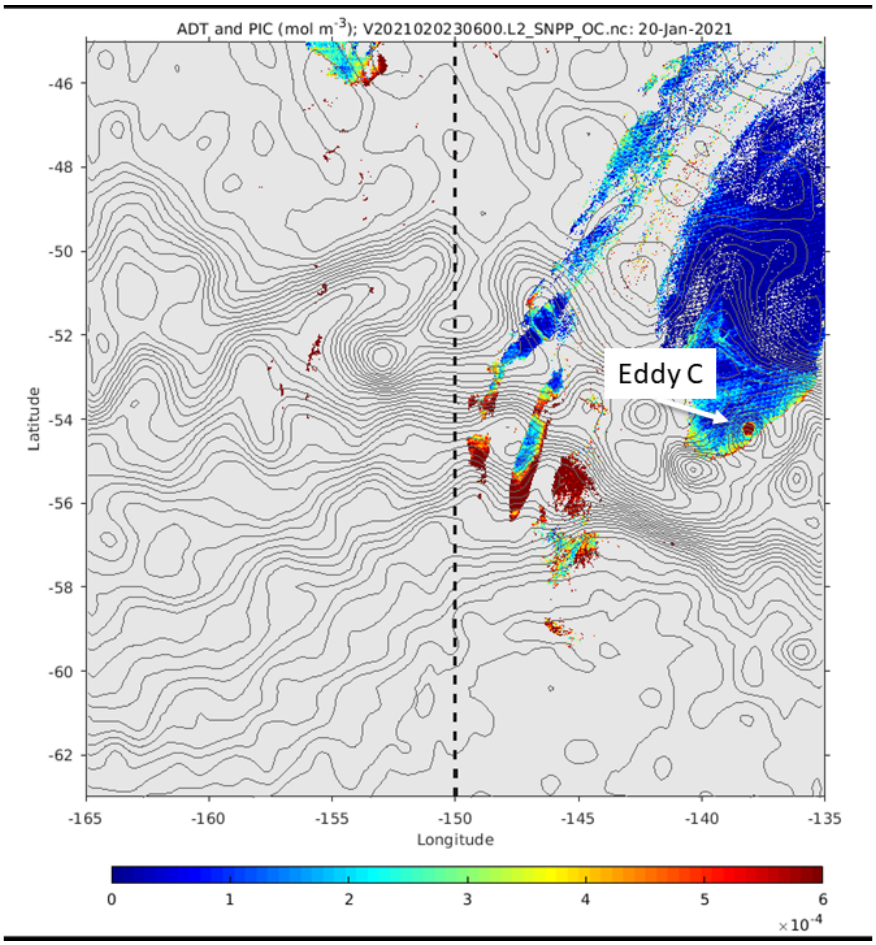

Figure 59. PIC image from 20 January highlighting Eddy C.

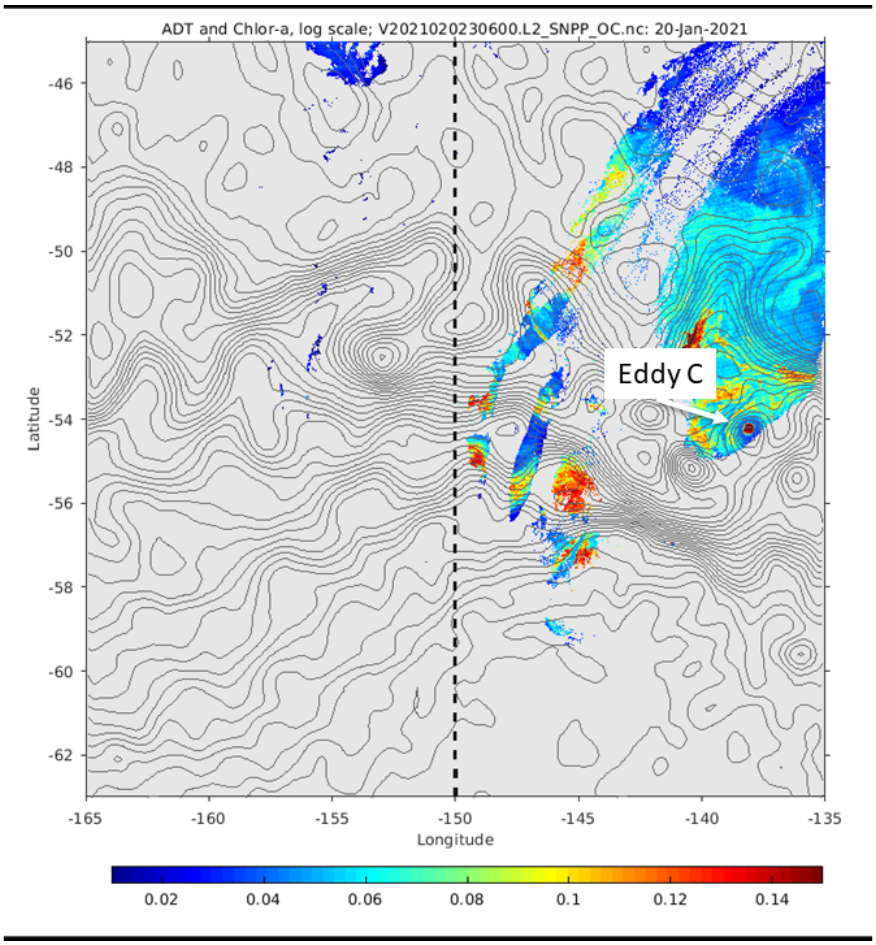

Figure 60. Chlorophyll image from 20 January highlighting Eddy C.

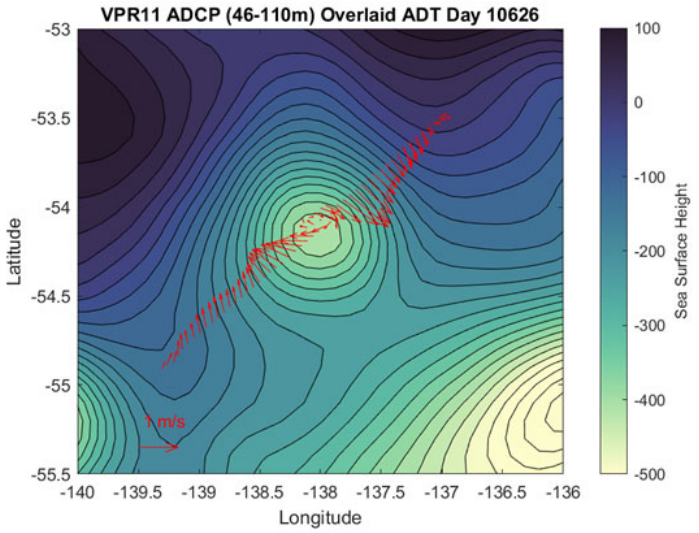

Figure 61. ADCP currents along VPR 11 track across Eddy C.

50

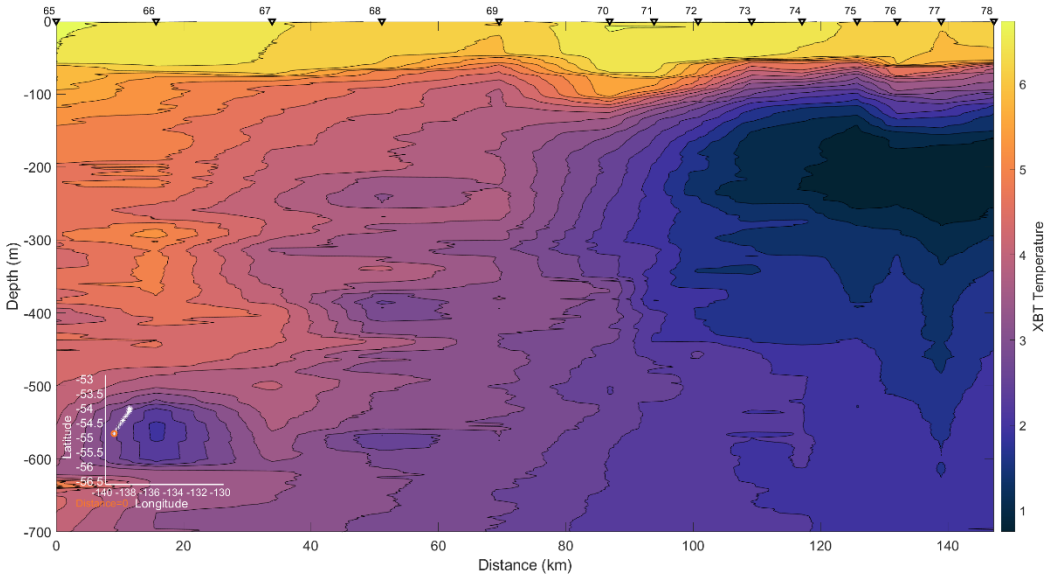

Figure 62. XBT survey used to help locate the center of Eddy C.

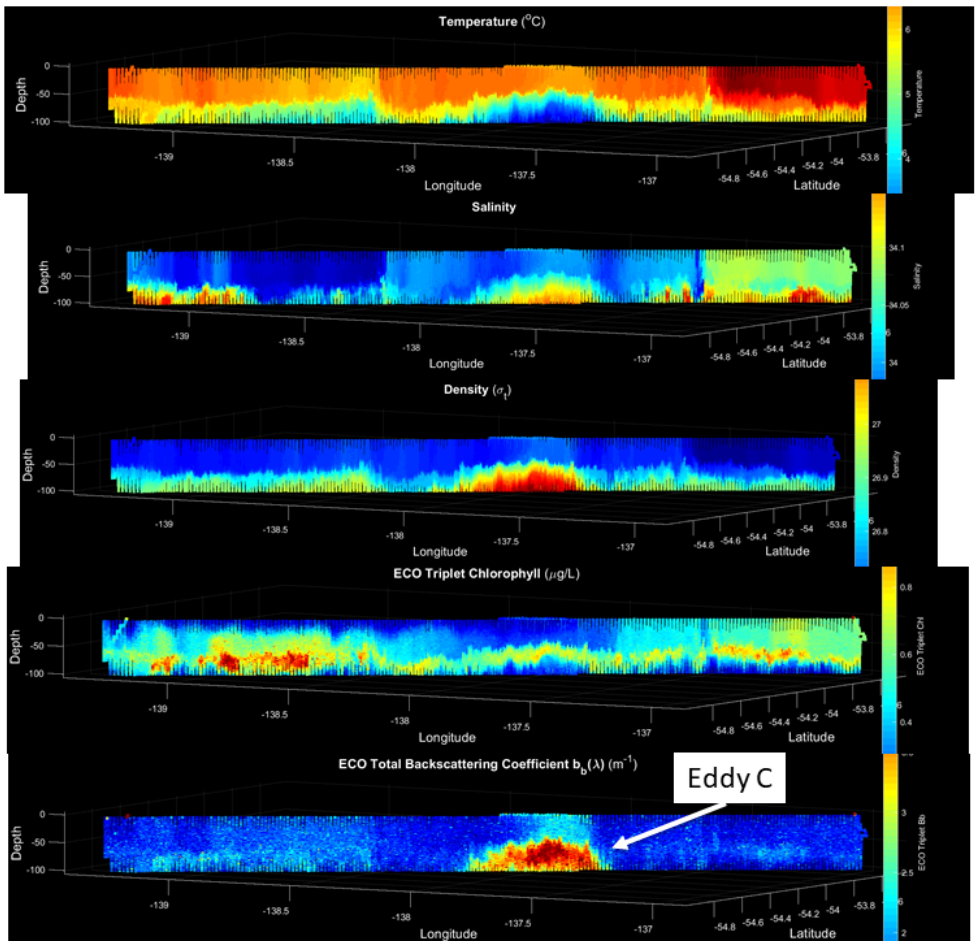

Figure 63. VPR 11 temperature, salinity, density, fluorescence, and backscatter.

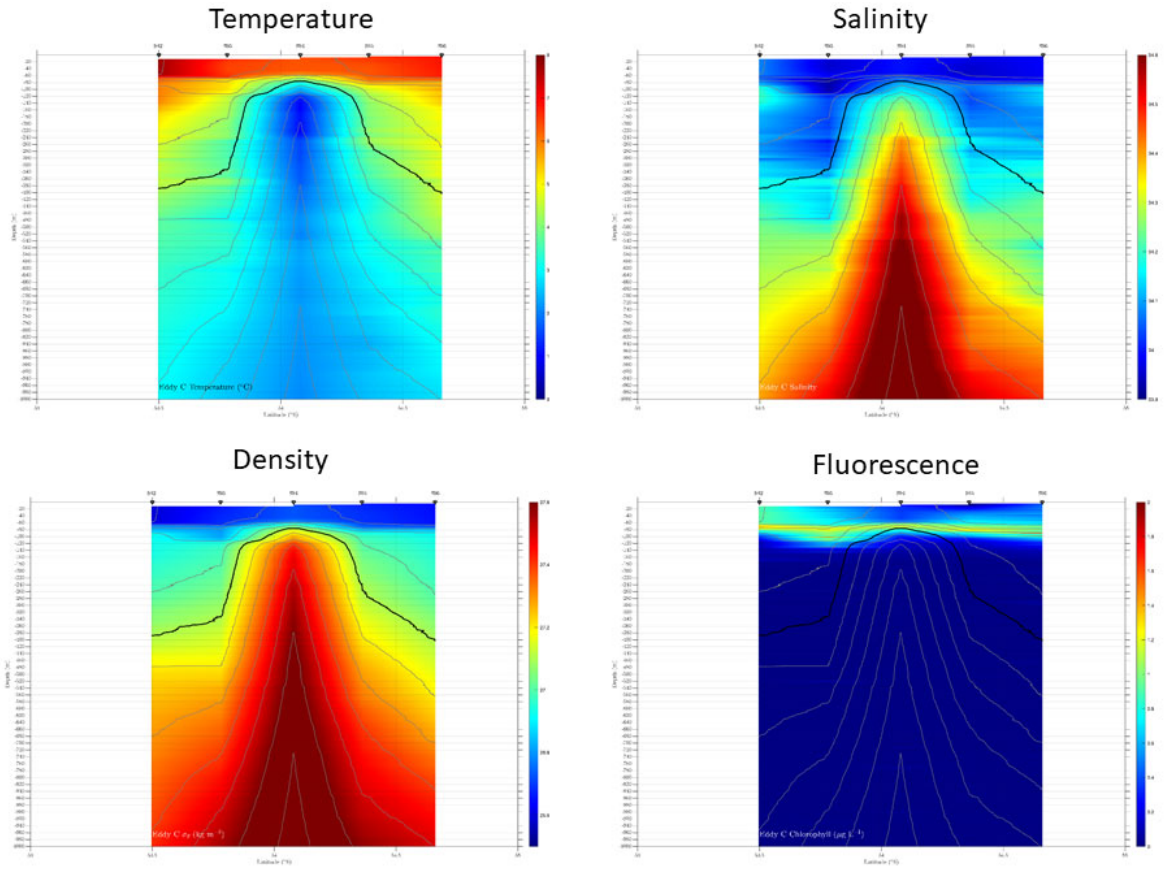

Figure 64. Cross sections of temperature, salinity, density, and fluorescence across Eddy C.

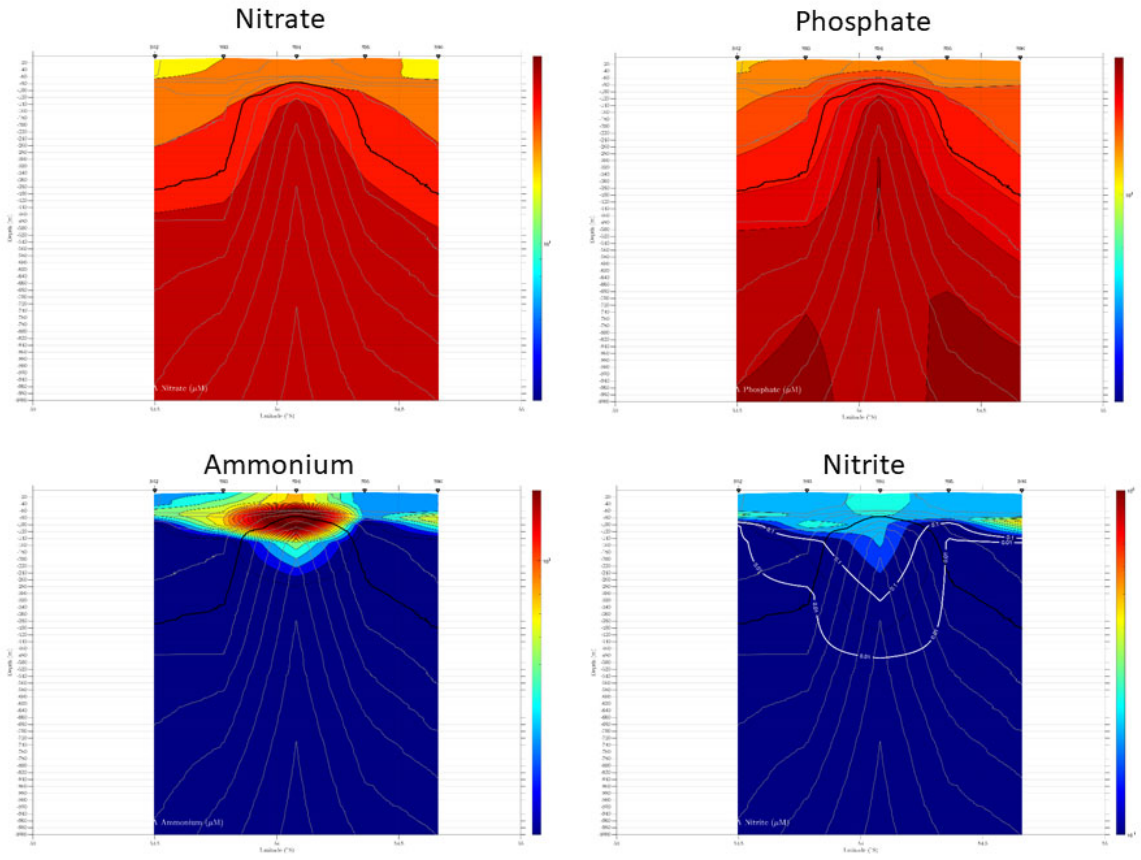

Figure 65. Cross sections of nitrate, phosphate, ammonium, and nitrite across Eddy C.

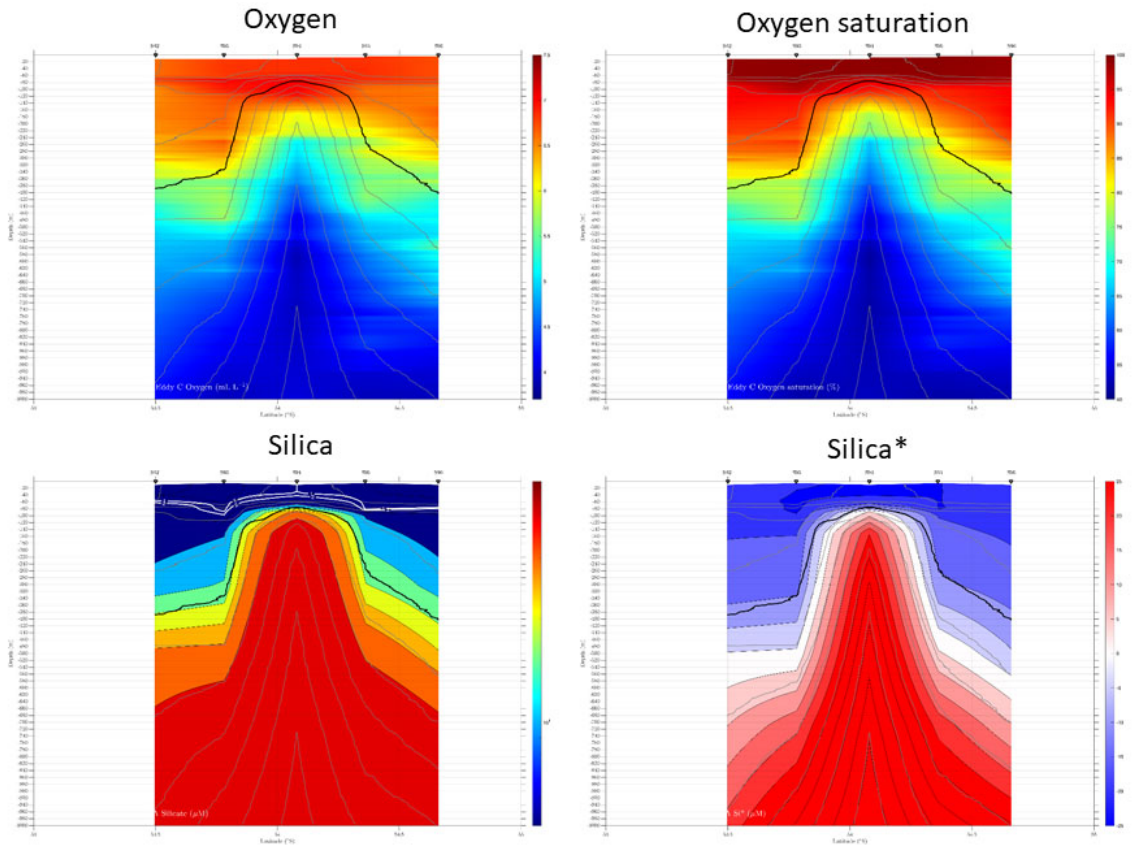

Figure 66. Cross sections of oxygen, oxygen saturation, silicate, and silicate across Eddy C.*

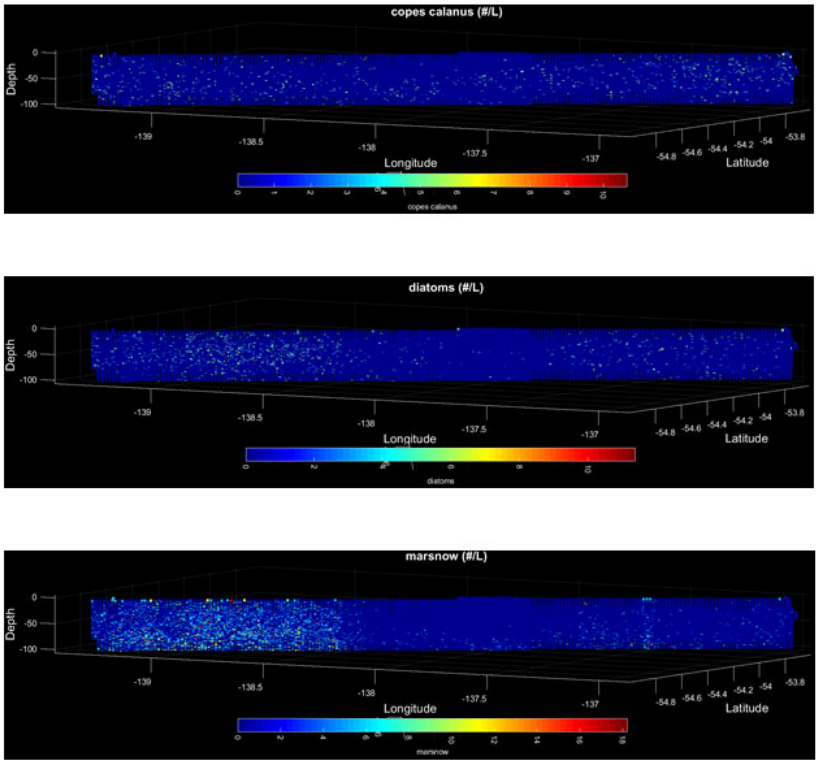

Figure 67. Taxon plots for VPR 11 transecting Eddy C.

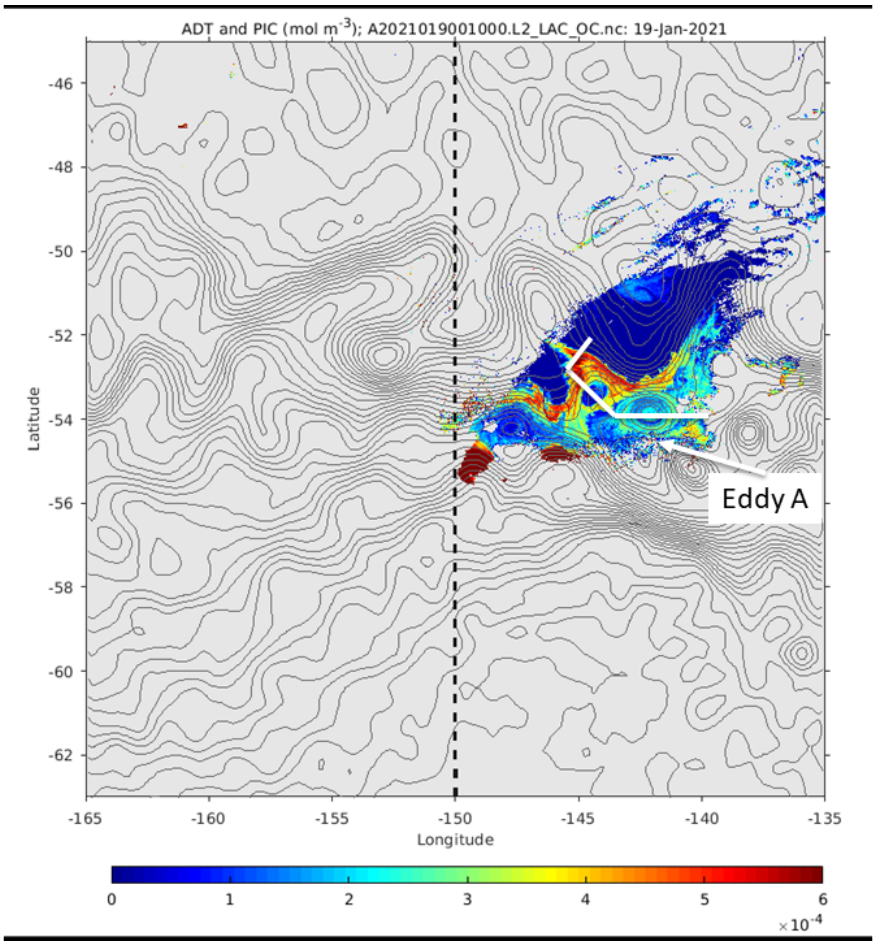

Figure 68. VPR 12 track through Eddy A, Eddy D, and the Subantarctic Front.

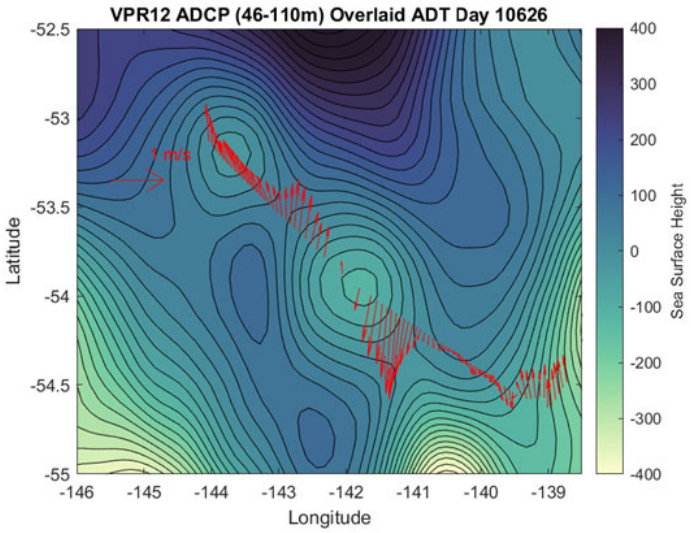

Figure 69. ADCP currents along VPR 12 track.

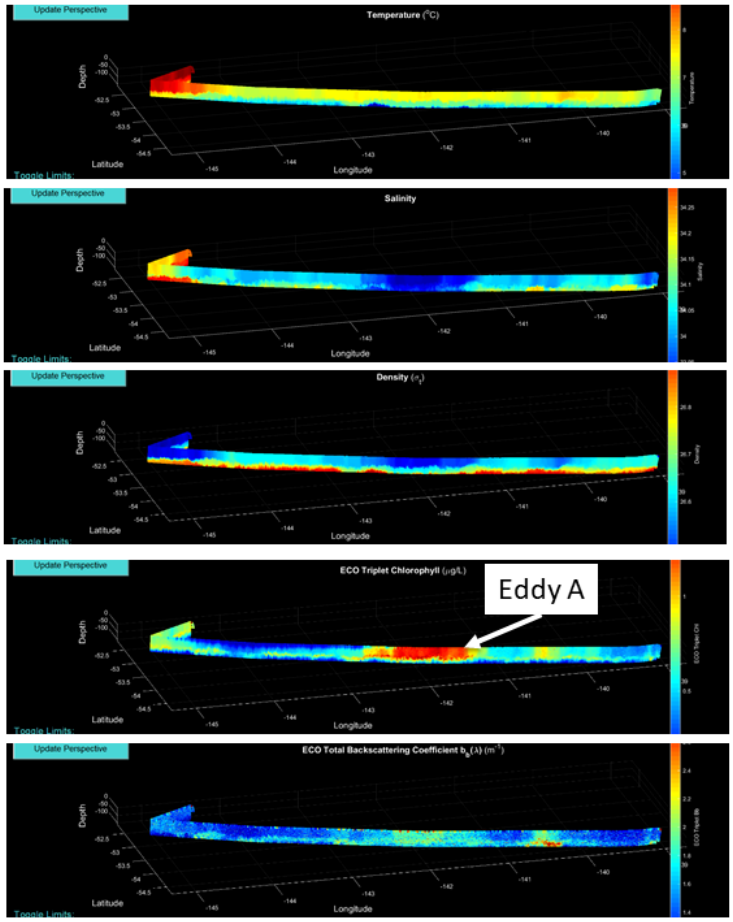

Figure 70. VPR 12 temperature, salinity, density, fluorescence, and backscatter.

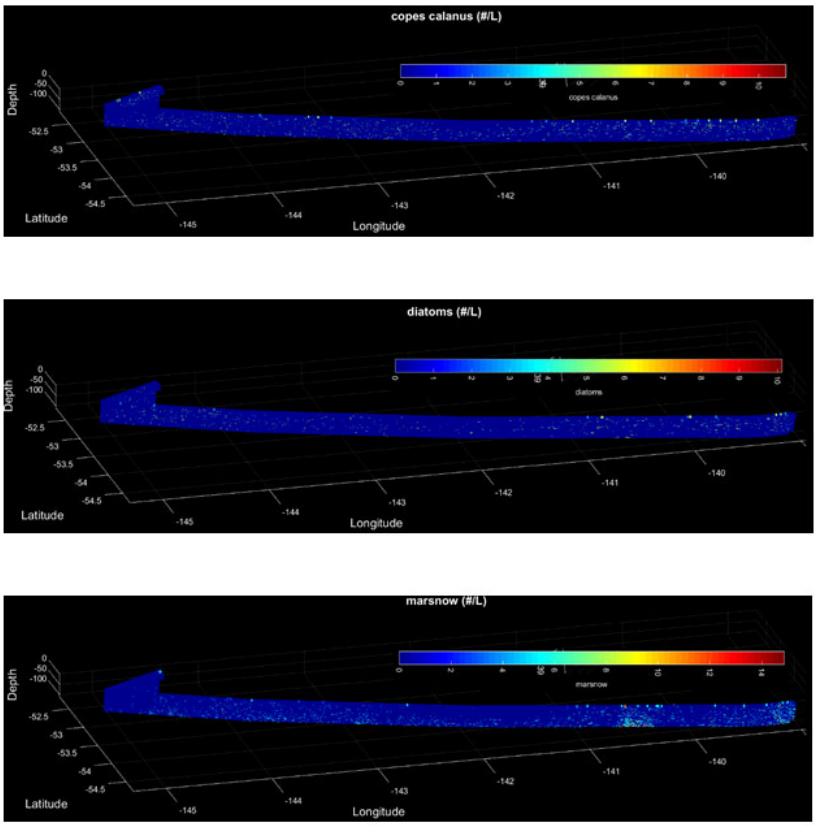

Figure 71. VPR 12 taxon plots.

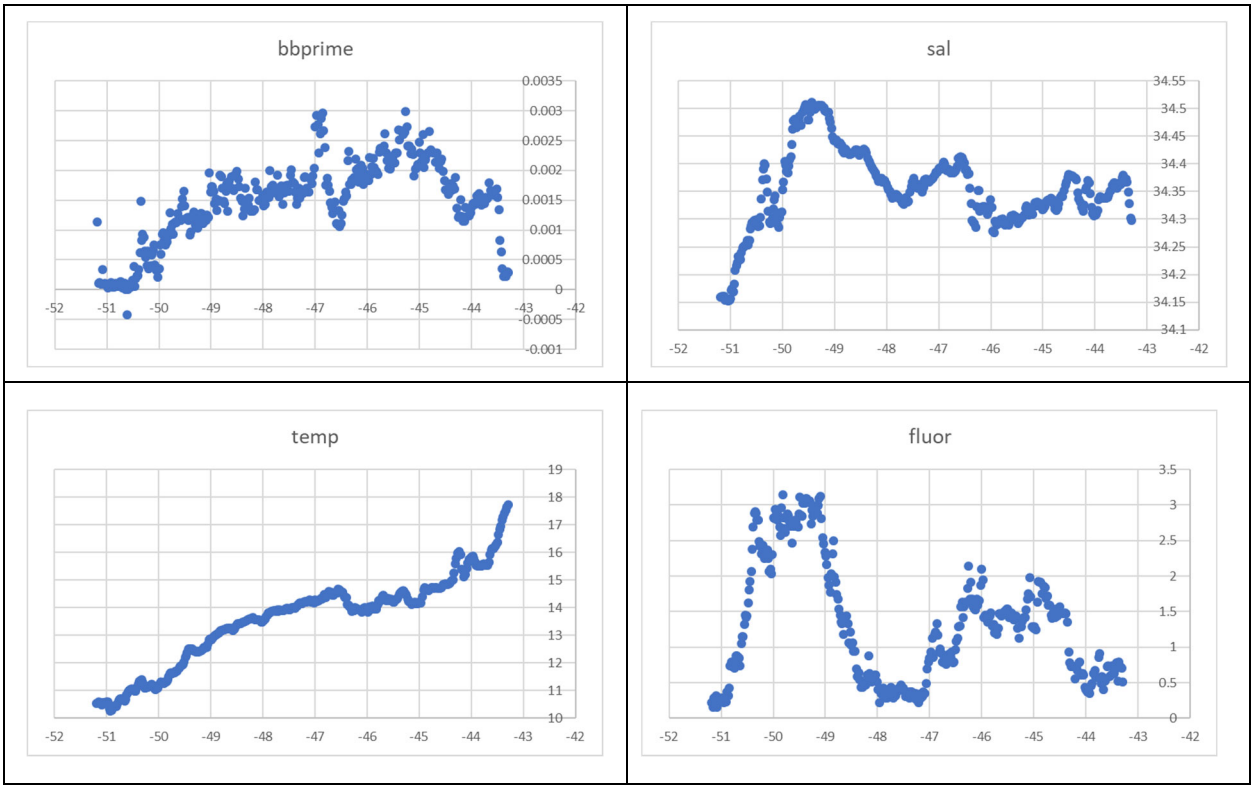

Figure 72. Balch lab underway data from northward transit: bb prime, temperature, salinity, and fluorescence.

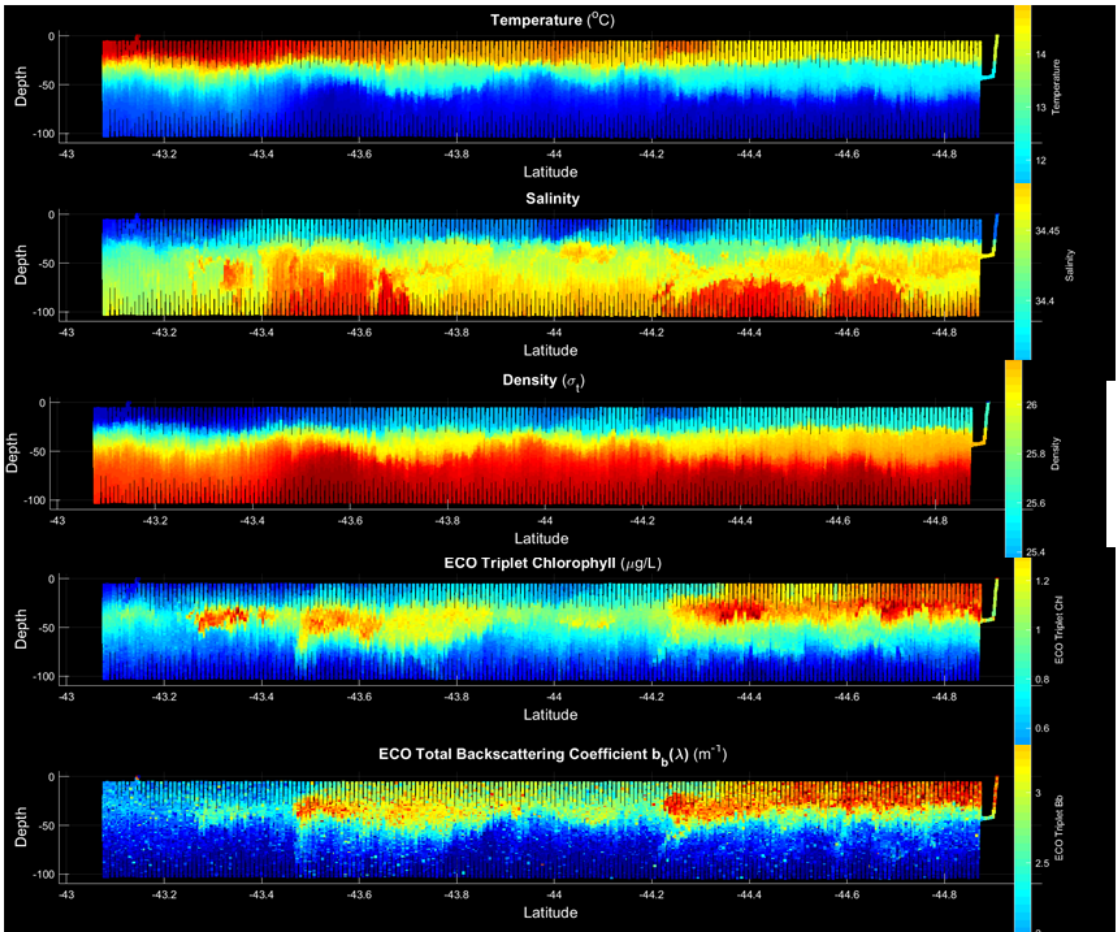

Figure 73. VPR 13 temperature, salinity, density, fluorescence, and backscatter.

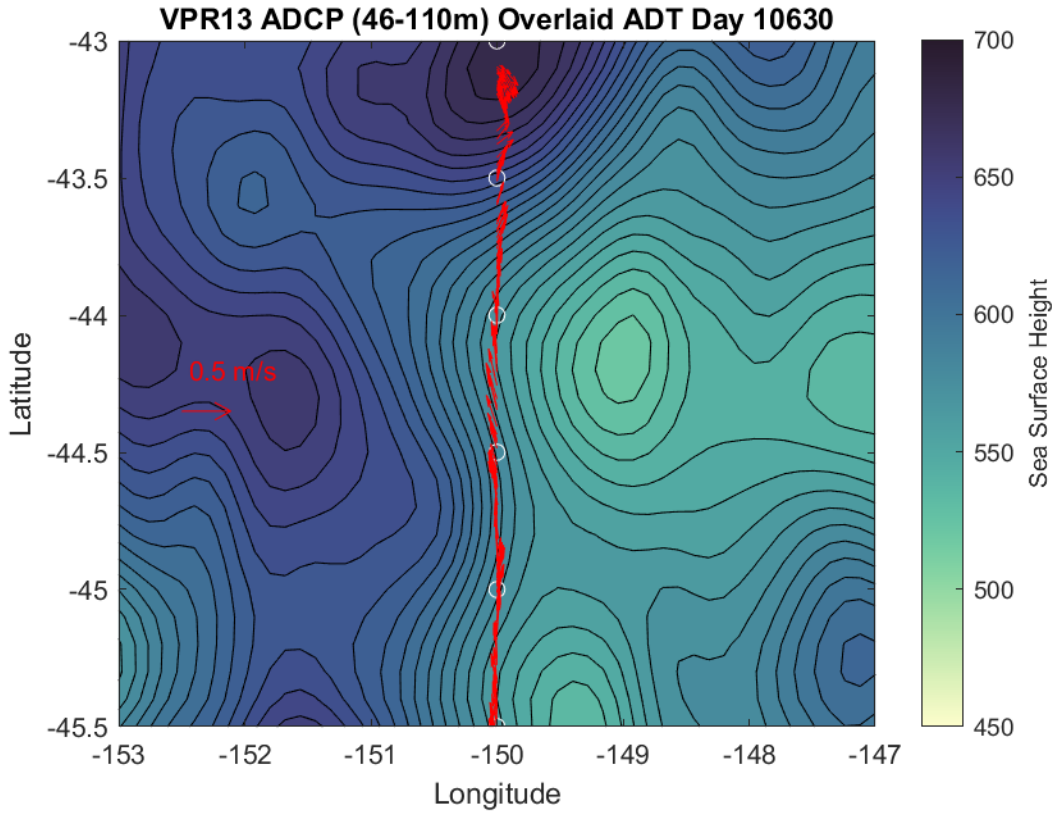

Figure 74. ADCP currents along VPR 13 track.

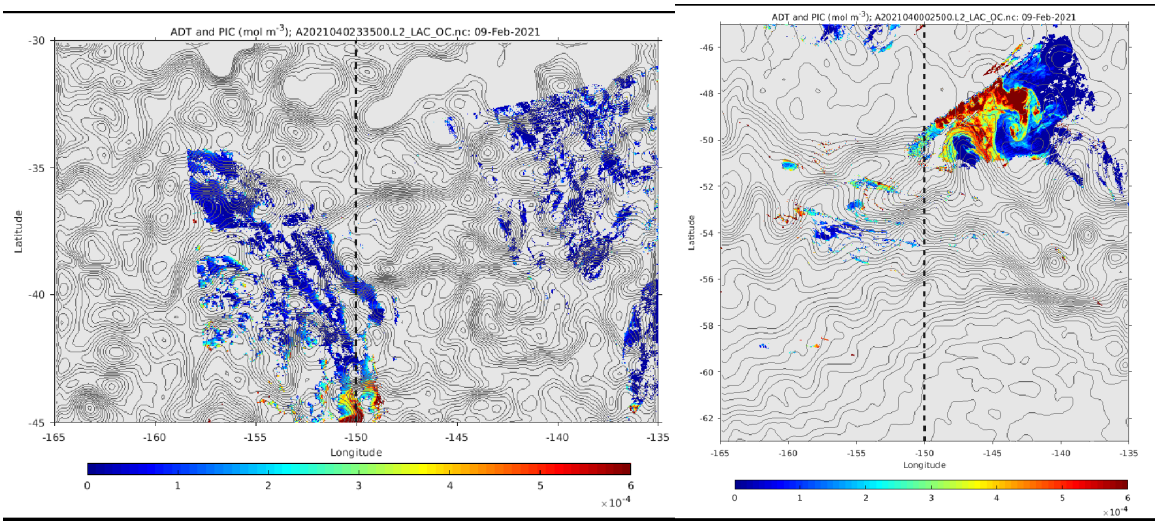

Figure 75. Satellite-derived PIC (color) with ADT contours overlaid. Images from 9 February indicate the dip in b_b' at 44S was associated with a meander; PIC-rich water to the east of the sampling area at approximately the same latitude high b_b' was encountered along 150W.

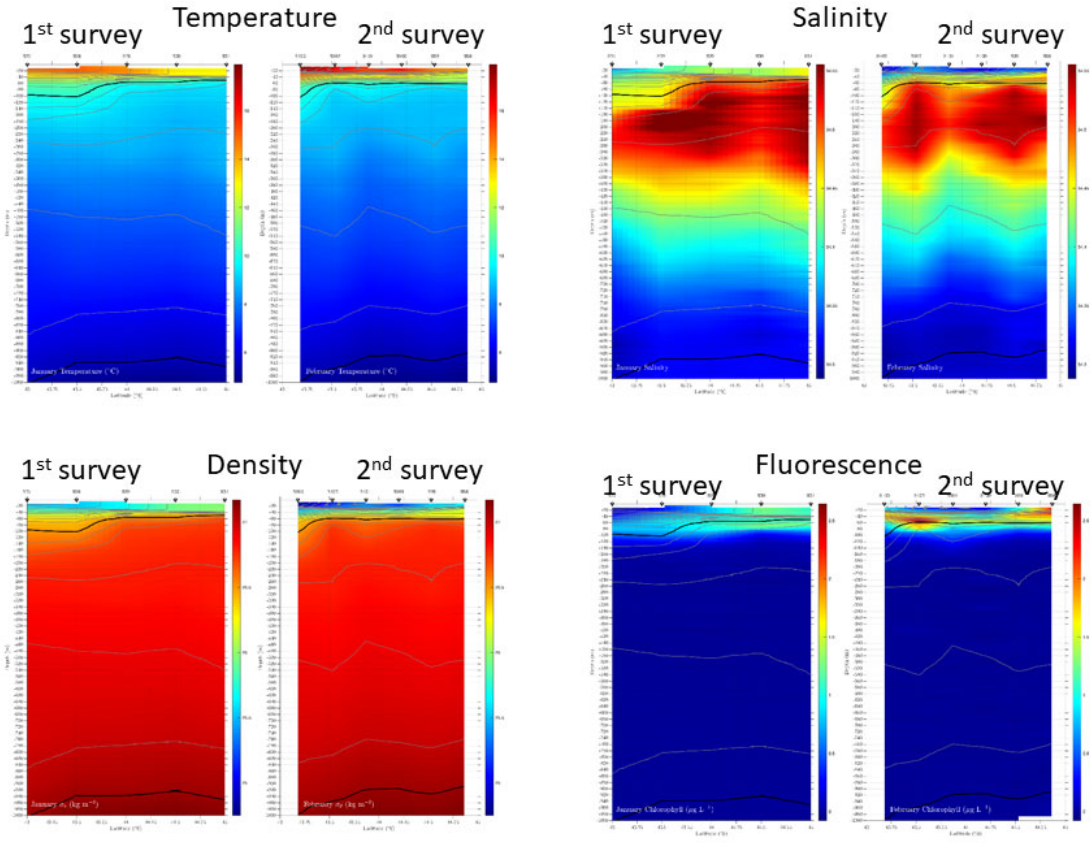

Figure 76. Comparison of CTD sections from the first and second surveys of the 150W transect between 43 and 45S.

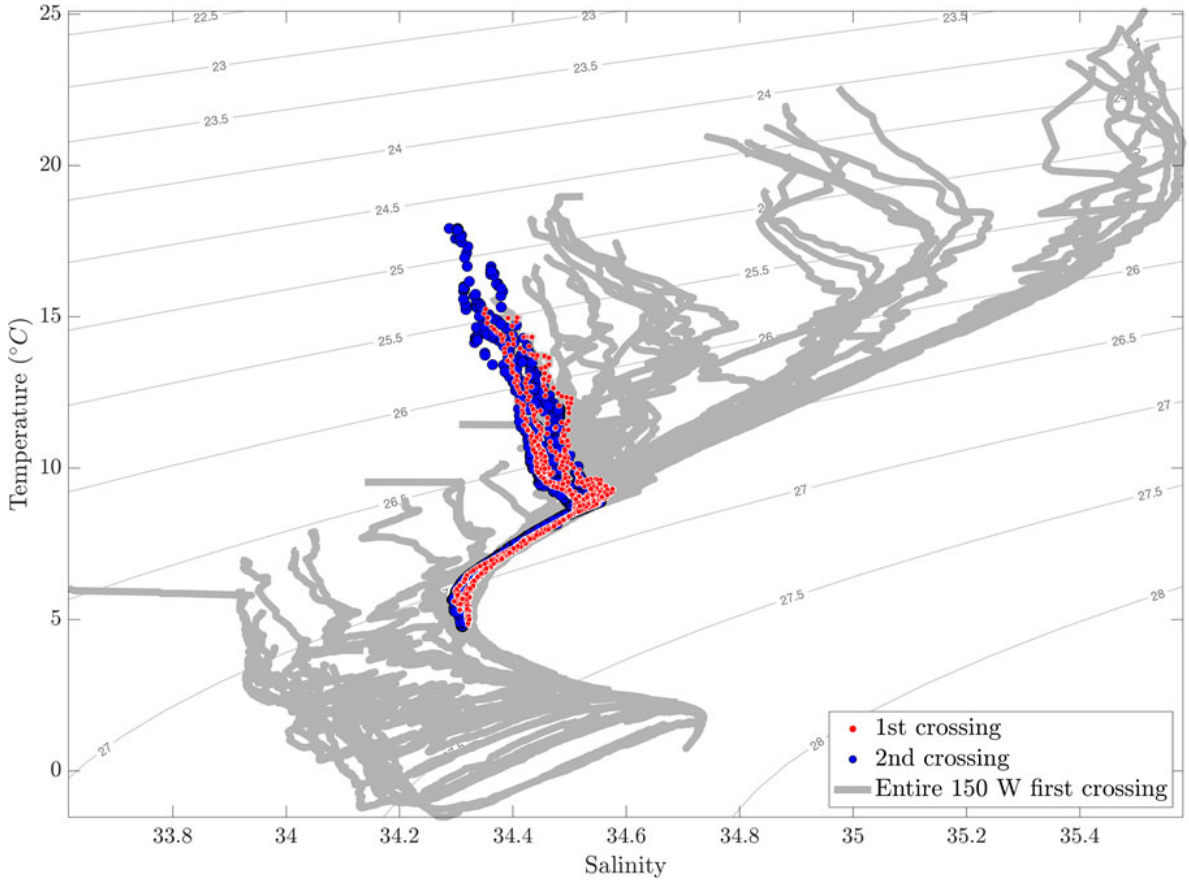

Figure 77. Temperature-salinity properties of the 43-45 S portion of the meridional transect, comparing the first and second occupations to the envelope of variability for all measurements.

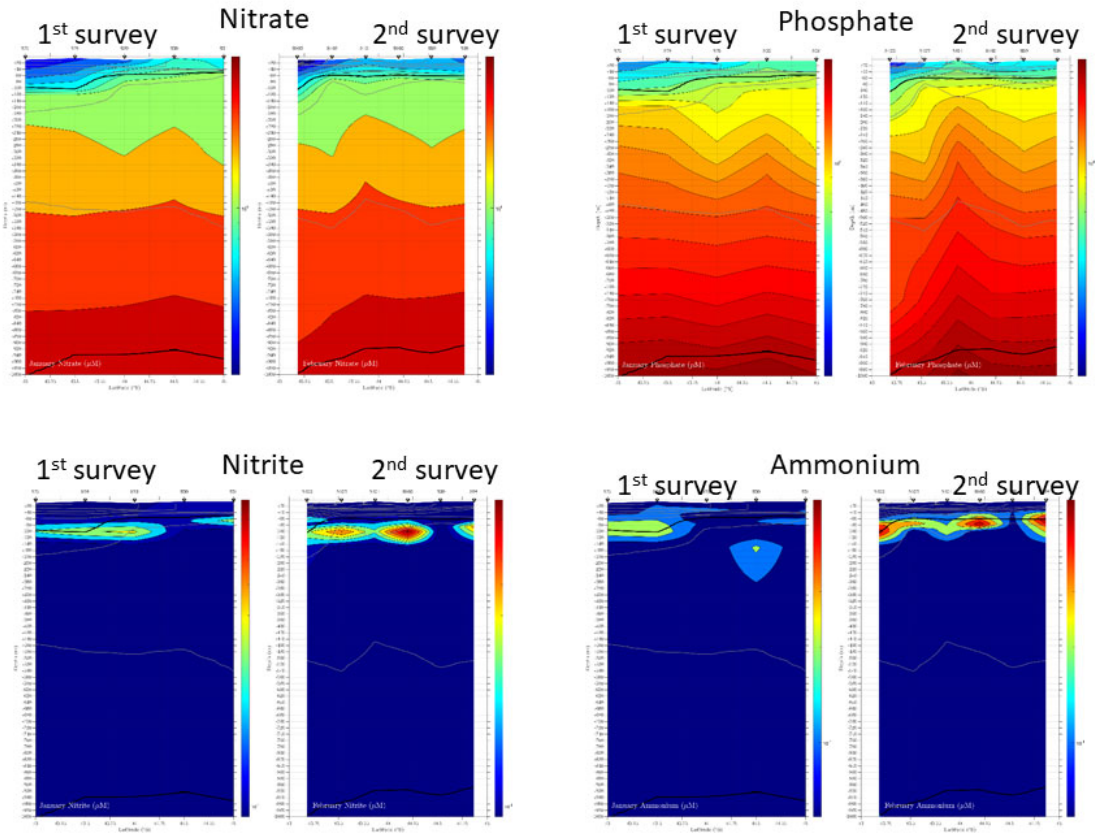

Figure 78. Comparison of nutrient sections from the first and second surveys of the 150W transect between 43 and 45S.

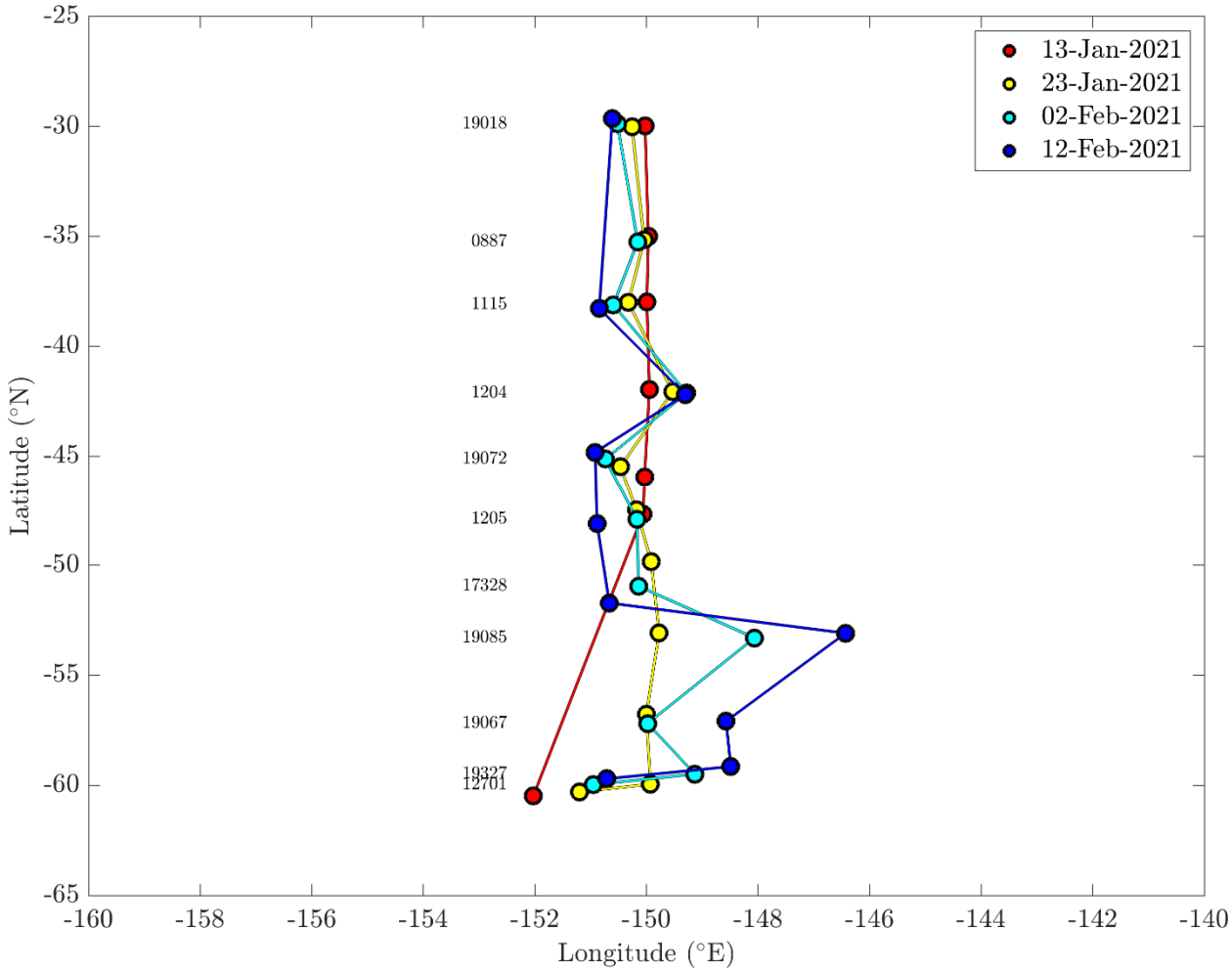

Figure 79. Locations of the 10 SOCCOM floats deployed during RR2004, and float 12701 for the four 10-day periods centered at 13 January, 23 January, 2 February, and 12 February 2021.

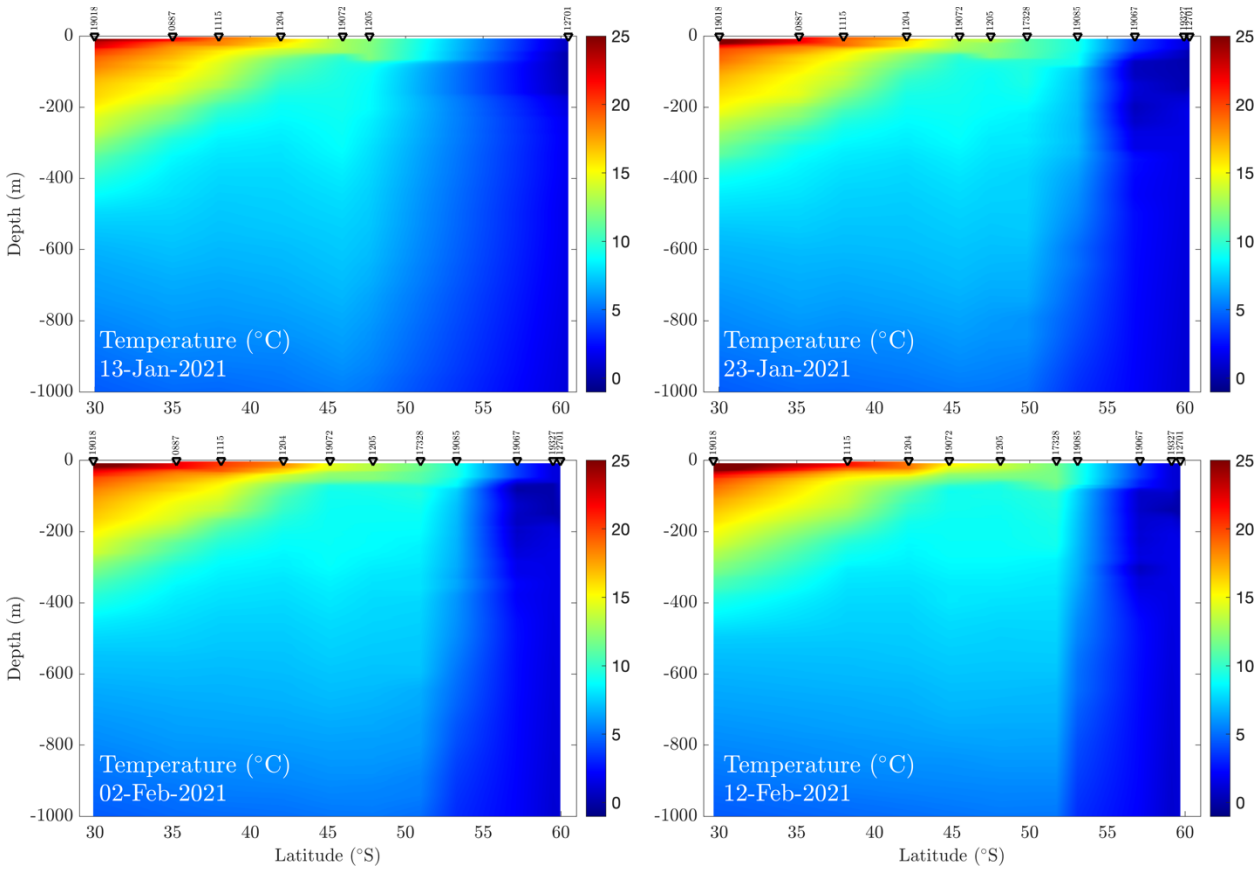

Figure 80. Cross-sections of temperature measured by SOCCOM floats for four 10-day periods centered at 13 January, 23 January, 2 February, and 12 February 2021. Float locations are plotted in Figure 79.

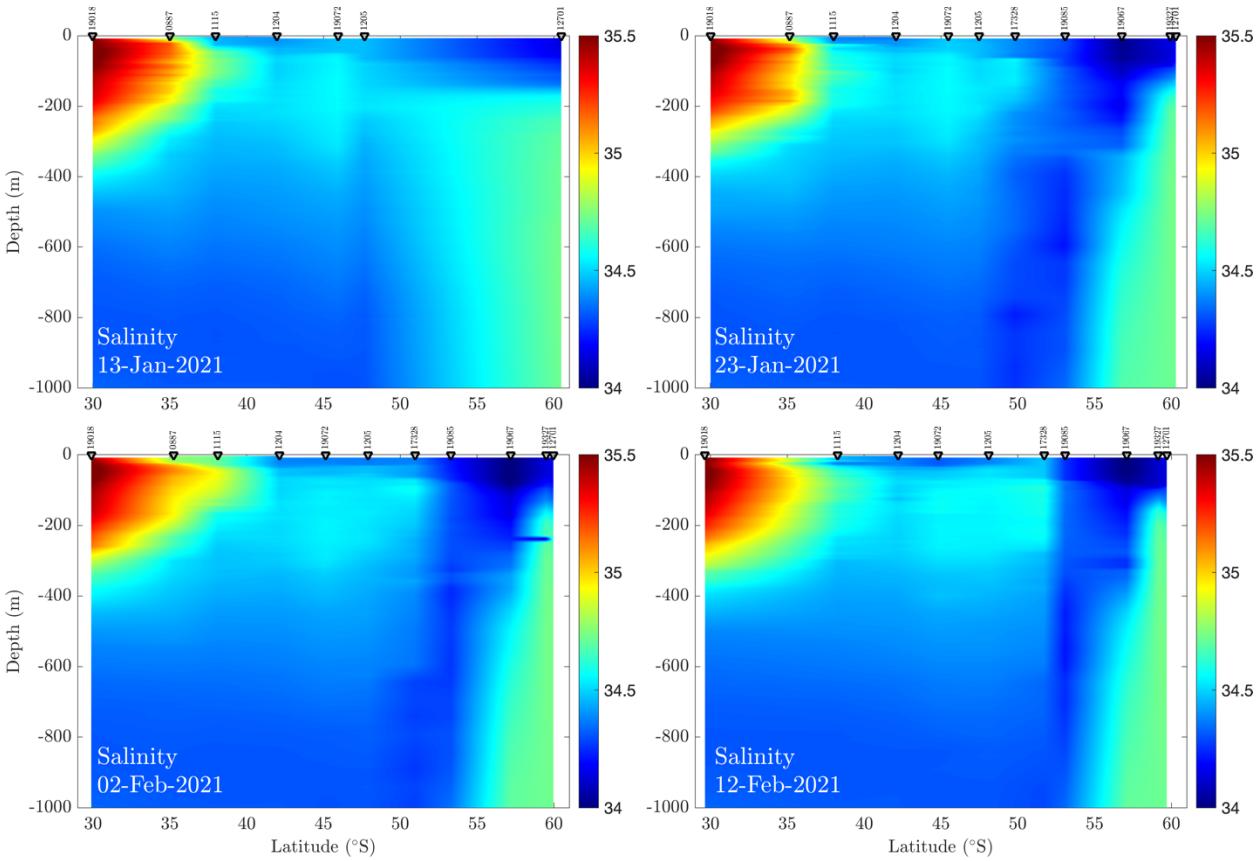

Figure 81. Cross-sections of salinity measured by SOCCOM floats for four 10-day periods centered at 13 January, 23 January, 2 February, and 12 February 2021. Float locations are plotted in Figure 79.

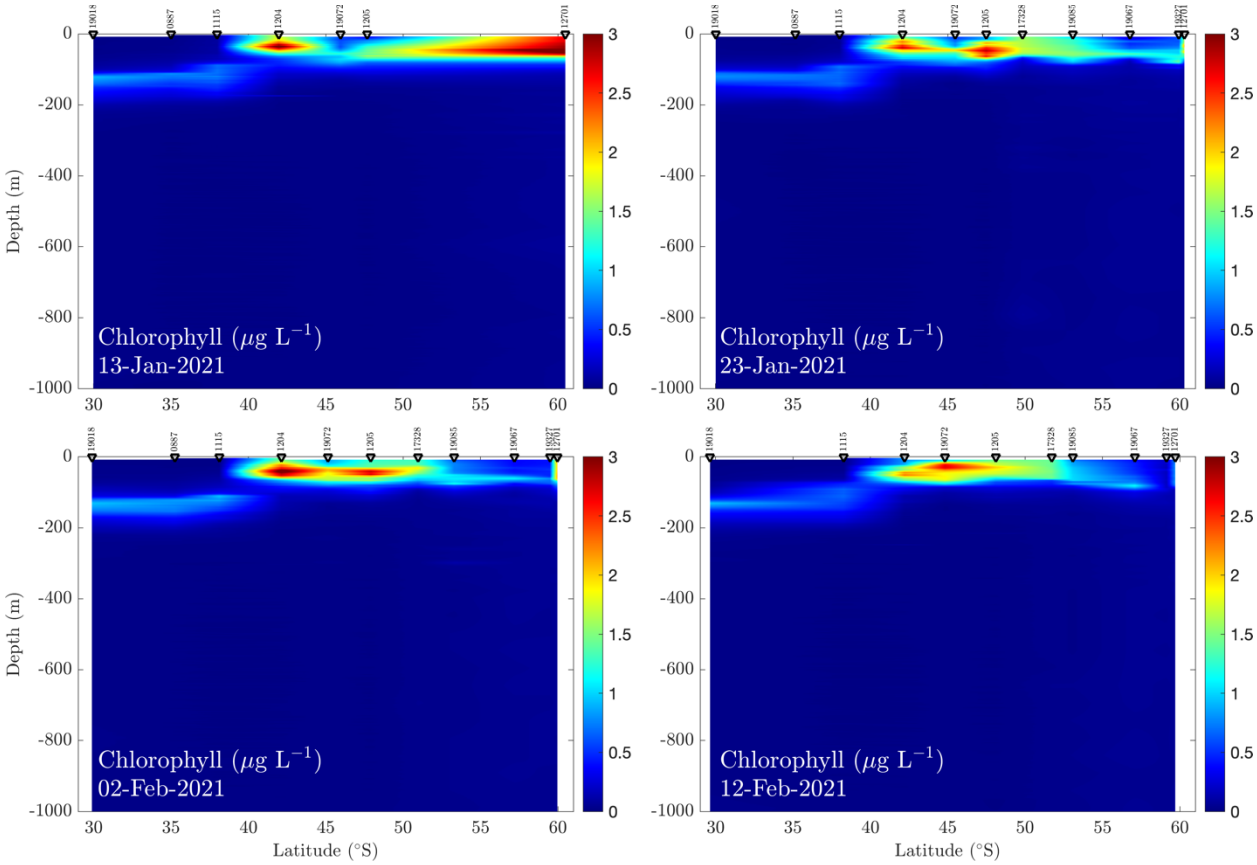

Figure 82. Cross-sections of chlorophyll concentrations estimated from SOCCOM float fluorometers for four 10-day periods centered at 13 January, 23 January, 2 February, and 12 February 2021. Float locations are plotted in Figure 79.

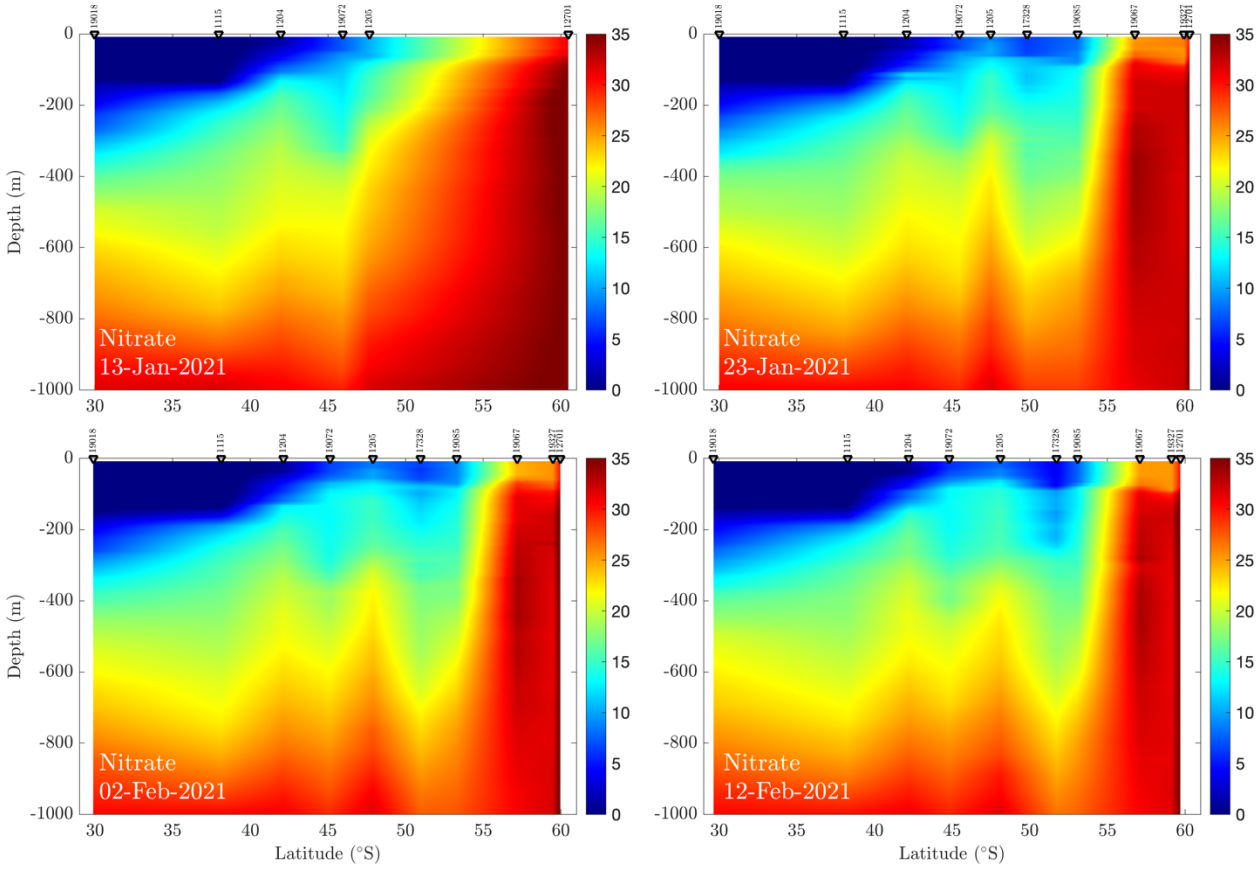

Figure 83. Cross-sections of nitrate estimated from SOCCOM float optical nitrate sensors for four 10-day periods centered at 13 January, 23 January, 2 February, and 12 February 2021. Float locations are plotted in Figure 79.

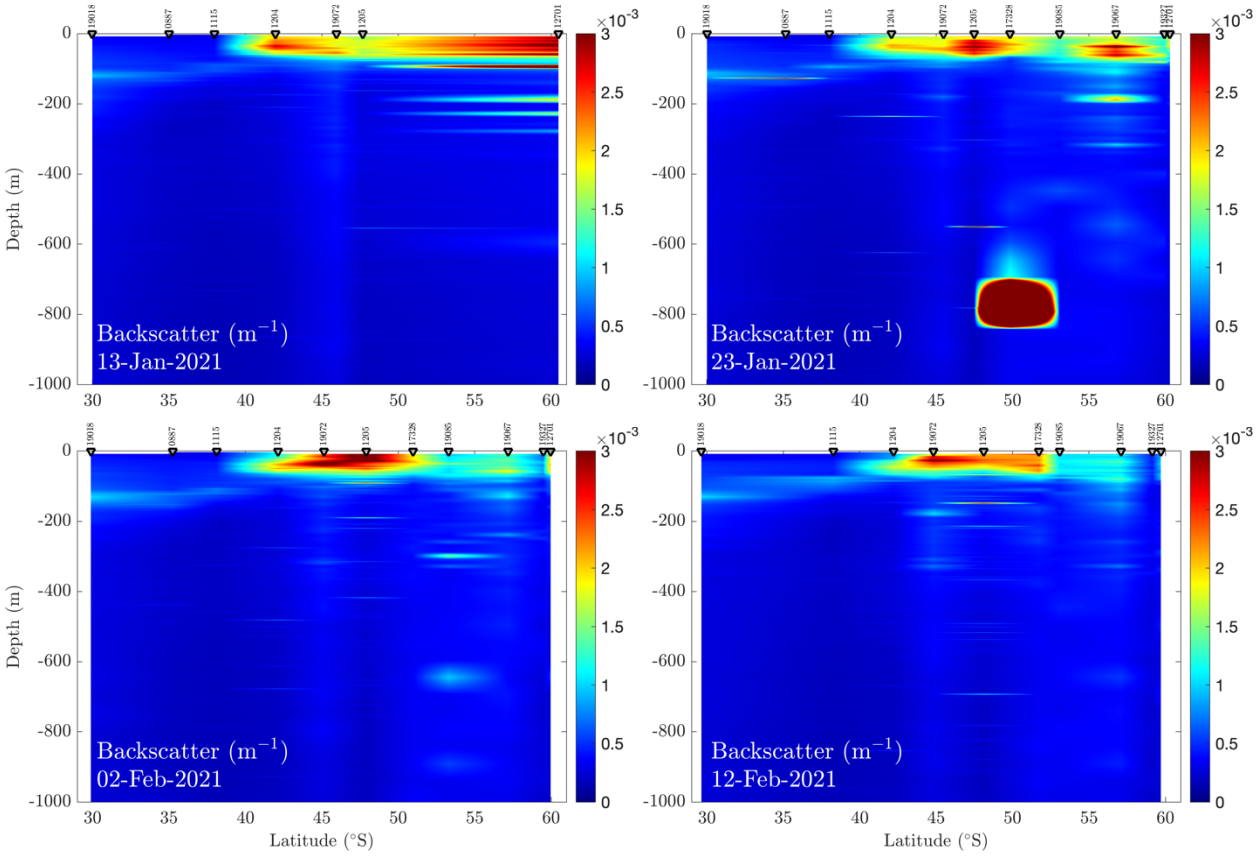

Figure 84. Cross-sections of backscatter (bbp700) measured by SOCCOM floats for four 10-day periods centered at 13 January, 23 January, 2 February, and 12 February 2021. Float locations are plotted in Figure 79.

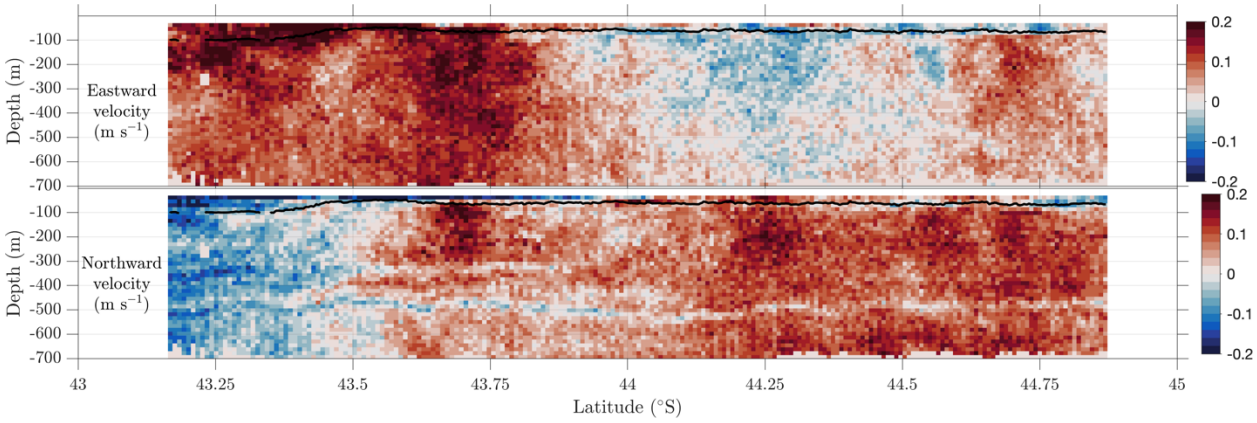

Figure 85. Cross-section of 75 KHz narrowband ADCP data recorded during VPR 13.

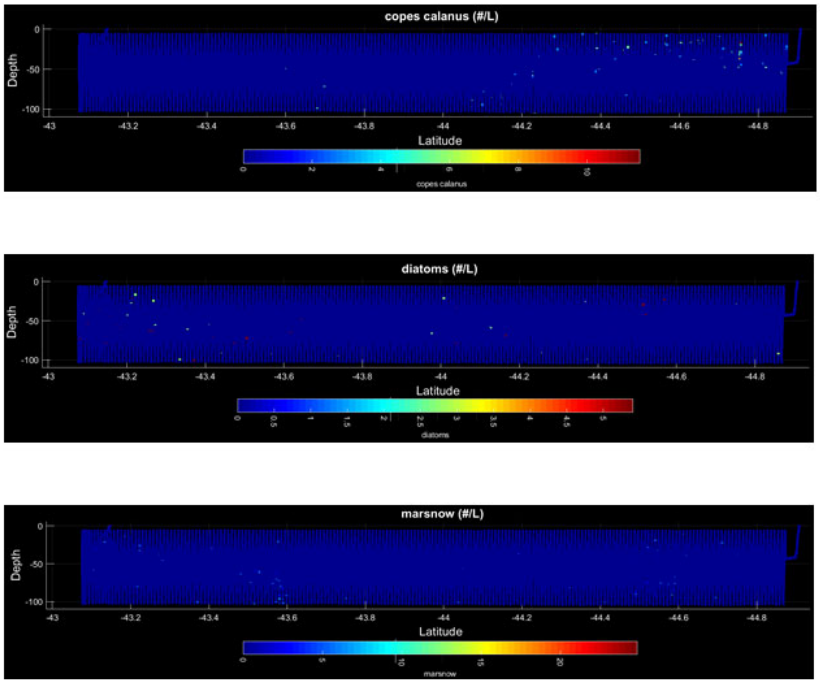

Figure 86. Taxon plot for VPR 13.

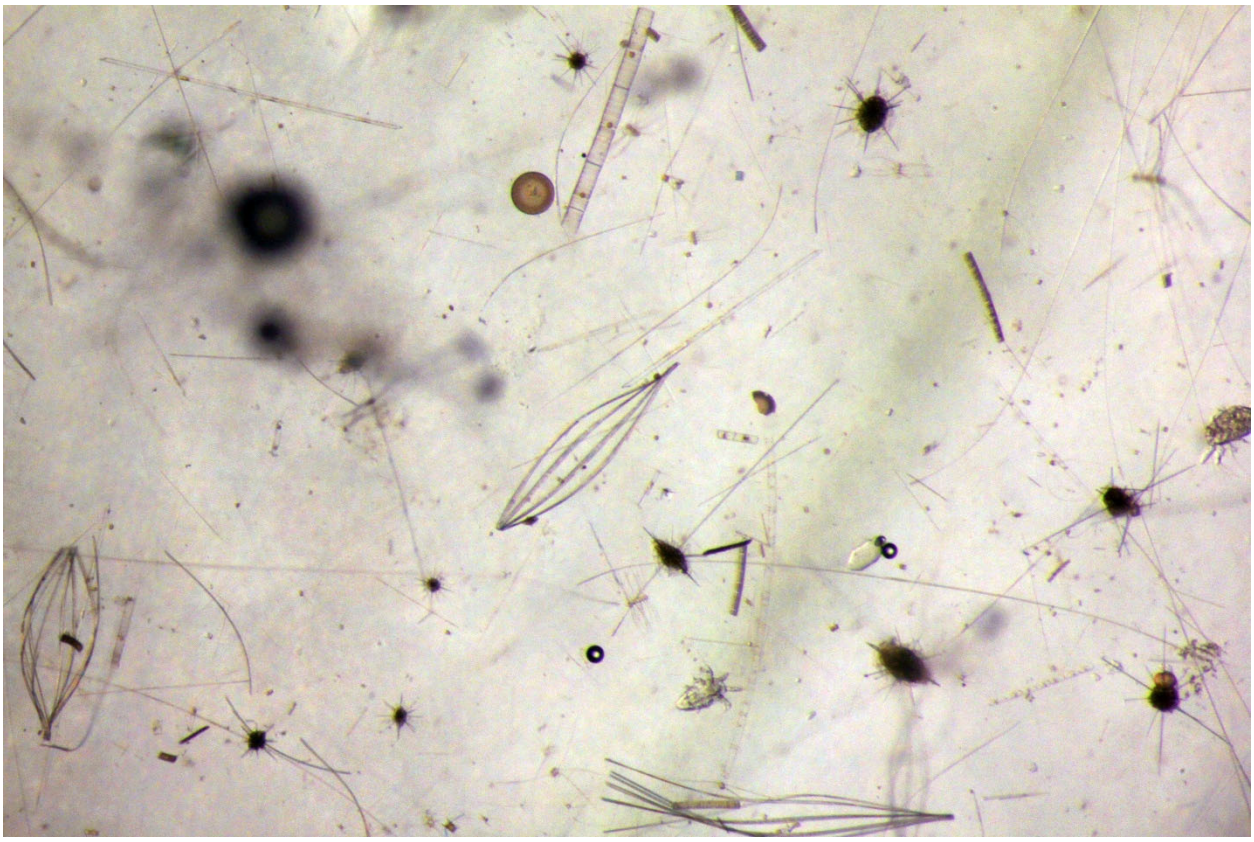

Figure 87. Microscope picture of Thalassiosira antarctica colonies, single cells, diatom chains, a centric diatom, acantharian & radiolarian protozoans, copepod nauplii from plankton net sample.

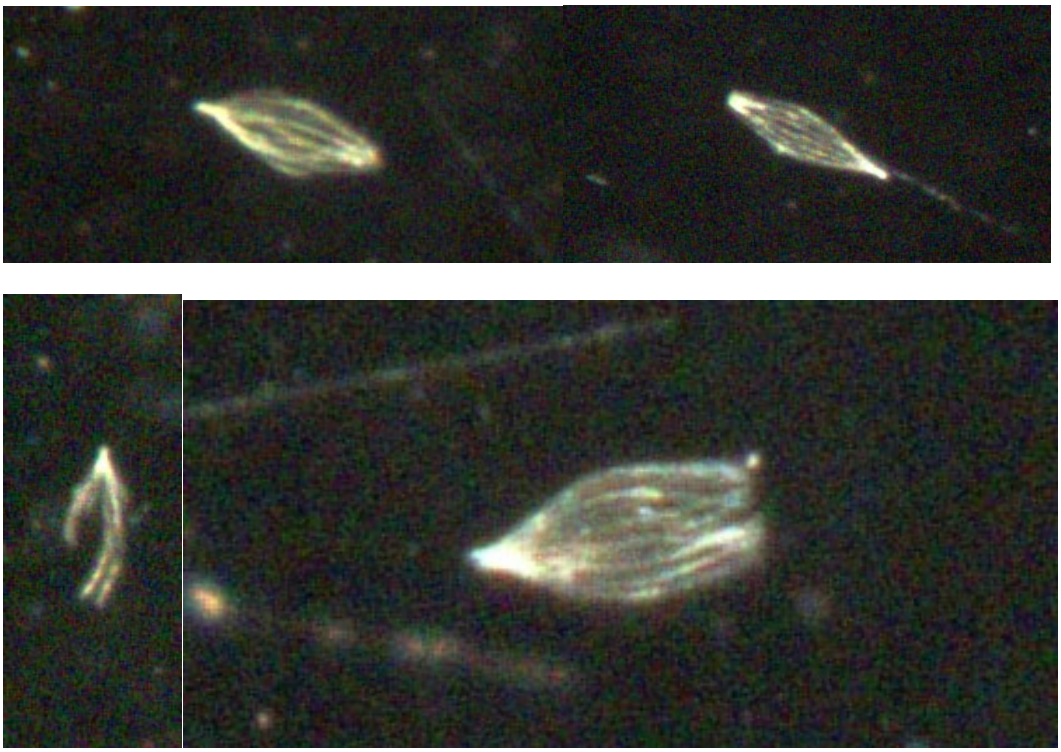

Figure 88. Diatom colonies, presumed to be Thalassiothrix antarctica in various configurations, from DAVPR video images.

Appendix 1. Evaluation and calibration of CTD conductivity and oxygen sensors

Salinity

For the first 62 stations of RR2004, there was a consistent salinity offset of 0.016 ± 0.033 between conductivity sensors. There was a 0.013 ± 0.006 difference in salinity estimated from the salinometer and conductivity sensor 1, and a -0.004 ± 0.034 difference for conductivity sensor 2. The large standard deviations in the offset for conductivity sensor 2 were due to casts 32 and 33, where the pump for CTD 2 became disconnected. Removing these stations reduces the salinometer/conductivity sensor 2 offset to -0.0005 ± 0.006. Given the high agreement of conductivity sensor 2 with the salinometer, conductivity sensor 1 was replaced for stations 63 through the end of the cruise. After switching out the sensor, the difference between salinities between conductivity sensor 1 and 2 was reduced to 0.004 ± 0.002 (Figure S1), with a difference between the salinometer and CTD 1 0.0001 ± 0.0233 and a difference between the salinometer and CTD 2 of -0.0039 ± 0.0233. The difference between CTD 1 and the salinometer and CTD 2 and the salinometer was statistically significant (Student's t-test, t = -49.9, 95% confidence interval: -0.0041 – -0.0038, $p < 0.001$, 452 degrees of freedom), and so the salinometer measurements are significantly better represented by salinities measured by CTD 1 than CTD 2 for stations 63 onwards.

To summarize: users of salinities from RR2004 conductivity sensors should consider 1) applying a correction factor of ~ 0.01 to conductivity sensor 1 salinities, at least for stations 32 and 33 where conductivity sensor 2 was not operational, 2) using salinities from conductivity sensor 2 for stations 1-62, except stations 32 and 33, 3) using salinities from conductivity sensor 1 for stations 63 onward.

Oxygen

Systematically low measurements recorded by CTD oxygen sensor during casts 1 and 2 led to its replacement for the remainder of the cruise. For stations 3 and onward, there was good agreement between the O_2 sensor and the oxygen measurements made in the Hydrolab (Figure S2), with

$$O2 = 1.0079[CTD\ O2] + 0.0643$$

which has $R^2 > 0.99$. For stations 1-2, the calibration is

$$O2 = 1.5205[CTD\ O2] + 0.9027$$

which has $R^2 = 0.91$.

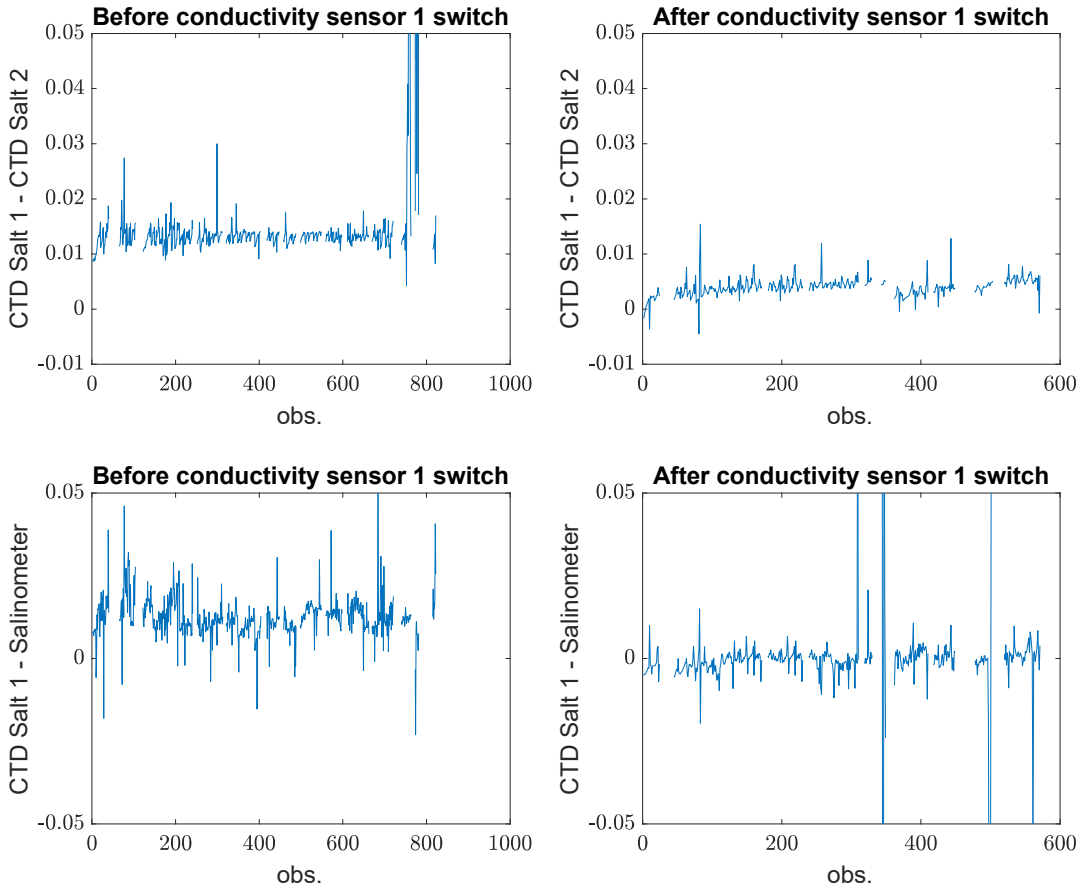

Figure S1. Differences between salinities for conductivity sensor 1 and conductivity sensor 2, and between conductivity sensor 1 and the salinometer.

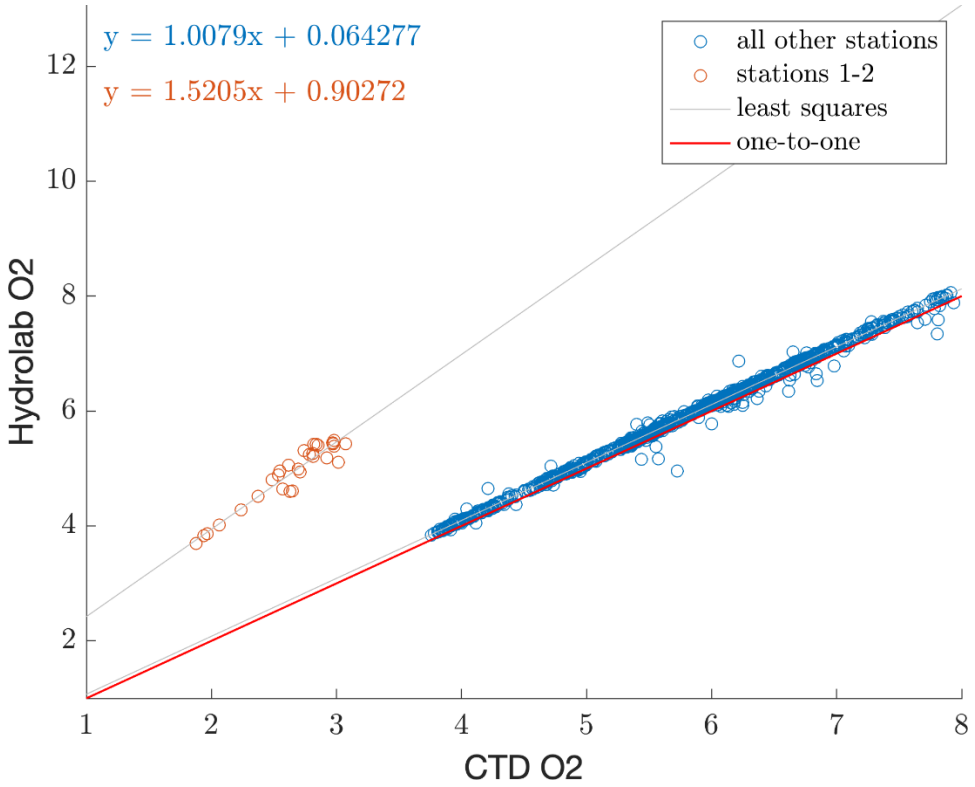

Figure S2. Agreement between the Hydrolab O2 measurements and the CTD oxygen sensor.

Appendix 2. Initial vetting of CNN classification of VPR imagery

The following table includes a summary of the most abundant taxa observed in RR2004. Two classifiers were used: CNN6 and CNN4(10b). All taxa with over 500 ROIs and/or were interesting for another reason (bloom, etc.). Overall CNN6 is more accurate for these purposes, although in a few cases CNN4(10b) performed better. Taxa for which the resulting distributions are reliable based on preliminary analysis are indicated in bold.

Tow 2 (47 S -> 50 S, Day 014-015):

Plotted	Classifier:	Taxon:	# ROIs in Taxon:	Other Notes:
Y	**CNN6**	**Acanth_spike**	**5979**	**Highly Accurate**
	CNN6	Alga_colonial	3228	All OOF or Bubbles
	CNN6	Chaetog	1501	Mostly Acanth, some bubbles
Y	**CNN6**	**Copes_calanus**	**521**	**Early tow is all krill, later hours are large copepods**
Y	**CNN6**	**Copes_small**	**2108**	**Highly Accurate**
Y	**CNN6**	**Diatoms**	**14900**	**Highly Accurate**
	CNN6	Fecal_strings	2565	Accurate, but distribution is pretty much a more sparsely populated version of marine snow
Y	**CNN6**	**Marsnow**	**10775**	**Accurate, with a some out of focus Acanth included**
	CNN6	Trichodesmium	600	Mostly copepods and marine snow

Tow 3 (50 S -> 53 S, Day 016-017):

Plotted	Classifier:	Taxon:	# ROIs in Taxon:	Other Notes:
Y	**CNN6**	**Acanth_spike**	**6828**	**Highly Accurate**
	CNN6	Alga_colonial	5416	All OOF or Bubbles
	CNN6	Chaetog	716	Mix of Acanth, gelatinous, krill, and chaetognaths
Y	**CNN6**	**Copes_calanus**	**1739**	**Predominately normal copepods, with a bias towards *Calanus*-like. Some krill.**
	CNN6	Copes_pseudo-calanus_w_eggs	973	Even split between actual copepods with egg sacs, marine snow, and too OOF to distinguish between the two
Y	**CNN6**	**Copes_small**	**4122**	**Highly Accurate**
Y	**CNN6**	**Diatoms**	**11720**	**Highly Accurate**
	CNN6	Diatoms_ coscinodiscus	542	Marine snow and blurry copepods
	CNN6	Fecal_strings	3887	Accurate, but distribution is pretty much a more sparsely populated version of marine snow

Y	**CNN6**	**Marsnow**	**26171**	**Highly Accurate**
	CNN6	Trichodesmium	1446	Mostly acanth and blurry copepods

Tow 4 (53 S -> 56 S, Day 019-020):

Plotted	Classifier:	Taxon:	# ROIs in Taxon:	Other Notes:
	CNN6	Chaetog	3004	Mix of copepods, chaetognaths, worms, and ghost colonies
Y	**CNN6**	**Copes_calanus**	**2042**	**Mostly copepods, some pteropods and worms.**
Y	CNN6	Copes_small	409	Accurate, with the occasional other taxa
Y	**CNN6**	**Diatoms**	**5144**	**Highly Accurate**
Y	CNN4(10b)	Diatoms	1949	Diatoms and fecal strings
Y	CNN4(10b)	Diatoms_bloom	521	Accurate, diatom dense conditions with about half showing colonial alga
Y	**CNN6**	**Diatoms_bloom _discrete**	**370**	**Highly Accurate**
Y	CNN6	Diatoms_bloom _snow	1122	Accurate, though the snow observed was predominately Phaeo/diatom mats
	CNN6	Fecal_strings	1249	Even split between fecal strings and worms
Y	CNN6	Marsnow	146557	Mostly colonial alga within blooms
Y	**CNN4(10b)**	**Marsnow**	**26260**	**Accurate**
Y	**CNN4(10b)**	**Phaeo**	**624**	***P. antarctica* and colonial algae**
Y	**CNN4(10b)**	**Phaeo_bloom**	**70997**	**Colonial algae with some *P. antarctica* and ghost colonies**

Tow 5 (56 S -> 60 S, Day 022-023):

Plotted	Classifier:	Taxon:	# ROIs in Taxon:	Other Notes:
	CNN6	Chaetog	6011	Complete mess of other taxa
Y	**CNN6**	**Copes_calanus**	**1786**	**Highly Accurate, all copepods**
	CNN6	Copes_pseudo-calanus_w_eggs	876	Some copepods with eggs, mostly marine snow
Y	CNN6	Copes_small	422	Accurate, but with low abundance
Y	**CNN6**	**Diatoms**	**10463**	**Highly Accurate**
Y	CNN4(10b)	Diatoms	2017	Mostly diatoms with some fecal strings
Y	**CNN6**	**Diatoms_bloom _discrete**	**222**	**Highly Accurate**

	CNN6	Fecal_strings	1919	Even split between fecal strings and worms, worms absent for second, southern bloom
Y	CNN6	Marsnow	51074	Mostly colonial algae within blooms
Y	**CNN4(10b)**	**Marsnow**	**10907**	**Accurate**
Y	**CNN4(10b)**	**Phaeo**	**342**	**Colonial algae throughout entire tow**
Y	**CNN4(10b)**	**Phaeo_bloom**	**27204**	**Phaeo_bloom (colonial algae for 56 S bloom, fecal strings and marine snow in bloom conditions for second, southern bloom (though Phaeo and marsnow (CNN6) taxa say there are some there)**

Tow 7 (Finish NE transit to Eddy A, SW->NE through Eddy A, Day 026-027)):
Strobe died d026, h18. Minimal ROIs were collected after this point.

Plotted	Classifier:	Taxon:	# ROIs in Taxon:	Other Notes:
	CNN6	Chaetog	11233	Worms, copepods, chaetognaths, some gelatinous organisms
Y	**CNN6**	**Copes_calanus**	**779**	**Accurate with occasional worms**
	CNN6	Copes_small	24	Accurate, but with low abundance
	CNN6	Decapods_misc	861	Various OOF
Y	**CNN6**	**Diatoms**	**948**	**Accurate, with an occasional copepod (after bloom)**
Y	CNN4(10b)	Diatoms	1092	Accurate with some fecal strings
Y	CNN6	Marsnow	6006	Not accurate, mostly other taxa
Y	**CNN4(10b)**	**Marsnow**	**2010**	**Accurate, with some colonial algae**
	CNN4(10b)	Phaeo	77	*P. antarctica* and colonial algae (located within frontal bloom). Omitted due to low abundance
	CNN4(10b)	Phaeo_bloom	21	Bubbles

Tow 9 (NW->SE through Eddy A, Day 027-028):

Plotted	Classifier:	Taxon:	# ROIs in Taxon:	Other Notes:
	CNN6	Chaetog	525	Worms, copepods, and chaetognaths
Y	**CNN6**	**Copes_calanus**	**1062**	**Accurate with occasional worms**
	CNN6	Copes_small	63	Accurate, but with low abundance
Y	CNN6	Diatoms	574	Inaccurate, mostly zooplankton

Y	CNN4(10b)	Diatoms	697	Inccurate, mostly zooplankton with some diatoms and fecal strings
Y	CNN6	Marsnow	5568	Accurate with some zooplankton
Y	**CNN4(10b)**	**Marsnow**	**4632**	**Accurate**
	CNN4(10b)	Phaeo	127	Almost entirely marine snow but there were a few *P. antarctica* within the eddy
	CNN4(10b)	Phaeo_bloom	46	Bubbles

Tow 10 (Cross through Polar Front South of Eddy B, Day 030-031):

Plotted	Classifier:	Taxon:	# ROIs in Taxon:	Other Notes:
	CNN6	Chaetog	2073	Colonial algae, chaetognaths, copepods
Y	**CNN6**	**Copes_calanus**	**1009**	**Accurate with occasional other taxa**
	CNN6	Copes_small	68	Accurate, but with low abundance
Y	**CNN6**	**Diatoms**	**2181**	**Accurate, with some fecal strings**
Y	CNN4(10b)	Diatoms	2040	Accurate, with some fecal strings
Y	**CNN6**	**Marsnow**	**12263**	**Accurate with some diatom mats**
Y	CNN4(10b)	Marsnow	9119	Accurate with some diatom mats
Y	CNN4(10b)	Phaeo	321	*P.* antarctica, colonial algae, marine snow, and pteropods
	CNN4(10b)	Phaeo_bloom	67	Bubbles

Tow 11 (Eddy C, Day 032-033):

Plotted	Classifier:	Taxon:	# ROIs in Taxon:	Other Notes:
	CNN6	Chaetog	1323	Chaetognaths and copepods with some other taxa
Y	**CNN6**	**Copes_calanus**	**1291**	**Accurate with occasional other taxa**
	CNN6	Copes_small	79	Accurate, but with low abundance
Y	**CNN6**	**Diatoms**	**1392**	**Accurate, with some fecal strings**
Y	CNN4(10b)	Diatoms	1268	Accurate, with some other taxa
Y	**CNN6**	**Marsnow**	**6143**	**Accurate with some diatom mats and pteropods**
Y	CNN4(10b)	Marsnow	4760	Accurate with some diatom mats and pteropods
Y	CNN4(10b)	Phaeo	142	*P.* antarctica, colonial algae, marine snow, and pteropods
	CNN4(10b)	Phaeo_bloom	30	Bubbles

Tow 12 (West of Eddy C through Eddy A, Eddy 0, and Subantarctic front, Day 034-035):

Plotted	Classifier:	Taxon:	# ROIs in Taxon:	Other Notes:
	CNN6	Chaetog	1274	Chaetognaths, gelatinous, copepods
Y	**CNN6**	**Copes_calanus**	**3261**	**Accurate with some worms**
	CNN6	Copes_small	210	Accurate, but with low abundance
Y	**CNN6**	**Diatoms**	**1744**	**Accurate, with some fecal strings**
Y	CNN4(10b)	Diatoms	1805	Accurate, with some other taxa
Y	**CNN6**	**Marsnow**	**6502**	**Highly Accurate**
Y	CNN4(10b)	Marsnow	5385	Accurate with some other taxa
Y	CNN4(10b)	Phaeo	266	Mostly marine snow
	CNN4(10b)	Phaeo_bloom	22	Bubbles

Tow 13 (NW->SE through Eddy A, Day 037-038):

Plotted	Classifier:	Taxon:	# ROIs in Taxon:	Other Notes:
	CNN6	Chaetog	176	Bubbles
Y	**CNN6**	**Copes_calanus**	**116**	**Accurate, though there are few ROIs**
	CNN6	Copes_small	10	Accurate, but with low abundance
Y	**CNN6**	**Diatoms**	**82**	**Accurate with some other taxa**
Y	**CNN6**	**Marsnow**	**156**	**Accurate with some other taxa**

Initial analysis of ROI data yielded some suggestions for additional taxa to add to future classifiers, summarized in the following table.

Preliminary taxon name:	Reason to add:	Sources in CNN:
Acanth w/ ID	Currently not a taxon, reduce false positives in other taxa	All tows: acanth_spike_amphilonche Tow 2, 3: chaetog Tow 2: marsnow Tow 3: trichodesmium
Amphipods	Currently not a taxon	Tow 9: Large ROIs
Colonial Algae	Currently not a taxon (though AR29 Phaeo works reasonably well)	Tow 4: Phaeo (CNN6, CNN4(10b))
Colonial Algae Bloom	Currently not a taxon (though AR29 Phaeo_bloom works reasonably well)	Tow 4: Marsnow (CNN6), Phaeo_bloom (CNN4(10b))
Diatoms _Chaetoceros	Split into several different subtaxa?	Tow6: Trichodesmium
Diatom Mats	Combine with diatoms_bloom _discrete? Or create new taxa?	VPR5: Southern bloom seems to be ideal
Eucalanus	Split copepods into better defined taxa	
Forams	Expand current trrois	CNN6 works well for most tows.

Gelatinous	Improve trrois, perhaps get enough to split into more specific taxa (medusas, salps, etc.)	All tows: gelatinous Can also find ROIs for large taxa by sorting by size
Krill	Currently not a taxon	All tows: copepod taxa (calanus best bet) Tow 3: chaetog
OOF_bubbles	VPRII bubbles are distinct	All Tows: At deployment and retrieval Decapods_misc is also usually bubbles.
Paracalanus	Split copepods into better defined taxa	
Phaeocystis antarctica	Currently not a taxon	Tow 4: marsnow (CNN6) in bloom conditions, Phaeo (CNN4(10b))
P. antarctica ghost colonies	Currently not a taxon	Tow 4: chaetog
Phaeod_knob_ Pcystida	Expand current trrois	CNN6 works well for most tows.
Phil's Unknown (Spindles?)	Currently not a taxon, cooccurs at bloom	Tow 4: No specific taxa
Pteropods	Missing most pteropods, would be good to grab more trrois	Tow 4: copes_calanus, copes_small
Worms	Currently not a taxon, cooccurs at bloom	Tow 4: copes_calanus, trichodesmium

Sample ROIs from RR2004 new taxa

Acanth w/ ID:

Amphipods:

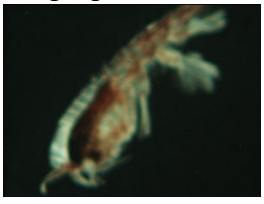

Colonial Alga (singular):

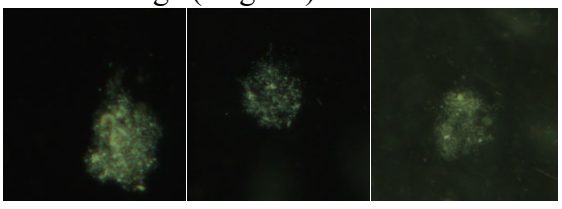

Colonial Alga (Bloom):

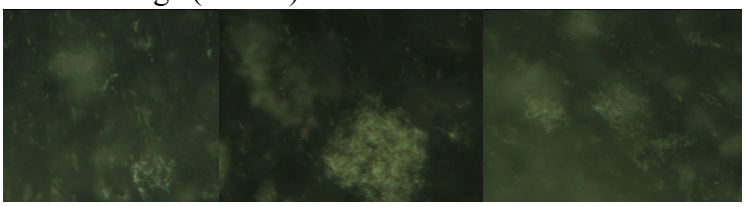

Diatoms_chaetoceros (Orthogonal):

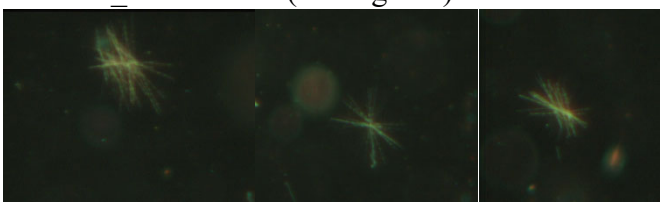

Diatoms_chaetoceros (planar):

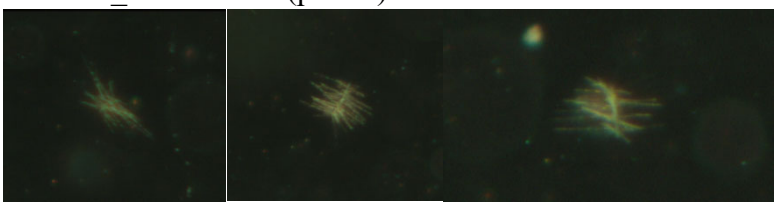

Diatoms_chaetoceros (fuzzy, short spines):

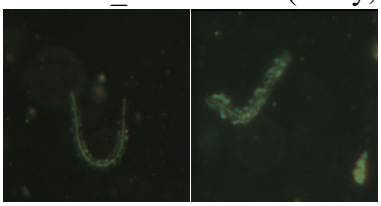

Diatom Mats:

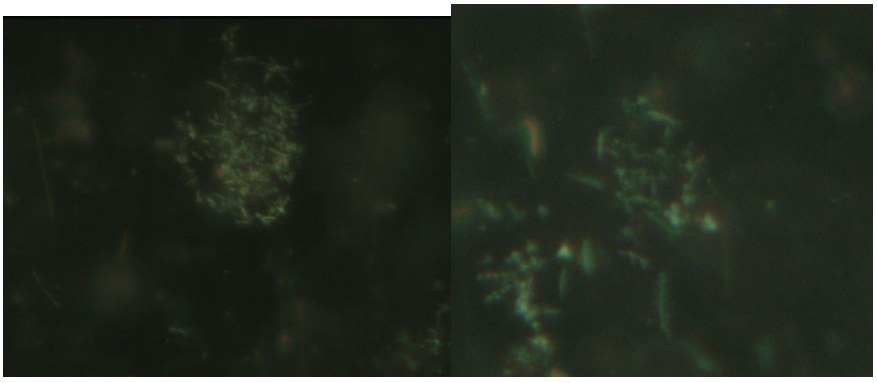

Gelatinous (medusa, in rr2004 ROIs as cool_jelly):

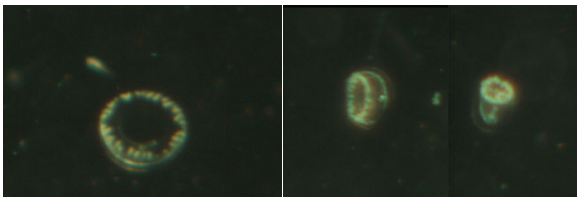

Gelatinous (salps):

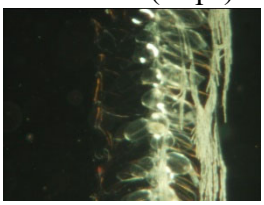

Gelatinous (siphonophores? Medusa 2?):

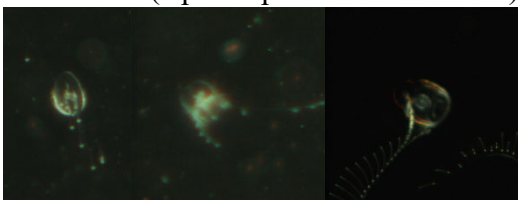

Gelatinous (other examples):

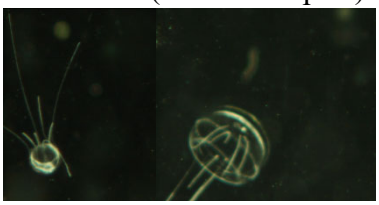

Krill (and krill-like):

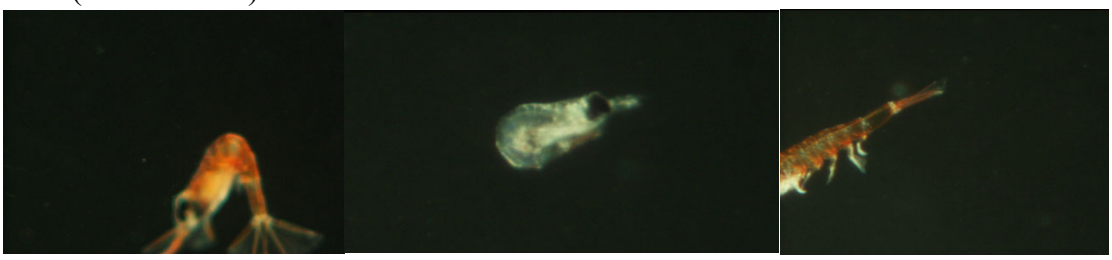

Phaeocystis antarctica:

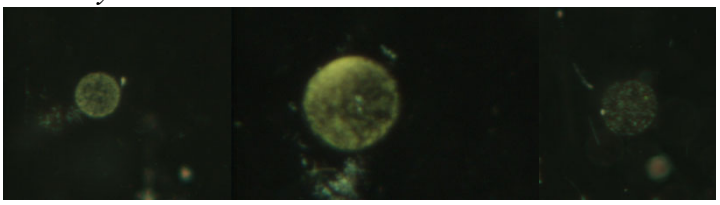

P. antarctica ghost colonies:

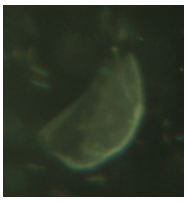

Phil's unknown spindles:

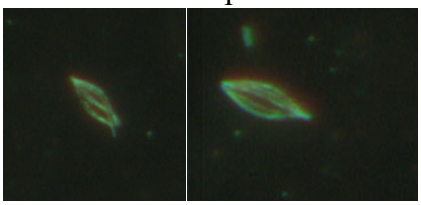

Pteropods:

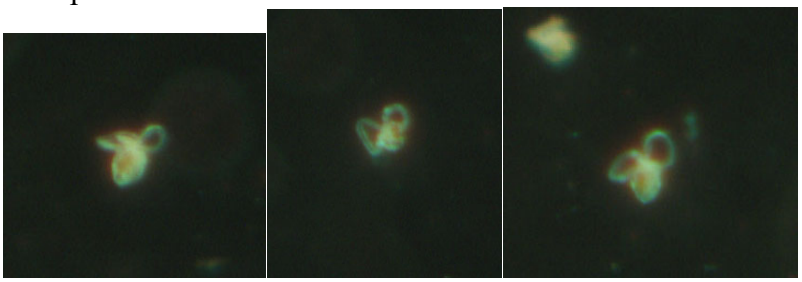

Worms (polychaetes):

Additional analysis was conducted to determine presence / absence of new and/or poorly classified taxa. These results are presented in the table below, as well as in the lower panels of the taxon plots presented in the main body of this report.

VPR 2:

Preliminary taxon name:	Hours:	Notes
Acanths	16-01	See taxon plots for distribution
Forams	Throughout tow	Rare, our CNN correctly classifies them. Identical in appearance TN368 (to 1st order).

Krill	Throughout tow	Rare, red and White Colorations
Large Copepods w/ and w/o dark spots	4, 5, 6, 10	Rare, likely eucalanus or paracalanus.
Long egg sac copes	7, 8, 9	Small, hours listed is for most common. Later hours have presence but low abundance.
Phaeod_knob_Pcystida	Throughout tow	Rare, our CNN correctly classifies them. Identical in appearance TN368 (to 1st order).
Red antennae and tail copepods	3, 5, 6	Calanus or calanoid, distinctive red antennae and band on tail. Low abundance in later hours.

VPR 3:

Preliminary taxon name:	Hours:	Notes
Acanths	Throughout tow	See taxon plots for distribution
Amphipods	14, 15	Rare
Blue backed Copes	13	Likely red antennae and tail copes with weird optics
Copes Microaggregations	4, 5, 14	Only present for isolated frames
Forams	Throughout tow	Rare, our CNN correctly classifies them. Identical in appearance TN368 (to 1st order).
Krill	Throughout tow	Rare, red ends 6, silver starts 9, white throughout.
Large Copepods w/ and w/o dark spots	7	Rare, likely eucalanus or paracalanus.
Long egg sac copes	4, 8	Small, hours listed is for most common. Other hours have presence but low abundance.
Phaeod_knob_Pcystida	Throughout tow	Rare, our CNN correctly classifies them. Identical in appearance TN368 (to 1st order).
Red antennae and tail copepods	23, 3, 11	Calanus or calanoid, distinctive red antennae and band on tail. Low abundance in other hours.
Smaller dark spot copes		Unknown if important, few found

VPR 4:

Preliminary taxon name:	Hours:	Notes
Amphipods	20, 0, 1, 5, 10	Rare
Chaetognaths	Throughout Tow	Rare, more common in dense bloom hours.
Copes Microaggregations	17	Only a single frame?
Forams	Throughout tow	Rare, our CNN correctly classifies them. Identical in appearance TN368 (to 1st order).

Gelatinous	17 onwards	More common during blooms, with 3 marking another increase in abundance and 6 an increase in diversity
Krill	Throughout Tow	More common in bloom hours
Large Copepods w/ and w/o dark spots	H18	Rare, likely eucalanus or paracalanus.
Long egg sac copes	15 – 18, Rare 19 and 20	Copes_small with distinct egg sacs
Phaeod_knob_Pcystida	Throughout tow	Rare, our CNN correctly classifies them. Identical in appearance TN368 (to 1st order).
Pteropods	19 onwards	Most abundant in bloom hours
Red antennae and tail copepods; Orange Butt is same?	15 – 18, Rare 19 and 20; 17	Calanus or calanoid, distinctive red antennae and band on tail.
Upside down, clear copes	18 onwards	Most abundant in bloom hours
Worms	19 onwards	Most abundant in bloom hours

Bloom Progress:
A_Col=Alga Colonial; Dia_Mat=Diatom Mats; Ghost=Ghost colonies; P_Ant=*Phaeocystis antarctica*.

Preliminary taxon name:	H18	H19	H20	H21	H22	H23	H00	H01	H02
# ROIs:	2954	3920	8514	7483	8308	7924	6684	6812	10774
A_Col	Low	High	Low	Low	Low	Low	Low	Low	Bloom
Dia_Mat	Low?	Low?	Low?	Low	Low	Low	Low	Low	Bloom
Ghost	Low	Low	Low	Low	High	High	Low	Low	Bloom
P_Ant	Low	High	Low	Low, Ill	Low	Low	Low	Low	Bloom
Spindles									

Preliminary taxon name:	H03	H04	H05	H06	H07	H08	H09	H10	H11
# ROIs:	16763	14961	15467	16021	16396	13475	17050	12819	8170
A_Col	Bloom	Bloom	Bloom	Bloom	Bloom	High	High	High	Low
Dia_Mat	Bloom	Bloom	Bloom	Bloom	Bloom	High	High	High	Low
Ghost	Bloom	Bloom	Bloom	Bloom	Bloom	High	Low?	Low?	Absent?
P_Ant	Bloom	Bloom	Bloom	Bloom	Bloom	High	Low?	Low?	Absent?
Spindles			Only 1?			Only 1?	Low	Low*	High*

*With increase in spindles, so too does Chaetoceros, regular marine snow, and segmented diatoms

VPR 5:

Preliminary taxon name:	Hours:	Notes
Amphipods	14, 17, 21	Rare
Chaetognaths	Throughout Tow	Rare, more common in dense bloom hours.
Polar Krill	H02-H07, H10, H12	Larger than normal krill below 58 S
Upside down, clear copes	Before H09	Included in H02-H07copepod increase

Hour (s):	Notes and Taxa:
H08:	Same as most of last tow: A_Col, P_Ant, Ghost, Pteropods, Worms
H09 & H10:	Chaetoceros, spindles, and segmented diatoms appear, other taxa fade
H11-H18:	No bloom, no A_Col or P_Ant. Present taxa are segmented diatom rods, spindles, worms, and pteropods
H19-H00	Bloom of diatoms (not mats, think diatoms_bloom_discrete) builds then falls. Spindles, segmented diatoms, chaetoceros common.
H01	Less of everything. A_Col appears, though it looks distinctly like marine snow and has no accompanying diatom mats
H02-H07	Lots of large zooplankton (Amphipods, polar krill, copes) and large fecal strings. Little to no phytoplankton (no spindles, Chaetoceros)
H08-H11	Salps particularly common.

Appendix 3. Atlas of the hydrographic, bio-optical, and taxonomic plots for all VPR tows combined

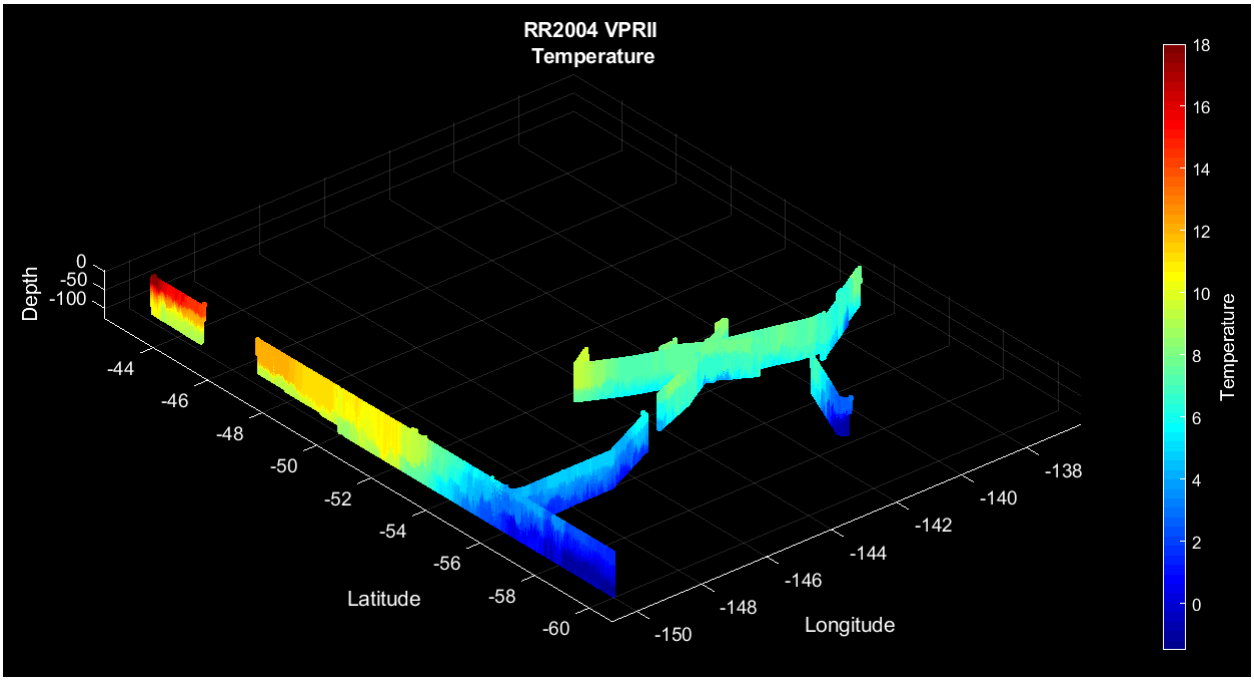

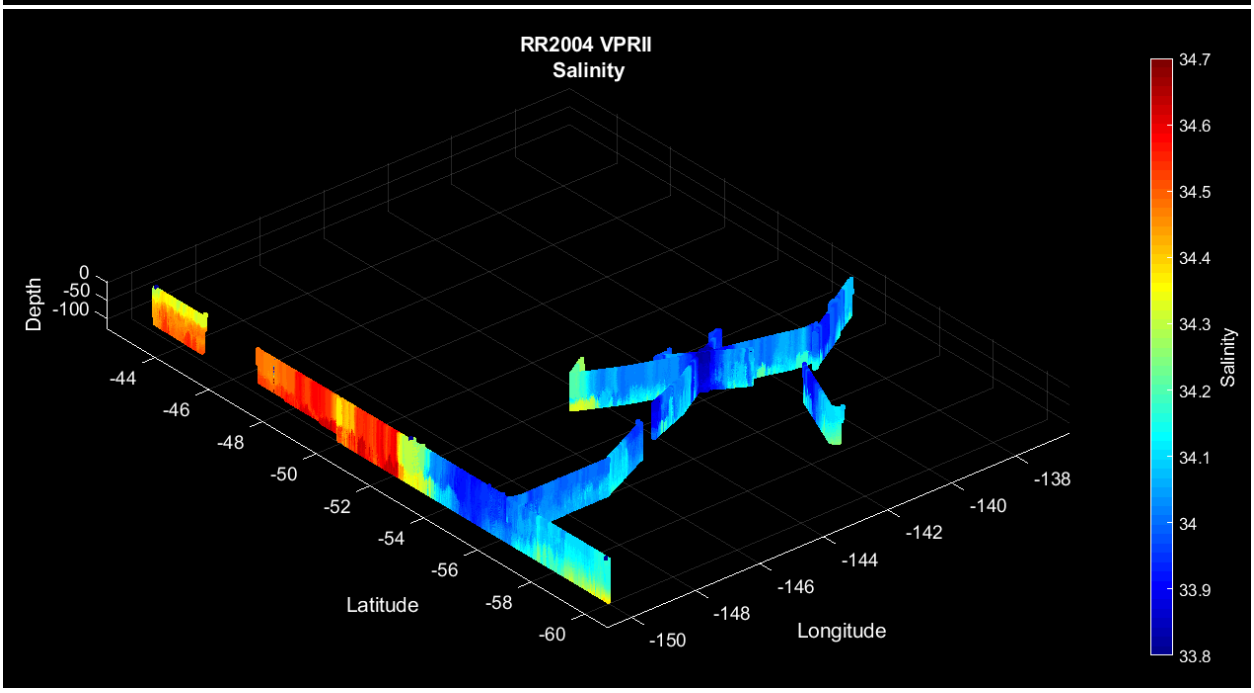

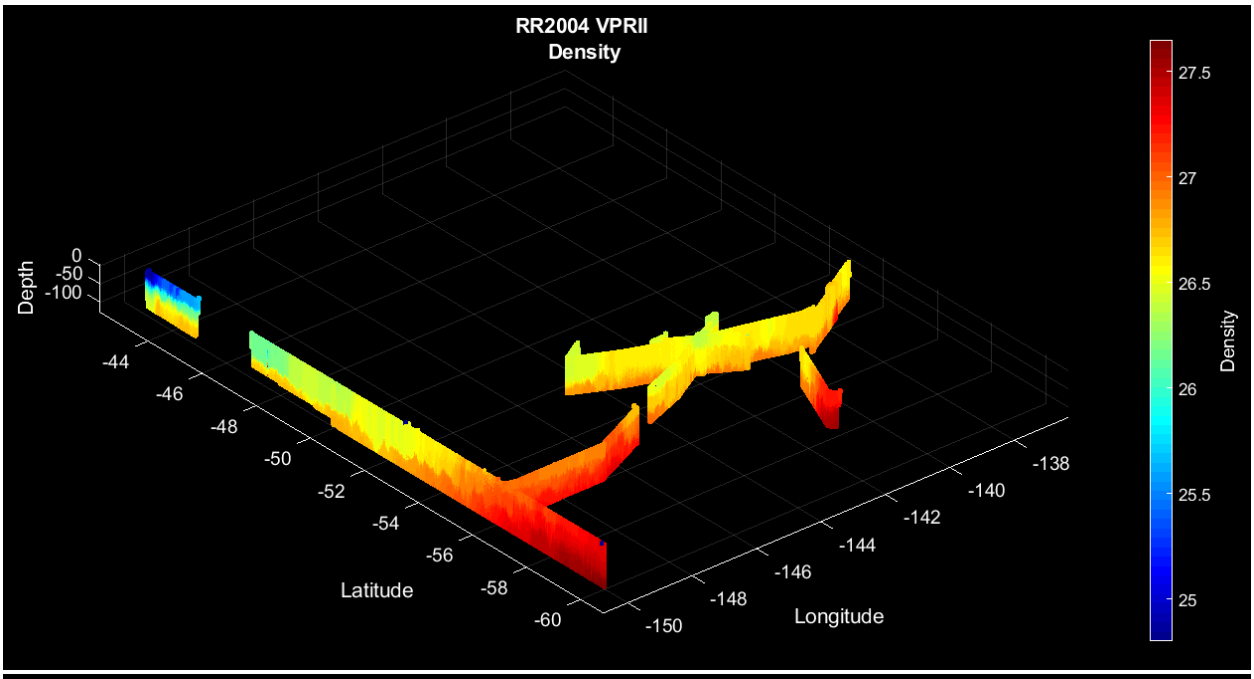
RR2004 VPRII
Density
Depth
0
-50
-100
-44
-46
-48
-50
-52
-54
-56
-58
-60
Latitude
-138
-140
-142
-144
-146
-148
-150
Longitude
27.5
27
26.5
26
25.5
25
Density

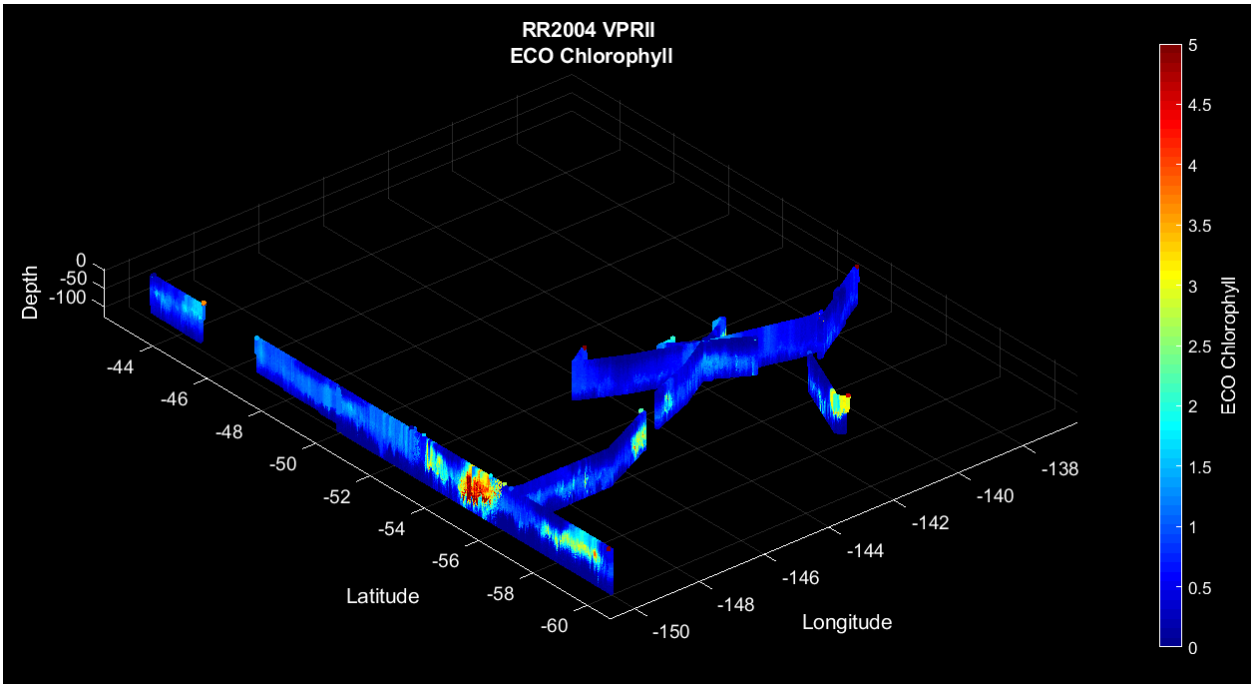
RR2004 VPRII
ECO Chlorophyll
Depth
0
-50
-100
-44
-46
-48
-50
-52
-54
-56
-58
-60
Latitude
-138
-140
-142
-144
-146
-148
-150
Longitude
5
4.5
4
3.5
3
2.5
2
1.5
1
0.5
0
ECO Chlorophyll

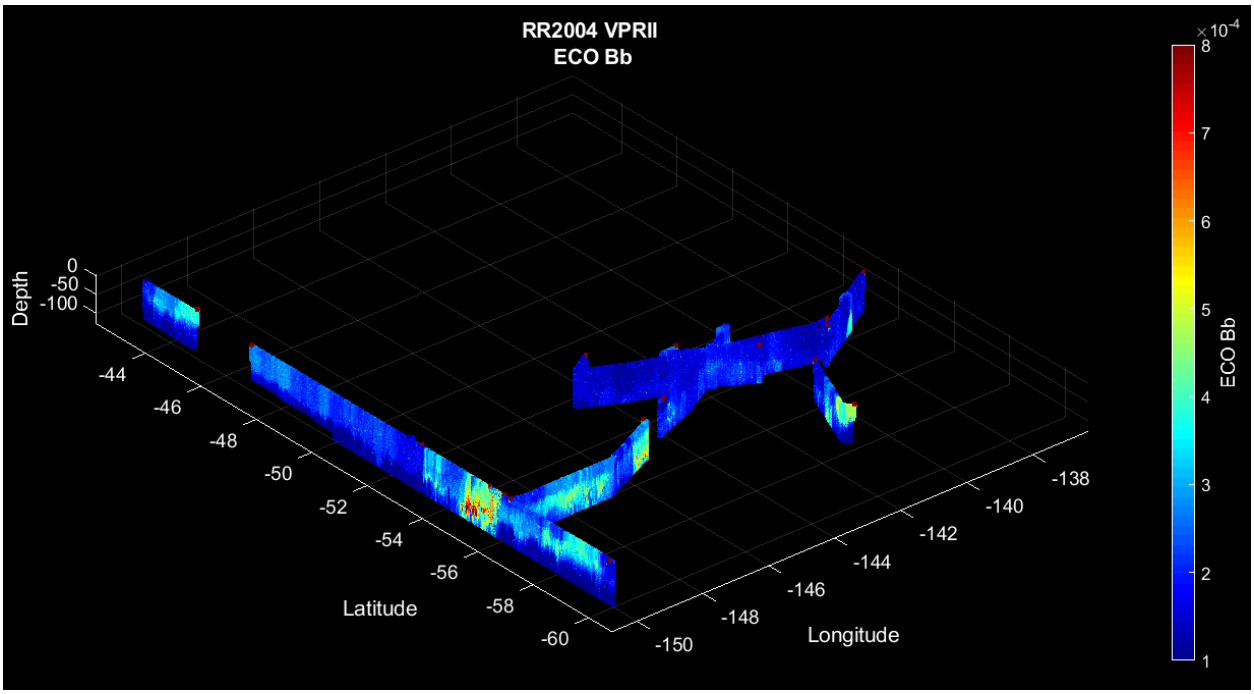
RR2004 VPRII
ECO Bb
Depth
0
-50
-100
-44
-46
-48
-50
-52
-54
-56
-58
-60
Latitude
-150
-148
-146
-144
-142
-140
-138
Longitude
×10^-4
8
7
6
5
4
3
2
1
ECO Bb

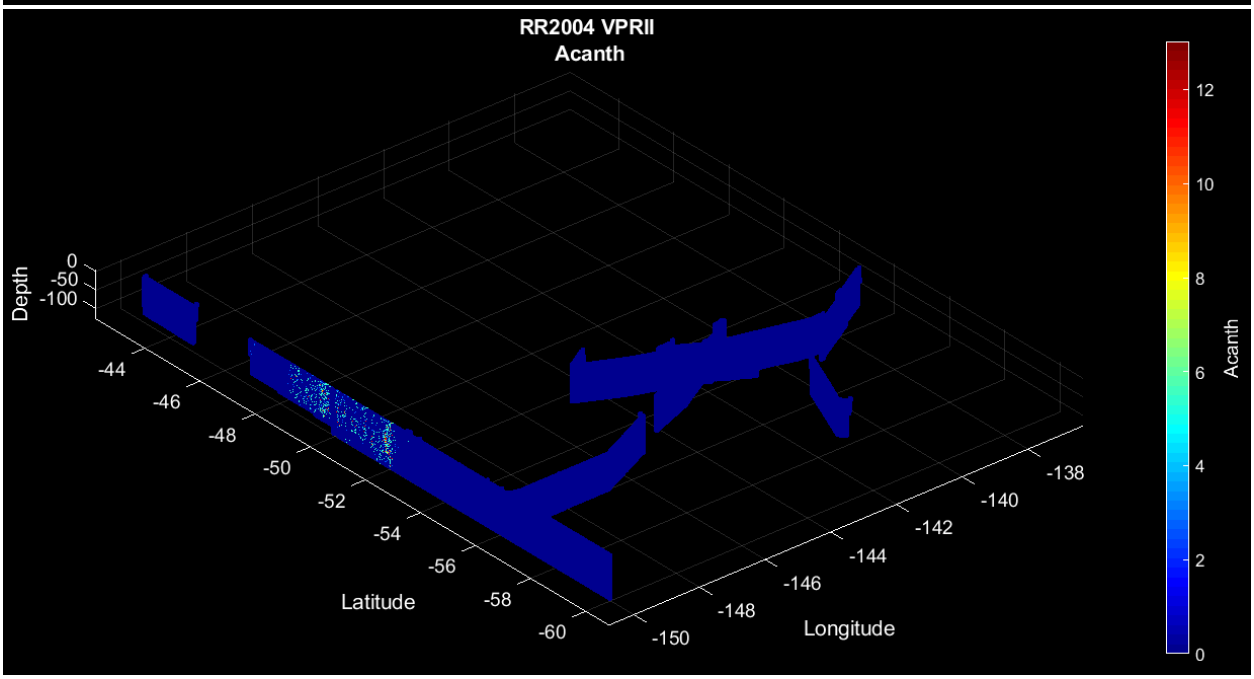
RR2004 VPRII
Acanth
Depth
0
-50
-100
-44
-46
-48
-50
-52
-54
-56
-58
-60
Latitude
-150
-148
-146
-144
-142
-140
-138
Longitude
12
10
8
6
4
2
0
Acanth

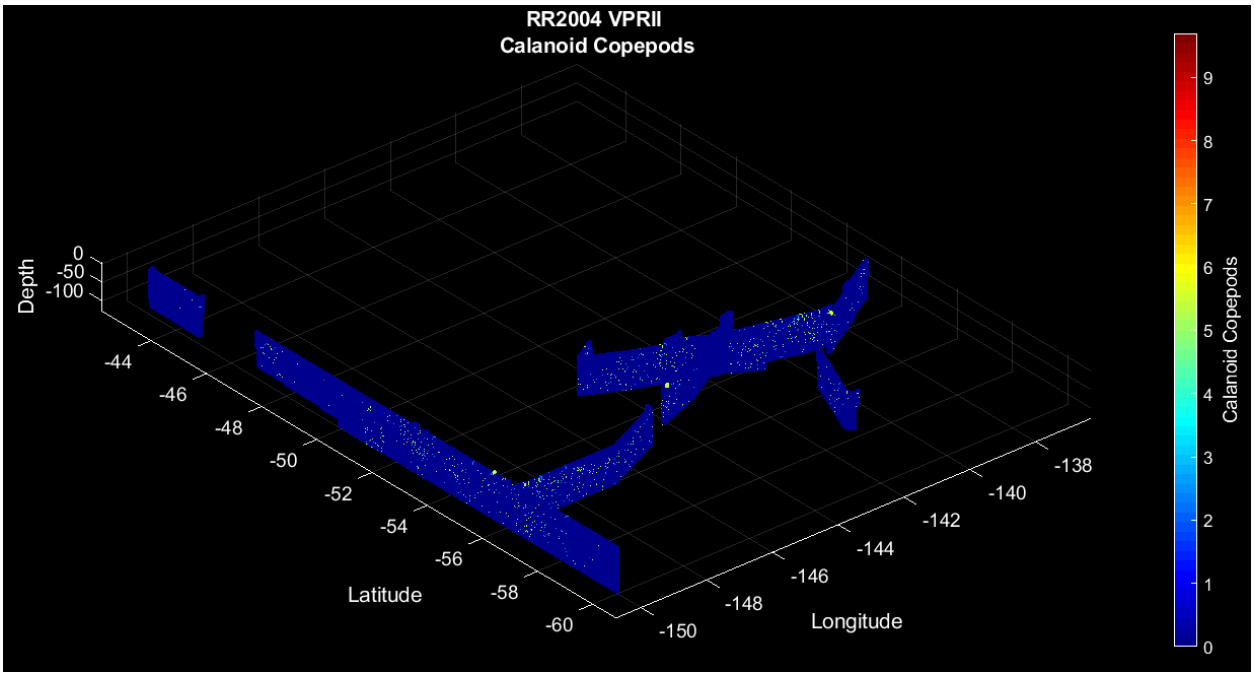

*CNN taxa copes_calanus

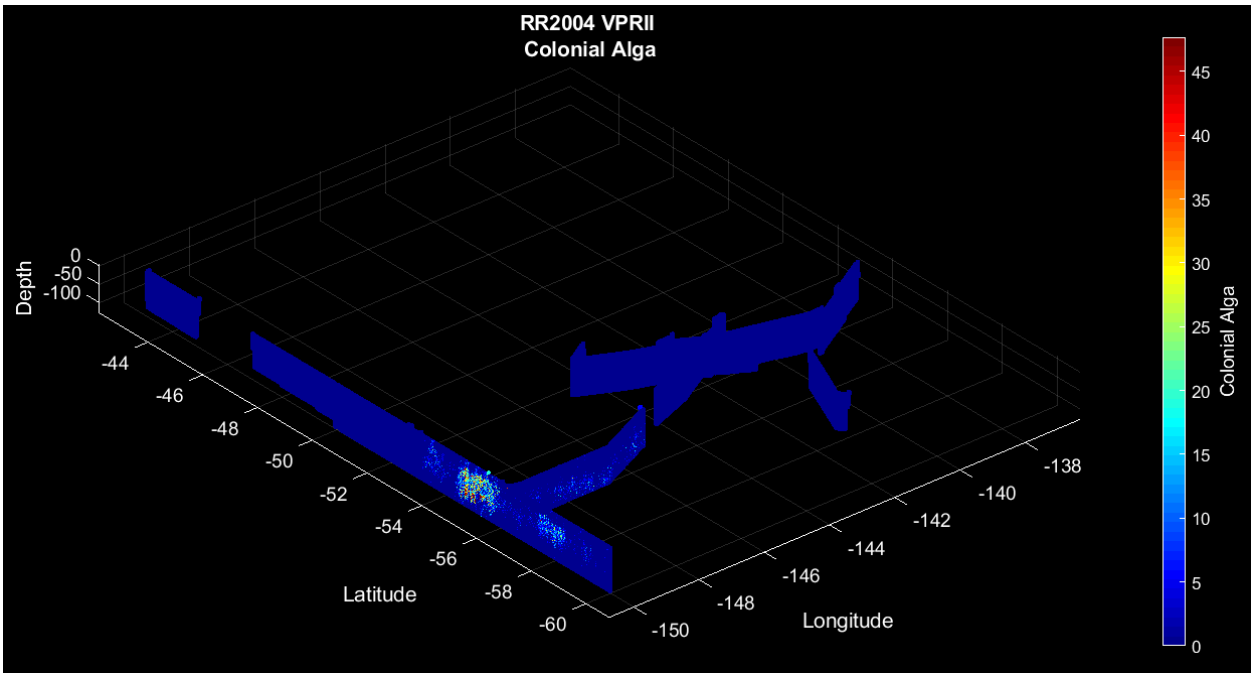

*CNN4(10b) taxa Phaeo_bloom

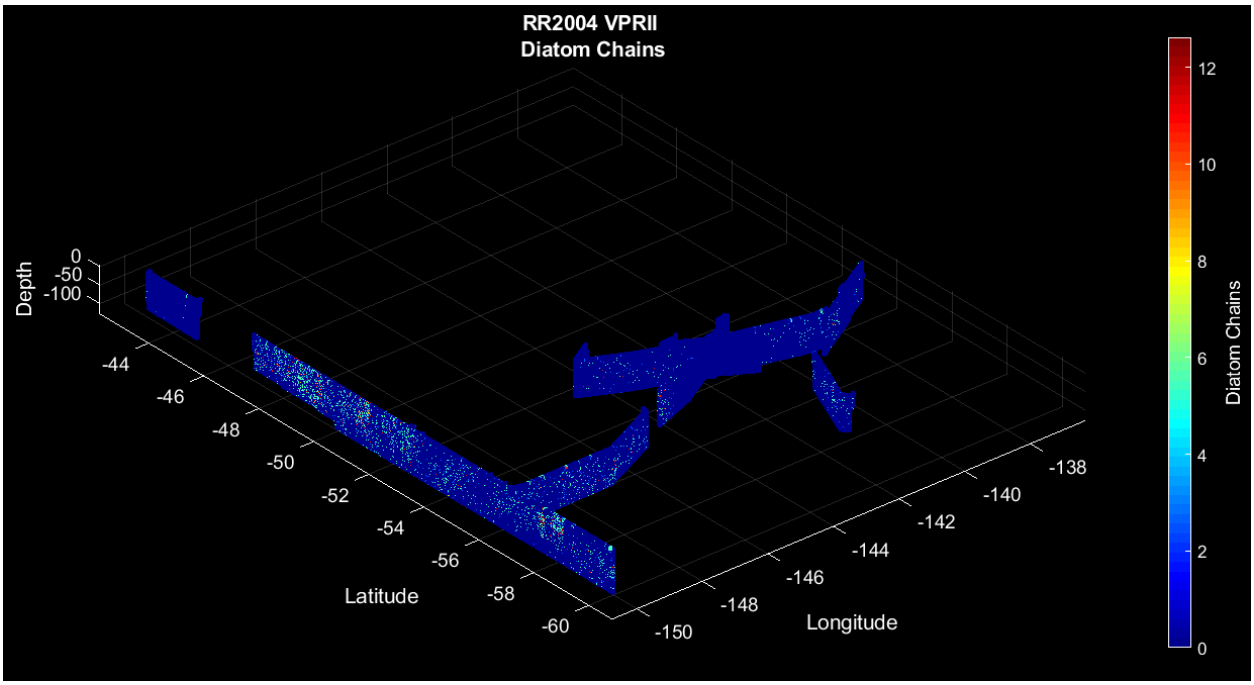
RR2004 VPRII
Diatom Chains
Depth
0
-50
-100
-44
-46
-48
-50
-52
-54
-56
-58
-60
Latitude
-138
-140
-142
-144
-146
-148
-150
Longitude
12
10
8
6
4
2
0
Diatom Chains

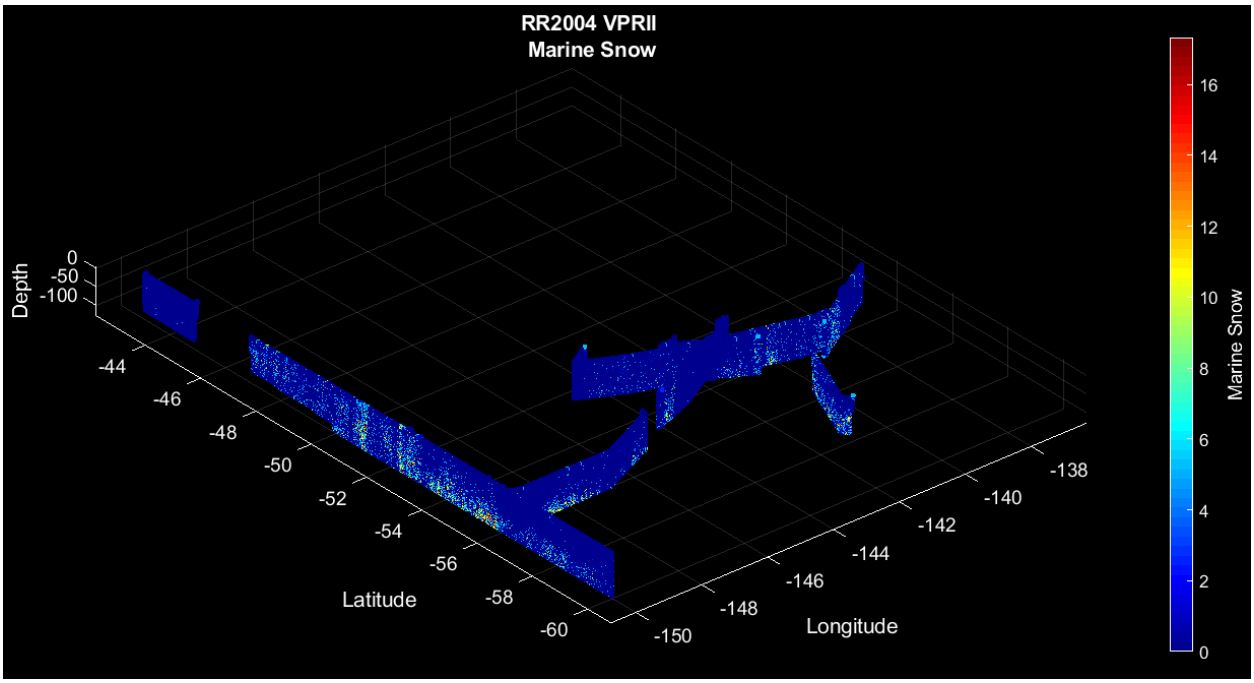
RR2004 VPRII
Marine Snow
Depth
0
-50
-100
-44
-46
-48
-50
-52
-54
-56
-58
-60
Latitude
-138
-140
-142
-144
-146
-148
-150
Longitude
16
14
12
10
8
6
4
2
0
Marine Snow

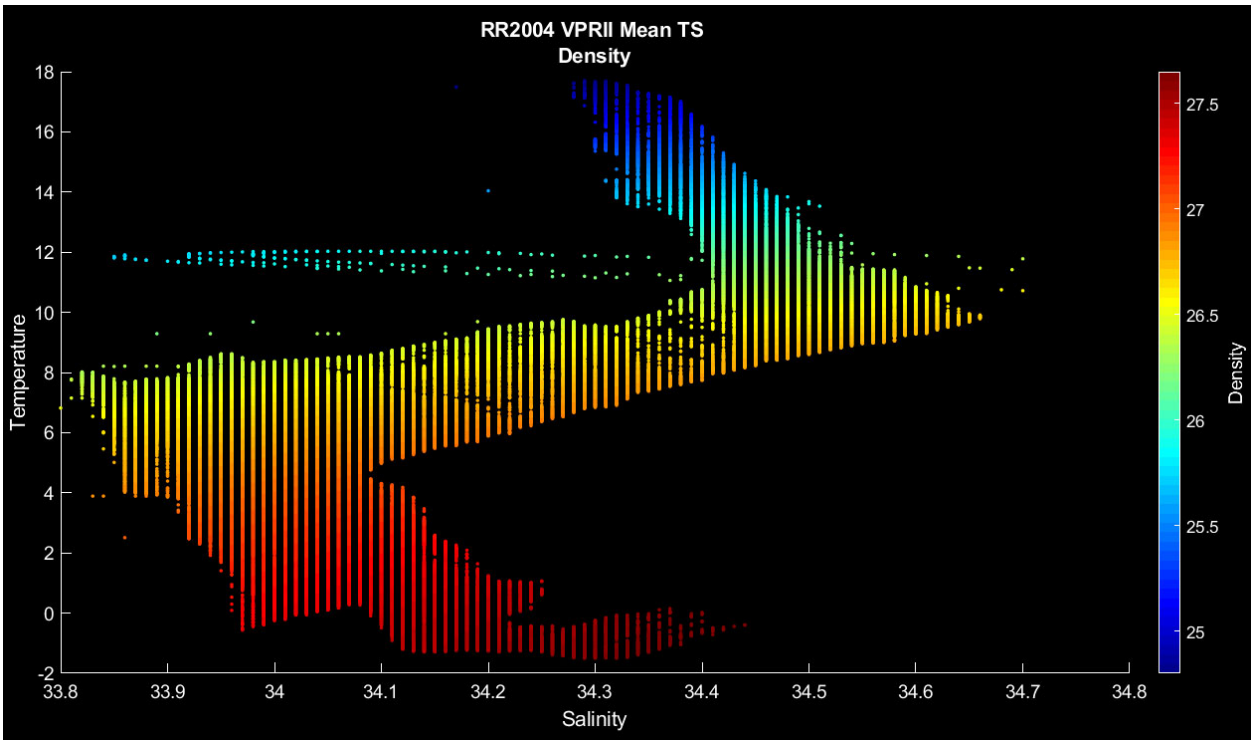
RR2004 VPRII Mean TS
Density
Temperature
Salinity
Density
18
16
14
12
10
8
6
4
2
0
-2
33.8
33.9
34
34.1
34.2
34.3
34.4
34.5
34.6
34.7
34.8
27.5
27
26.5
26
25.5
25

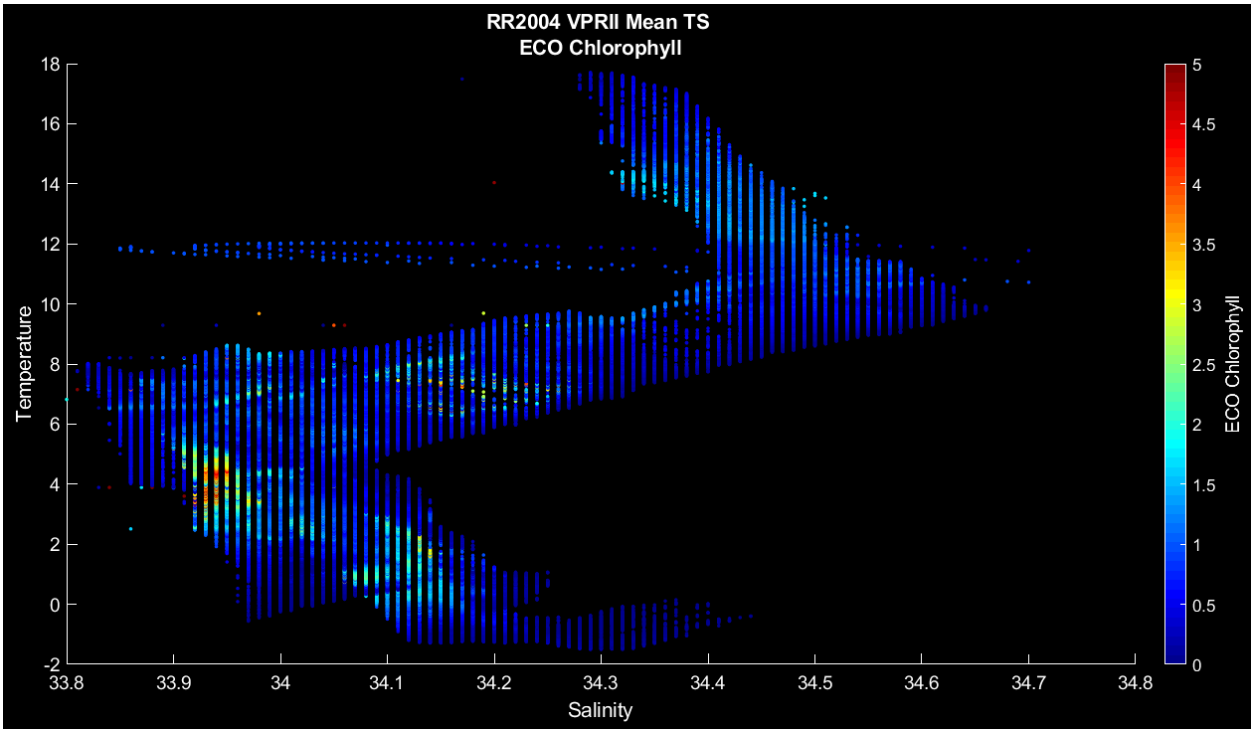
RR2004 VPRII Mean TS
ECO Chlorophyll
Temperature
Salinity
ECO Chlorophyll
18
16
14
12
10
8
6
4
2
0
-2
33.8
33.9
34
34.1
34.2
34.3
34.4
34.5
34.6
34.7
34.8
5
4.5
4
3.5
3
2.5
2
1.5
1
0.5
0

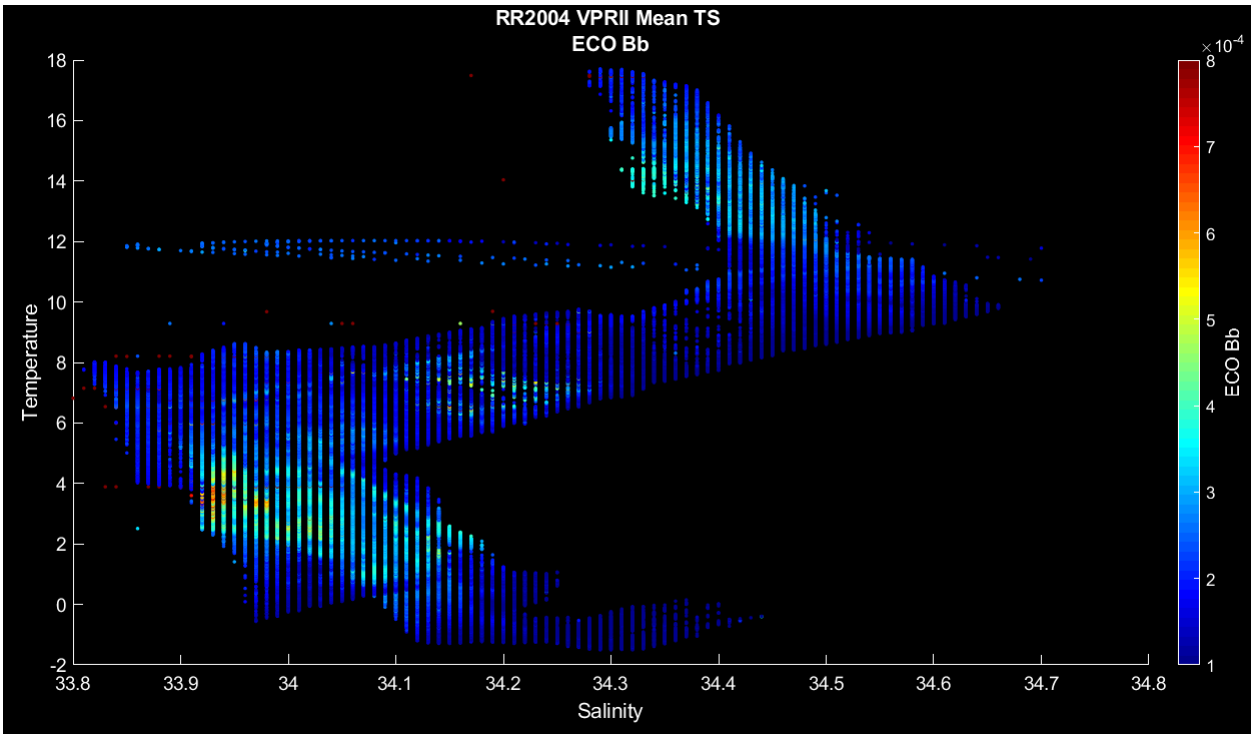
RR2004 VPRII Mean TS
ECO Bb
Temperature
Salinity
ECO Bb
×10^-4
18
16
14
12
10
8
6
4
2
0
-2
33.8
33.9
34
34.1
34.2
34.3
34.4
34.5
34.6
34.7
34.8
8
7
6
5
4
3
2
1

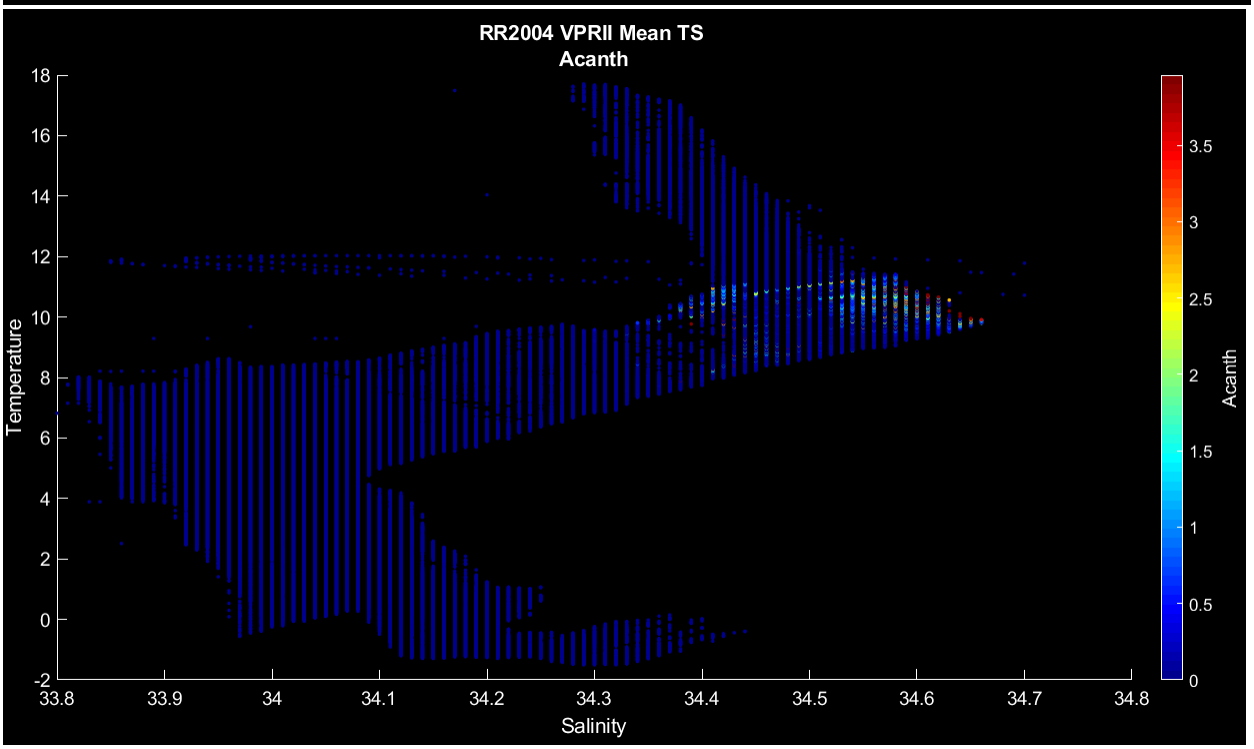
RR2004 VPRII Mean TS
Acanth
Temperature
Salinity
Acanth
18
16
14
12
10
8
6
4
2
0
-2
33.8
33.9
34
34.1
34.2
34.3
34.4
34.5
34.6
34.7
34.8
3.5
3
2.5
2
1.5
1
0.5
0

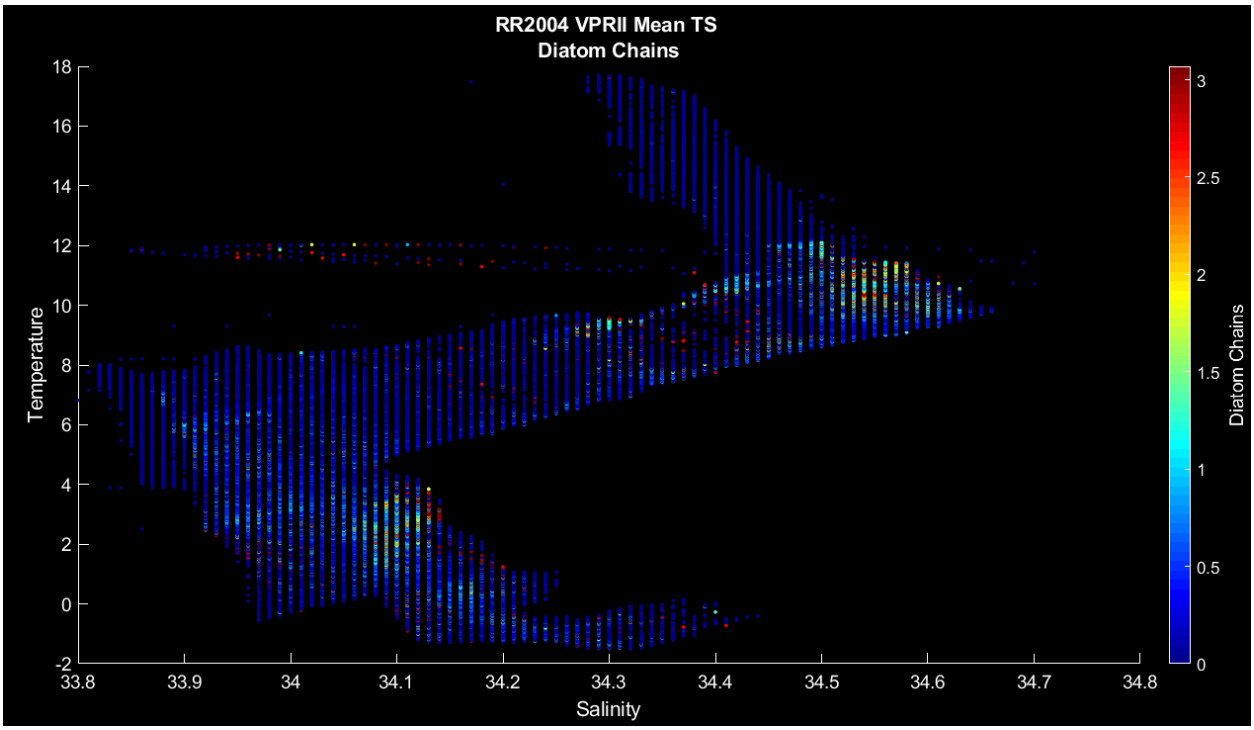

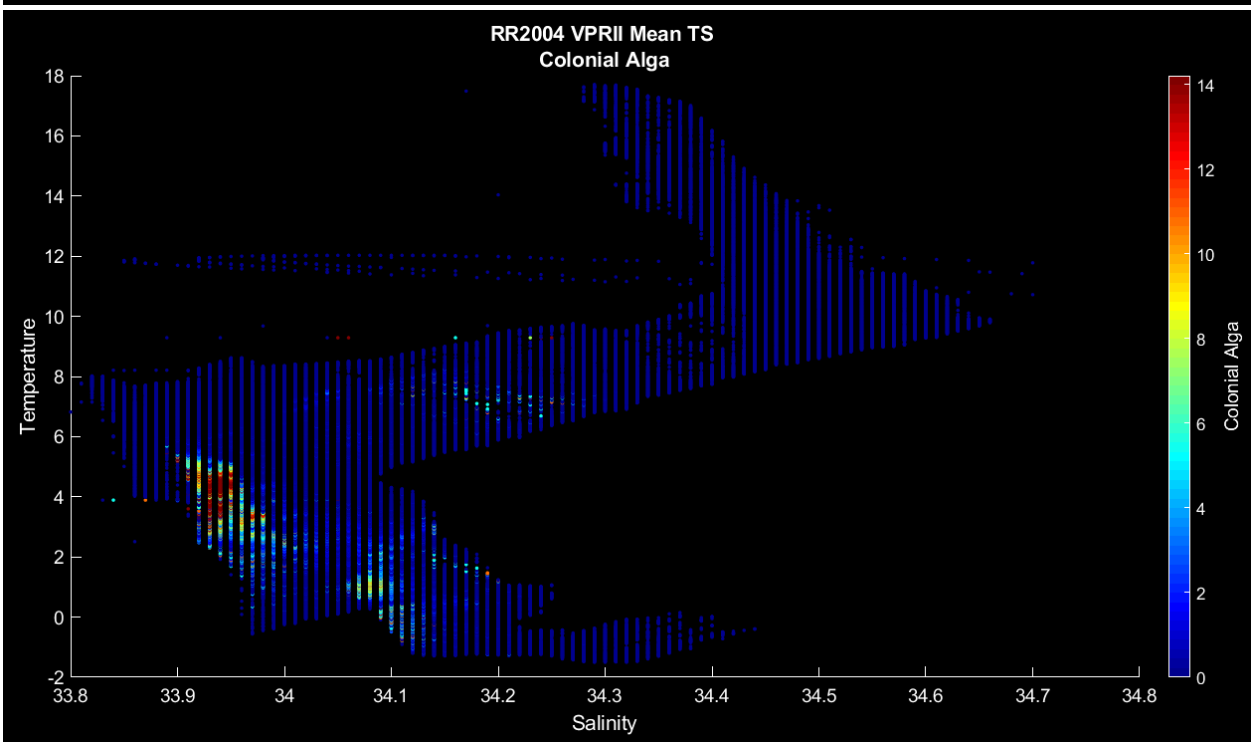

*CNN4(10b) taxa Phaeo_bloom

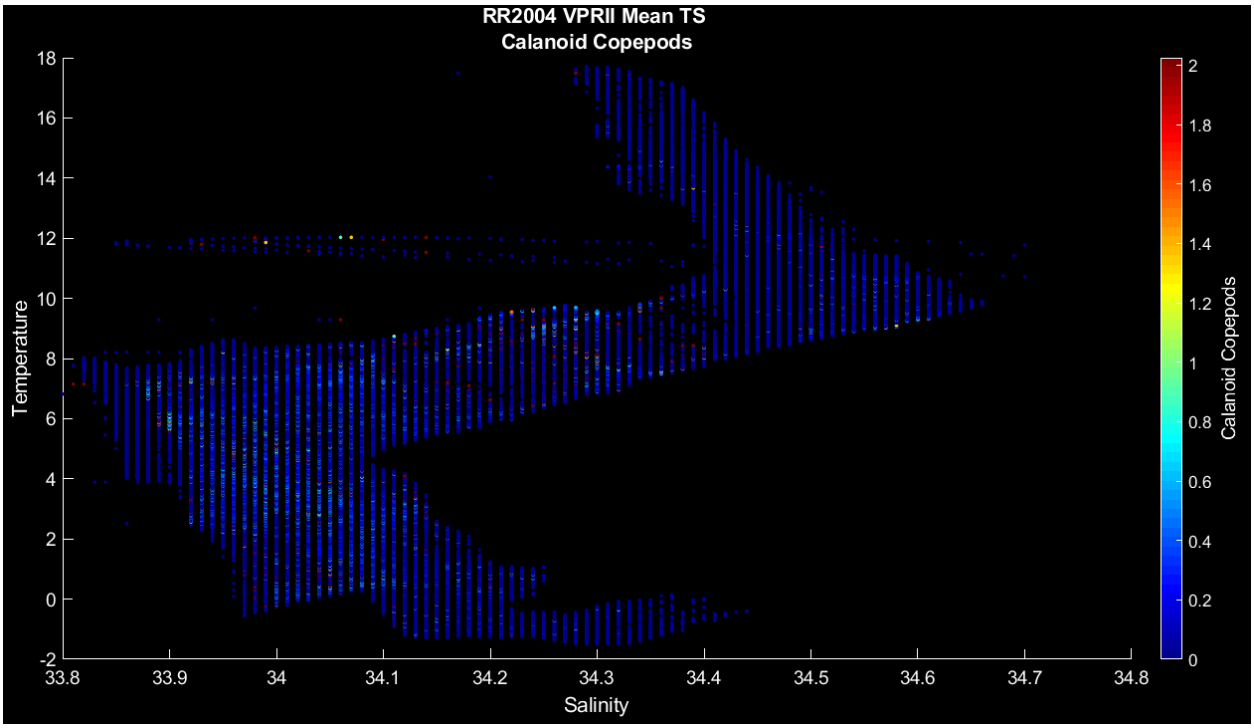

*CNN taxa copes_calanus

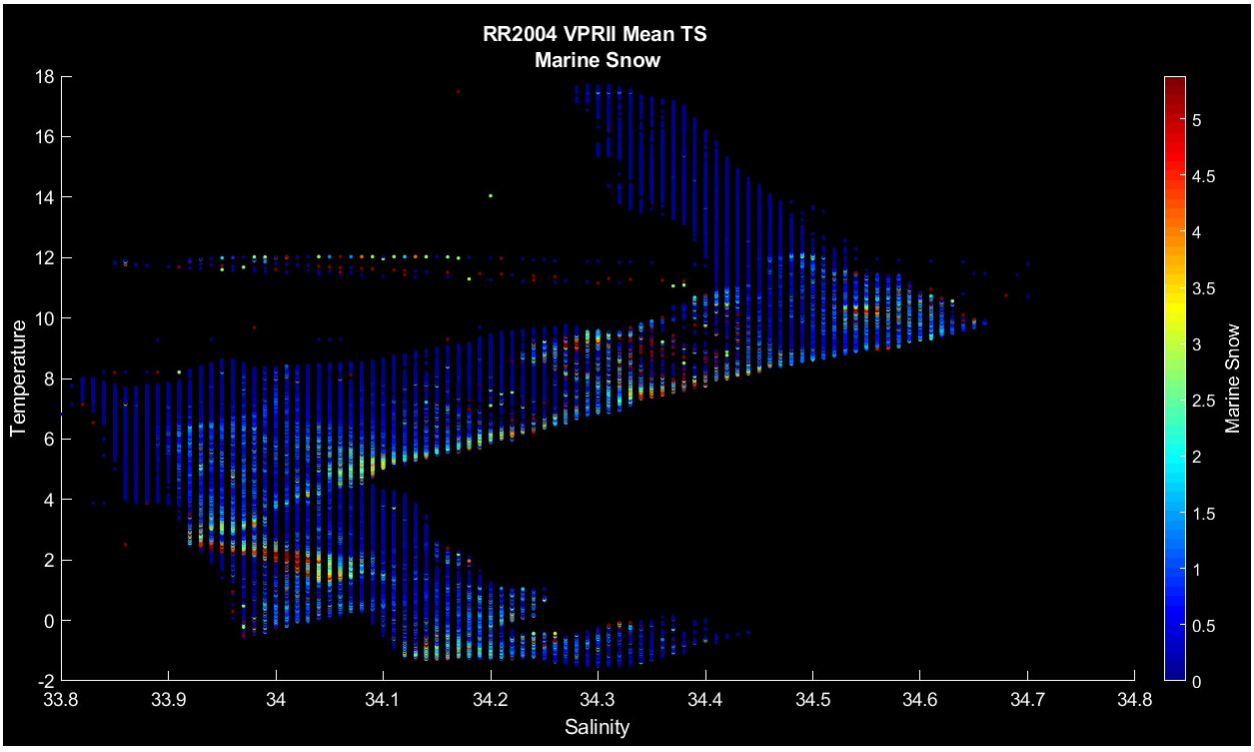

Appendix 4. VPR 3-4 overlap region

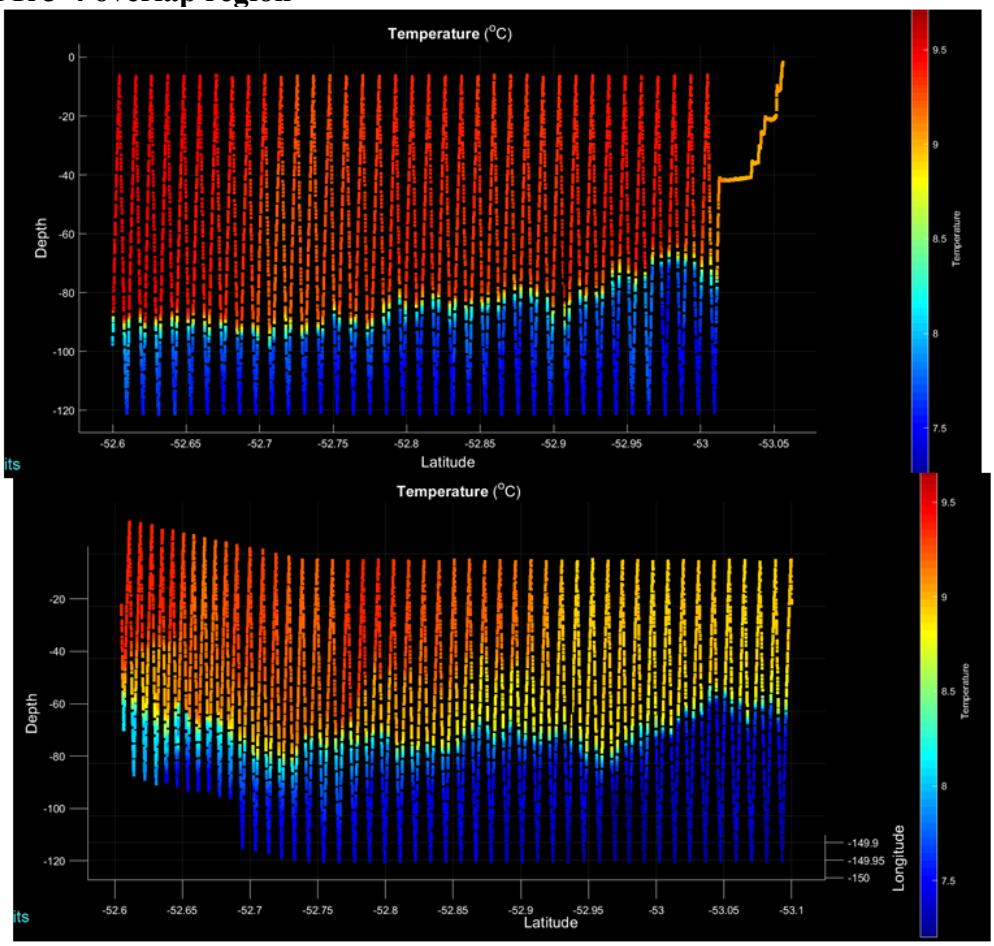

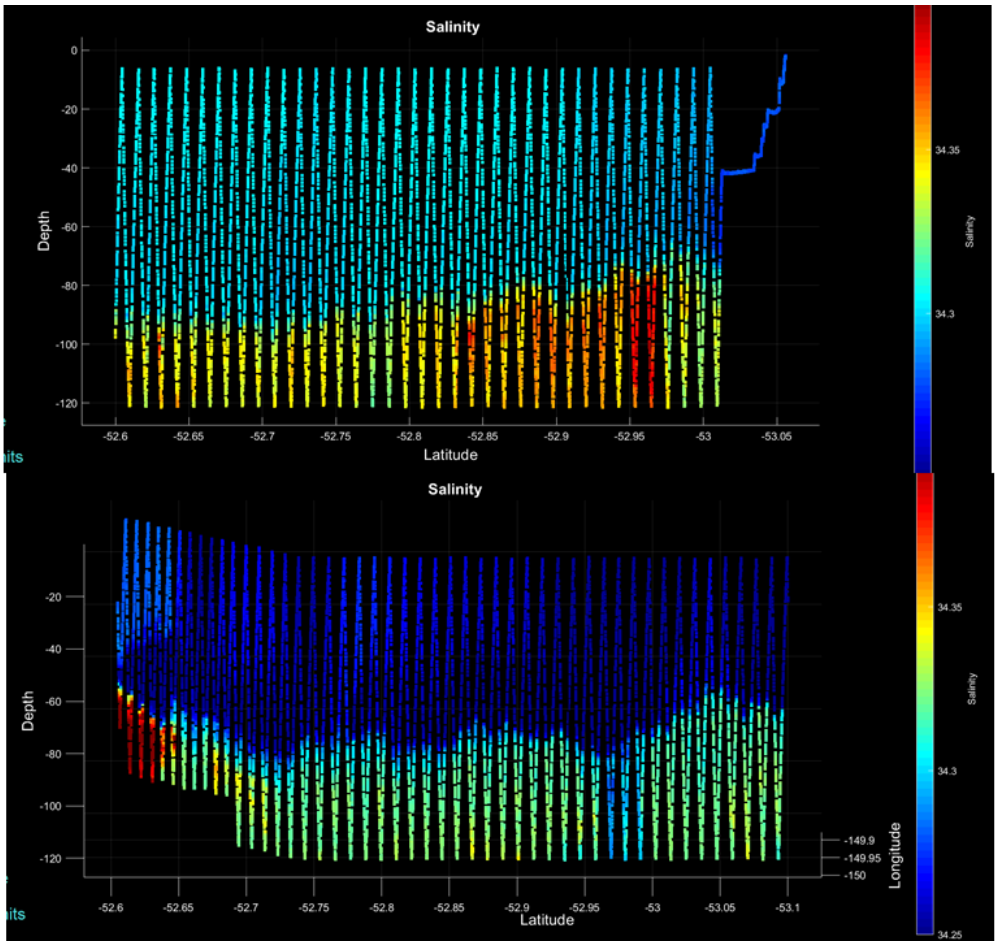
Salinity
Depth
0
-20
-40
-60
-80
-100
-120
-52.6
-52.65
-52.7
-52.75
-52.8
-52.85
-52.9
-52.95
-53
-53.05
Latitude
34.35
34.3
Salinity
Salinity
Depth
-20
-40
-60
-80
-100
-120
-52.6
-52.65
-52.7
-52.75
-52.8
-52.85
-52.9
-52.95
-53
-53.05
-53.1
Latitude
-149.9
-149.95
-150
Longitude
34.35
34.3
34.25
Salinity

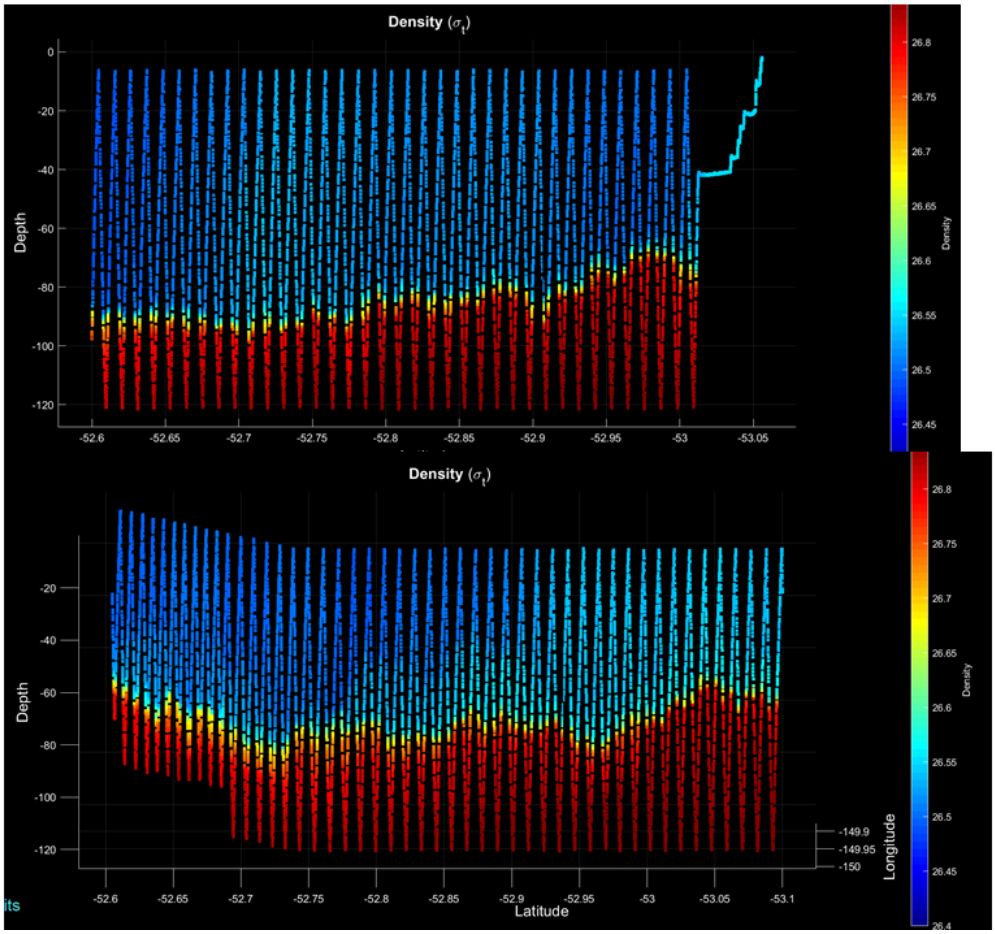
Density (σ_t)
Depth
0
-20
-40
-60
-80
-100
-120
-52.6
-52.65
-52.7
-52.75
-52.8
-52.85
-52.9
-52.95
-53
-53.05
Density
26.8
26.75
26.7
26.65
26.6
26.55
26.5
26.45
Density (σ_t)
Depth
-20
-40
-60
-80
-100
-120
-52.6
-52.65
-52.7
-52.75
-52.8
-52.85
-52.9
-52.95
-53
-53.05
-53.1
Latitude
-149.9
-149.95
-150
Longitude
Density
26.8
26.75
26.7
26.65
26.6
26.55
26.5
26.45
26.4

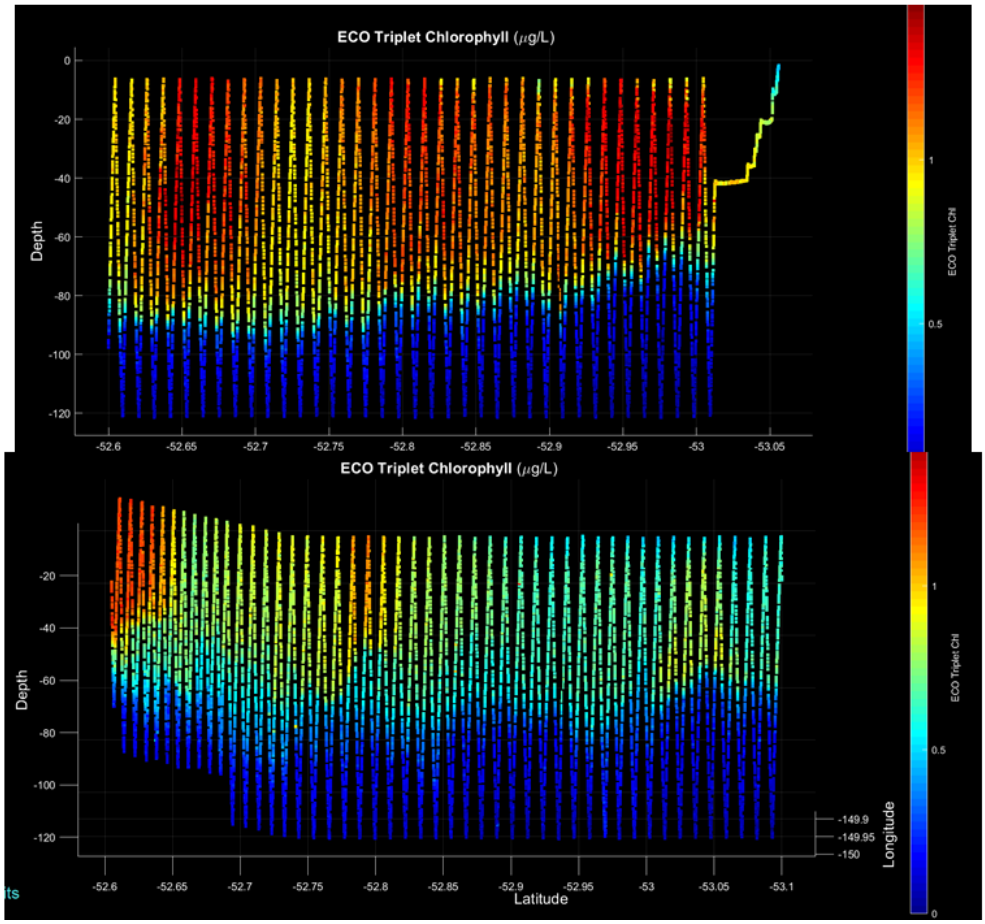
ECO Triplet Chlorophyll (μg/L)
Depth
0
-20
-40
-60
-80
-100
-120
-52.6
-52.65
-52.7
-52.75
-52.8
-52.85
-52.9
-52.95
-53
-53.05
ECO Triplet Chl
1
0.5
ECO Triplet Chlorophyll (μg/L)
Depth
-20
-40
-60
-80
-100
-120
-52.6
-52.65
-52.7
-52.75
-52.8
-52.85
-52.9
-52.95
-53
-53.05
-53.1
Latitude
-149.9
-149.95
-150
Longitude
ECO Triplet Chl
1
0.5
0

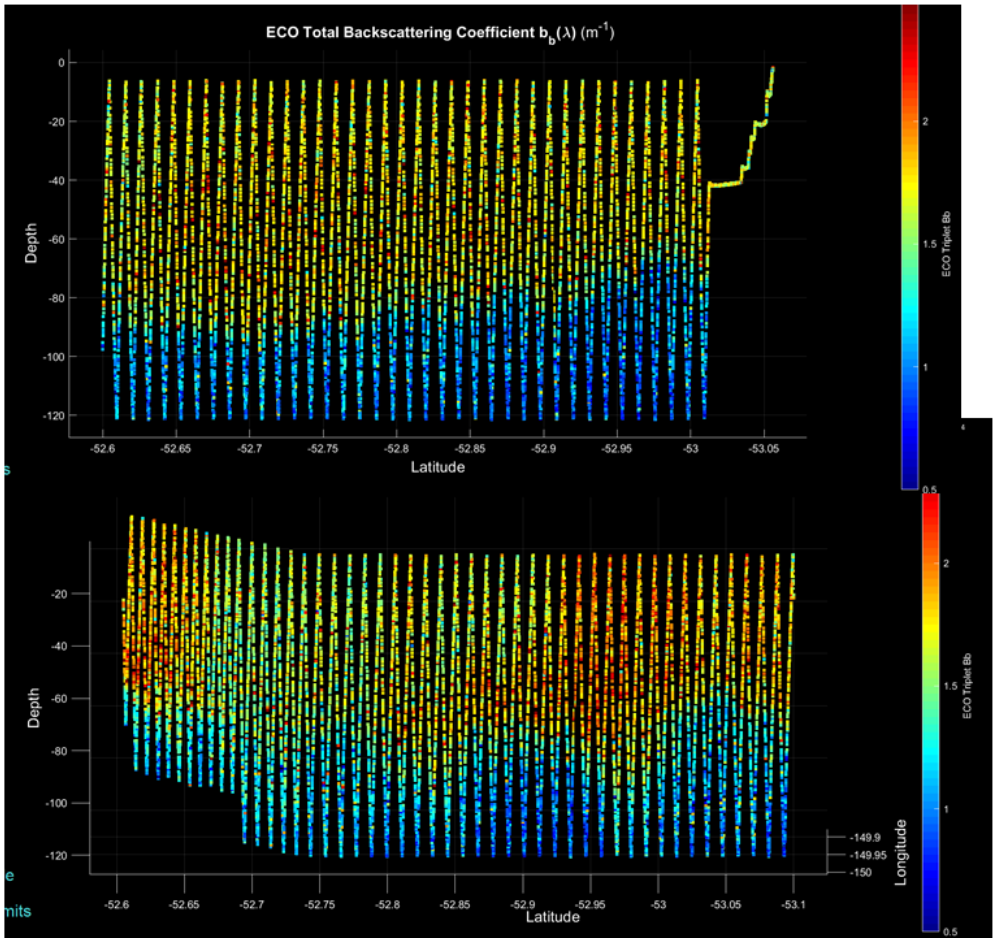
ECO Total Backscattering Coefficient $b_b(\lambda)$ (m^{-1})
Depth
Latitude
ECO Triplet Bb
Depth
Latitude
Longitude
ECO Triplet Bb

Appendix 5. VPR 4-5 overlap region

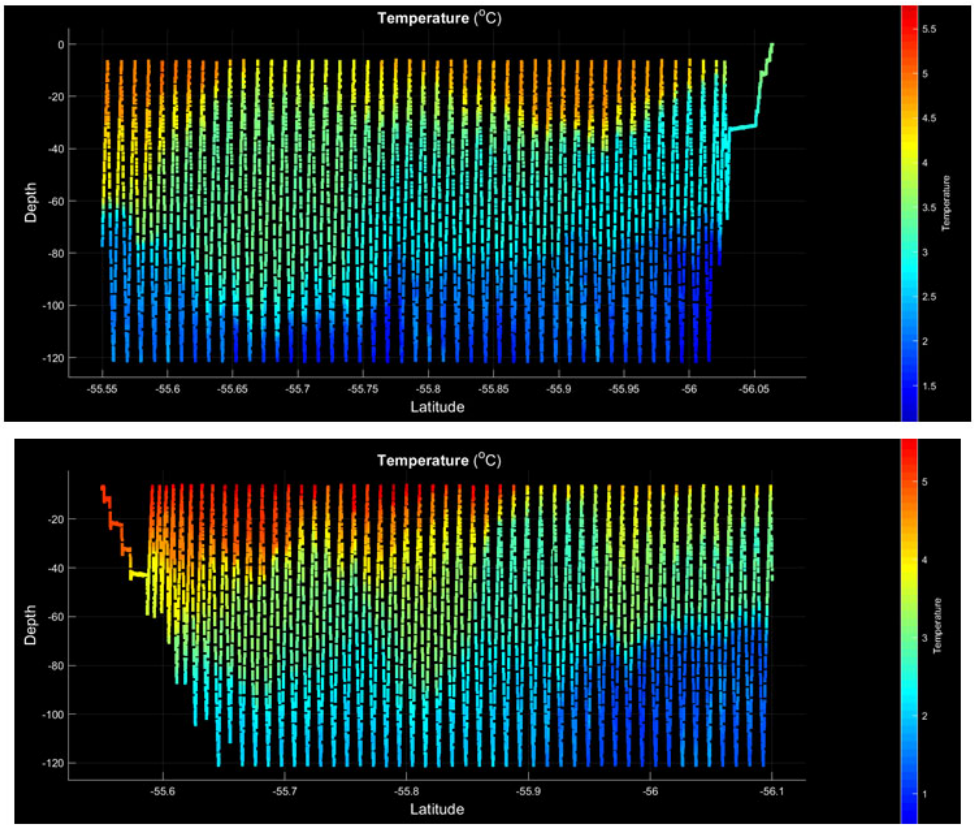

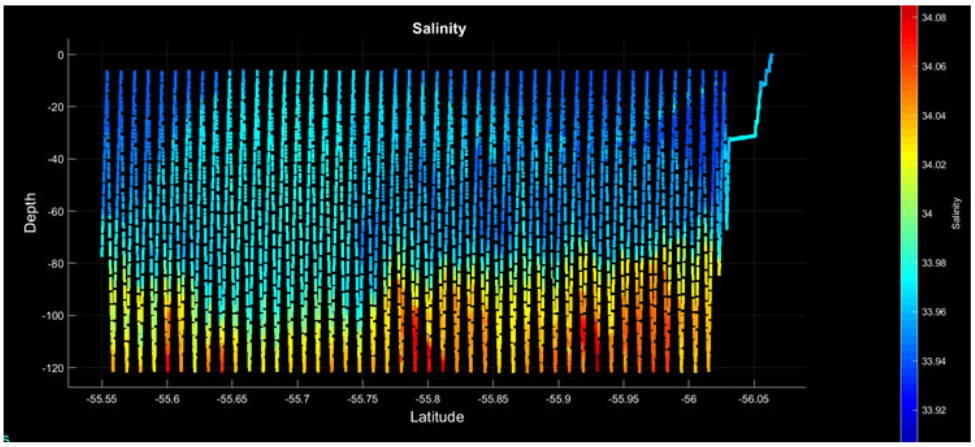
Salinity
Depth
0
-20
-40
-60
-80
-100
-120
-55.55
-55.6
-55.65
-55.7
-55.75
-55.8
-55.85
-55.9
-55.95
-56
-56.05
Latitude
34.08
34.06
34.04
34.02
34
33.98
33.96
33.94
33.92
Salinity

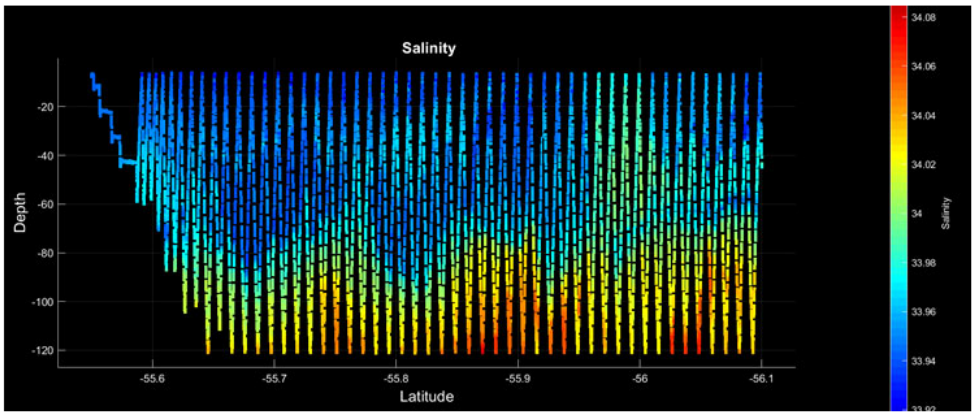
Salinity
Depth
-20
-40
-60
-80
-100
-120
-55.6
-55.7
-55.8
-55.9
-56
-56.1
Latitude
34.08
34.06
34.04
34.02
34
33.98
33.96
33.94
Salinity

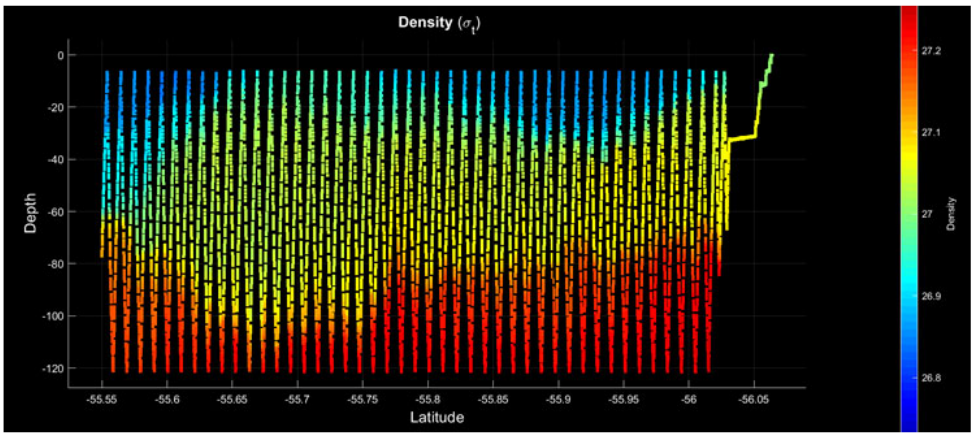
Density (σ_t)
Depth
0
-20
-40
-60
-80
-100
-120
-55.55
-55.6
-55.65
-55.7
-55.75
-55.8
-55.85
-55.9
-55.95
-56
-56.05
Latitude
27.2
27.1
27
26.9
26.8
Density

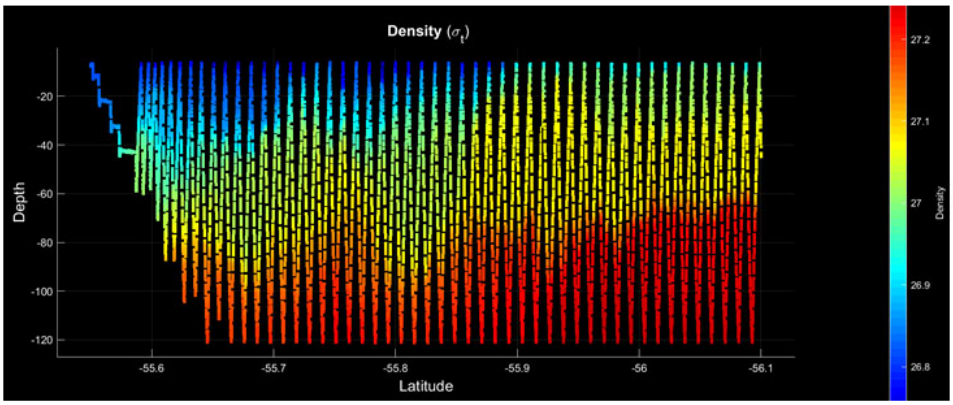
Density (σ_t)
Depth
-20
-40
-60
-80
-100
-120
-55.6
-55.7
-55.8
-55.9
-56
-56.1
Latitude
27.2
27.1
27
26.9
26.8
Density

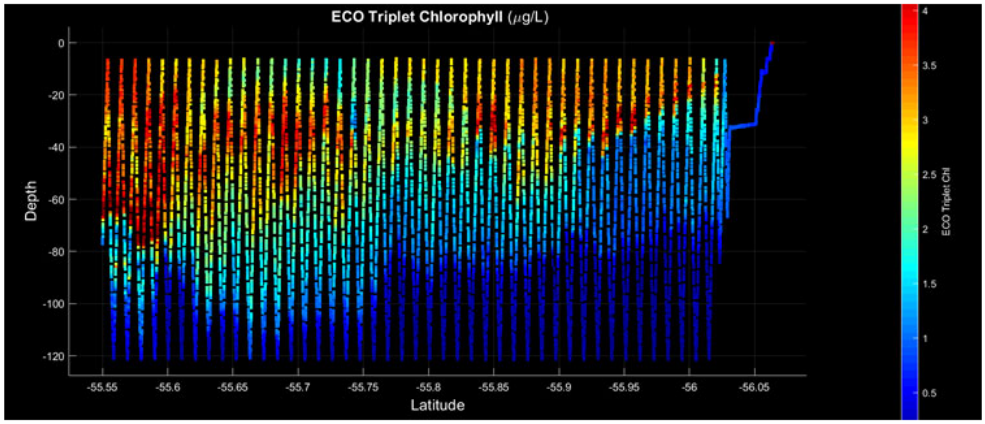
ECO Triplet Chlorophyll (μg/L)
Depth
0
-20
-40
-60
-80
-100
-120
-55.55
-55.6
-55.65
-55.7
-55.75
-55.8
-55.85
-55.9
-55.95
-56
-56.05
Latitude
ECO Triplet Chl
4
3.5
3
2.5
2
1.5
1
0.5

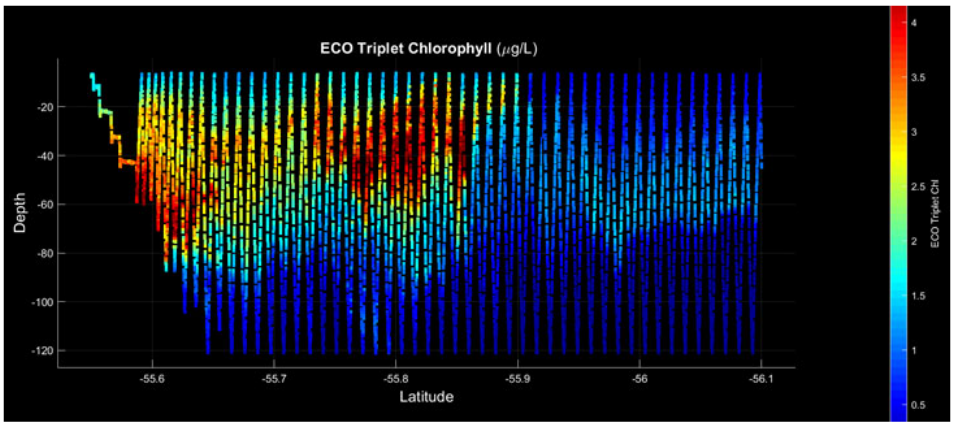
ECO Triplet Chlorophyll (μg/L)
Depth
-20
-40
-60
-80
-100
-120
-55.6
-55.7
-55.8
-55.9
-56
-56.1
Latitude
ECO Triplet Chl
4
3.5
3
2.5
2
1.5
1
0.5

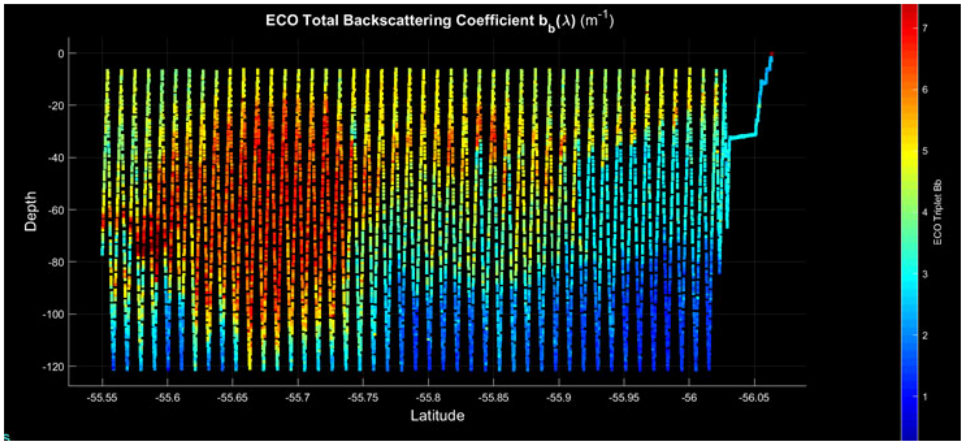
ECO Total Backscattering Coefficient $b_b(\lambda)$ (m^{-1})
Depth
0
-20
-40
-60
-80
-100
-120
-55.55
-55.6
-55.65
-55.7
-55.75
-55.8
-55.85
-55.9
-55.95
-56
-56.05
Latitude
ECO Triplet Bb
7
6
5
4
3
2
1

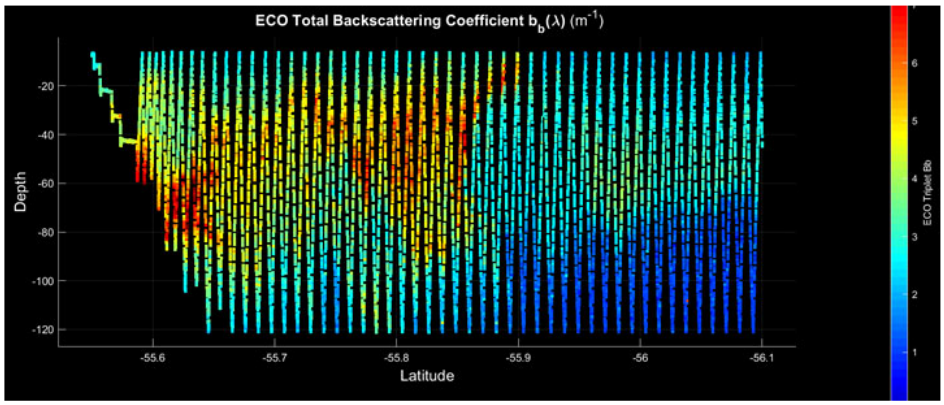
ECO Total Backscattering Coefficient $b_b(\lambda)$ (m^{-1})
Depth
-20
-40
-60
-80
-100
-120
-55.6
-55.7
-55.8
-55.9
-56
-56.1
Latitude
ECO Triplet Bb
6
5
4
3
2
1

Bio-optical, Biological and Biogeochemical Measurements

William Balch, Dave Drapeau, Bruce Bowler, Sunny Pinkham
Bigelow Laboratory for Ocean Sciences
E. Boothbay, ME 04575

Giuliana Viglione
Freelance Writer
Washington, DC

Hannah Primiano
Undergraduate Intern
Drew University
Madison, NJ

Benjamin Gustafson
Undergraduate Intern
Colby College
Waterville, ME

The Balch lab was involved in sampling a number of variables from the bottle casts, running an optical surface underway system, measuring discrete samples for a variety of water samples (see below). We also were involved in the carboy experiments. The Balch group sampled from 55 CTD/full water cast stations during the cruise (taking water from 8 of the 12 Niskin bottles each cast). Of those 8 bottles, 7 were usually from the euphotic zone and one from deeper in the water column (300-1000m). Samples were also taken from the 48 "trip-on-fly" casts (5m sample only). For all Niskin bottles sampled, aliquots were drawn for particulate organic carbon (POC) and particulate organic nitrogen (PON), particulate inorganic carbon ($CaCO_3$ or PIC), biogenic silica, and coccolithophore counts (to be processed ashore using polarized light microscopy). The latter technique is identical to the Canada Balsam technique for enumeration of calcite particles (Haidar and Thierstein, 2001) except we use Norland #74 brand optical adhesive instead of Canada Balsam. Chlorophyll *a* extractions ((JGOFS, 1996) were performed and for surface bottles always run in triplicate to have an estimate of precision; deeper samples were run as single measurements). Flow-cam samples ((Sieracki *et al.*, 1998) were taken from the eight depths of each Niskin cast for enumeration of net and nanoplankton as well as deriving size distribution functions. At each productivity station, two samples (surface mixed layer and deep euphotic zone (fluorescence maximum)) were taken and samples concentrated for microscopy. The Filter Transfer Freeze (FTF) technique (Hewes and Holm-Hansen, 1983) was used in which typically 250mL of sample were concentrated onto a 25mm, 0.4um-poresize, polycarbonate filter and the particles transferred to a glass microscope slide for examination using an American Optical polarizing microscope equipped with epifluorescence (with excitation wavelengths at about 480nm and 530nm). Samples were examined at any of four magnifications (100X, 200X, and 400X, the vast majority on this trip were photographed at 400X) under four types of illumination: bright field, polarized (to visualize calcium carbonate coccoliths) and epifluorescence (for discriminating autofluorescent, autotrophic cells versus

heterotrophic, nonfluorescent cells). High resolution photos were taken with a Canon EOS Rebel digital camera mounted on the trinocular head of the microscope.

Samples were also taken for measuring photosynthesis and calcification rates from 21 morning, full-CTD stations over the course of the trip (here called Productivity Stations). For these measurements, Niskin bottles were tripped at specific light depths throughout the euphotic zone (0.56%, 3.86%, 7.10%, 23.4%, 42.2% and 73.6%). During casts where there was sufficient light to measure PAR throughout the euphotic zone, these depths were calculated assuming a constant diffuse attenuation coefficient. For samples taken during the nighttime, estimation of those light depths was performed based on the assumption that the fluorescence maximum was located at the 1% light depth (Poulton *et al.*, 2017). Water samples for incubation were transferred from Niskin bottles to incubation bottles, typically inside the ship's enclosed hanger, under subdued light conditions. Water samples were pre-filtered through 120μm nitex mesh to remove large grazers. Incubations were performed in 70 mL polystyrene tissue culture bottles that were previously acid-cleaned, rinsed with ethanol, reverse-osmosis water, then rinsed 5x with each sea water sample prior to filling. Photosynthesis and calcification were measured using the microdiffusion technique (Paasche and Brubak, 1994) with modifications by Balch et al. (2000) (see also Fabry (2010)). ^{14}C bicarbonate (~30 μCi) was added for each water sample. Incubations were performed in triplicate (with an additional 2% buffered formalin sample (final concentration) used as a killed control) in simulated *in situ* conditions on-deck, corrected for both light quantity (extinction using bags made of neutral-density shade cloth) and quality (spectral narrowing) using blue acetate bag inserts. Bottle transfers between the incubators and radioisotope van were always done in darkened bags to avoid light shock to the phytoplankton. Deck incubators consisted of blue plastic tubs open to sky light, chilled using surface seawater from the ship's flowing sea water system. Calibration of those light levels in the bag were previously made using a Biospherical OSR2100 scalar PAR sensor inserted into each bag relative to a scalar PAR sensor outside the bag. All filtrations were performed using 0.4 μm pore-size polycarbonate filters. Following sample filtration, polycarbonate filters were rinsed three times with filtered seawater, then carefully given a "rim rinse" to make sure that all ^{14}C-HCO_3 in interstitial seawater in the filters was rinsed out. Filters and sample "boats" were placed in scintillation vials with 7mL of Ecolume scintillation cocktail. Samples were counted using a high sensitivity Beckman Tricarb liquid scintillation counter with channel windows set for ^{14}C counting. Counts were performed for sufficient time to reach 1% precision or 25 minutes for samples with lower counts. Blank ^{14}C counts were always run for scintillation cocktail as well as the phenethylamine CO_2 absorbent. Standard equations were used for calculating primary production and calcification from the ^{14}C counts with a 5% isotope discrimination factor assumed for the physiological fixation of ^{14}C-HCO3 as opposed to ^{12}C-HCO_3.

We discovered that our calcification blanks during the cruise had consistently higher DPMs than the photosynthesis blanks. We ran an extra experiment on the formalin blanks to see whether the buffer in the buffered formalin used to kill the cells, was causing the artificially high blanks. We performed this experiment using highly oligotrophic, 0.2μm filtered water found north of the Subtropical front in which there was no measurable phytoplankton fluorescence. We filled 10 productivity bottles with this water, and added buffered formalin (buffered to pH 8.8) to half of them (leaving the other five bottles "live" despite the fact that all particles >0.2mm diameter had been filtered out), then incubated all bottles with 30uCi ^{14}C bicarbonate in the dark for 24h. All 10 bottles were subsequently filtered onto 0.4um polycarbonate filters and subjected

to the microdiffusion technique. The calcification blanks for the filtered, non-killed samples had radioactivity that was 46% lower than the blank samples "killed" with buffered formalin. Given the state of oligotrophy in the original water samples, and that they were incubated in darkness, we conclude that the buffered formalin-killed calcification blanks caused a chemical artifact. That is, that the buffer injected with the formalin into the incubation bottles was driving the carbonate equilibrium to precipitate a small amount of the ^{14}C-bicarbonate, which was then caught on the filter. For this reason, for all of our calcification blanks, we subtracted the blank formalin values from filters that were acidified prior to counting (which drove off any residual ^{14}C-carbonate precipitate (artifact) or residual ^{14}C bicarbonate solution left in the interstices of filters).

The Balch lab bio-optical underway system was run continuously for 37d of the trip. This system has been described elsewhere (Balch *et al.*, 2008). Basically it measures temperature, salinity, chlorophyll *a* fluorescence and backscattering at 531nm (using a WETLabs ECOVSF sensor aimed into a specially-designed flow-through container which minimizes wall reflectance, hence maximizing the light scattering signal associated with marine particulate matter). First, the system measures backscattering of 531nm light with raw seawater (pH=8.1) running through the system for one minute. After 60 seconds of data collection (or whatever time period was set in order to achieve statistically-significant measurements), the acid controller injected 0.2um-filtered, 10% glacial acid into the seawater stream, passing through a static mixing coil to thoroughly mix it with the seawater, *upstream* of the ECOVSF. This reduced the pH to 5.5, below the dissociation point for calcium carbonate. A pH sensor *downstream* of the sample chamber measured the pH constantly. Once the pH dropped below pH 5.4, the backscattering was re-measured for 60s after which the acid additions stopped and the pH re-equilibrated and the entire cycle repeated. The difference in backscattering between raw seawater and acidified seawater represented "acid-labile backscattering" (b_b'), which can be directly related to the concentration of suspended calcium carbonate (Balch *et al.*, 1996).

The Balch lab bio-optical underway system had a separate flow loop that passed through a WETLabs ac-9, to measure spectral absorption and attenuation. In the flow path to the ac-9 was a solenoid that diverted the seawater stream through a 1um filter, then a 0.2 um filter prior to running the water through the ac-9. Every two minutes, the solenoid would alternate between filtered and unfiltered seawater, thus providing absorption and attenuation (at 9 spectral wavelengths across the visible spectrum) for raw and filtered seawater. In turn, this allows calculation of the absorption and attenuation of total suspended particles and dissolved organic matter. The difference between raw and dissolved ac-9 measurements represents particulate absorption and beam attenuation. Calibrations of the complete underway system were performed two ways: 1) daily, ultra-filtered 0.2um seawater was run through the entire system in order to estimate signals derived from ultra-clean seawater 2) approximately bi-weekly a calibration was performed by taking the instruments apart, cleaning and drying the sensors, and reassembly. This was done over the cruise as well as a final calibration at the completion of the cruise. These calibrations are used to estimate biofouling corrections during each operation period. The protocol was to run 0.2um filtered RO water from the ship's Milli-Q system, under pressure, through the entire flow path prior to cleaning ("a dirty calibration" which provides the endpoint for estimating the optical contribution of biofouling). Then the system is carefully disassembled and cleaned, reassembled and a "clean calibration" performed (which represents the beginning

calibration for the next operational segment, with no bio-fouling. Post cruise, the biofouling corrections are interpolated between each initial clean calibration and the following dirty calibration.

On the bow of the *R/V Thompson* was a hyperspectral radiometer system (HyperSAS) mounted to an Underway Aiming System (UAS), used to estimate water-leaving radiance from the ship, analogous to to the nLw derived by the SeaWiFS and MODIS satellite sensors, but free from atmospheric error (hence, it can provide radiometric data below clouds). The system consisted of a down-looking radiance sensor and a sky-viewing radiance sensor, both mounted on UAS. A downwelling irradiance sensor was mounted as far as possible from any potentially shading structures. These data were used to estimate normalized water-leaving radiance as a function of wavelength. The radiance detector was set to view the water at 40º from nadir as recommended by Mueller et al. (2003b). The water radiance sensor was able to view over an azimuth range of ~200º across the ship's heading with no contamination from the ship's wake. The direction of the sensor was adjusted to view the water 120 º from the sun's azimuth, to minimize sun glint. This was continually adjusted as the time and ship's heading were used to calculate the sun's position using an astronomical solar position subroutine interfaced with a stepping motor which was attached to the radiometer mount (designed and fabricated at Bigelow Laboratory for Ocean Sciences). Protocols for operation and calibration were performed according to Mueller (Mueller *et al.*, 2003a; Mueller *et al.*, 2003b; Mueller *et al.*, 2003c). Data for this system were only accepted is the solar zenith angle was >20º. Post-cruise, the 1 Hz data are filtered to remove as much residual white cap and glint as possible (we accept the lowest 5% of the data).

Carboy Experiments

Five carboy experiments were performed during the 60d cruise. For a complete description of the experiments, see the report of Peter Morton in this report. The purpose of the experiments was to assess the impact of different nutrient amendments on phytoplankton-related variables measured by the Balch lab: phytoplankton biomass, POC/PON, PIC, counts of plated coccolithophores and detached coccoliths, nutrient concentrations, biogenic silica, flowcam counts of various classes of algae, particle size distributions. As outlined earlier, the 18 cubitainors were divided as follows: three controls (no amendments), then triplicate amendments for various additions depending on the experiment and location. These amendments included: nitrate, 5% 0.2um-filtered SAMW, silicate, iron (0.4nM), iron+silicate, Antarctic Intermediate Water (AIW), super iron (4nM), eddy edge water (for experiment run in Eddy A). See section from the Morton lab for all the specifics for collecting trace-metal-clean surface seawater for these experiments. All cubitainors were then placed in blue seawater incubators maintained at ambient seawater temperatures using a a chiller/heater system kept in the ship's hanger. Cubitainors were kept in neutral-density screen (which reduced the total irradiance to about 50% of incident).

Samples processed

The Balch group performed five carboy experiments over the SAMW'21 cruise, and sampled all CTD/full water casts plus the top bottles of Trip-on-Fly casts to serve as calibration samples for the underway system. Underway samples were also taken every three hours during long steams

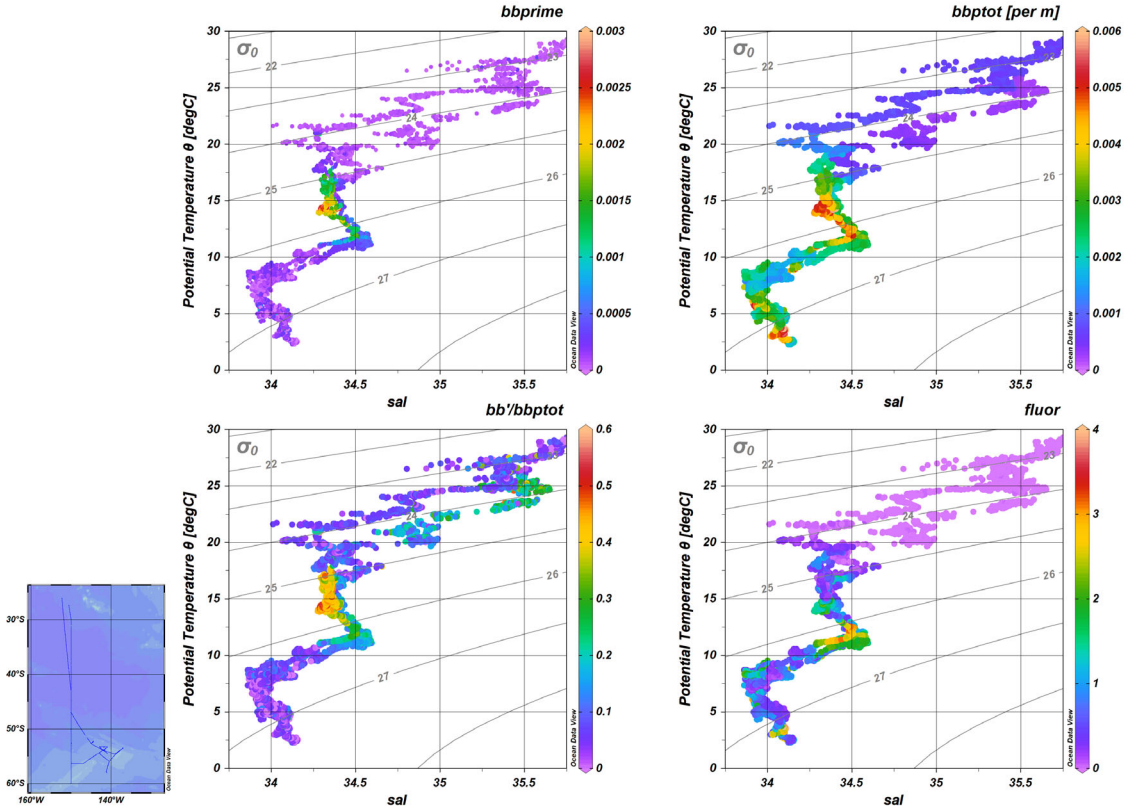

Fig. 1- TS diagrams for surface underway data from RR#2004. Cruise track shown in lower left corner. Top left- acid-labile backscattering is shown on the Z axis of the TS plot. Water along the 25.5 isopycnal showed peak amounts of acid-labile backscattering in the cool, fresh part of the TS diagram. Upper right panel- Total particulate backscattering at 532nm also showing peak values in the Sub-Antarctic Frontal water, decreasing as the ship moved in progressively more oligotrophic environments. Lower left panel: fraction of acid-labile backscattering (bb') normalized to total particle backscattering. Lower right panel: Fluorescence of chlorophyll *a* shown in TS space, showing similar pattern to total backscattering. It can be seen that in the SAMW density range, that fraction approaches 60% of the total particle backscattering, which decreases to 20-30% in the subtropical water (σ_0< 25; southbound transit) and 5-10% in the northbound transit.

for calibration of the underway system. In total, 725 water samples were processed for all variables listed above: 90 full samplings of measurements were performed for shipboard experiments on nutrient/trace metal amendments, plus 49 underway samples.

Data archival

The data collected from this voyage will be ultimately archived with the Biological and Chemical Oceanographic Data Management Office (BCO-DMO) at Woods Hole Oceanographic Inst. (sponsored by NSF).

Preliminary Results

Our surface underway system illustrated that the peak coccolithophore populations were found in moderate temperatures (14-15oC water) and fresher salinities (34.3-34.4) in the density ranges of

Table 1- Summary of all 14C incubations for measuring integrated photosynthesis and calcification. Color-coded columns show values as well as relative values for comparison between stations. Chlorophyll-normalized carbon fixation values are also shown.

Description	Station	Event	Lat. (°S)	Lon (°W)	Int Calc/Psy	Int Prod (mg C m^{-2} d^{-1})	Int Calc (mg C m^{-2} d^{-1})	Int Chl (mg m^{-2})	Int Prod/Int Chl (mgC (mg chl)$^{-1}$ d^{-1})	Int Calc/Int Chl (mgC (mg chl)$^{-1}$ d^{-1})
Merid 32S	5.01	20210108.1559	-31.999	-150.000	0.175	92.5	16.19	14.90	6.21	1.09
Merid 34S	9.01	20210109.1023	-34.000	-150.001	0.073	86.4	6.30	17.31	4.99	0.36
Merid 37S	15.01	20210110.1600	-36.998	-159.999	0.220	46.0	10.13	14.98	3.07	0.68
Merid 40S	9.01	20210111.1722	-39.999	-150.000	0.082	87.9	7.25	7.00	12.55	1.04
Merid 42S	25.01	20210112.1053	-42.000	-150.000	0.036	221.7	7.94	10.74	20.64	0.74
Merid 45S	31.01	20210113.1515	-44.998	-149.999	0.086	331.2	28.58	17.27	19.18	1.66
Merid 47S	35.01	20210114.1722	-46.998	-149.999	0.022	253.5	5.61	40.94	6.19	0.14
Merid 47.7S	37.01	20210116.1654	-47.667	-150.002	0.034	164.8	5.63	14.80	11.13	0.38
Merid 49.7S	43.01	20210117.1438	-49.665	-149.998	0.043	456.9	19.73	53.61	8.52	0.37
Merid 53S	45.01	20210118.1717	-53.000	-149.998	0.037	376.9	14.12	46.90	8.03	0.30
Merid 51S	51.01	20210119.1529	-51.000	-149.999	0.069	241.6	16.58	40.12	6.02	0.41
Merid 56S- Polar Front	54.01	20210121.1306	-55.999	-149.998	0.027	407.8	10.87	96.05	4.25	0.11
Merid 54S	60.01	20210122.1130	-53.999	-149.999	0.045	399.0	18.13	85.06	4.69	0.21
Merid 60S	63.01	20210124.1313	-59.998	-150.000	0.205	57.4	11.75	17.29	3.32	0.68
Merid 58S	69.01	20210125.1228	-58.000	-150.000	0.059	143.6	8.46	38.62	3.72	0.22
Eddy A edge	79.01	20210129.1759	-53.329	-142.922	0.068	330.6	22.32	71.30	4.64	0.31
Eddy A center	82.02	20210130.1504	-53.924	-141.924	0.030	192.0	5.71	40.54	4.74	0.14
Cross Front	87.01	20210201.1458	-57.480	-141.113	0.144	183.9	26.43	35.11	5.24	0.75
Eddy C Center	94.01	20210203.1627	-54.079	-138.022	0.106	71.7	7.58	18.40	3.89	0.41
Meander Station	97.02	20210205.1357	-52.666	-144.997	0.038	216.4	8.29	34.01	6.36	0.24
Bloom Stn	98.02	20210208.1333	-44.865	-149.999	0.058	344.6	20.06	36.74	9.38	0.55

Subantarctic Mode Water (SAMW) (Fig 1) between 25.6 and 26.1 sigma-theta isopycnals. It also appears that as that water moves northward along this isopycnal (verified in satellite ocean color images and altimetry), it is being conditioned such that below the SAMW isopycnal (moving into subtropical water, the water is no longer amenable to coccolithophore growth. It is also significant that at its peak, the suspended calcium carbonate accounted for up to 60% of the total backscattering of the particulate material. It is no wonder that these features are visible from space. This percentage is similar to the percentages observed previously in the Patagonian Shelf part of the Great Calcite Belt. The phytoplankton fluorescence was also greatest in this moderate temperature, fresh water, consistent with the hypothesis that the total algal populations in the SAMW as well as in the PF were actively growing.

A summary of the integrated primary production and calcification results is given in Table 1. They show that the highest integrated calcification rates were observed near 45ºS latitude as well as the Cross Frontal station near the Polar Front. The former location is where SAMW outcropped at the surface whereas at the latter location, there was only moderate acid-labile backscattering so the source of the elevated reflectance there does not appear to be coccolithophores (or at least not enough PIC has accumulated there to account for the elevated reflectance). Micrographs of the water showed small <1um diameter birefringent particles (see below). The identity of this material must await the results of our particulate analyses to be done ashore. Integrated calcification rates in the coccolithophore bloom were moderate. The greatest

integrated photosynthesis rates were observed between 45°S and 56°S, where the highest integrated chlorophylls were also observed.

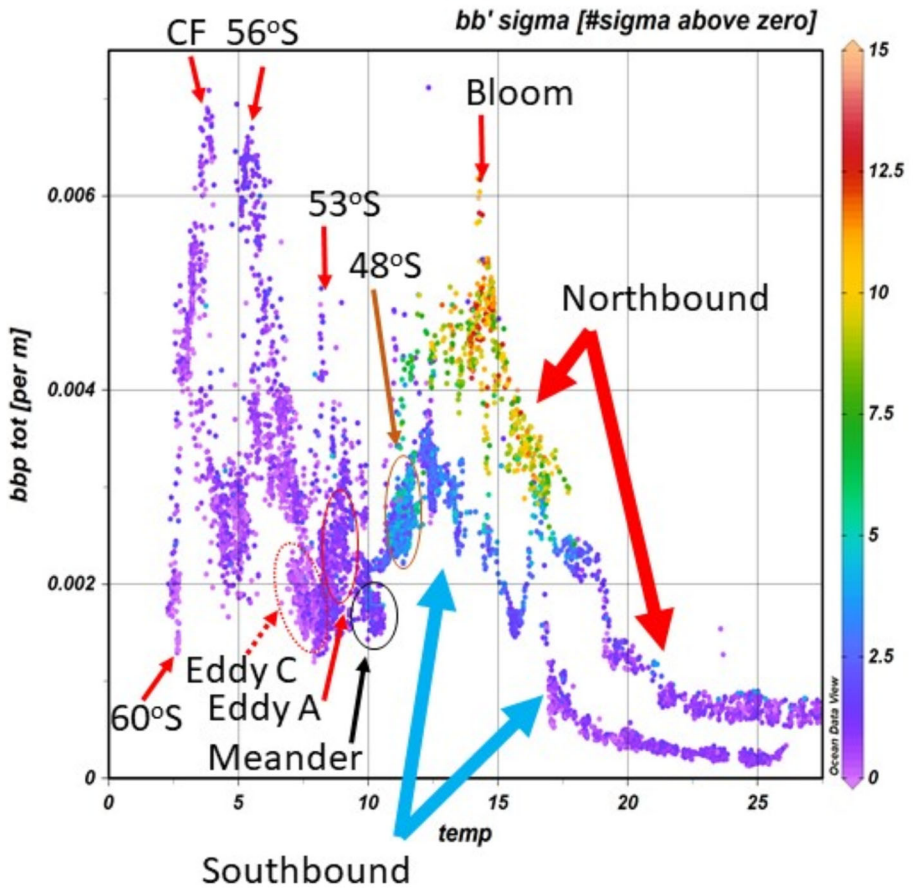

Fig. 3- Plot of total particle backscattering at 531nm versus temperature at 5m depth. The Z aaxis shows the number of standard deviations above zero that the bb' values are. Data groupings for different features are shown.

A temperature analysis of the most statistically-significant b_b' levels (determined as the number of standard deviations above zero the b_b' values were (where any value >2 is significant at a confidence level of >95%). The results (Fig. 3) demonstrate that the most significant peaks in b_b' were in the temperature range of 14-15°C which falls within the Subantarctic frontal zone. The waters of specific features studied during SAMW'21 are designated in Figure 3 and show that for the colder features, the coccolithophore backscattering was not highly significant. In these features, diatoms generally dominated. The colder the water, the more that diatoms were favored in the populations.

A summary of some of the high-reflectance features described in Fig. 3 and found in satellite imagery during RR#2004 is given in Fig 4. Cloud contamination of satellite imagery

was a major problem during the cruise, so features were only clearly seen in rare overpasses. The best image of the SAF and PF was on 10 January, 2021 (Fig. 4A, red and yellow arrows respectively). An early view of various features to the east of our study region was taken on 15 December, 2020. The features visible in this PIC image were the PF (cyan arrow), Eddy A (red arrow) and Eddy C (yellow arrow; Fig. 4B). A later image of the smaller and more distinct Eddy C was made on 18 January, 2021 (Fig. 4C). A region of elevated PIC along the SAF was spotted on 18 January 2021 (Fig. 4D. The coccolithophore bloom in the Great Calcite Belt was obscured by clouds virtually every day except on 9 February, 2021, when a hole in the clouds developed along its northern boundary along the 150oW meridian (Fig. 4E).

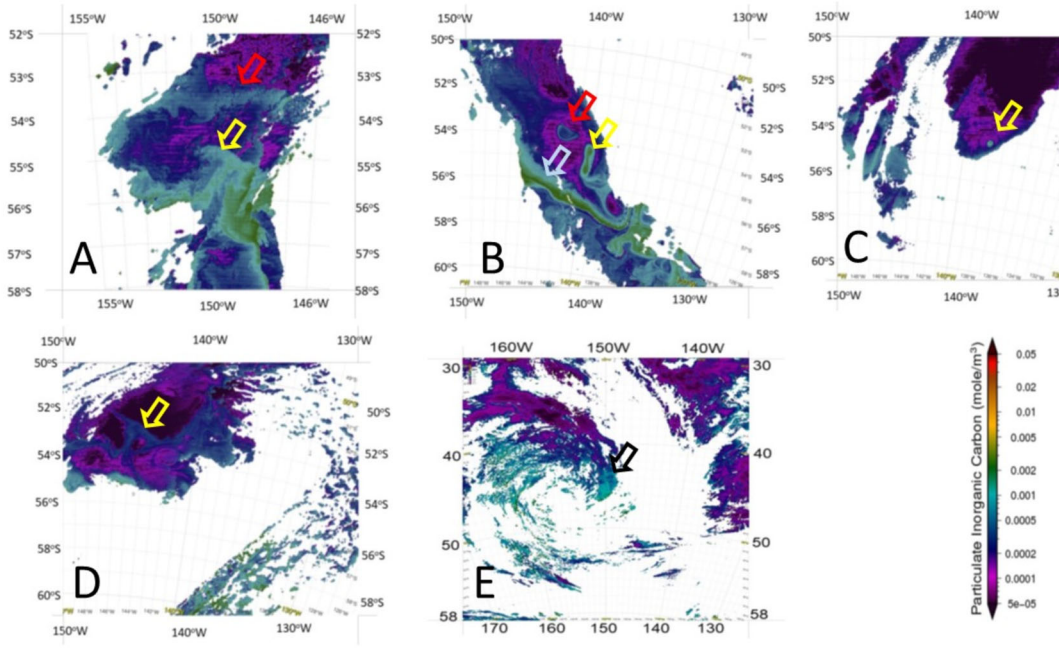

Fig. 4- VIIRS NPP images for select scenes showing high reflectance and elevated PIC concentratons observed during SAMW #2004: (A) SAF 10 Jan'21 (red arrow) & PF (yellow arrow); (B) three features sampled during the trip: topographically-steered PF (cyan arrow) Eddy C in the process of formation (yellow arrow), Eddy A (red arrow) 15Dec'20; (C) Eddy C (yellow arrow) on 20 January, 2021; (D) SAF on 18 Jan'21(yellow arrow); (E) North side of cocco bloom, north of SAF 9 Feb'21 (black arrow). The color bar for all of the images is given in the lower right of the figure.

Photomicrographs of the high-reflectance features observed during RR#2004 are shown in Figure 5. The coccolithophore bloom (Fig. 5A) showed the expected high numbers of plated coccolithophores (~900 ml^{-1}) and detached coccoliths (~10,000 mL^{-1}). The center of Eddy C (Fig. 5B) certainly qualified as a high reflectance feature, although not as bright as the coccolithophore bloom (Fig. 5A). It had many very small, birefringent particles that were lacking the tell-tail 4-pole birefringent cross-nichols of regular detached coccoliths and instead showing what we commonly refer to as "singlets". Diatoms (both occasional live cells but mostly empty frustules) were evident. The chlorophyll and total particle scattering were low in the center of Eddy C (Fig. 3). The waters from the cross frontal transect (Fig 5D) had some of the highest total particle backscattering observed on the cruise (Fig. 3) but also looked similar to the waters at the center of Eddy C, with mostly empty diatom frustules and small birefringent

"singlets" <1um in diameter. The reflective waters of the SAF meander (Fig. 5C) also showed the birefringent singlets along with some detached coccoliths as well as some plated cells. Until we process the PIC and BSi samples, however, we won't know the relative importance of these two minerals in generating the observed high-reflectance signature observed by satellite. If the small particles are indeed made of calcium carbonate, their extremely small size (<1um) could give them a significantly larger backscattering cross section, potentially even greater than that of 2um diameter *E. huxleyi* coccoliths.

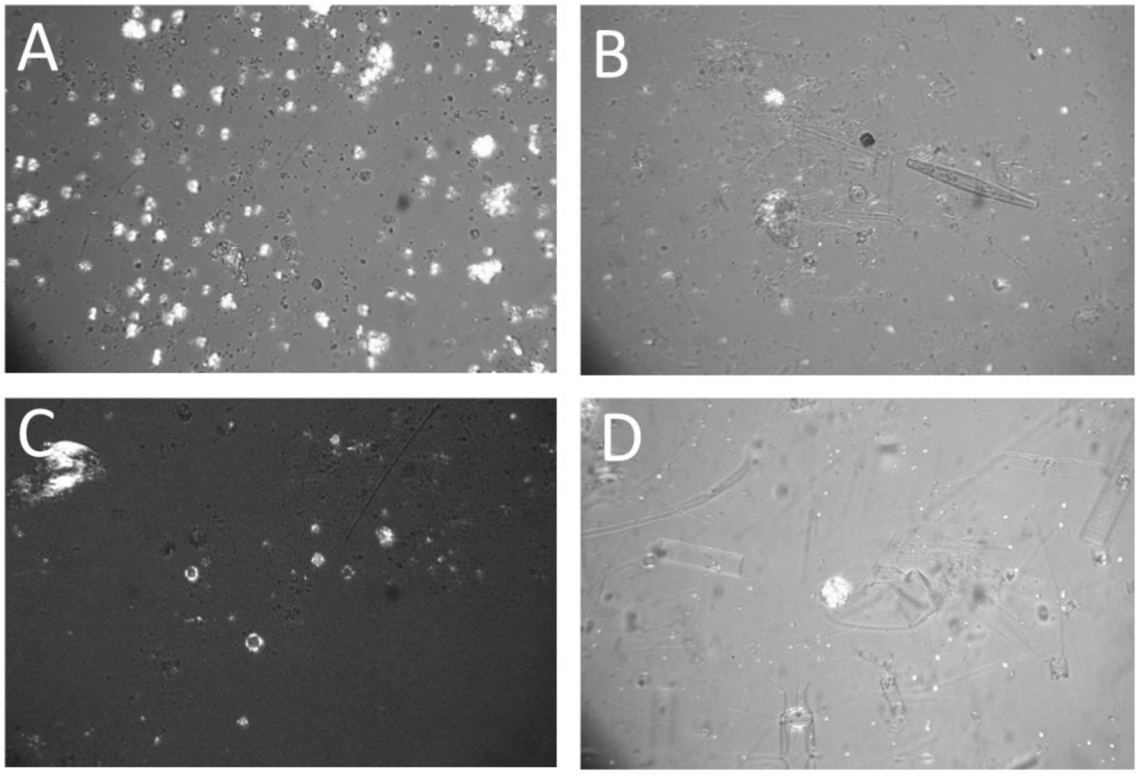

Figure 5- Polarization birefringence micrographs from four high-reflectance features observed during RR#2004. All micrographs taken at 400X magnification. FTF slides prepared according to Hewes and Holm-Hansen (1983) after filtration of 150mL of sample through a 0.4um pore-size polycarbonate filter: (A), station 9801, 5m depth from the coccolithophore bloom; (B) eddy C underway sample from eddy center; (C) SAF meander station 97;(D) cross-front underway sample. Dimension of each image: 281µm x 187.5µm

References

Balch, W.M., Drapeau, D., Fritz, J., 2000. Monsoonal forcing of calcification in the Arabian Sea. Deep-Sea Research II 47, 1301-1337.

Balch, W.M., Drapeau, D.T., Bowler, B.C., Booth, E.S., Windecker, L.A., Ashe, A., 2008. Space-time variability of carbon standing stocks and fixation rates in the Gulf of Maine, along the GNATS transect between Portland, ME and Yarmouth, NS. Journal of Plankton Research 30 (2), 119-139.

Balch, W.M., Kilpatrick, K., Holligan, P.M., Harbour, D., Fernandez, E., 1996. The 1991 coccolithophore bloom in the central north Atlantic. II. Relating optics to coccolith concentration. Limnology and Oceanography 41, 1684-1696.

Fabry, V.J., Balch, W.M., 2010. Direct measurements of calcification rates in planktonic organisms. In: Riebeseil, U., Fabry, V.J., Hansson, L., Gattuso, J.-P. (Eds.), Guide to Best Practices in Ocean Acidification Research and Data Reporting. European Project on Ocean Acidification (EPOCA), Bremerhaven, Germany, pp. 185-196.

Haidar, A.T., Thierstein, H.R., 2001. Coccolithophore dynamics off Bermuda (N. Atlantic). Deep Sea Research 48 (8-9), 1925-1956.

Hewes, C.D., Holm-Hansen, O., 1983. A method for recovering nanoplankton from filters for identification with the microscope: The filter-transfer-freeze (FTF) technique. Limnology and Oceanography 28, 389-394.

JGOFS, 1996. Protocols for the Joint Global Ocean Flux Study (JGOFS) core measurements. In: Knap, A. (Ed.), Report no. 19 of the Joint Global Ocean Flux Study. Scientific committee on oceanic research, international council of scientific unions. Intergovernmental Oceanographic Commission, Bergen, Norway, p. 170.

Mueller, J.L., Austin, R.W., Morel, A., Fargion, G.S., McClain, C.R., 2003a. Ocean optics protocols for satellite ocean color sensor validation, Revision 4, Volume I: Introduction, background, and conventions. Goddard Space Flight Center, Greenbelt, MD, p. 50.

Mueller, J.L., Morel, A., Frouin, R., Davis, C., Arnone, R., Carder, K., Lee, Z.P., Steward, R.G., Hooker, S.B., Mobley, C.D., McLean, S., Holben, B., Miller, M., Pietras, C., Knobelspiesse, K.D., Fargion, G.S., Porter, J., Voss, K., 2003b. Ocean optics protocols for satellite ocean color sensor validation, Revision 4, Volume III: Radiometric measurements and data analysis protocols Goddard Space Flight Center, Greenbelt, MD, p. 78.

Mueller, J.L., Pietras, C., Hooker, S.B., Austin, R.W., Miller, M., Knobelspiesse, K.D., Frouin, R., Holben, B., Voss, K., 2003c. Ocean optics protocols for satellite ocean color sensor validation, Revision 4, Volume II: Instrument specifications, characterization,and calibration. Goddard Space Flight Center, Greenbelt, MD.

Paasche, E., Brubak, S., 1994. Enhanced calcification in the coccolithophorid *Emiliania huxleyi* (Haptophyceae) under phosphorus limitation. Phycologia 33, 324-330.

Poulton, A.J., Holligan, P.M., Charalampopoulou, A., Adey, T.R., 2017. Coccolithophore ecology in the tropical and subtropical Atlantic Ocean: New perspectives from the Atlantic meridional transect (AMT) programme. Progress in Oceanography, doi: 10.1016/j.pocean.2017.1001.1003.

Sieracki, C.K., Sieracki, M.E., Yentsch, C.S., 1998. An imaging-in-flow system for automated analysis of marine microplankton. Marine Ecology Progress Series 168, 285-296.

Nutrient limitation by major and trace metals

Peter Morton, Lauren Hearn
National High Magnetic Field Laboratory/Florida State University
Tallahassee, Florida 32310

Julia Middleton, Logan Tegler
Woods Hole Oceanographic Institution
Woods Hole, Massachusetts 02543

The transect along the 150ºW meridian (30-60ºS) in the South Pacific crosses three major nutrient regimes: the low-nutrient low-chlorophyll conditions of the subtropical gyre, the high-nitrate high-phosphate (but low-silicate) low-chlorophyll conditions of the subantarctic gyre, and the nutrient-rich (but iron-limited) conditions of the Southern Ocean. Each of these regions has the potential to support greater levels of primary productivity, but are potentially limited by one or more nutrients (e.g., silicate and/or iron).

Vertical profiles of trace elements

To characterize the nutritional values of these waters and determine the limiting nutrient(s) in each regime, uncontaminated seawater samples (**n=173**) were drawn from **21 deployments** of nine 5-L Niskin-X bottles suspended from Kevlar line at varying depths between 30 m and 1050 m.

Three modifications to the sampling system made for much more reliable sampling operations on this expedition.

First, a small Ronstan Series 60 Single Orbit block (model #7298755) was used instead of the large General Oceanics metering block (borrowed from URI on the 2020 expedition), which eliminated the risk of the line jumping the sheave and the need for a deck-mounted snatch block. The block was attached to the squirt boom which allowed for the Niskin-X bottles to be attached to the Aracom line without having to lean too far over the side of the ship.

Second, in order to better estimate the depths at which the bottles were deployed, a miniature temperature and pressure sensor (centi-TD, by Star Oddi) was secured to the deepest bottle deployed. This sensor recorded the temperature and pressure (i.e., depth) at preset intervals (every 60 seconds). The pauses in the recording at specific depths revealed the exact depth at which each subsequent Niskin-X was attached, and the distances between the bottles were used to calculate the deployment depths. These depths are double-checked by comparing the salinity and nutrient values determined in samples from each Niskin-X bottle against (1) the temperature and salinity values from the ship's CTD sensors and (2) discrete salinity and nutrient concentrations determined from the ship's bottles.

Third, the Niskin-X bottles were deployed from the starboard side of the ship instead of the fantail (R/V Thompson, SAMW 2020) by securing the Hawboldt winch at an angle, just aft of the ResTech locker. This allowed the Aracom line to be threaded through the Ronstan block mounted to the squirt boom. Even in heavier seas, the Niskin-X bottles were deployed reliably

and reproducibly due to this arrangement (which was designed by Matt Durham, UCSD ResTech).

Niskin-X subsampling

In general, unfiltered samples were drawn from each Niskin-X for salinity and major nutrient measurements (ODF). The remainder of the volume was filtered using 47 mm, 0.4 μm pore-size Isopore membrane filters installed in Advantec filter cartridges. The filters were folded and stored in acid-washed 2 mL centrifuge tubes and stored refrigerated at 4°C. The filtrate was collected into trace metal-cleaned (acid-washed) bottles for dissolved trace metal concentrations (125 mL) and barium concentrations and isotopic composition (60 mL).

As is customary, trace metal analysis will occur at the home institutions under strictly controlled environments to prevent contamination of precious seawater samples.

Dissolved trace metals

Dissolved trace metal samples will be extracted using solid-phase extraction (Nobias Chelate PA-1 or Toyopearl AF-Chelate 650-M) to remove metals from the high salinity matrix and concentrate the metals into a pure nitric acid matrix suitable for direct injection and analysis by high resolution inductively coupled plasma mass spectrometry (HR-ICP-MS). The analysis will produce total dissolved concentrations of Fe, Mn, Cd, Co, Cu, Ni, and Zn, which describes the standing inventories of bioactive metal nutrients. In addition, dissolved concentrations of Al and Pb can be used as tracers of mineral dust and anthropogenic aerosols, respectively. Based on previous analyses of this region, we expect dissolved Fe concentrations to be sparingly low (<0.2 nM), dissolved Mn to be <0.5 nM unless enriched in surface waters by recent dust deposition events, and concentrations of the other bioactive elements to be low unless enriched by cross-frontal intrusions of enriched subantarctic waters where surface dissolved trace metal concentrations are much higher than in oligotrophic subtropical waters.

Dissolved barium analysis will be conducted by Julia Middleton at WHOI (see section on Ba isotopic composition).

Dissolved Pb and Al will be measured at all stations and depths as part of our usual multielement suite. Concentrations of these elements will be compared against NOAA HYSPLIT air mass back trajectories to estimate atmospheric deposition of trace elements (especially Fe) from the relatively nearby Australian deserts. It is worth noting that our location is downwind of the Austral summer seasonal winds which cross the Fe-rich region of the Australian Lake Eyre Basin and could potentially deposit material to our study region.

Particulate trace elements

Particulate trace element samples will be subjected to two primary chemical treatments to determine the labile and refractory fractions of trace elements. First, the filtered samples will be brought to room temperature, folded twice to contain the suspended particulate material (SPM) in the center of the filter, and submerged into a 25% acetic acid solution with the mild reducing agent hydroxylamine hydrochloride (Berger et al. 2008). This treatment releases biogenic (e.g., soft components of marine microorganisms) and lithogenic phases of trace metals (e.g., Fe and Mn oxides), providing an estimate of the total elemental SPM concentration that easily remineralizes and is likely bioavailable for nutrient recycling. The second treatment involves an

aggressive mixture of nitric, hydrochloric, and hydrofluoric acids, that completely breaks down the more refractory mineral (e.g., aerosol dust and resuspended sediments) and biogenic phases (e.g., frustules and tests). When considered together, the concentrations of trace and major elements in each of the labile and refractory fractions, along with their relative ratios (Fe/P, Zn/Si), can be used to tease apart the biogenic, lithogenic, and authigenic composition of marine particles. Using HR-ICP-MS, a suite of elements can be simultaneously detected and their concentrations quantified, including the bioactive trace metals (e.g., Fe and Zn), mineral tracers (e.g., Al and Ti), biominerals (e.g., Ba and Si), and other tracers like P (biology), Pb (coal combustion), and V (diesel fuel combustion).

Deckboard incubations

To estimate the potential for major or trace nutrient limitation, five series of nutrient amended whole water incubations were conducted throughout the cruise. Surface whole water was collected from the starboard side of the ship using a clean sampling hose (¾" Bev-a-line and ¾" drinking water hose) kept at sea-surface depth using a modified otter boat ("Big Jon") with a snorkel that extends below and forward of the otter boat itself.

Surface samples were collected with great attention to preventing and minimizing the possibility of accidental trace or major nutrient contamination (especially iron and nitrogen species). All cubitainers, tubing, fittings, pumps, and subsample bottles were acid-washed with dilute hydrochloric acid (~10%) and thoroughly rinsed with UHPW and/or freshly collected seawater. The surface seawater was pumped into the wet lab using an air-operated double-diaphragm Teflon pump (Ingersoll-Rand PD07P-APS-PTT) at ~ 10 L/min into two 200 L acid-cleaned tanks simultaneously through a tee that improved homogeneity of the water in each tank. The cubitainers were filled with 20 L of surface seawater directly from Big Jon (in the case of the Control incubations) and from one tank at a time (without use of the tee) using the same Teflon pump, with the hoses configured in reverse. Eighteen (Incubations A-C) or nine (Incubations D and E) cubitainers were filled per experiment and amended in triplicate with one or more nutrients or filtered subsurface water, except for a set of Controls which contained only surface seawater.

Nutrient amendment stocks were carefully evaluated before the cruise for unwanted concentrations of either trace metals (especially Fe) or other major nutrients.

Nitrate

The nitrate standard was prepared at sea by dissolving approximately 2.5 g of sodium nitrate salt ($NaNO_3$), carefully weighed and bottled at NHMFL/FSU before the cruise, into ~ 125 mL of UHPW from the Thompson's UHPW system. The solution was then cleaned twice by passing over a small column of Chelex-100 that had been cleaned with freshly prepared 10% HCl (v/v; reagent grade) and thoroughly flushed with UHPW to rinse away residual acid and any associated metals released from the Chelex. The stock nitrate concentration was confirmed by the SIO-ODF team to be free of contamination from other major nutrients (e.g., ammonia or silicate), and preliminary tests at home

Surface sampler: modified otter boat, also known as "Big Jon"

demonstrated the efficient removal of trace metals like Fe from the stock by using the same Chelex method; nevertheless, the nitrate stock will be reevaluated at NHMFL/FSU for any potential trace metal contamination.

Silicate

Unlike nitrate, solutions of dissolved silicate salts cannot be cleaned of trace metals by Chelex resin, since dissolved silicate naturally produces a solution of pH greater than 12, which is above the effective complexation capacity of Chelex (effective at pH values 2-10). Therefore, a stock solution of Si produced by High Purity Standards (Charleston, South Carolina) was purchase for these experiments. This solution is certified for numerous elements, including Fe, which effectively contributes 80 pM for every 10 µM of silicate added to a 20-L cubitainer. While this amount of Fe is exceedingly low (especially for a silicate standard), it is worth noting that the South Pacific/Southern Ocean is so Fe-starved that even the addition of 80-160 pM of Fe might be enough to alleviate Fe-limiting conditions.

Iron

The Fe standard used to amend the +Fe and +Fe+Silicate incubations was prepared from a stock solution by High Purity Standards (Charleston, South Carolina). The standard is acidified using 2% HNO_3 acid (0.32 M). Incubations amended with this standard will also have nitrate introduced to the experiment (1.6 µM nitrate per 1 nM Fe). However, as noted before the cruise using nutrient data from previous occupations of 150ºW (WOCE/CLIVAR/GO-SHIP P16S line), surface nitrate concentrations were expected to be high (> 6 µM) throughout our survey, so the addition of nitrate from the Fe standard would not affect the incubation adversely.

Subsurface Water

Before each incubation experiment, a vertical Niskin-X cast was conducted to both characterize the vertical water column structure and collect subsurface water to simulate an upwelling or mixing event into surface waters. These subsurface waters were subsampled differently, by using an Acropak-200 capsule filter to rapidly draw 0.2 µm filtered water into three 1-L FEP bottles. Before filling the subsurface water-amended cubitainers with surface seawater from the tanks, one of the 1-L subsurface samples was added to each of the cubitainers, and then the tank water pumped in to thoroughly mix. If the cubitainers are assumed to contain ~20 L total volume, then the addition of 1-L of filtered subsurface water would produce a final mixture of ~5% subsurface water with 95% surface seawater. While the initial nutrient and salinity concentrations from the Control experiment were assumed to be identical across all the other incubation amendments before they were amended, separate nutrient and salinity samples were drawn for each of the subsurface-amended cubitainers.

Chemical properties of each incubation (starting concentrations and amendments)

Incubation A: Station 37 (47.7°S 150°W)
Nitrate = 7.9 µM
Phosphate = 0.6 µM
Silicate = 0.6 µM
Amendments (n=6)
Control
10 µM nitrate
1 nM Fe
20 µM silicate
20 µM silicate+1 nM Fe
Subsurface amendment:
SAMW (520 m; nitrate = 21 µM, phosphate = 1.5 µM, silicate = 7 µM)

Incubation B: Station 54 (56°S 150°W)
Nitrate = 21 µM
Phosphate = 1.4 µM
Silicate = 0.4 µM
Amendments (n=6)
Control
1 nM Fe
4 nM Fe
20 µM silicate
20 µM silicate+1 nM Fe
Subsurface amendment:
AAIW (153 m; nitrate = 31 µM, phosphate = 2.2 µM, silicate = 32 µM)

Incubation C: Station 82, Eddy Center (53.9°S 141.9°W)
Nitrate = 20.1 µM
Phosphate = 1.4 µM
Silicate = 1.0 µM
Amendments (n=6)
Control
1 nM Fe
20 µM silicate
20 µM silicate+1 nM Fe
Subsurface amendment:
Eddy Edge (Stn 79/92 m; nitrate = 22 µM, phosphate = 1.7 µM, silicate = 6 µM)
Winter Mixed Depth (Stn 82/311 m; nitrate = 32 µM, phosphate = 2.2 µM, silicate = 38 µM)

Incubation D: Station 97, Meander (52.7ºS 145ºW)
Nitrate = 14.3 µM
Phosphate = 1.1 µM
Silicate = 1.2 µM
Amendments (n=3)
Control
2 nM Fe
Subsurface amendment:
Winter Mixed Depth (267 m; nitrate = 19 µM, phosphate = 1.4 µM, silicate = 5.4 µM)

Incubation E: Station 98, Great Calcite Belt (44.9ºS 150ºW)
Nitrate = 5.9 µM
Phosphate = 0.5 µM
Silicate = 0.3 µM
Amendments (n=3)
Control
2 nM Fe
Subsurface amendment:
Winter Mixed Depth (304 m; nitrate = 17 µM, phosphate = 1.2 µM, silicate = 4 µM)

Subsampling the incubation cubitainers
Subsamples were drawn directly from the tanks for "t=0" time points, except for trace metal samples which were drawn immediately after each cubitainer was amended. Thereafter, each cubitainer was subsampled approximately every 24-48 hours for nutrients, DIC/alkalinity, POC/PIC, chlorophyll a, biogenic silica, and dissolved and particulate trace metals. Trace metal samples were drawn into a 1-L acid-washed FEP Teflon bottle and filtered offline (0.4 um Isopore PCTE) for dissolved and particulate trace metals. Additional subsamples were drawn at the first and final time points for DNA/RNA analysis for D. Sturm (Plymouth University), where ~600 mL from each of the three replicates was combined to produce a single "average" sample of 2 L.

Incubation A preliminary results

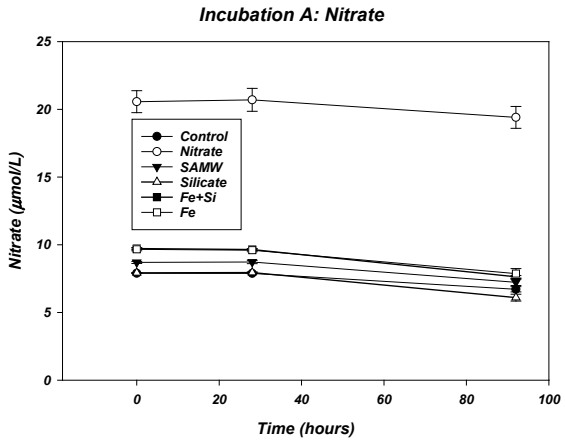

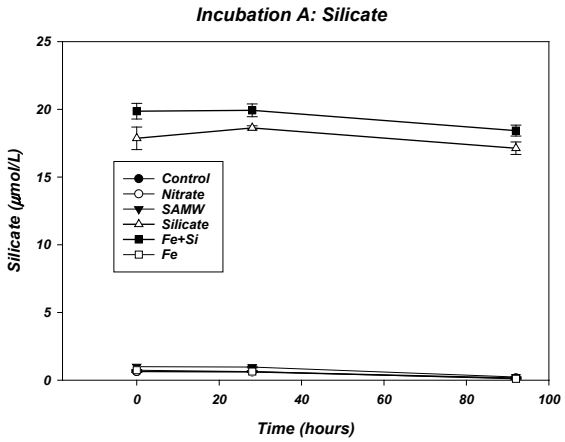

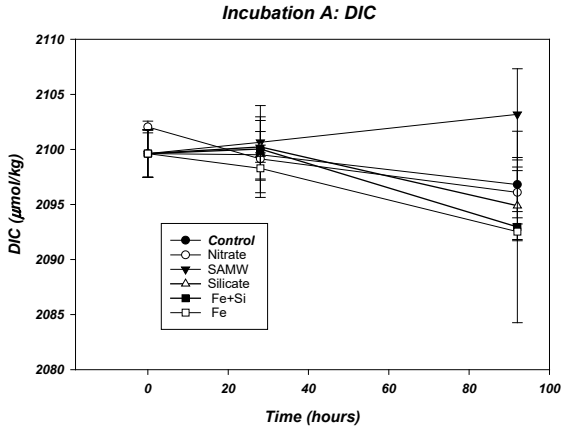

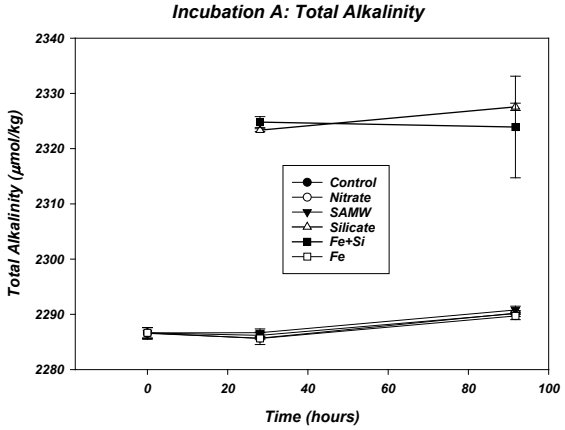

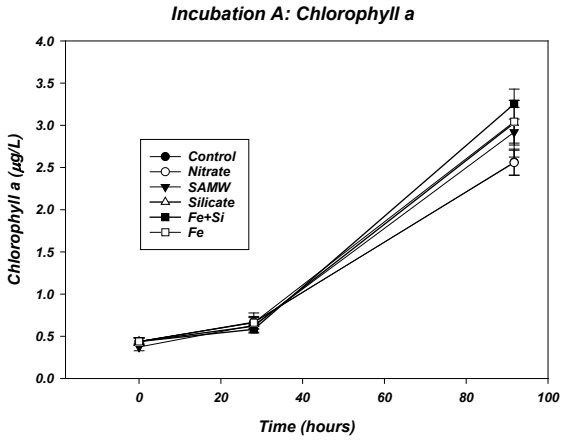

Incubation B preliminary results

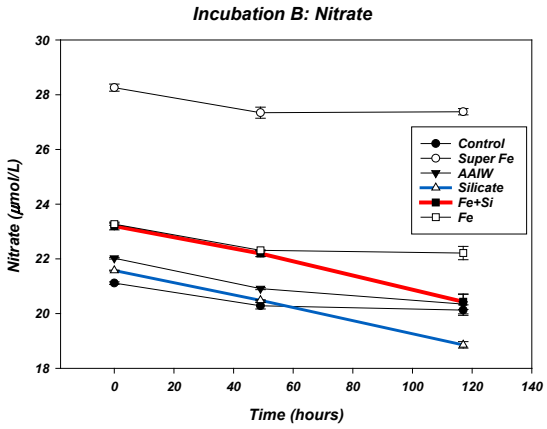

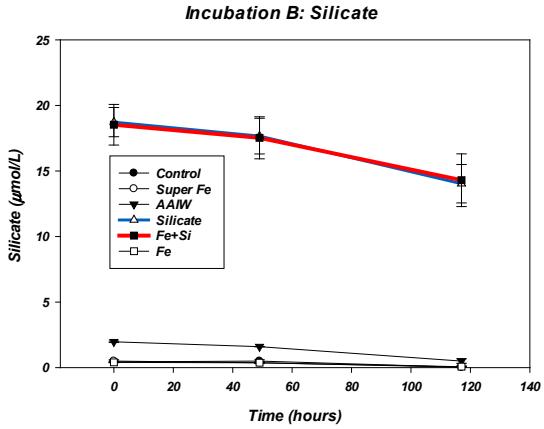

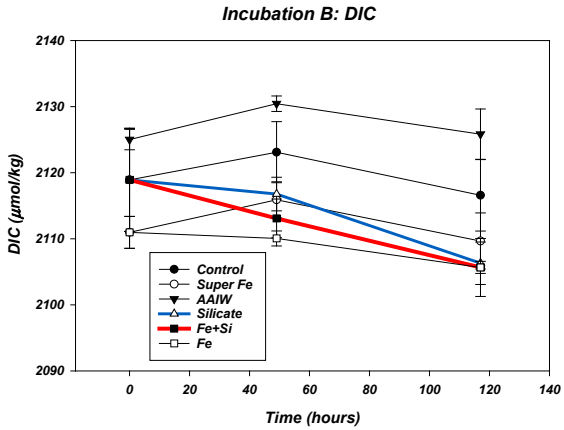

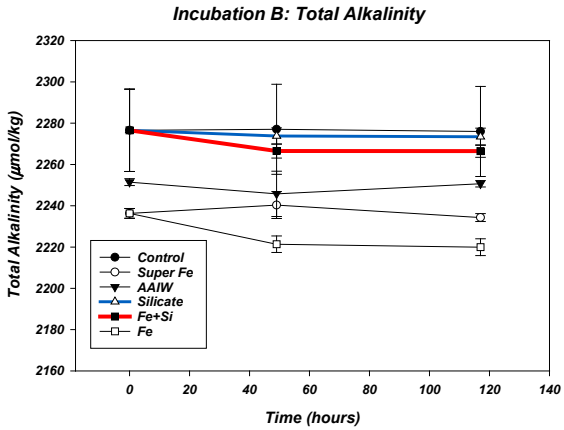

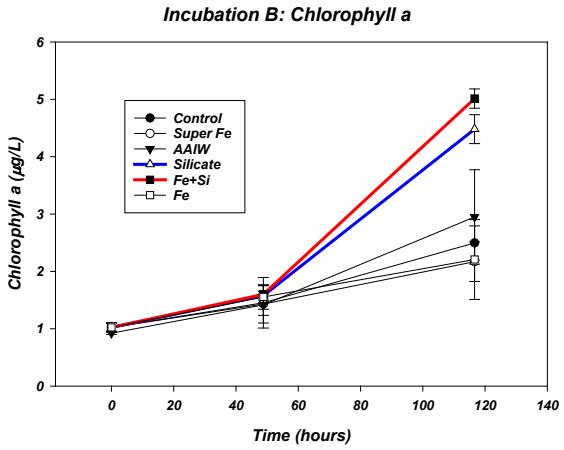

Incubation C preliminary results

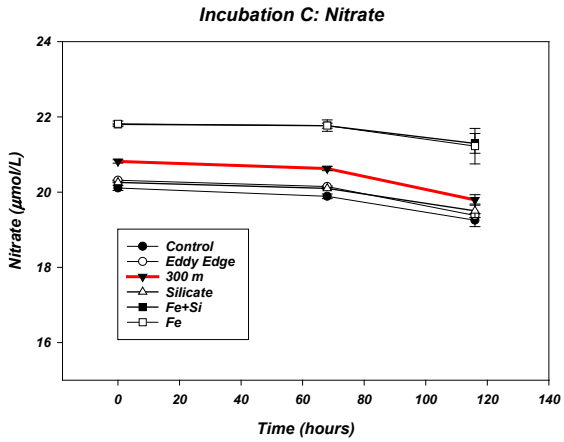

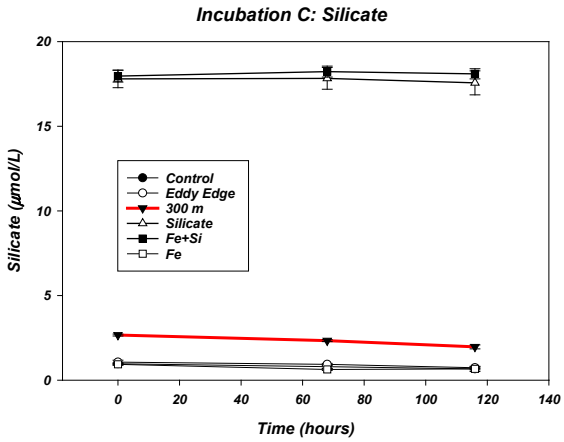

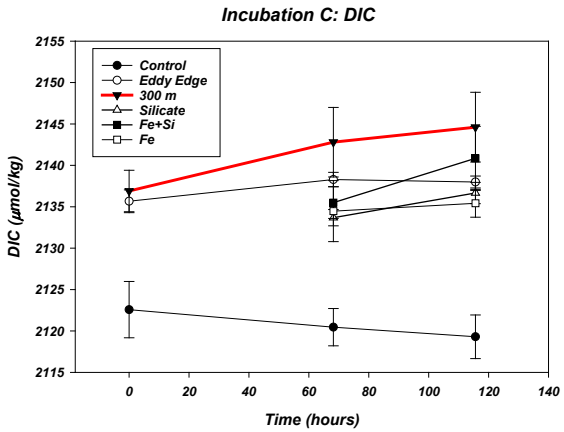

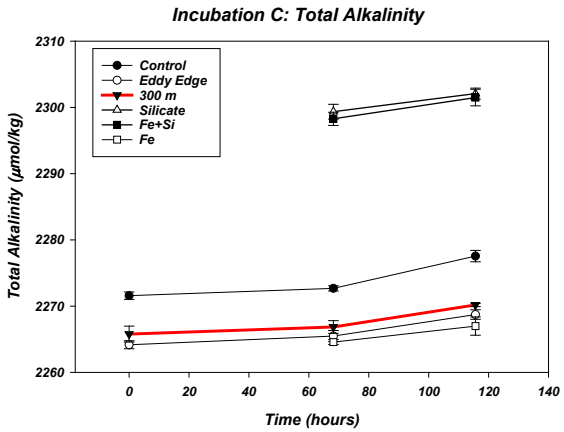

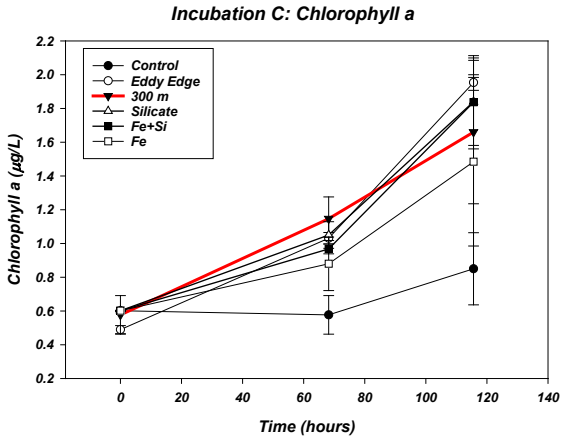

Incubation D preliminary results

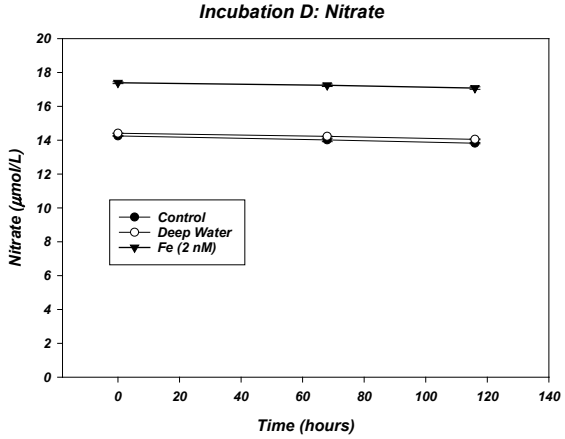

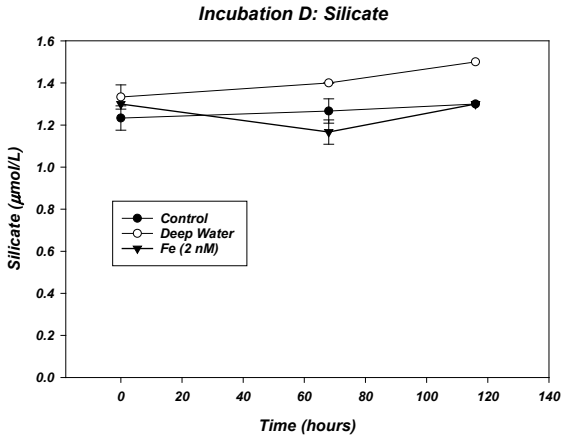

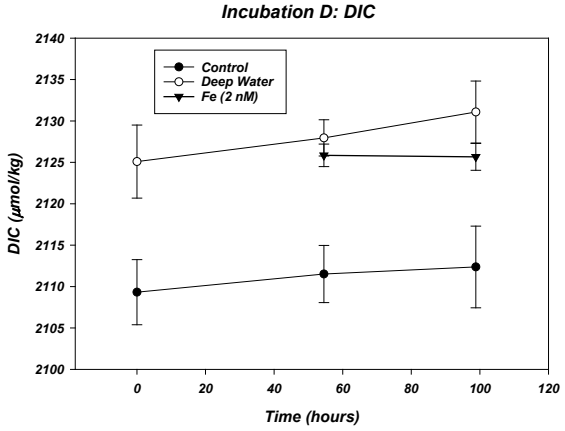

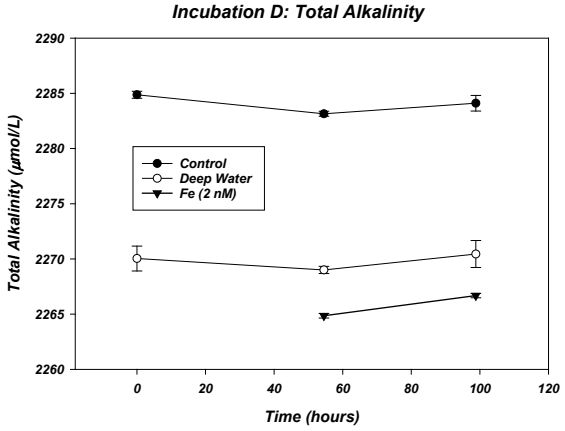

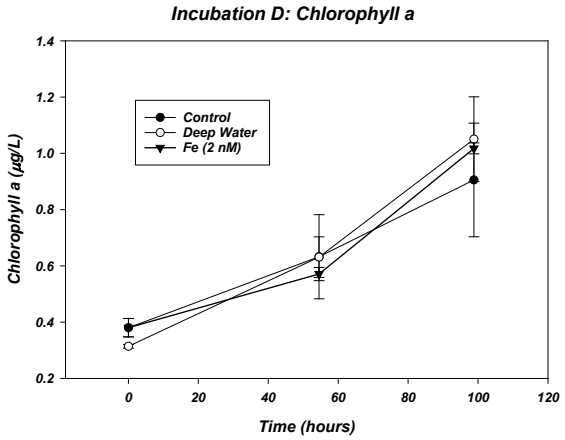

Incubation E preliminary results

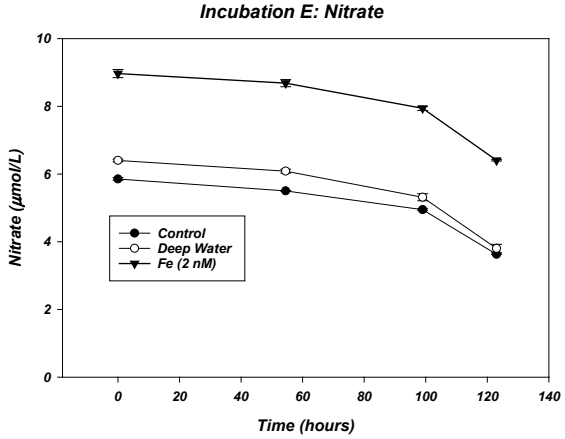

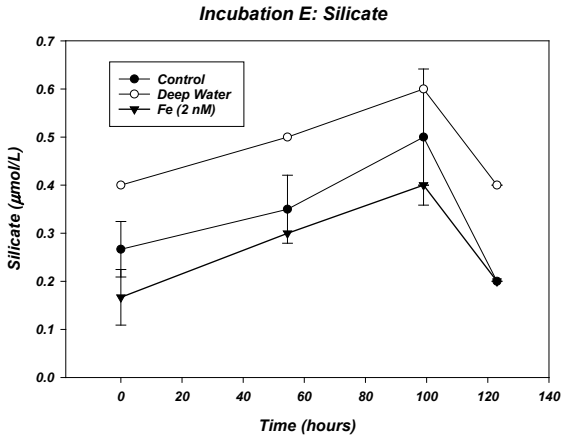

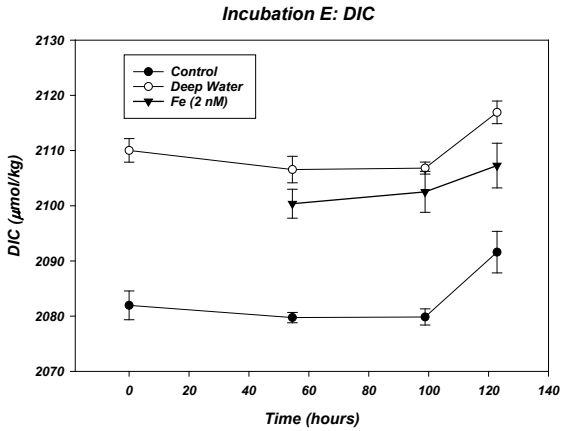

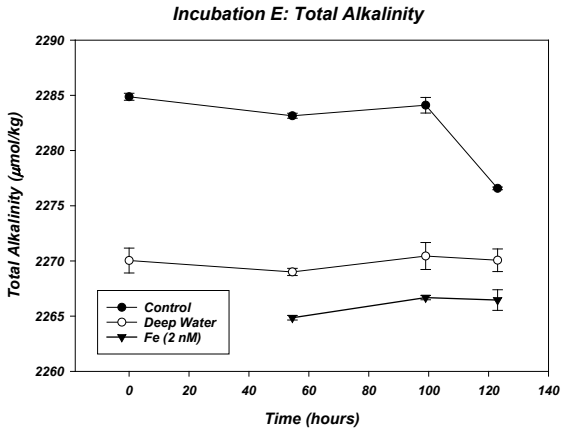

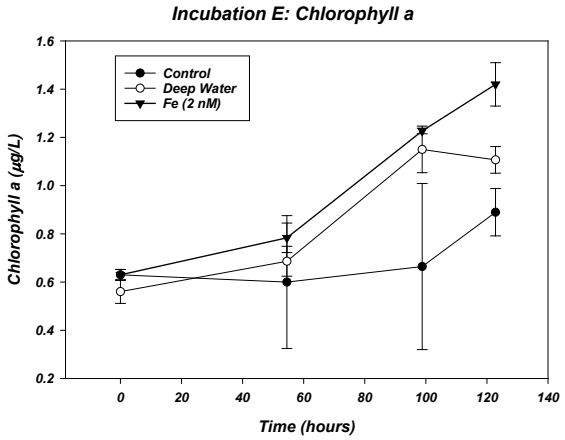

DNA sampling

Peter Morton, Lauren Hearn
National High Magnetic Field Laboratory/Florida State University
Tallahassee, Florida 32310

Samples for community DNA were collected on 0.22 µm MF Millipore filters (47 mm diameter) using the same offline vacuum filtration rigs used for the dissolved and particulate trace metal samples. Samples were drawn from the ship's rosette (surface and deep chlorophyll maximum) at full CTD casts, and from the initial and final timepoints of each incubation study. Volumes were 1-2 L, depending on sample availability and processing time.

Filtered samples were folded twice and stored in new 1.5-mL Eppendorf snap-cap centrifuge tubes at -80ºC. During the course of the cruise, the Plymouth University lab determined that DNA samples from the 2020 expedition had probably degraded during the transport from Mauritius to the UK, but the RNA samples – collected in exactly the same way but preserved using RNALater (Invitrogen, AM7020) – performed much better during PCR amplification than the DNA samples. Therefore, at the request of the Plymouth University lab, the 2021 DNA samples were preserved using RNALater (shipped directly to Dr. C. Measures, University of Hawaii-Manoa and brought to the Revelle in port) before shipping to Plymouth from San Diego.

DNA samples

								CTD		*Filter*	*Filter*		*Personnel*		
Station	Date (local)	**Lat (S)**	**Long (W)**	**CTD Bottle #**	**Type (s/d)**	**Depth**	**Filter volume**	**Sample time**	**Start time**	**End time**	**Sampler**	**Filterer**	**Notes**	
1	1/7/2021	30	150	24	surface	5	***2***	16:45	16:50	17:05	PLM	PLM		
1	1/7/2021	30	150	16	DCM	125	***2***	16:45	16:50	17:05	PLM	PLM		
3	1/7/2021	31	150	24	surface	5	2.13	23:00			LEH	LEH		
3	1/7/2021	31	150	10	DCM	140	2.16	23:00			LEH	LEH		
5	1/8/2021	32	150	24	surface	5	2.16	10:25	10:30	10:45	PLM	PLM		
5	1/8/2021	32	150	14	DCM	150	2.16	10:25	10:30	10:45	PLM	PLM		
7	1/8/2021	33	150	24	surface	5	2.20	18:15	18:20	19:00	PLM	PLM		
7	1/8/2021	33	150	12	DCM	115	2.12	18:15	18:20	19:00	PLM	PLM		
9	1/9/2021	34	150	24	surface	5	2.21	1:00	4:05	4:30	PLM	PLM		
9	1/9/2021	34	150	14	DCM	135	2.12	1:00	4:05	4:30	PLM	PLM		
11	1/9/2021	35	150	24	surface	5	2.06	11:56	12:00	12:30	PLM	PLM		
11	1/9/2021	35	150	10	DCM	133	2.08	11:56	12:00	12:30	PLM	PLM		
13	1/9/2021	36	150	24	surface	5	***2***	23:00			LEH	LEH		
13	1/9/2021	36	150	11	DCM	135	***2***	23:00			LEH	LEH		
15	1/10/2021	37	150	24	surface	5	2.22	7:30	9:50	10:20	PLM	PLM		Barney: dinos under microscope
15	1/10/2021	37	150	14	DCM	95	2.06	7:30	9:50	10:20	PLM	PLM		Barney: cocco under microscope (living and tests only)
17	1/10/2021	38	150	24	surface	5	2.20	19:20	19:25	19:55	PLM	PLM		
17	1/10/2021	38	150	17	DCM	125	2.12	19:20	19:25	19:55	PLM	PLM		
19	1/11/2021	39	150	23	surface	5	2.12	1:30	1:45	2:15	LEH	LEH		
19	1/11/2021	39	150	13	DCM	80	2.25	1:30	1:45	2:15	LEH	LEH		
21	1/11/2021	40	150	24	surface	5	2.01	9:00	11:05	11:30	PLM	PLM		
21	1/11/2021	40	150	14	DCM	94	2.24	9:00	11:05	11:30	PLM	PLM		diatoms
23	1/11/2021	41	150	24	surface	5	***2***	18:38	18:40	19:10	PLM	PLM		
23	1/11/2021	41	150	14	DCM	75	***2***	18:38	18:40	19:10	PLM	PLM		
25	1/12/2021	42	150	24	surface	5	2.10	3:00	4:25	5:05	PLM	PLM		lots of diatoms (pennates and centrics), dinos, few coccos
25	1/12/2021	42	150	15	DCM	35	2.24	3:00	4:25	5:05	PLM	PLM		"a real soup": diatoms, coccos, dinos, cryptomonads
27	1/12/2021	43	150	24	surface	5	2.02	13:00	13:15	13:50	PLM	PLM		
27	1/12/2021	43	150	14	DCM	75	2.04	13:00	13:15	13:50	PLM	PLM		
29	1/12/2021	44	150	24	surface	5	***2***	21:00			LEH	LEH		
29	1/12/2021	44	150	16	DCM	60	***2***	21:00			LEH	LEH		
31	1/13/2021	45	150	24	surface	5	2.12	5:45			PLM	PLM		Mostly diatoms and dinos and coccos
31	1/13/2021	45	150	14	DCM	64	2.25	5:45			PLM	PLM		mostly cyanobacteria
33	1/14/2021	46	150	24	surface	5	1.30	22:40	22:45	23:05	PLM	PLM		
33	1/14/2021	46	150	23	DCM	80	1.26	22:40	22:45	23:05	PLM	PLM		
35	1/14/2021	47	150	24	surface	5	2.12	7:30	11:00	11:25	PLM	PLM		mostly diatoms, some dinos and coccos
35	1/14/2021	47	150	14	DCM	58	2.19	7:30	11:00	11:25	PLM	PLM		mostly big diatoms, some dinos and coccos
43	1/17/2021	49.7	150	24	surface	5	1.10	5:15	16:44	16:53	PLM	PLM		stored in fridge; mix of diatoms, coccos, dinos
43	1/17/2021	49.7	150	18	DCM	26	1.08	5:15	16:55	17:07	PLM	PLM		stored in fridge; fewer diatoms, some big dinos and moderate coccos
45	1/18/2021	53	150	24	surface	5	1.08	9:00	13:00	13:15	PLM	PLM		lots of cyanobacteria
45	1/18/2021	53	150	13	DCM	65	1.08	9:00	13:15	13:25	PLM	PLM		few dinos, few coccos, few more diatoms and lots of cyanos
47	1/18/2021	52.3	150	24	surface	5	2.07	16:30	20:50	21:20	LEH	LEH		
47	1/18/2021	52.3	150	16	DCM	60	2.19	16:30	20:50	21:20	LEH	LEH		
49	1/18/2021	51.7	150	24	surface	5	1.06	23:30	9:25	9:40	LEH	LEH		
49	1/18/2021	51.7	150	16	DCM	50	1.03	23:30	9:25	9:40	LEH	LEH		
51	1/19/2021	51	150	24	surface	5	1.03	6:00	10:00	10:20	LEH	LEH		stored in fridge
51	1/19/2021	51	150	14	DCM	65	1.01	6:00	10:00	10:20	LEH	LEH		stored in fridge
53	1/20/2021	50.3	150	24	surface	5	1.03	15:40	15:50	16:09	LEH	LEH		
53	1/20/2021	50.3	150	16	DCM	65	1.00	15:40	15:50	16:09	LEH	LEH		
~~60~~	~~1/22/2021~~	~~54~~	~~150~~	~~24~~	~~surface~~	~~5~~		~~3:30~~			~~PLM~~	~~PLM~~		~~stored in FREEZER; did not filter~~
~~60~~	~~1/22/2021~~	~~54~~	~~150~~	~~13~~	~~DCM~~	~~85~~		~~3:30~~			~~PLM~~	~~PLM~~		~~stored in FREEZER; did not filter~~
63	1/24/2021	60	150	24	surface	13	1.98	7:00	9:38	9:56	PLM	PLM	ODF lab	
63	1/24/2021	60	150	15	DCM	50	2.24	6:15	6:26	6:47	PLM	PLM	ODF lab	
65	1/24/2021	59.3	150	24	surface	5	1.97	13:30	14:48	15:23	PLM	PLM	ODF lab	
65	1/24/2021	59.3	150	16	DCM	50	2.13	13:30	15:30	15:55	PLM	PLM	ODF lab	
67	1/24/2021	58.7	150	24	surface	5	2.06	20:45	21:05	21:35	LEH	LEH	ODF lab	
67	1/24/2021	58.7	150	18	DCM	40	2.20	20:45	21:40	22:11	LEH	LEH	ODF lab	
69	1/25/2021	58	150	24	surface	5	2.09	4:00	6:55	7:13	PLM	PLM	ODF lab	
69	1/25/2021	58	150	14	DCM	60	2.26	4:00	7:17	7:39	PLM	PLM	ODF lab	
69	1/25/2021	58	150	UHPW	UHPW	UHPW	0.48				PLM	PLM	ODF lab	UHP water blank (~500 mL UHPW poured through unrinsed/unwashed filter rig and filter)
71	1/25/2021	57.3	150	24	surface	5	2.12	12:30	14:35	14:57	PLM	PLM	ODF lab	
71	1/25/2021	57.3	150	16	DCM	55	2.21	12:30	15:00	15:23	PLM	PLM	ODF lab	
71	1/25/2021		UHPW	UHPW	UHPW	UHPW	0.60		15:30	15:35	PLM	PLM	ODF lab	UHP water blank (~600 mL UHPW poured through unrinsed/unwashed filter rig and filter)
73	1/26/2021	56.7	150	24	surface	5	2.06	20:00	20:18	20:40	LEH	LEH	ODF lab	
73	1/26/2021	56.7	150	18	DCM	60	2.09	20:00	20:40	21:08	LEH	LEH	ODF lab	
73	1/26/2021		UHPW	UHPW	UHPW	UHPW	0.60		21:10	21:15	LEH	LEH	ODF lab	UHP water blank (~600 mL UHPW poured through unrinsed/unwashed filter rig and filter)
75	1/28/2021	54.5	141	24	surface	5	1.96	18:00	18:47	19:07	PLM	PLM	ODF lab	Eddy A, SE corner
75	1/28/2021	54.5	141	12	DCM	85	2.03	18:00	19:09	19:25	PLM	PLM	ODF lab	Eddy A, SE corner
79	1/29/2021	53.3	143	24	surface	5	2.03	10:00	12:50	13:09	PLM	PLM	ODF lab	Eddy A, NW corner
79	1/29/2021	53.3	143	14	DCM	90	1.98	10:00	13:14	13:40	PLM	PLM	ODF lab	Eddy A, NW corner
80	1/29/2021	53.3	141	24	surface	5	2.05	18:30	18:55	19:21	PLM	PLM	ODF lab	
80	1/29/2021	53.3	141	16	DCM	60	2.13	18:30	19:24	19:54	PLM	PLM	ODF lab	
82	1/30/2021	53.9	141.9	24	surface	5	2.08	7:00	9:50	10:10	PLM	PLM	ODF lab	
82	1/30/2021	53.9	141.9	14	DCM	60	2.09	7:00	10:10	10:30	PLM	PLM	ODF lab	
84	1/31/2021	54.4	143	24	surface	5	1.95		14:31	14:52	PLM	PLM	ODF lab	
84	1/31/2021	54.4	143	14	DCM	75	2.10		14:55	15:27	PLM	PLM	ODF lab	(saw an iceberg, paused filtration)
85	2/1/2021	58	141.1	24	surface	5	1.87	1:30	10:00	10:25	PLM	PLM	ODF lab	Refrigerated after collection
85	2/1/2021	58	141.1	20	DCM	30	1.94	1:30	10:26	10:48	PLM	PLM	ODF lab	Refrigerated after collection
89	2/1/2021	56.85	140.8	24	surface	5	2.06	15:00	15:30	15:55	PLM	PLM	ODF lab	
89	2/1/2021	56.85	140.8	14	DCM	73	2.12	15:00	16:14	17:04	PLM	PLM	ODF lab	
91	2/1/2021	56	140.5	24	surface	5	1.85	22:18	14:00	14:23	PLM	PLM	ODF lab	
91	2/1/2021	56	140.5	14	DCM	85	1.89	22:18	14:25	14:44	PLM	PLM	ODF lab	
94	2/3/2021	53.1	138	24	surface	5	2.03	8:00	10:45	11:08	PLM	PLM	ODF lab	
94	2/3/2021	53.1	138	14	DCM	60	2.15	8:00	11:10	11:36	PLM	PLM	ODF lab	
96	2/3/2021	54.7	139	24	surface	5	2.04	16:50	18:37	18:58	PLM	PLM	ODF lab	
96	2/3/2021	54.7	139	12	DCM	85	2.11	16:50	19:00	19:23	PLM	PLM	ODF lab	
97	2/5/2021	52.7	145	24	surface	5	2.12	5:30	8:35	8:55	LEH	LEH	ODF lab	
97	2/5/2021	52.7	145	14	DCM	75	2.25	5:30	8:53	9:16	LEH	LEH	ODF lab	
98	2/8/2021	44.9	150	24	surface	5	2.08	4:00	10:02	10:27	LEH	LEH	ODF lab	
98	2/8/2021	44.9	150	18	DCM	30	2.21	4:00	9:38	10:00	LEH	LEH	ODF lab	
100	2/8/2021	44.2	150	24	surface	5	2.07	10:15	14:17	14:42	PLM	PLM	ODF lab	
100	2/8/2021	44.2	150	16	DCM	55	2.19	10:15	14:43	15:06	PLM	PLM	ODF lab	
102	2/8/2021	43.5	150	24	surface	5	2.06	17:30	17:45	18:10	PLM	PLM	ODF lab	
102	2/8/2021	43.5	150	18	DCM	50	2.10	17:30	18:15	18:40	PLM	PLM	ODF lab	
103	2/8/2021	43.2	150	24	surface	5	1.93	21:00	8:10	8:35	PLM	PLM	ODF lab	Refrigerated after collection
103	2/8/2021	43.2	150	18	DCM	43	1.99	21:00	8:37	9:00	PLM	PLM	ODF lab	Refrigerated after collection

DaNielA samples

Incubation	Date	Time Point	Amendment	Filter volume	*Filter* Start time	*Filter* End time	Notes
A	1/16/2021	0	Control	1.08	16:20	16:27	
A	1/16/2021	0	SAMW	1.05	16:32	16:42	
A	1/20/2021	Final	Control	2.08			
A	1/20/2021	Final	Nitrate	2.02			
A	1/20/2021	Final	SAMW	1.04			
A	1/20/2021	Final	Silicate	1.06			
A	1/20/2021	Final	Fe+Silicate	1.02			
A	1/20/2021	Final	Fe	1.06			
B	1/21/2021	0	Control	2.00			
B	1/21/2021	0	AAIW	1.36			
B	1/26/2021	Final	Control	1.06	13:37	13:46	
B	1/26/2021	Final	+4Fe	1.02	13:50	13:58	
B	1/26/2021	Final	AAIW	1.06	14:03	14:13	
B	1/26/2021	Final	Silicate	0.99	14:16	14:33	
B	1/26/2021	Final	Fe+Silicate	1.04	15:37	14:46	
B	1/26/2021	Final	Fe	1.05	14:49	14:58	
C	1/30/2021	0	Control	2.08	18:22	18:45	
C	1/30/2021	0	300 m/AAIW	1.43	18:48	19:02	
C	1/26/2021	Final	Control	1.07			
C	1/26/2021	Final	Eddy Edge	1.13			
C	1/26/2021	Final	300 m/AAIW	1.06			
C	1/26/2021	Final	Silicate	1.06			
C	1/26/2021	Final	Fe+Silicate	1.05			
C	1/26/2021	Final	Fe	1.04			
D	2/5/2021	0	Control	2.09	8:34	8:52	
D	2/10/2021	Final	Control	1.08	10:45	11:06	
D	2/10/2021	Final	DW (Deep Water)	2.00	10:45	11:05	
D	2/10/2021	Final	+2Fe	2.24	11:00	11:27	
E	2/8/2021	0	Control	2.11			
E	2/8/2021	0	300 m/DW	2.10			
E	2/12/2021	Final	Control	2.08			
E	2/12/2021	Final	DW (Deep Water)	2.22			
E	2/12/2021	Final	+2Fe	2.13			

Barite formation experiments and barium isotope measurements

Julia Middleton, jemiddle@mit.edu, Woods Hole Oceanographic Inst, Woods Hole, MA 02543

The ultimate burial of particulate organic carbon (POC) represents a climatically significant sink of the CO_2 drawn down by photosynthetic organisms in the sunlit surface ocean. However, quantification of marine export production and POC burial in the sediments, and its ultimate effects on global climate, has remained a delicate problem described by a handful of proxies, each with caveats. Marine barites have emerged as one powerful proxy option based on the barite formation pathway currently invoked in the literature. Despite this potential, controls on the formation of barite in the water column are greatly understudied. Currently, consensus does not exist as to the mechanism of barite formation (Chow & Goldberg 1960, Van Beek et al 2007, Gonzalez-Muñoz et al 2012) or the depth of barite formation in the water column (Van Beek et al 2007, Horner et al 2015). Although pelagic surface waters are under saturated with respect to barite, microcrystalline barite appears throughout the water column. To overcome this apparent paradox, much of the current literature invokes the microenvironment model: Barite precipitation occurs exclusively within locally supersaturated microenvironments contained within sinking POM, of which POC is a fraction. Supersaturation occurs through the release of dissolved barium during the microbial degradation of POM. To Investigate the controls on this precipitation mechanism, incubation experiments using a stable ^{135}Ba tracer were carried out during the SAMW 2020 cruise.

Barite formation experiments were initiated at the same stations as the Balch/Morton nutrient amendment incubations (Stations 39, 54, 83, 98) and were carried out within two stations of the productivity and trace metal casts (i.e. where a productivity cast was at Stn 001, a barite experiment was run at Stn 002 or 003). From the main CTD casts, water samples from the fluorescence peak, maximum gradient in beam transmission (region of decreasing particle load), and oxygen minimum were used to target areas with high phytoplankton growth, particle degradation, and microbial action, respectively. Samples were first spiked with ^{135}Ba to $\Omega barite \approx 1$ to allow tracing of new barite precipitation during the course of the experiment. Ba-135 spike additions were calculated using [Si] measured by ODF on stations within a few latitude degrees, following the [Ba]:[Si] relationship described by Bates et al. (2017), where [Ba] = 0.6296*[Si] + 38.63. We explored the influence of particulate availability (microenvironments) and microbial action at each of these depths. Four conditions were carried out at each depth: 1) Unadulterated water, 2) Filtered to 5 µm (no particulates/microenvironments), 3) poisoned with mercuric chloride (no microbial action), 4) filtered to 5 µm and poisoned (control). Three time points were taken over the course of one week, with replicates performed for the latter two time points. The particulate fraction was saved for shore-side analysis. Pre-cruise experiments show that the uptake of ^{135}Ba into the particulate fraction can be observed over this time period. All analytical measurements for these experiments will be carried out at the Woods Hole Oceanographic Institution (WHOI) ICP Facility.

Stn #	Niskin	Depth (m)	Depth Name	*In-situ* Temp (℃)	Incubator temp (℃)	Goal [Ba]	Samples
39	18	50	Flourescence max.	11.7	12 ± 1	160	23
	16	60	Max. gradient in transmissivity	11.6	12 ± 1	153	23
	2	1000	Oxygen minimum (cast)	5.3	5 ± 1	135	23
54	16	50	Flourescence max.	4.4	5 ± 1	154	23
	14	75	max. gradient in transmissivity	2.8	5 ± 1	141	23
	2	1000	Oxygen minimum (cast)	2.7	5 ± 1	109	23
83	20	60	Flourescence max.	6.6	8 ± 1	136	23
	18	80	Max. gradient in transmissivity	5.9	8 ± 1	134	23
	1	1000	Oxygen minimum (cast)	2.8	8 ± 1	112	23
98	17	30	Flourescence max.	12.2	15 ± 2	158	23
	15	47	Max. gradient in transmissivity	11.9	15 ± 2	152	23
	1	1000	Oxygen minimum (cast)	4.8	15 ± 2	129	23
						Total Samples	276

Additionally, dissolved barium samples (collected post filter, 0.4μm Isopore polycarbonate track-etch filter) were collected from every depth of the trace metal casts. Samples along the meridional transect are of particular interest, as they offer information pertinent to controls on global barium cycling and the relationship between barium and silica cycling. Marine chemists have speculated on the barium-silica relationship since the 1970's, when the linear correlation between dissolved silicon and barium was first observed throughout the world's oceans. The prevailing paradigm posits that the silicon–barium correlation arises from similarities in the remineralization length scale of the major particulate carrier phases of silicon and barium (diatom opal and barite, respectively; *sensu* Broecker and others). However, recent advances in barium stable isotope mass spectrometry have generated datasets suggesting that mixing, mediated via the Southern Ocean 'hub' may be more adept in describing the major features of marine barium distributions, particularly at the low latitudes (Fig. 1a, *sensu* Sarmiento and others). **A simple test to discriminate between these two models is to examine the patterns of dissolved silicon, barium, and barium stable isotope distributions in water masses as they are being labeled in the high-latitude Southern Ocean (Figure 1).**

How does water mass labeling occur for silicon and barium? For Si, water parcels are labeled by extreme Si depletion, relative to nitrate and phosphate, associated with significant diatom productivity in euphotic waters of the Southern Ocean. In contrast, labeling for Ba is thought to occur via Ba removal into discrete micron-sized crystals of barite; these crystals form in the upper mesopelagic in association with organic matter remineralization. Thus, the processes labeling water masses for silicon and barium have fundamentally different boundary conditions: one is drawn out of seawater by the production of organic matter and the other by its degradation. Should the remineralization mechanism of global silicon–barium coupling be correct, we hypothesize that a coupled fingerprint should exist across the Southern Ocean (Fig. 1b). Alternatively, should the mixing-mediated model set the chemical fingerprints for dissolved silicon and barium, we expect strong silicon-barium decoupling in the SAMW formation region, where water parcels are labeled for Si *before* labeling for Ba (Fig. 1c).

As our cruise track had the specific aim of tracking the SAMW, and therefore represents a significant opportunity to acquire samples hand-picked for their applicability to SAMW conditioning questions. Having now collected these samples, I will carry out shore-side quantification of barium-silica (de)coupling using high-precision Ba stable isotope analyses of upstream water samples collected between 30—60 °S during the meridional survey. These analyses will be carried out in the WHOI ICP Facility. **Sampling Sub-Antarctic Mode Water from the origin at the surface into the Indian Ocean will be used to refine Ba-based productivity proxies and will illuminate controls on a historically enigmatic relationship between barium and silica distributions.**

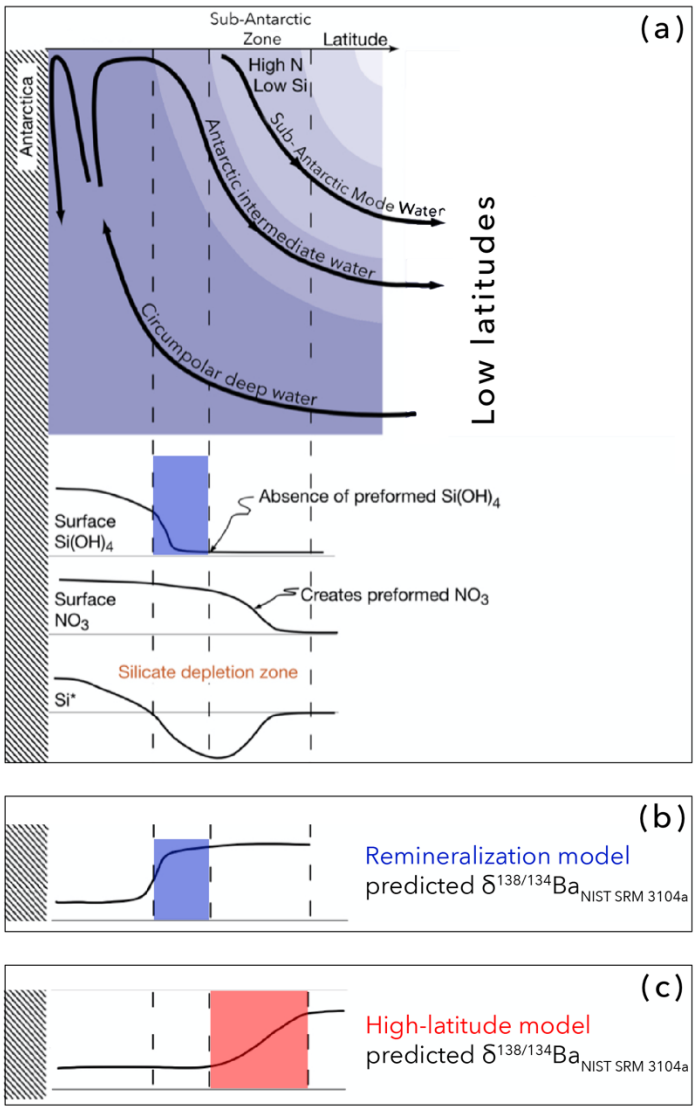

Figure 1. Schematic of surface silicic acid, nitrate, and Si* changes across the Antarctic Intermediate Water (AAIW) and Sub-Antarctic Mode Water (SAMW) outcropping regions, modified from Sarmiento et al. (2004). Here used as a tracer for the SAMW, $Si^* = [Si(OH)_4] - [NO_3^-]$. Panel (b) shows remineralization model for global barium cycling, which predicts changes barite precipitation the same region as $Si(OH)_4$ draw down, as seen through an enrichment in $\delta^{138/134}Ba_{NIST\ SRM\ 3104a}$ across the AAIW outcropping zone. In contrast, a high-latitude mixing mediated model predicts $\delta^{138/134}Ba_{NIST\ SRM\ 3104a}$ enrichment during the subduction of the SAMW, *after* particulate organic matter enters the upper mesopelagic and begins to degrade, promoting barite precipitation.

Dissolved Ba samples	
# of stations	21
# of samples	172

Cadmium Authigenic Formation during a Biomass Decay Experiments
Cruise Report for SAMW Cruise on *R/V Roger Revelle* #2004

Logan Tegler – Graduate Student, Woods Hole Oceanographic Institution; ltegler@mit.edu
PhD Advisors – Tristan Horner & Sune Nielsen

I. Introduction and Objectives

Cadmium (Cd) isotopes exhibit a nutrient-type profile in the water column that reflects a prominent biological control. Thus, due to its connection to biological processes, Cd can be used as a paleoproxy for nutrient utilization (e.g., Georgiev et al., 2015; Hohl et al., 2019). However, recent studies have suggested that Cd that forms authigenically in the water column and may represent an important missing sink of Cd. The authigenic Cd may form either due to the formation of insoluble sulfides in microenvironments, especially in oxygen-depleted waters (e.g. Janssen et al., 2014; Conway and John et al., 2015), or particulate Cd that forms in association with Cd uptake by prokaryotes (Ohnemus et al., 2016).

The purpose of these experiments is to (i) characterize authigenic precipitation of Cd during phytoplankton decay experiments, (ii) understand how Cd is trapped in an authigenic phase in the upper several hundred meters of the water column, and (iii) help determine whether this formation is a biogeochemically important sink of Cd. During the SAMW Cruise on the R/V Roger Revelle, we have performed isotopic ^{111}Cd tracer in decay experiments at four stations in the Southern Ocean to monitor the rates and drivers of authigenic Cd precipitation under a variety of experimental conditions—filtered to 5µm and unfiltered seawater and with the addition of $HgCl_2$ and absence of poison. The filtered trials will allow us to isolate effects that are attributed to microenvironments created during biomass decay and the poisoned trials will allow us to isolate effects to do with biological processing during decay by prokaryotes. Each trial iteration will then be examined to answer the following: Over what timescales does authigenic precipitation occur? How much precipitation is there? How efficient is the precipitation relative to remineralization? And Where does the precipitation ultimately come from (direct precipitation with seawater or in association with organic matter)?

These experiments will be conducted in two distinct ocean regions: the well-oxygenated waters of the Southern Ocean and an oxygen minimum zone (OMZ) in the Costa Rica Dome. The first set of experiments, which are detailed in this cruise report, will inform Cd particulate cycling in the Southern Ocean. These experiments will be repeated on a future cruise in an oxygen minimum zone the Costa Rica Dome. The goal of these studies is to compare and contrast authigenic Cd formation in these regions.

Understanding the formation of authigenic Cd under various oxygen conditions is essential for interpretation the Cd cycle in both the past and future as the ocean has experienced variable oxygen conditions in the geological past and oxygen minimum zones are expected to increase in the future.

II. Methods

At each station, 40L of water was collected in two 20L cubitainers from a trace metal clean surface sampler (Big Jon). 1L of seawater was be collected and taken as the baseline to confirm the natural abundances. The remaining seawater was broken into two 20L aliquots. One aliquot was filtered through a 5µM PES filter (minimizing the potential for microenvironments) and the other was left unfiltered.

After the water was taken and filtered, if necessary, it was placed into clean 1L bottles (14 that were filtered and 14 that were left unfiltered). From each of these, half poisoned with 200µL of concentrated mercuric chloride and the other half were not poisoned (see Fig. 1). Finally, the appropriate amount of spike will be added based on previous dissolved Cd, d[Cd], in the region. The amount of spike was calculated by adding 1.5 times the natural d[Cd] in the water column. In the event that the d[Cd] < 0.2nM, 0.2nM was added.

All 1L bottles were placed in a dark plastic bag and subsequently transferred to a shipping crate strapped down on the outside deck (to provide cool temperatures). The experiments are sampled as following:t_0 (1

replicate), t_1 (2replicates), and t_2 (2 replicates), t_3 (2 replicates) timepoints. A filter blank was processed alongside every time point. See below for a cartoon of the experimental setup (Fig. 1).

Table 1 gives the stations where water was collected, the approximate natural dissolved Cd in the region, and the amount of ^{111}Cd spike added to each experiment. The starting natural dissolved Cd values that the spike was calculated by were courtesy of Dr. Angela Milne and Dr. Peter Morton. These values are in the process of publication and thus have not been directly included in this cruise report.

After the samples are transported off of the R/V Revelle, they will be brought to the NIRVANA laboratory at the Woods Hole Oceanographic Institution where they will be processed in a Class 100 trace metal clean lab. Here, they will be leached using the Bishop method (0.6 M HCl in Teflon, 16 hours, at 80˚C) and analyzed on a quadrupole inductively-coupled plasma mass spectrometer (Q-ICP-MS) in the WHOI Plasma Facility.

III. Tables and Figures

Station	Latitude	Longitude	^{111}Cd (nM)	Temp (˚C)
37	-47.685	-150.001	0.20	12 ± 1
55	-55.669	-149.998	0.34	5 ± 1
82	-53.927	-141.927	0.40	8 ± 1
98	-44.865	-149.999	0.20	15 ± 2

Table 1. Station location, natural Cd concentration, and spiking addition.

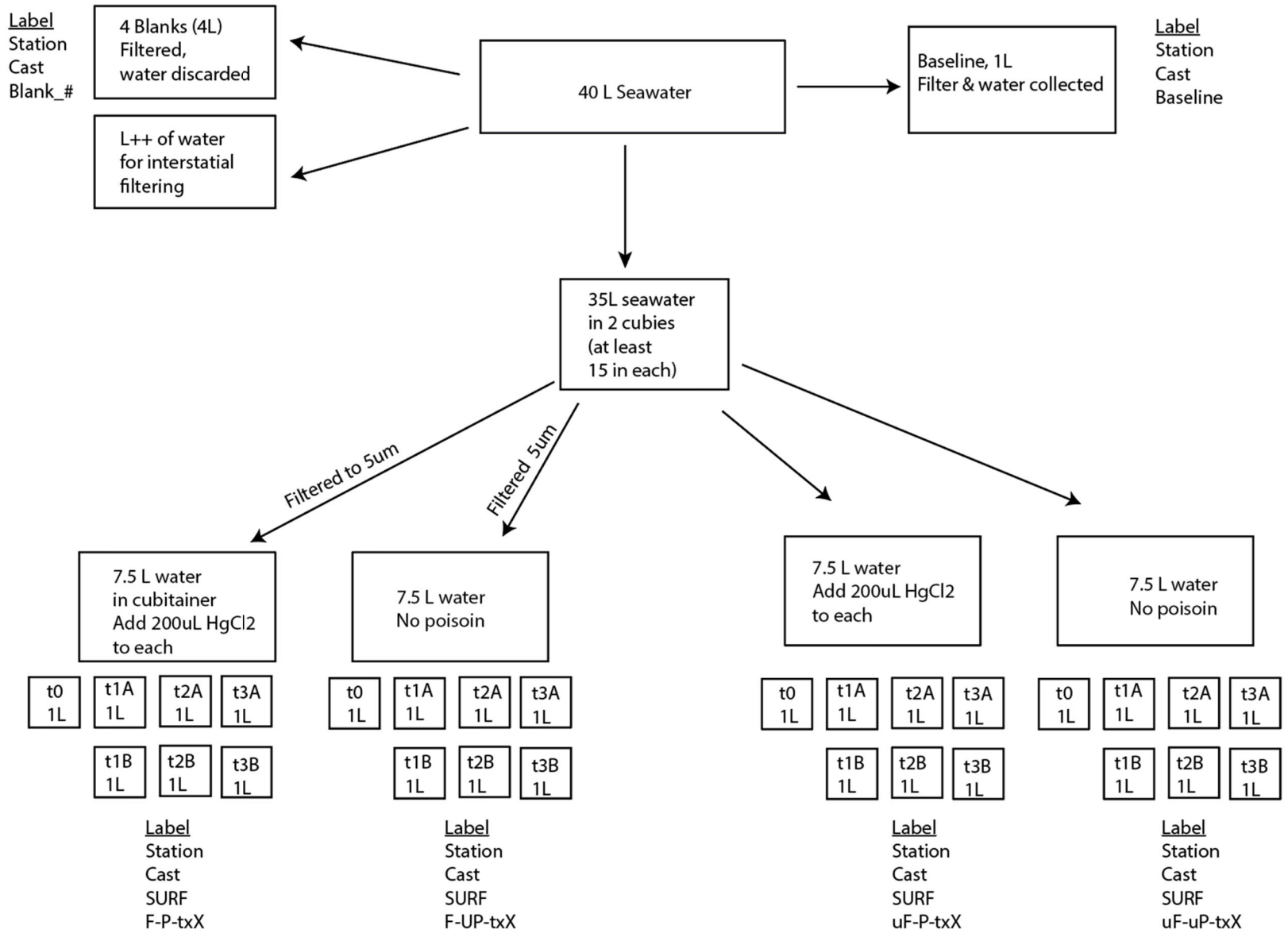

Figure 1. Experimental Set up

References:

Georgiev, S. V., Horner, T. J., Stein, H. J., Hannah, J. L., Bingen, B., & Rehkämper, M. (2015). Cadmium-isotopic evidence for increasing primary productivity during the Late Permian anoxic event. *Earth and Planetary Science Letters*, *410*, 84-96.

Hohl, S. V., Jiang, S. Y., Wei, H. Z., Pi, D. H., Liu, Q., Viehmann, S., & Galer, S. J. (2019). Cd isotopes trace periodic (bio) geochemical metal cycling at the verge of the Cambrian animal evolution. *Geochimica et Cosmochimica Acta*, *263*, 195-214.

Ohnemus, D. C., Rauschenberg, S., Cutter, G. A., Fitzsimmons, J. N., Sherrell, R. M., & Twining, B. S. (2017). Elevated trace metal content of prokaryotic communities associated with marine oxygen deficient zones. *Limnology and Oceanography*, *62*(1), 3-25.

RR2004
Carbon System Measurements
Nick Bates Group
Bermuda Institute of Ocean Sciences (BIOS)

Group Members:
Rebecca Garley (BIOS)
Matt Enright (BIOS)

Objectives:

To undertake high quality dissolved inorganic carbon (DIC) and total alkalinity (TA) measurements throughout the cruise from both the CTD rosette and the ships underway system. Sampling especially in features with high PIC and/or coccolithophore biomass in order to understand the influences on biogeochemistry, carbon dynamics (including biological pump of carbon) and air-sea gas exchange on Sub Antarctic Mode Water (SAMW). Also, to support other biogeochemical measurements on the cruise as a means to understand Southern Ocean ecosystem dynamics.

We will use the carbon chemistry measurements to help understand the dynamics of preconditioning of the SAMW formed in the Southern Ocean. Inputting the DIC and TA data into CO2SYS (Lewis and Wallace, 1998; using the constants from Mehrbach et al., 1973 refit by Dickson and Millero, 1987) to compute other carbonate parameters (e.g. pH, pCO2, calcium carbonate mineral saturation states) to further understand the carbonate system of these waters.

Methods:

Samples for DIC and TA were collected in 250ml borosilicate glass bottles according to standard JGOFS methods. Milli-Q cleaned bottles were rinsed out 3 times, bottom filled using silicone tubing, allowed to overflow at least 1 times the bottle volume, ensuring no bubbles are in the sample and sealed with a small headspace to allow for water expansion.

Water samples were collected from all depths the CTD-rosette sampled on full casts and from 8 depths on the 'trip-on-fly' casts. Two samples were collected from each niskin bottle on the full casts. The first sample was poisoned with 100µl saturated mercuric chloride solution for analysis back at the BIOS lab. The second sample was not spiked and stored in the dark for no longer than 12 hours (to minimise any biological activity altering the sample) before being run on board, DIC first then TA. In addition to sampling from the rosette, samples were also collected and analysed on board from the underway system. Underway sampling was on the final leg through higher PIC water on the return to the meridional transect and up to the Tahitian EEZ. Also, samples for the 5 incubation experiments were analysed; 6-9 initial T=0 samples, then one sample from each of the 18 cubitainers for the further time points of the experiment. Both the underway and carboy samples were un-spiked, stored in the dark and analysed on board.

Samples were analysed on the VINDTA 3S (Versatile Instrument for the Determination of Titration Alkalinity) and the AIRICA (Automated Infra-Red Inorganic Carbon Analyzer) (www.marianda.de).

TA is measured on the VINDTA 3S by titration with a strong acid (HCl). The titration curve shows 2 inflection points, characterising the protonation of carbonate and bicarbonate respectively, where consumption of acid at the second point is equal to the titration alkalinity.

DIC is measured on the AIRICA by the extraction of total dissolved inorganic carbon content from the sample by phosphoric acid addition. The liberated CO_2 flows with a N_2 carrier gas into a Li-Cor non-dispersive IR gas analyser where the CO_2 levels are measured.

For both instruments, within bottle replicates were run consecutively on start up to check the precision, continuing once the instrument precision was ±2µmol kg^{-1} or better. These were followed by a combination of Certified Reference Materials (CRMs) produced by the Marine Physical Laboratory at UCSD and low nutrient surface water from the Bermuda Atlantic Time Series (BATS) site, which were run every 20-24 samples on the VINDTA and every 6 samples on the AIRICA, to determine the accuracy and precision of the measurements and to correct for any discrepancies. The TA system CRM values did not vary more than 2umol within each batch of HCl acid. The AIRICA can be more susceptible to drift and can be affected by the lab temperature which is why CRMs were run much more often on the AIRICA, the system did not drift much and the lab temperature did not really vary. The AIRICA did have 2 shifts in CRM value after replacement of system parts. The Scripps MPL lab had been closed due to Covid-19 and no more CRMs were available. Our lab already had 20 bottles but we made our own reference water and filled 100, 500ml glass stopper borosilicate bottles with the BATS surface water, measured 15 bottles pre-cruise at the BIOS lab, analysed 60 during the cruise and will measure the rest upon return to BIOS to confirm the DIC and TA values were stable.

The values for DIC and TA were used to calculate other parameters of the carbonate system using CO2sys (Lewis and Wallace, 1998). Parameters able to be calculated are pH, fCO_2, pCO_2, $[HCO_3^-]$, $[CO_3^{2-}]$, $[CO_2]$, alkalinity from borate; hydroxide ion; phosphate and silicate, Revelle Factor, plus the saturation states of calcite and aragonite.

Underway Systems:

BIOS used a SAMIpCO2 from Sunburst Sensors to measure the pCO_2 from the underway system every 30 minutes. pCO2 was also measured with the installed General Oceanics Equilibrator pCO2 underway system. The UCSD system has 5 standards measured every 4-5 hours. The Scripps Li-Cor 7000 gas analyser was not functioning but we had a spare which we installed for the duration of this cruise.

pH was measured using the AFT-pH (Autonomous Flow Through instrument) analyser from Sunburst Sensors. This measured pH every 30 minutes.

TA was measured underway by the Hydro FIA TA system. The system was standardized using Scripps Certified Reference Material and discrete surface samples taken at CTD stations. The CONTROS HydroFIA® TA is a flow through system for the determination of the total alkalinity in seawater. It can be used for continuous monitoring during surface water applications as well as for discrete sample measurements A defined amount of seawater is acidified by injection of a fixed amount of hydrochloric acid (HCl). After acidification the generated CO_2 in the sample is removed by means of a membrane based degassing unit resulting in a so-called open-cell titration. The subsequent pH determination is carried out by means of an indicator dye (Bromocresol green) and VIS absorption spectrometry. Together with salinity and temperature, the resulting pH is directly used for the calculation of total alkalinity.

Sample	# of stations	# of samples	analysis
CTD DIC/TA	103	1102	Analysed on board
CTD DIC/TA replicate bottles	103	728	Future processing at BIOS
Underway DIC/TA discrete bottles	127	44	Analysed on board
Incubation DIC/TA	5	189	Analysed on board
Underway TA	-	7000	Underway measurements
Underway GO pCO2	-	12000	Underway measurements
Sunburst SAMIpCO2		2000	Underway measurements

Table 1: Summary of sample collection and analysis

Initial Findings:

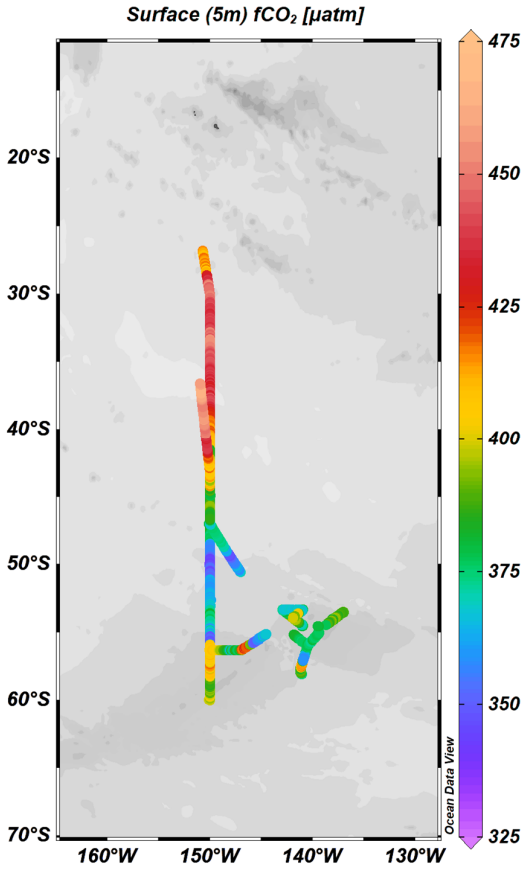

Fig. 1: Surface pCO_2, measurements from the underway General Oceanics pCO_2 system.

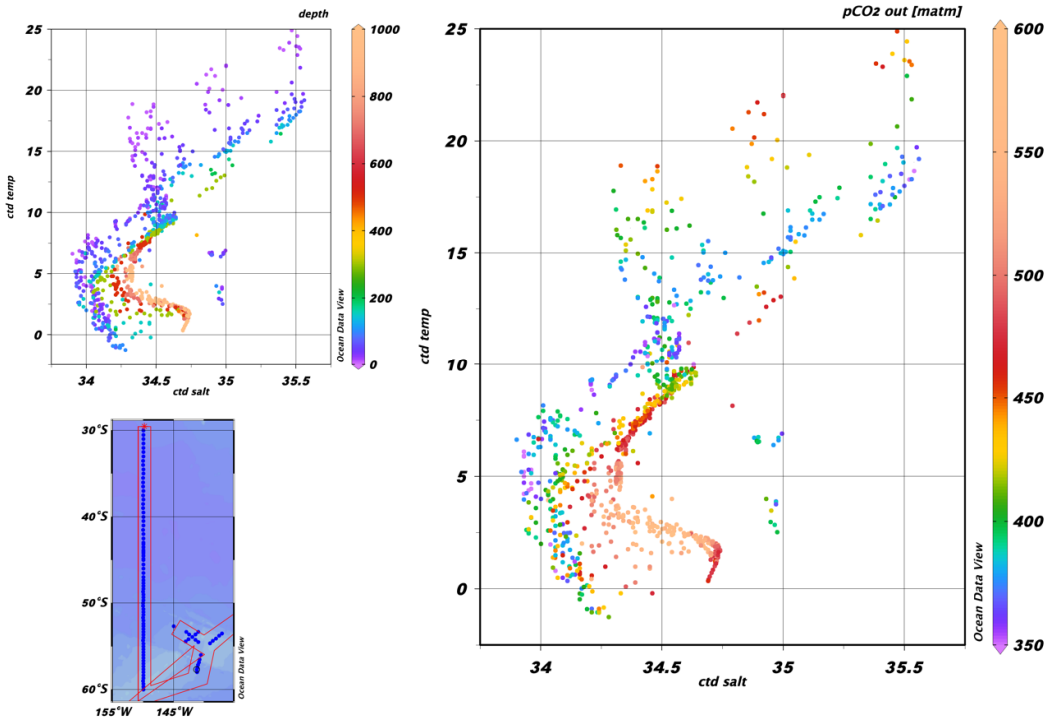

Fig. 2: Temperature - salinity scatter plots with z-axis of depth (top left) and pCO_2 (right) for all CTD data. pCO_2 has been calculated from DIC and TA samples.

See the VPR Team cruise report, figure 15, for section plots of DIC, TA and pCO2 from the meridional transect 30-60°S.

Above atmospheric surface pCO_2 was measured in the lower latitudes of the meridional transect, north of the subtropical front, on the first leg. There was also low nTA (salinity normalized to a salinity of 35) in the surface waters north of the STF, with values of 2295-2315 umol/kg.

South of ~43°S the surface water pCO_2 was below atmospheric levels. The return to the meridional transect on the final leg with the higher PIC water, saw similar surface pCO_2 levels compared to the first sampling, ranging 380-423ppm, also, similar nTA values around 2322umol/kg.

Further comparisons between the survey sites will be made within the carbonate chemistry data set and with the rest of the cruise data in particular examining the biogeochemical conditioning of the SAMW. Also, comparisons between DIC and TA sample analysis on board and back at the lab in Bermuda.

References:

Lewis, E., and D. W. R. Wallace. 1998. Program Developed for CO2 System Calculations. ORNL/CDIAC-105. Carbon Dioxide Information Analysis Center, Oak Ridge National Laboratory, U.S. Department of Energy, Oak Ridge, Tennessee.

Robbins, L.L., Hansen, M.E., Kleypas, J.A., and Meylan, S.C., 2010, CO2calc—A user-friendly seawater carbon calculator for Windows, Max OS X, and iOS (iPhone): U.S. Geological Survey Open-File Report 2010–1280, 17 p.

NUTRIENT ANALYSIS

Technicians:
Melissa Miller, UC San Diego/Scripps Institution of Oceanography,
Shipboard Technical Support, Oceanographic Data Facility (ODF)

Megan Roadman, UC San Diego/Scripps Institution of Oceanography
Shipboard Technical Support, Oceanographic Data Facility

Summary of Analysis

• 1581 nutrient samples were collected analyzed. This includes:
- ❖ 1140 samples from 105 CTD casts (103 stations), including 1 that was mis-sampled
- ❖ 173 samples from 21 trace metal stations
- ❖ 224 samples from 5 trace metal incubation experiments
- ❖ 43 underway samples

• The cruise started with new pump tubes and they were changed 2 times.
• 3 sets of primary standards were made up over the course of the cruise.
• The cadmium column efficiency was checked periodically and new column was put on if the efficiency fell below 97% or injected with air. See Analytical Problems section for details.

Equipment and Techniques

Nutrient analyses (phosphate, silicate, nitrate+nitrite, nitrite, and ammonia) were performed on a Seal Analytical continuous-flow AutoAnalyzer 3 (AA3). The methods used are described by Gordon et al [Gordon1992] Hager et al. [Hager1972], and Atlas et al. [Atlas1971]. Details of modification of analytical methods used in this cruise are also compatible with the methods described in the nutrient section of the GO-SHIP repeat hydrography manual (Hydes et al., 2010) [Hydes2010].

Nitrate/Nitrite Analysis

A modification of the Armstrong et al. (1967) [Armstrong1967] procedure was used for the analysis of nitrate and nitrite. For nitrate analysis, a seawater sample was passed through a cadmium column where the nitrate was reduced to nitrite. This nitrite was then diazotized with sulfanilamide and coupled with N-(1-naphthyl)-ethylenediamine to form a red dye. The sample was then passed through a 10mm flowcell and absorbance measured at 520nm. The procedure was the same for the nitrite analysis but without the cadmium column.

REAGENTS

Sulfanilamide: Dissolve 10g sulfamilamide in 1.2N HCl and bring to 1 liter volume. Add 2 drops of 40% surfynol 465/485 surfactant. Store at room temperature in a dark poly bottle.
Note: 40% Surfynol 465/485 is 20% 465 plus 20% 485 in DIW.

N-(1-Naphthyl)-ethylenediamine dihydrochloride (N-1-N): Dissolve 1g N-1-N in DIW, bring to 1 liter volume. Add 2 drops 40% surfynol 465/485 surfactant. Store at room temperature in a dark poly bottle. Discard if the solution turns dark reddish brown.

Imidazole Buffer: Dissolve 13.6g imidazole in ~3.8 liters DIW. Stir for at least 30 minutes to completely dissolved. Add 60 ml of CuSO4 + NH4Cl mix (see below). Add 4 drops 40% Surfynol 465/485 surfactant. Let sit overnight before proceeding. Using a calibrated pH meter, adjust to pH of 7.83-7.85 with 10% (1.2N) HCl (about 10 ml of acid, depending on exact strength). Bring final solution to 4L with DIW. Store at room temperature.

NH4Cl + CuSO4 mix: Dissolve 2g cupric sulfate in DIW, bring to 100 m1 volume (2%). Dissolve 250g ammonium chloride in DIW, bring to l liter volume. Add 5ml of 2% CuSO4 solution to this NH4Cl stock. This should last many months.

Phosphate Analysis

Ortho-Phosphate was analyzed using a modification of the Bernhardt and Wilhelms (1967) [Bernhardt1967] method. Acidified ammonium molybdate was added to a seawater sample to produce phosphomolybdic acid, which was then reduced to phosphomolybdous acid (a blue compound) following the addition of dihydrazine sulfate. The sample was passed through a 10mm flowcell and absorbance measured at 880nm.

REAGENTS

Ammonium Molybdate: H2SO4 solution: Pour 420 ml of DIW into a 2 liter Ehrlenmeyer flask or beaker, place this flask or beaker into an ice bath. SLOWLY add 330 ml of conc H2SO4. This solution gets VERY HOT!! Cool in the ice bath. Make up as much as necessary in the above proportions. Dissolve 27g ammonium molybdate in 250ml of DIW. Bring to 1 liter volume with the cooled sulfuric acid solution. Add 3 drops of 15% DDS surfactant. Store in a dark poly bottle.

Dihydrazine Sulfate: Dissolve 6.4g dihydazine sulfate in DIW, bring to 1 liter volume and refrigerate.

Silicate Analysis

Silicate was analyzed using the basic method of Armstrong et al. (1967). Acidified ammonium molybdate was added to a seawater sample to produce silicomolybdic acid which was then reduced to silicomolybdous acid (a blue compound) following the addition of stannous chloride. The sample was passed through a 10mm flowcell and measured at 660nm.

REAGENTS

Tartaric Acid: Dissolve 200g tartaric acid in DW and bring to 1 liter volume. Store at room temperature in a poly bottle.

Ammonium Molybdate: Dissolve 10.8g Ammonium Molybdate Tetrahydrate in 1000ml dilute H2SO4. (Dilute H2SO4 = 2.8ml conc H2SO4 or 6.4ml of H2SO4 diluted for PO4 moly per liter DW) (dissolve powder, then add H2SO4) Add 3-5 drops 15% SDS surfactant per liter of solution.

Stannous Chloride stock: (as needed) Dissolve 40g of stannous chloride in 100 ml 5N HCl. Refrigerate in a poly bottle. NOTE: Minimize oxygen introduction by swirling rather than shaking the solution. Discard if a white solution (oxychloride) forms.

Stannous Chloride working: (every 24 hours) Bring 5 ml of stannous chloride stock to 200 ml final volume with 1.2N HCl. Make up daily - refrigerate when not in use in a dark poly bottle.

Ammonia Analysis

Ammonia is analyzed using the method described by Kerouel and Aminot [Kero97]. The sample is combined with a working reagent made up of ortho-phthalaldehyde, sodium sulfite and borate buffer and heated to 75degC. Fluorescence proportional to the NH4 concentration is emitted at 460nm following excitation at 370nm.

REAGENTS

Ortho-phthalaldehyde stock (OPA): Dissolve 10g of ortho-phthalaldehyde in 250mls ethanol and mix thoroughly. Store in a dark glass bottle and keep refrigerated.

Sodium sulfite stock: Dissolve 0.8g sodium sulfite in DIW and dilute up to 100ml. Store in a glass bottle, replace weekly.

Borate buffer: Dissolve 120g disodium tetraborate in DIW and bring up to 4L volume.

Working reagent:
In the following order and proportions combine:
1L borate buffer
20ml stock orthophthalaldehyde
2 ml stock sodium sulfite
4 drops 40% Surfynol 465/485 surfactant and mix.
Store in a glass bottle and protect from light. Replace weekly. Make this up at least one day prior to use. Store in dark bottle and protect from outside air/nh4 contamination.

Sampling

Nutrient samples were drawn into 40 ml polypropylene screw-capped centrifuge tubes. The tubes and caps were cleaned with 10% HCl and rinsed 3 times with sample before filling. Samples were analyzed within 1-12 hours after sample collection, allowing sufficient time for all samples to reach room temperature. If stored longer than 1 hour, samples were placed in the fridge and always protected from light. The centrifuge tubes fit directly onto the sampler.

Data Collection and Processing

Data collection and processing was done with the software (ACCE ver 7.10) provided with the instrument from Seal Analytical. After each run, the charts were reviewed for any problems during the run and final concentrations (micro moles/liter) were calculated, based on a linear curve fit. Once the run was reviewed and concentrations calculated, the data was saved as an

.xlsx file, nitrate was determined by subtracting nitrite from N+N values, and the file was reviewed for possible problems.

Standards and Glassware Calibration

Primary standards for silicate (Na_2SiF_6), nitrate (KNO_3), nitrite ($NaNO_2$), phosphate (KH_2PO_4), and ammonia ($(NH_4)_2SO_4$) were obtained from Johnson Matthey Chemical Co. and/or Fisher Scientific. The supplier reports purities of >98%, 99.999%, 97%, and 99.999 respectively. All glass volumetric flasks and pipettes were gravimetrically calibrated prior to the cruise. The primary standards were dried and weighed out to 0.1mg prior to the cruise. The exact weight was noted for future reference. When primary standards were made, the flask volume at 20C, the weight of the powder, and the temperature of the solution were used to buoyancy-correct the weight, calculate the exact concentration of the solution, and determine how much of the primary was needed for the desired concentrations of secondary standard. Primary and secondary standards were made up every 7-10 days. The new standards were compared to the old before use.

All the reagent solutions, primary and secondary standards were made with fresh distilled deionized water (DIW). Secondary nitrite and ammonia standard was made up at least every 24 hours. Standardizations were performed at the beginning of each group of analyses with working standards prepared at least every 12 hours from a secondary. Working standards were made up in low nutrient seawater (LNSW). One batch of LNSW was used on the cruise and was collected and filtered prior to the cruise. The actual concentration of nutrients in this water was empirically determined during the standardization calculations.

The concentrations in micro-moles per liter of the working standards used were:

	N+N (uM)	PO_4 (uM)	Sil (uM)	NO_2 (uM)	NH_4 (uM)
SW	0.0	0.0	0.0	0.0	0.0
3	15.50	1.2	60	0.50	2.0
5	31.00	2.4	120	1.00	4.0
7	46.50	3.6	180	1.50	6.0

Quality Control

All final data was reported in micro-moles/L. NO_3, PO_4, NO_2, and NH_4 were reported to two decimals places and SIL to one. Accuracy is based on the quality of the standards the levels are:

NO_3 0.05 µM
PO_4 0.004 µM
SIL 2-4 µM
NO_2 0.05 µM
NH_4 0.1 µM

Reference materials for nutrients in seawater (RMNS) were used as a check sample analyzed with almost every run, at least once per day. The RMNS preparation, verification, and suggested

protocol for use of the material are described by [Aoyama2006], [Aoyama2007], [Aoyama2008], and Sato [Sato2010]. RMNS batch CM was used on this cruise, with each bottle being used twice before being discarded and a new one opened. Data are tabulated below.

Parameter	Concentration (uM)	stddev	Assigned conc. (uM)
NO3	33.596	0.186	33.998
PO4	2.453	0.311	2.437
SIL	103.358	0.575	102.91
NO_2	0.004	0.006	0.018
NH_4	0.671	0.124	n/a

Analytical Problems

The first few days of station work were accompanied by multiple unrelated problems with the AA3 and then the rest of the cruise went very smoothly.

It was later determined that no NH4Cl/CuSO4 mix had been added to the imidazole buffer, which led to the quick degradation of the cadmium columns used to determine nitrate concentrations. Multiple columns were changed out and other fixes attempted before the cause was determined. Many of the columns reactivated once the mix was added to a new batch of buffer and were able to be used for the rest of the cruise without issues. Nitrate data from stations 1-28 have been corrected using the average RMNS value from the remainder of the cruise.

Backpressure issues were also present off and on the first few days, evidenced by backward-twitching bubbles in the phosphate and nitrite channels. The software can generally account for this, but some peaks had to be moved and some samples re-run. No samples were lost. Syringing air and water through the sample lines didn't fix the issue.

The pump with the silicate and ammonia channel, as well as the water for the sampler wash pot, failed. Its roller stops rotating of its own accord and required restarting the pump's power and toggling the fast/normal speed switch repeatedly during one run.

It also became clear that the heater connected to the ammonia channel was clogged and created backpressure in that channel, as well as others. It was replaced with a spare and the clog was cleared by syringing air, water, and dilute acid into the coils.

Backpressure issues continued after the heater was replaced and so the sample probe was swapped out for a spare. No timing issues occurred after that.

References

.. [Armstrong1967] Armstrong, F.A.J., Stearns, C.A., and Strickland, J.D.H., "The measurement of upwelling and subsequent biological processes by means of the Technicon Autoanalyzer and associated equipment," Deep-Sea Research, 14, pp.381-389 (1967).

.. [Atlas1971] Atlas, E.L., Hager, S.W., Gordon, L.I., and Park, P.K., "A Practical Manual for Use of the Technicon AutoAnalyzer in Seawater Nutrient Analyses Revised," Technical Report 215, Reference 71-22, p.49, Oregon State University, Department of Oceanography (1971).

.. [Aoyama2006] Aoyama, M., 2006: 2003 Intercomparison Exercise for Reference Material for Nutrients in Seawater in a Seawater Matrix, Technical Reports of the Meteorological Research Institute No.50, 91pp, Tsukuba, Japan.

.. [Aoyama2007] Aoyama, M., Susan B., Minhan, D., Hideshi, D., Louis, I. G., Kasai, H., Roger, K., Nurit, K., Doug, M., Murata, A., Nagai, N., Ogawa, H., Ota, H., Saito, H., Saito, K., Shimizu, T., Takano, H., Tsuda, A., Yokouchi, K., and Agnes, Y. 2007. Recent Comparability of Oceanographic Nutrients Data: Results of a 2003 Intercomparison Exercise Using Reference Materials. Analytical Sciences, 23: 1151-1154.

.. [Aoyama2008] Aoyama M., J. Barwell-Clarke, S. Becker, M. Blum, Braga E. S., S. C. Coverly,E. Czobik, I. Dahllof, M. H. Dai, G. O. Donnell, C. Engelke, G. C. Gong, Gi-Hoon Hong, D. J. Hydes, M. M. Jin, H. Kasai, R. Kerouel, Y. Kiyomono, M. Knockaert, N. Kress, K. A. Krogslund, M. Kumagai, S. Leterme, Yarong Li, S. Masuda, T. Miyao, T. Moutin, A. Murata, N. Nagai, G.Nausch, M. K. Ngirchechol, A. Nybakk, H. Ogawa, J. van Ooijen, H. Ota, J. M. Pan, C. Payne, O. Pierre-Duplessix, M. Pujo-Pay, T. Raabe, K. Saito, K. Sato, C. Schmidt, M. Schuett, T. M. Shammon, J. Sun, T. Tanhua, L. White, E.M.S. Woodward, P. Worsfold, P. Yeats, T. Yoshimura, A.Youenou, J. Z. Zhang, 2008: 2006 Intercomparison Exercise for Reference Material for Nutrients in Seawater in a Seawater Matrix, Technical Reports of the Meteorological Research Institute No. 58, 104pp.

.. [Bernhardt1967] Bernhardt, H., and Wilhelms, A., "The continuous determination of low level iron, soluble phosphate and total phosphate with the AutoAnalyzer," Technicon Symposia, I,pp.385-389 (1967).

.. [Gordon1992] Gordon, L.I., Jennings, J.C., Ross, A.A., Krest, J.M., "A suggested Protocol for Continuous Flow Automated Analysis of Seawater Nutrients in the WOCE Hydrographic Program and the Joint Global Ocean Fluxes Study," Grp. Tech Rpt 92-1, OSU College of Oceanography Descr. Chem Oc. (1992).

.. [Hager1972] Hager, S.W., Atlas, E.L., Gordon L.I., Mantyla, A.W., and Park, P.K., " A comparison at sea of manual and autoanalyzer analyses of phosphate, nitrate, and silicate ," Limnology and Oceanography, 17,pp.931-937 (1972).

.. [Hydes2010] Hydes, D.J., Aoyama, M., Aminot, A., Bakker, K., Becker, S., Coverly, S., Daniel,A.,Dickson,A.G., Grosso, O., Kerouel, R., Ooijen, J. van, Sato, K., Tanhua, T., Woodward, E.M.S., Zhang, J.Z., 2010. Determination of Dissolved Nutrients (N, P, Si) in Seawater with High Precision and Inter-Comparability Using Gas-Segmented Continuous Flow Analysers, In: GO-SHIP Repeat Hydrography Manual: A Collection of Expert Reports and Guidelines. IOCCP Report No. 14, ICPO Publication Series No 134.

.. [Kerouel1997] Kerouel, R., Aminot, A., “Fluorometric determination of ammonia in sea and estuarine waters by direct segmented flow analysis.” Marine Chemistry, vol 57, no. 3-4, pp. 265-275, July 1997.

.. [Sato2010] Sato, K., Aoyama, M., Becker, S., 2010. RMNS as Calibration Standard Solution to Keep Comparability for Several Cruises in the World Ocean in 2000s. In: Aoyama, M., Dickson, A.G., Hydes, D.J., Murata, A., Oh, J.R., Roose, P., Woodward, E.M.S., (Eds.), Comparability of nutrients in the world's ocean. Tsukuba, JAPAN: MOTHER TANK, pp 43-56.

DISSOLVED OXYGEN ANALYSIS

Technicians:
Melissa Miller, UC San Diego/Scripps Institution of Oceanography,
Shipboard Technical Support, Oceanographic Data Facility (ODF)

Megan Roadman, UC San Diego/Scripps Institution of Oceanography
Shipboard Technical Support, Oceanographic Data Facility

Summary of Analysis

- 1141 oxygen samples were collected and analyzed from 105 CTD casts, with 3 values were lost due to operator error.

Equipment and Techniques

Dissolved oxygen analyses were performed in the ship's hydro lab with an SIO/ODF-designed automated oxygen titrator using photometric end-point detection based on the absorption of 365 nm wavelength ultra-violet light. The titration of the samples and the data logging were controlled by PC LabView software. Sodium thiosulfate was dispensed by a Brinkmann Dosimat 665 burette driver fitted with a 1.0 mL burette. ODF used a whole-bottle modified Winkler titration with concentrations of potassium iodate standard (approximately 0.012N) and sodium thiosulfate solution (approximately 55 g/L). Pre-made liquid potassium iodate standards were run every day of station work, and/or if changes were made to the system or reagents. Reagent/distilled water blanks were determined with every standardization to account for presence of oxidizing or reducing agents. Large enough batches of all the reagents were made in port and used throughout the cruise.

Sampling and Data Processing

Samples were collected for dissolved oxygen analyses soon after the rosette was brought onboard. On some stations, freon samples were collected first but on all others, oxygen was the first sample drawn. Nominal 125 mL volume-calibrated iodine flasks were rinsed 3 times with minimal agitation using a silicone drawing tube, then filled with the tube at the bottom of the flask and allowed to overflow for at least 3 flask volumes to ensure no air bubbles remained within the sample. The sample drawing temperatures were measured with an electronic thermometer embedded in the drawing tube. These temperatures are essential to calculate dissolved oxygen concentrations in umol/kg, and were used as a quick diagnostic check of bottle integrity. Pickling reagents ($MnCl_2$ followed by NaI/NaOH solution) were added in excess (1 mL of each) to fix the dissolved oxygen before stoppering. The flasks were checked again for bubble contamination following reagent addition before shaking thoroughly (10-12 inversions) to assure thorough dispersion of the precipitate. Samples were shaken again after about 30-40 minutes.

Samples were analyzed within 1-18 hours of collection. Sodium thiosulfate normalities were calculated for each standardization and corrected to 20°C. The corrected normalities and blanks were plotted versus time and were reviewed for irregularities that would suggest a possible problem. Sodium thiosulfate normality was monitored throughout the cruise and stayed within acceptable limits, except for one point. The thiosulfate container was cleaned and the solution swapped out for more from the batch made up in port, and the values returned to earlier, lower levels.

After station 2, Melissa Miller noticed that the bottle oxygen data didn't match the values of the CTD sensor trace (which was left open on a computer screen nearby). Upon further research, it was clear that the CTD sensor was giving incorrect readings and the restech Matt Durham swapped out for a new sensor. Data were compared to CTD bottle files by Hilde Oliver of the VPR group to allow for QC at a basic level. A few outlying data points were found to be due to incorrect numbering in the files provided by ODF, which were updated.

Roughly half of the total CTD casts during this cruise were trip-on-fly, meaning that the CTD wasn't stopped or even slowed down on the upcast. There may be issues using that data to calibrate sensors as the sensor readings would not have stabilized.

Volumetric Calibration

Oxygen flask volumes were determined gravimetrically with degassed deionized water to determine flask volumes at ODF's chemistry laboratory. This is done once before using flasks for the first time and periodically thereafter when a suspect volume is detected. The volumetric flasks used in preparing iodate standards were volume-calibrated by the same method, as was the 10 mL Dosimat burette used to dispense standard iodate solution.

Standards

Liquid potassium iodate standards were prepared in 6-liter batches and bottled in sterile glass bottles at ODF's chemistry laboratory prior to the expedition. The normality of the liquid standard was determined by calculation from weight. The standard was supplied by Alfa Aesar and has a reported purity of 99.4-100.4%. All other reagents were "reagent grade" and were tested for levels of oxidizing and reducing impurities prior to use.

Narrative

Temperature sensors for the sodium thiosulfate and iodate standard burettes disagreed on initial setup (difference > 1.5°C),

Station sampling and analysis went very well. Three samples were lost at the analysis stage due to the analyst not properly priming the dispenser on the acid, resulting in less than 1mL of volume being added, which wasn't noticed until the titration didn't complete normally.

SALINITY ANALYSIS

Technicians:
Melissa Miller, UC San Diego/Scripps Institution of Oceanography,
Shipboard Technical Support, Oceanographic Data Facility (ODF)

Megan Roadman, UC San Diego/Scripps Institution of Oceanography
Shipboard Technical Support, Oceanographic Data Facility

Summary of Analysis

- 1337 salinity samples were collected and analyzed. This includes:
  - ❖ 1141 samples from 105 CTD casts (103 stations), including 1 that was mis-sampled
  - ❖ 173 samples from 21 trace metal casts
  - ❖ 23 samples from 5 trace metal incubation experiments

Equipment and Techniques

A Guildline Autosal 8400B (S/N 57-526) was set up in the hydro lab and used for all salinity measurements. The water bath temperature was set to 24°C for stations 1-62 and 98-103 but was changed to 21°C for stations 63-97 due to colder laboratory temperatures. The air temperature was monitored during and between each run. We considered moving the salinometer into one of Revelle's temperature stable rooms, but decided against it since we had multiple people helping us with analysis and it was easier to have them in the room in case questions arose.
Samples were analyzed after they had been left to equilibrate to laboratory temperature (typically 12-36 hours after collection). The salinometer was standardized for each group of samples analyzed at the beginning and end of the sample run using IAPSO Standard Seawater Batch P-162. The salinometer readings were logged using a LabView program developed by Carl Mattson. The software prompted the analyst to flush the instrument's cell and change samples when appropriate.
Sample analysis was largely done by Melissa Miller and Megan Roadman, but scheduled required other help. Other people who analyzed samples are Charlie Brooks, Matt Durham, Giuliana Viglione, and Lauren Hearn. The initials of the analyzer are in each individual file.

Sampling and Data Processing

Salinity samples were collected in 200 mL Kimax high-alumina borosilicate bottles that had been rinsed at least three times with sample water prior to filling. The bottles were sealed with custom-made plastic insert thimbles and Nalgene screw caps. This assembly provides very low container dissolution and sample evaporation. PSS-78 salinity was calculated for each sample from the measured conductivity ratios. Any offset between the initial standard seawater value and its reference value was always within instrument precision, so no offset was made to following sample values. The difference (if any) between initial and final standards was noted so that a drift correction could be applied.
Bottle fire CTD data were compared with salinity sample data by Hilde Oliver of the VPR team to allow for QC at a basic level. At the beginning of the cruise, a few samples were run on the wrong suppression setting on the Autosal, retruning reading of 1.90XXX instead of 2.00XXX. These were changed in the data and updated files were used for QC. An offset between primary and secondary CTD sensors was noted, with the bottle data used to determine that CTD 1 should be changed out. Beginning with station 63, CTD sensor 3 was swapped in.
Roughly half of the total CTD casts during this cruise were trip-on-fly, meaning that the CTD wasn't stopped or even slowed down on the upcast. There may be issues using that data to calibrate sensors as the sensor readings would not have stabilized.

Analytical Problems

Lab temperature was an issue in the hydro lab. As mentioned earlier, the decision was made to leave the salinometer there so that analysis by other people could be overseen. The engineers and electrician onboard were notified of the issue of laboratory temperature. The system is new after the ship's midlife refit so they were still getting used to the systems and thermometer, but were able to adjust the temperature. Thankfully, we had enough bottles to store samples so that we could wait until the lab temperature had been stable for a time before performing any analyses.

SOCCOM Cruise Report, for SAMW Cruise on *R/V Roger Revelle* #2004

PI: Dr. Lynne Talley, Scripps Institution of Oceanography (SIO)

Team: Melissa Miller and Megan Roadman, Scripps Institution of Oceanography

Andrew Meyer, University of Washington (set up in port prior to cruise)

Rationale: The SOCCOM (Southern Ocean Carbon and Climate Observations and Modeling) project deploys autonomous biogeochemical floats to study the Southern Ocean and its impact on the climate. Ten SOCCOM floats were deployed during the 2021 SAMW cruise on *R/V Roger Revelle*.

Aims and Objectives: SOCCOM floats include sensors measuring nitrate, pH, fluorescence, backscatter, oxygen, salinity, temperature, and pressure. CTD casts were performed at each location in order to calibrate each float's sensors. Niskin bottle samples were taken at various depths between the surface and 1500 meters (on 8 casts) and the seafloor (2 already-scheduled deep casts), with some samples analyzed onboard and others sent back for analysis on shore.

order deployed	station	target latitude	serial number(s)	Adopted Name
1	1	30S	9066 / 19018	***The Mighty Mussel***
2	11	35S	0887	***Moana***
3	17	38S	1115	***NOAA-EPP/MSI***
4	25	42S	1204	***Hawk-eye***
5	33	46S	9069 / 19072	***Lizzy***
6	37	48S +/1	1205	***The Sea Lion***
7	43	50S +/-	8690 / 17328	***Fernando***
8	45	53S +	8925 / 19085	***Rocket Penguin***
9	63	60S -	8917 / 19327	***Aquaty***
10	73	57S +/-	8926 / 19067	***Alvin***

Methods:

With the ship moving at 1-2 knots, the restech looped a rope through the float's upper ring and lowered it gently over the starboard-side stern.

The CTD winch was operated by a member of the crew and the software run by Dave Drapeau or Barney Balch from the computer lab. An FLBB sensor was added to the rosette and configured

by restechs Matt Durham and Charlie Brooks during the load period. A dark test was performed on station 16 by covering the light path with electrical tape.

Nutrients (nitrate, nitrite, phosphate, silicate, and ammonia) were measured using a SEAL Analytical continuous-flow Auto-Analyzer (AA3) operated in the hydro lab by Melissa Miller and Megan Roadman. Primary and secondary standards, as well as reagents, were made up in deionized (DI) water. Working standards were made up in low nutrient seawater (LNSW), brought from coastal California. Reference materials (RMNS) from Kanso were analyzed with most sample runs.

30ml of water was collected for each sample. Nutrients were sampled by Melissa Miller or Megan Roadman, with help from the Balch group when possible. The AA3 and AACE software required some troubleshooting throughout the cruise (see nutrients section).

Dissolved oxygen was measured using an automated titrator designed at Scripps Institution of Oceanography and operated in the hydro lab by Melissa Miller and Megan Roadman. Pre-made standards were run at every 24 hours.

Dissolved oxygens were sampled into 125ml glass flasks by Melissa Miller or Megan Roadman.

Salinity samples were measured using a Guidline Autosal in the hydro lab. 250ml of water was collected and samples after they had adjusted to lab temperature over 12 hours. Melissa Miller and Megan Roadman analyzed many of the samples, with help from restechs Charlie Brooks and Matt Durham, as well as Clay Tompkins, Giuliana Viglione, and Lauren Hearn. OSIL IAPSO standard seawater batch P162 was used with each run. Salinities were sampled by Melissa Miller and Megan Roadman, with help from the Balch group when possible.

HPLC samples were taken from Niskin bottles at the surface and chlorophyll maximum. 1-2L of water was sampled, and filtered immediately in the hydro lab by Melissa Miller or Megan Roadman. Filters were then stored in the -80C and will be transported to Scripps on dry ice and then shipped to NASA in a dry shipper. HPLC samples were taken by Melissa Miller or Megan Roadman.

pH/alkalinity samples will ride the ship back to San Diego for analysis by Dr. Andrew Dickson's lab at SIO. 500ml of water was collected, and poisoned with mercuric chloride before being sealed. Melissa Miller or Megan Roadman took all pH/alkalinity samples with help from the Balch group when possible.

Preliminary Results: Data sets were returned from each float within 24 hours of deployment, and every 10 days thereafter. Data will be posted online as it is collected. The nitrate sensor on float 0887 has been determined to be bad.
http://soccom.princeton.edu/content/data-access
Shore-based members of the SOCCOM project are responsible for converting bottle data into a format suitable to calibrate the sensors. Melissa Miller will submit bottle data analyzed onboard for this purpose, as well as the pCO2 data.

Issues/recommendations: All ten floats were deployed successfully. Operations were done in sea states ranging from calm to moderately stormy, and all were performed safely. The order of stations changed due to weather and order of VPR transits, but everything got done.

Outreach: All floats were adopted by schools and decorated with their given names and associations before being deployed. Melissa Miller posted a weekly blog on the site:
http://soccomatsea.blogspot.com

Broader impacts
Giuliana Viglione, Freelance Science Writer, Washington, D.C.

In order to broaden the audience of the scientific objectives of the project and to engage with K–12 educators across the country, a freelance science writer was brought along on the SAMW 21 cruise. The objectives of the science writer, broadly defined and established in advance with Barney Balch, were to keep a regular blog, connect with classrooms across the country, make posts on social media, take photos and videos of scientists on board, and assist with scientific duties and operations.

Bigelow Lab hosted the blog on their website. Over the course of the cruise, the science writer wrote 18 posts for a general audience. Every member of the science party was featured on the blog at least once and individual posts highlighted each science group on board as well as the overall scientific mission. Part of each blog post was also dedicated to informing the public about the realities of life aboard a research vessel.

Two of the undergraduate students on the cruise also kept blogs as part of their independent study duties on board, totaling more than 15 posts between the two of them. The science writer helped the undergraduates formulate ideas and edited blog posts.

Before the cruise, the science writer connected with teachers in 6 classrooms across 4 US states. They also connected with WeatherBlur, an NSF-funded program that has a reach of 10+ classroom teachers across New England and the Gulf Coast. WeatherBlur promoted the blog and encouraged people to send in questions via their weekly email newsletter. Students from across the country sent in dozens of questions over the course of the cruise; five blog posts were ultimately dedicated to answering as many of these questions as possible.

Twitter was the primary social media platform used to communicate science aboard the ship. Over the course of the cruise, 35+ tweets were sent by the science writer. These ranged from brief descriptions of science to photos of ship operations to snippets of life on board the vessel. Overall, the tweets amassed around 45,000 impressions. Twitter was also used to promote new blog posts and drive traffic to the blog. The blog was also promoted on Twitter by Bigelow Lab, WHOI, Scripps, and the SOCCOM program.

On 19 February, the science writer also used the social media platform Reddit to host an “Ask me Anything”, or AMA. The purpose of an AMA is for people to respond in real time to text-based questions posed by the general public. Reddit was selected as an outreach venue because its user base is quite distinct from the other outreach efforts conducted during the cruise. A team of scientists and ship technicians helped answer questions throughout the two-hour AMA. Over the course of the event, we received and answered more than 30 questions from the public.

The science writer also took photos of scientists in action during all major scientific operations on board the vessel. These photos are being provided to both individual scientists and their

institutions for promotional materials in the future. Some institutions, such as Bigelow Lab, have already been using these photos on both social media and for donor solicitations.